VNIVERSITAT DE VALÈNCIA

SCHOOL OF MEDICINE AND DENTISTRY

DEPARTMENT OF PHYSIOLOGY

DOCTORAL PROGRAM IN PHYSIOLOGY

MUSCLE ARCHITECTURE DETERMINED BY ULTRASOUND FOR THE DIAGNOSIS OF FRAILTY WITH CORRELATION OF CLINICAL, PHYSICAL AND BIOCHEMICAL MARKERS

Doctoral thesis presented by:

JELENA VUCETIC

And supervised by
CONSUELO BORRÁS BLASCO

GOITZANE MARCAÍDA BENITO

REBECA MIRÓN MOMBIELA

JANUARY, 2023

Dña **Consuelo Borrás Blasco**, Catedrática del Departamento de Fisiología de la Facultad de Medicina y Odontología, Universitat de València.

Dña **Goitzane Marcaída Benito**, Jefa del Servicio de Análisis Clínicos del Hospital General Universitario de Valencia.

Dña **Rebeca Mirón Mombiela**, Médica Adjunta del Servicio de Radiología del Hospital Herlev of Gentofte de Dinamarca.

CERTIFICAN:

Que la presente memoria, titulada "Muscle architecture determined by ultrasound for the diagnosis of frailty with correlation of clinical, physical and biochemical markers", corresponde al trabajo realizado bajo su dirección por D/Dña. Jelena Vucetic, para su presentación como Tesis Doctoral en el Programa de Doctorado en Fisiología de la Universitat de València.

Y para que conste firman el presente certificado en Valencia, a 20 de enero de 2023.

GOIZANE| MARCAIDA| BENITO

Fdo. Dra Consuelo Borrás Blasco | Fdo. Dra Goitzane Marcaída Benito | Fdo. Dra Rebeca Mirón Mombiela

Acknowledgments

To the people that taught and guided me and the people that stood by me during this journey, and with special emphasis:

To Consuelo Borrás, I know I came to you as an appendix of sorts, being Rebe´s ´little´ resident, trying to fill her shoes. Thank you for having patience with me and being at my side. You gave me more than I was hoping for as a tutor and a director, you paid attention to my needs and you guided me all the way. Thank you for believing in me and pushing me forward.

To Goitzane Marcaída, thank you for giving me an opportunity and accepting this collaboration. Your guidance has been invaluable, you helped me merge and understand different fields of study and without your input, this work would not be the same. Also, I would like to mention that you have been a true inspiration to me as a woman and a leader, thank you for showing me it can be achieved.

To Rebeca Mirón, I am certain I could not have done this without you. Not only have you made the investigation fun and approachable, you have also shown me the practicals, the logistics and the planning that goes into any serious project. Thank you for not letting me be mediocre, for encouraging critical thinking and giving me the opportunity to shine.

To Jenny Cárdenas, it has been a pleasure working by your side; you enriched my life professionally and personally.

To my parents and brother, it goes without saying, I would not be where I am without all of you.

I hope to make you proud.

To my uncle, you were my first professor, you opened the world of science and made me fall in love with medicine and I thank you for that. I wish you could see me today.

To my grandmother, this work is for you, after all, you helped me add a close and personal touch to it. I hope I made some difference.

And last but not the least, to my partner, thank you for being my guinea pig for this project and letting me practise on you, you were lucky I have not chosen any surgical field. Instead, the photos of your leg are famous in the science world. And seriously, thank you for not complaining for the long hours, for understanding and supporting me through all ups and downs, I feel lucky to share a life with a person like you.

Contents

INDEX OF ABBREVIATIONS

µM – micromole

A.U. – arbitrary units

AGEs – advanced glycosylation end-products

ALT – alanine aminotransaminase

ASCA – anatomical cross-sectional area

ASM – apendicular skeletal muscle mass

AST – aspartate aminotransferase

AUC – area under the curve

BIA – bioelectrical impedance

BMI – body mass index

CHGUV – Consorcio Hospital General Universitario de Valencia

CI – confidence interval

COPD – chronic obstructive pulmonary disease

CPK – creatine phosphokinase

CRP – C-reactive protein

CT – computed tomography

DHEA – dehydroepiandrosterone

DM – diabetes mellitus

DXA – dual-energy X-ray absorptiometry

EDTA – Ethylenediaminetetraacetic acid

EI – echointensity

ELISA – enzyme-linked immunosorbent assay

EWGSOP – European Working Group on Sarcopenia in Older People

FDR – false discovery rates

GFR – glomerular filtration rate

HDL – high-density lipoprotein

HGB – haemoglobin

HPLC – High-performance liquid chromatography

i.e. – that is

ICC – intraclass correlation coefficient

IFN – interferon

IGF – insulin-like growth factor

IL – interleukin

IPAQ – International Physical Activity Questionnaire

ITAC – interferon-inducible T-cell alpha chemoattractant

kg – kilogram

LDL – low-density lipoprotein

m – meter

MCH – mean corpuscular haemoglobin

MCHC – mean corpuscular haemoglobin concentration

MCV – mean corpuscular volume

MDA – malondialdehyde

MIP – macrophage Inflammatory Protein

MRI – magnetic resonance imaging

MT – muscle thickness

OR – odds ratio

PA – pennate angle

PAC – pennate angle in contraction

PACS - Picture Archiving and Communication System

PE – phycoerythrin

PSCA – physiological cross-sectional area

PTH – parathormone

QIB – Quantitative imaging biomarker

RBC – red blood cells

RF – rectus femoris

ROC – receiver operating characteristic

ROI – region of interest

s – second

SASP – senescence-associated secretory phenotype

SDS – sodium dodecyl sulphate

SPPB – Short Physical Performance Battery

TBA – thiobarbituric acid

TIA – transitory ischaemic attack

TNF – tumour necrosis factor

TS – transferrin saturation

TSH – thyroid-stimulating hormone

TUG – Timed-Up and Go test

VI – vastus intermedius

VIF – Variance Inflation Factor

VL – vastus lateralis

VM – vastus medialis

λ – wavelength

INDEX OF TABLES

INDEX OF FIGURES

RESUMEN TESIS DOCTORAL

INTRODUCCIÓN

La fragilidad se define como un síndrome clínico de mayor vulnerabilidad a factores externos que pueden desencadenar efectos adversos para la salud y llevar a la muerte. Este síndrome se caracteriza por una disminución acelerada de las reservas funcionales, donde los pacientes son susceptibles a eventos aparentemente menores (por ejemplo, una infección o un nuevo medicamento) que pueden provocar un empeoramiento grave de la salud con períodos prolongados de recuperación y repercusiones en el nivel general de funcionamiento. Los efectos adversos asociados con la fragilidad incluyen caídas, discapacidad, hospitalización y mortalidad. La prevalencia estimada de personas frágiles mayores de 65 años en los países europeos oscila entre el 5,8 % y el 27,3 %.

La fragilidad es prevenible y parcialmente reversible si se diagnostica a tiempo, por lo que existe un especial interés en desarrollar biomarcadores para la identificación de personas en riesgo e implementar intervenciones oportunas con el fin de reducir los eventos adversos. En este sentido, el desarrollo de biomarcadores cuantitativos para el diagnóstico de fragilidad es de suma importancia.

El diagnóstico clínico de fragilidad se basa en la definición operativa de Fried basada en cinco criterios y es el método más utilizado para identificar a las personas frágiles y prefrágiles en el entorno clínico. Aunque es una herramienta ampliamente validada, tiene algunas limitaciones en la práctica clínica. Por ejemplo, tiene una capacidad limitada para predecir la progresión de un estado robusto o prefrágil a uno frágil. Además, algunos de los criterios de fragilidad son subjetivos y pueden dificultar la evaluación en varios escenarios clínicos (por ejemplo, en pacientes con deterioro cognitivo o depresión).

Hasta la fecha, no existe un biomarcador cuantitativo específico para el diagnóstico de fragilidad, aunque se están investigando muchos marcadores circulantes y de imagen. Un buen biomarcador debe ser accesible, rentable, preciso y fiable. En los últimos años, el concepto de paneles de biomarcadores en lugar de biomarcadores individuales está ganando más importancia.

Aunque se están investigando varios parámetros ecográficos, no está claro si los parámetros de tamaño muscular o de calidad muscular o una combinación de ambos muestran un mejor rendimiento en el diagnóstico de pacientes frágiles. Además, la falta de protocolos

estandarizados para realizar ecografías musculares en pacientes ancianos con sarcopenia puede disminuir la fiabilidad y la reproducibilidad de los resultados y presenta una importante limitación para la implementación clínica.

No hay estudios que hayan investigado la combinación de marcadores circulantes y de parámetros de imagen ecográfica para el diagnóstico de fragilidad. Esto es importante ya que los hallazgos de imagen deben respaldarse con datos biológicos para comprender los perfiles histológicos y moleculares de los parámetros visuales.

Aunque la ecografía muscular no forma parte de los protocolos actuales para el diagnóstico de sarcopenia, esta técnica podría ser útil en el ámbito clínico, ya que puede medir cambios en el volumen, la composición y la arquitectura del músculo.

Por lo tanto, asumimos que las imágenes ecográficas se pueden usar de manera fiable para evaluar la sarcopenia siempre que se haya aplicado el protocolo apropiado y el operador esté capacitado para realizar el examen. Asimismo, postulamos que el protocolo con una combinación de parámetros ecográficos que evalúen tanto la masa como la calidad muscular pueda distinguir a los individuos en riesgo de fragilidad entre los pacientes ambulatorios. Además, planteamos la hipótesis de que la combinación de parámetros ecográficos y circulantes sería una buena herramienta cuantitativa para diagnosticar pacientes con riesgo de fragilidad en el entorno clínico.

METODOLOGÍA

Este fue un estudio experimental realizado en un entorno clínico ambulatorio. La parte experimental del estudio incluyó ecografía muscular y análisis de sangre. El estudio se realizó en humanos tras obtener la aprobación del comité de ética del CHGUV.

Los criterios de inclusión para el grupo experimental:

- 60 años o más,

- capacidad para caminar de forma independiente (incluso con la ayuda de un bastón/andador),

- acceso a la historia clínica.

Los criterios de exclusión:

- trastornos neuromusculares o enfermedades agudas o crónicas que alterarían la arquitectura muscular o interferirían con la medición de la fuerza de prensión usando un dinamómetro manual,

- pacientes oncológicos en tratamiento (quimio o radioterapia),

- pacientes institucionalizados o pacientes que no pueden llegar al centro de investigación utilizando sus propios medios de transporte,

- demencia grave que influiría en la capacidad del paciente para comprender el consentimiento informado y el cuestionario.

Se invitó a participar como grupo de control a sujetos sanos entre 20 y 59 años.

Ecografía muscular

Se escanearon las cuatro cabezas del músculo cuádriceps femoral. El primer conjunto de imágenes se tomó en el punto medio entre la espina ilíaca anterosuperior y el cóndilo femoral lateral en planos transversal y longitudinal y se utilizó para evaluar las cabezas de los músculos recto femoral y vasto intermedio. Luego, con la sonda sostenida en posición longitudinal, se le pidió al paciente que contrajera el músculo cuádriceps y se tomaron las imágenes en contracción. Desde este punto, la sonda se colocó lateralmente al mismo nivel para incluir la cabeza del músculo vasto lateral. Las imágenes se tomaron en planos transversal y longitudinal, en reposo y en contracción. Finalmente, la sonda se colocó en posición medial y ligeramente distal y se exploró la cabeza del vasto medial en ambos planos (longitudinal y transversal) en reposo y durante la contracción.

Las imágenes se procesaron con ImageJ software. La ecointensidad (EI) y el grosor muscular (MT) se midieron a partir de las imágenes tomadas en el plano transversal y se utilizó el valor medio de las tres medidas para el análisis estadístico. Para la ecointensidad se trazó un ROI manual incluyendo la mayor parte del músculo visible en la imagen y evitando la aponeurosis y el hueso. El grosor muscular se midió a partir de imágenes transversales como la distancia máxima entre las dos aponeurosis, utilizando la herramienta de regla y se utilizó el valor medio para el análisis. Los ángulos penados (PA) se midieron a partir de imágenes longitudinales en reposo y en contracción utilizando la herramienta de ángulo. Se eligió un fascículo claramente visible y se trazó el ángulo entre el fascículo y su inserción en la aponeurosis profunda. Finalmente, el área del recto femoral se midió a partir de las imágenes tomadas con el transductor convexo utilizando ROI manual.

La fuerza de prensión de la mano dominante se midió utilizando un dinamómetro de mano. Medición de la velocidad de la marcha se midió con la aplicación de cronómetro del teléfono Android.

Cuestionario – se registraron los datos epidemiológicos y antropométricos, comorbilidades y factores de riesgo.

Se utilizaron los criterios de fragilidad propuestos por Fried y colegas para determinar el fenotipo de fragilidad. Estos criterios evalúan la pérdida de peso no intencionada, el agotamiento, la baja actividad física, la marcha lenta y la debilidad muscular.

Cada criterio positivo se puntuó con un punto. La puntuación final fue la suma de los cinco criterios. Según el número de puntos, los pacientes se clasificaron en:

Robusto – 0 puntos,

Pre-frágil – 1 o 2 puntos,

Frágil – 3-5 puntos.

Análisis bioquímicos

Se extrajo sangre después de al menos 8 horas de ayuno. Se analizaron los siguientes analitos: leucocitos con fórmula leucocitaria, hematíes, hemoglobina, hematocrito, plaquetas, proteínas, proteína C reactiva, albúmina, glucosa basal, urea, creatinina, filtrado glomerular, calcio, fósforo, transaminasas, cloro, potasio, sodio, colesterol total, triglicéridos, colesterol HDL y LDL, creatinfosfoquinasa, homocisteína, ferritina, hierro, índice de saturación de transferrina, vitamina D, cortisol, insulina, parathormona (PTH), tirotropina (TSH) y factor de crecimiento insulínico tipo 1 (IGF-1).

La muestra de plasma se utilizó para la determinación de malondialdehído (MDA) y carbonilación de proteínas como marcadores de estrés oxidativo.

Las citoquinas pro y antiinflamatorias se evaluaron en muestras de plasma. Se utilizó un kit de ensayo Luminex comercial para la detección y cuantificación de las siguientes citoquinas: ITAC, Fractalkine, IFN-γ, IL-10, MIP-3α, IL-12p70, IL-13, IL- 17a, IL-1β, IL-2, IL-4, IL-23, IL-6, IL-7, IL-8, TNF-α.

Análisis estadístico

El análisis estadístico se realizó utilizando el software SPSS, versión 22.0 para Windows (IBM, SPSS Inc.). Todas las variables continuas se presentaron como medias ± desviaciones estándar, mientras que las variables ordinales se presentaron como cantidad y porcentajes. La distribución de las variables continuas se evaluó con la prueba de normalidad de Kolmogorov-Smirnov. Para evaluar las diferencias entre sexos se utilizó la prueba t-student para las variables con distribución normal (variables paramétricas) y la prueba de Mann-Whitney para las variables no paramétricas. Las diferencias de las variables de estudio según el fenotipo de fragilidad se evaluaron mediante la prueba ANOVA para variables paramétricas seguida de la prueba post-hoc de Bonferroni, mientras que para las variables no paramétricas se utilizó la prueba de Kruskal-Wallis.

Se realizó un análisis de correlación para evaluar las relaciones entre las características físicas, ecográficas y los parámetros bioquímicos. La fuerza de la correlación se dividió arbitrariamente en tres categorías: débil, moderada y fuerte, y se interpretó como débil para valores r<0,399, moderada para valores r de 0,400 a 0,699 y fuerte para valores r>0,700.

La precisión de los parámetros ecográficos se evaluó utilizando áreas bajo la curva ROC (por sus siglas en inglés Receiver Operating Characteristic). La precisión de la técnica de medición se evaluó utilizando los coeficientes de correlación intraclase (ICC) y los límites de concordancia de Bland-Altman.

Se realizó un análisis de regresión logística con parámetros ecográficos y bioquímicos ajustados con características físicas para determinar los mejores modelos predictivos de fragilidad. El fenotipo de fragilidad se utilizó como variable dependiente, creando dos grupos: no frágiles y de riesgo. Los pacientes robustos y los controles jóvenes se asignaron al grupo no frágil, y los pacientes frágiles y prefrágiles se asignaron al grupo de riesgo. El nivel de influencia de las variables independientes sobre la fragilidad se expresó mediante razones de probabilidad.

La significación estadística se definió como p<0,05.

RESULTADOS

La muestra consistió en 128 pacientes, de los cuales 66 fueron mujeres (51%) y 62 hombres (49%). La muestra fue homogénea entre sexos en cuanto a edad, índice de masa corporal (IMC), velocidad de la marcha y actividad física. Hubo diferencias significativas entre sexos en peso, talla, fuerza muscular, actividad física intensa y moderada y tiempo sentado durante el día.

Hubo 36 controles (28%), 22 robustos (17%), 53 prefrágiles (41%) y 17 pacientes frágiles (13%). Hubo diferencias significativas entre los grupos en edad, talla, IMC, fuerza muscular, velocidad de la marcha, actividad física intensa y marcha. No hubo diferencias significativas en peso, actividad física moderada y tiempo sentado. Finalmente, la muestra se distribuyó homogéneamente entre los grupos en cuanto al sexo.

En cuanto a los parámetros ecográficos, hubo diferencias significativas entre sexos en casi todos los parámetros, excepto en los ángulos penados del recto femoral, vasto intermedio y vasto lateral, así como del grosor muscular del vasto lateral.

Los parámetros ecográficos según el fenotipo de fragilidad mostraron los siguientes hallazgos: hubo diferencias significativas entre los grupos para todos los parámetros del recto femoral. El grosor muscular de todas las cabezas del cuádriceps femoral mostró diferencias significativas entre los grupos. En cuanto a la ecointensidad, hubo diferencias significativas entre los grupos para el recto femoral, mientras que el vasto intermedio, vasto medial y vasto lateral no mostraron diferencias entre los grupos. Los ángulos penados en reposo y en contracción mostraron diferencias significativas entre los grupos para todas las cabezas del cuádriceps excepto el vasto medial en reposo.

Se analizaron un total de 61 muestras de sangre. Había 34 mujeres (56%) y 27 hombres (44%) individuos. Hubo 18 (29%) sujetos asignados al grupo control y 8 (13%) pacientes robustos, 26 (43%) prefrágiles y 9 (15%) pacientes frágiles. Se realizó analítica general de sangre y estado hormonal. Además, se evaluaron los parámetros de estrés oxidativo.

Se realizó un análisis de correlación de todas las variables del estudio con el fin de evaluar las posibles relaciones entre los parámetros ecográficos, físicos y bioquímicos. Luego, estos parámetros se seleccionaron y utilizaron en el análisis de regresión para determinar su valor predictivo de fragilidad.

Las correlaciones del fenotipo de fragilidad con la ecografía y los parámetros funcionales: hubo una correlación inversa moderada entre el fenotipo de fragilidad y el área del recto femoral (r = -0,612). El fenotipo de fragilidad mostró una correlación negativa moderada con el grosor muscular del recto femoral, vasto interno y el vasto lateral (r = -0,563, -0,483 y -0,403 respectivamente). Por otro lado, se mostraron correlaciones positivas moderadas entre la fuerza muscular y el área del recto femoral, así como el grosor muscular del vasto medial (r=0,425 y 0,474 respectivamente). Inversamente, hubo correlaciones negativas entre la fuerza muscular y la ecointensidad, moderadas para el recto femoral (r=-0,451) y débiles para el vasto medial y el

vasto lateral (r=-0,380 y –0,382 respectivamente). Se encontraron correlaciones inversas débiles entre la velocidad de la marcha y el grosor muscular del recto femoral, vasto medial y vasto lateral (r=-0,260, -0,280 y -0,323), área del recto femoral (r=- 0.334), así como con ángulo penado en contracción del recto femoral y vasto intermedio y ángulo pennado del vasto lateral en reposo y contraído. No hubo correlaciones entre la velocidad de la marcha y la ecointensidad de ninguna de las cabezas del cuádriceps femoral.

Se detectaron correlaciones negativas débiles entre las caídas y el área del recto femoral, el grosor muscular del recto femoral, vasto medial y lateral, así como el ángulo penado en la contracción del recto femoral y el vasto medial. Además, hubo correlaciones positivas débiles entre la obesidad y la ecointensidad de todas las cabezas de los cuádriceps, así como el grosor de la grasa superficial.

El factor de crecimiento insulínico tipo 1 tuvo una correlación positiva moderada con el área del recto femoral y el fenotipo de fragilidad (r=0,510 y 0,582 respectivamente), y una débil correlación negativa con la ecointensidad del recto femoral, r=-0,378. También hubo correlaciones positivas débiles con el grosor muscular del recto femoral y del vasto medial (r=0,374 y 0,356 respectivamente), así como con el ángulo penado en la contracción del vasto intermedio, r=0,352. La parathormona mostró una correlación positiva débil con el fenotipo de fragilidad, r=0,352 y una correlación negativa débil con el ángulo penado del vasto lateral, r=-0,302. El cortisol, la insulina y la hormona estimulante de la tiroides en su mayoría no tuvieron correlaciones significativas con los parámetros ecográficos.

Con el fin de evaluar el rendimiento de los parámetros ecográficos como biomarcadores de imagen y su utilidad clínica, los analizamos para determinar su exactitud y precisión.

Para determinar la exactitud o el poder discriminativo de los parámetros ecográficos, se analizaron las áreas bajo la curva ROC. El área del recto femoral y el grosor muscular del recto femoral mostraron un poder de discriminación excelente (AUC = 0,838) y aceptable (AUC = 0,793), respectivamente. El área del recto femoral mostró el poder discriminativo mejor que la fuerza muscular. El resto de los parámetros se comportaron de pobre a aceptable.

Para valorar la precisión de los parámetros ecográficos se evaluaron los coeficientes de correlación intraclase (ICC) y los límites de concordancia de Bland-Altman. Comparamos mediciones repetidas para cada uno de los parámetros ecográficos obteniendo un ICC excelente para la mayoría de ellos, excepto el ángulo pennado de los músculos vasto intermedio y vasto

lateral, que mostró un buen ICC. La mayoría de los parámetros tenían alta repetibilidad (o bajo error de medición).

Modelos de fragilidad con análisis de regresión logística

Se realizó un análisis de regresión logística utilizando parámetros ecográficos y bioquímicos y características físicas para estimar su poder diagnóstico de fragilidad. Se desarrollaron múltiples modelos predictivos utilizando diferentes parámetros ecográficos (grosor muscular, ecointensidad, ángulos penados y área del recto femoral) ajustados con parámetros bioquímicos (parámetros bioquímicos generales, panel de citoquinas y hormonas) y con las características físicas (velocidad de la marcha, fuerza muscular, sexo, IMC).

1) Parámetros ecográficos y características físicas

El modelo de análisis de regresión logística BEST US fue estadísticamente significativo en el primer paso ($\chi 2$ (5) = 64.447, p<0.001). El modelo explicó el 54,2% de la varianza del fenotipo de fragilidad y clasificó correctamente el 79% de los casos. Cuando se ajustó por características físicas, el bloque y el modelo fueron estadísticamente significativos (p<0,001). El modelo explicó el 74,5% de la varianza del fenotipo de fragilidad y clasificó correctamente el 91,9% de los casos. Área de recto femoral (p<0,001), grosor muscular de vasto medial (p=0,05), ángulo pennado en contracción de vasto medial (p=0,036), IMC (p=0,027), sexo (p=0,014) y fuerza muscular (p<0,001) contribuyeron significativamente al modelo final. El grosor muscular del vasto lateral fue significativo solo en el primer paso, mientras que el grosor de la grasa superficial del recto femoral y la ecointensidad del vasto lateral no influyeron significativamente en la fragilidad. El aumento de un centímetro cuadrado del área del recto femoral, y manteniendo el resto de variables constantes, disminuye la probabilidad de fragilidad 1,95 veces. El aumento de un centímetro de grosor muscular del vasto medial disminuye las probabilidades de fragilidad 4,18 veces. El aumento de un grado del ángulo penado en contracción del vasto medial aumenta las probabilidades de fragilidad 1,16 veces. El aumento de un kg de fuerza muscular disminuye las probabilidades de fragilidad 1,27 veces y el aumento de una unidad de IMC aumenta las probabilidades de fragilidad 1,22 veces. Finalmente, las probabilidades de fragilidad fueron 14,08 veces mayores en mujeres que en hombres.

2) Parámetros ecográficos y bioquímicos con características físicas

Se construyeron los modelos utilizando el área del recto femoral o el grosor del recto femoral (como los parámetros con el AUC más alto). Se evaluaron diferentes parámetros bioquímicos, en concreto, los que mostraron diferencias significativas entre los grupos de fragilidad. Las

citoquinas y hormonas que mostraron correlaciones con el fenotipo de fragilidad también se eligieron para este análisis.

El modelo de análisis de regresión logística BIO 1 utiliza el grosor muscular del recto femoral combinado con los mejores parámetros bioquímicos generales. El modelo fue significativo en el primer paso (p<0,001), explicó el 47% de la varianza del fenotipo de fragilidad prediciendo correctamente el 75,8% de los casos. Al ajustar con parámetros bioquímicos, el bloque y el modelo permanecieron significativos (p<0,001), el modelo explicó el 69,4% de la varianza y la predicción correcta fue del 87,1%. Finalmente, al ajustar con las características físicas, el bloque y el modelo resultaron significativos (p<0,001), el modelo explicó el 83,8% de la varianza y predijo correctamente el 93,5% de los casos. El grosor muscular del recto femoral (p=0,035), las proteínas (p=0,022), la velocidad de la marcha (p=0,047) y la fuerza muscular (p=0,046) contribuyeron significativamente al modelo final. La glucosa fue significativa en el segundo paso (p=0,016) y no alcanzó significación estadística en el paso final. El aumento de un centímetro de grosor muscular del recto femoral y el mantenimiento de todas las demás variables constantes, disminuye 333 veces las probabilidades de fragilidad. El aumento de una unidad de proteínas disminuye las probabilidades de fragilidad 143 veces. El aumento de un segundo del tiempo de marcha (disminución de la velocidad de la marcha) aumenta las probabilidades de fragilidad 8,87 veces. El aumento de un kg de fuerza muscular disminuye las probabilidades de fragilidad 1,26 veces.

Para el modelo BIO 2 los parámetros utilizados fueron MIP-3a e IL-1β. Ambos parámetros mostraron correlaciones con el área del recto femoral así como con el fenotipo de fragilidad. El modelo fue significativo en los tres pasos (p<0,001). Cuando se ajustó con parámetros bioquímicos y características físicas, el modelo explicó el 87,2% de la varianza y predijo correctamente el 95,1% de los casos. Por cada centímetro cuadrado de aumento del área del recto femoral y manteniendo constantes el resto de variables, la probabilidad de fragilidad disminuye 2,69 veces. El aumento de una unidad de MIP-3a reduce las probabilidades de fragilidad 1,17 veces. El aumento de una unidad de IL-1β disminuye las probabilidades de fragilidad 12,34 veces. El aumento de una unidad de IMC aumenta las probabilidades de fragilidad 1,67 veces. El aumento de un kilogramo de fuerza muscular disminuye las probabilidades de fragilidad 1,6 veces. Las probabilidades de fragilidad eran 5000 veces mayores en las mujeres.

El modelo BIO 3, utiliza IGF-1 e IFN-γ, ambos parámetros tuvieron una correlación significativa con el fenotipo de fragilidad. El modelo fue significativo en los tres pasos (p<0,001). En el paso

final, cuando se ajustó con los parámetros bioquímicos y las características físicas, el modelo explicó el 80,1% de la varianza y predijo correctamente el 93,3% de los casos. El grosor muscular del recto femoral (p=0,030), el IFN-γ (p=0,016) y la fuerza muscular (p=0,029) contribuyeron significativamente al modelo final. IGF-1 fue significativo en el segundo paso (p=0,037), y cuando se ajustó con características físicas, no alcanzó significación estadística (p=0,08). La disminución de un centímetro de grosor muscular del recto femoral aumenta las probabilidades de fragilidad 58,8 veces. El aumento de una unidad de IFN-γ reduce las probabilidades de fragilidad 1,12 veces. El aumento de un kg de fuerza muscular disminuye las probabilidades de fragilidad 1,18 veces.

DISCUSIÓN

Los resultados de este estudio confirman que la ecografía muscular podría utilizarse en pacientes ambulatorios como método de cribado y es posible diagnosticar sujetos en riesgo de fragilidad con una precisión de hasta el 95 % utilizando modelos de fragilidad que combinan parámetros ecográficos y bioquímicos. Varios hallazgos importantes respaldan este resultado:

1. La ecografía muscular es una herramienta útil para evaluar el volumen y la arquitectura muscular en el contexto del síndrome de fragilidad, con alta precisión y exactitud y podría considerarse como una alternativa válida a los métodos estándar para la evaluación de masa muscular en un entorno clínico. Los parámetros de ecografía muscular por sí solos, como el área del recto femoral y el grosor del músculo recto femoral, fueron capaces de identificar un tamaño muscular bajo y tuvieron un buen poder de discriminación para la fragilidad con AUC de 0,84 y 0,79 respectivamente y fueron comparables con la fuerza muscular, AUC= 0,80 (IC 95% 0,73-0,88) y la velocidad de la marcha, AUC=0,74 (IC 95% 0,67-0,83). La sensibilidad para detectar fragilidad fue del 87% y 86% para el grosor muscular y el área del recto femoral respectivamente (con valores de corte de 1,72 cm para el grosor muscular y 6,72 cm2 para el área del recto femoral).

2. Los modelos de análisis de regresión logística demostraron que la tasa de predicción de fragilidad de los parámetros de la arquitectura muscular por sí solos osciló entre el 76,5 % y el 82,5 %, y cuando se ajustaron con las características físicas, los modelos clasificaron correctamente hasta el 91,9 % de los casos.

3. La combinación de parámetros de arquitectura muscular y parámetros bioquímicos ajustados con características físicas mostró buenos resultados y predijo fragilidad hasta en el 95% de los casos. Tanto la disminución del grosor muscular como del área del recto femoral aumentaron la

probabilidad de fragilidad en todos los modelos mostrados. Varios parámetros bioquímicos, citocinas y hormonas mostraron correlaciones significativas con el fenotipo de fragilidad y se utilizaron para el análisis de regresión.

4. El tamaño muscular tuvo correlaciones positivas tanto con la fuerza muscular como con la velocidad de la marcha, mientras que la calidad muscular se asoció con la fuerza muscular pero no con la velocidad de la marcha.

5. Varios analitos bioquímicos mostraron correlaciones con los parámetros ecográficos, así como con el fenotipo de fragilidad. Hubo correlaciones positivas entre el tamaño muscular y los niveles de hemoglobina. Los niveles altos de glucosa basal se correlacionaron con un bajo grosor y área del recto femoral, así como con el fenotipo de fragilidad. IGF-1 mostró una correlación positiva con el tamaño del músculo y una correlación negativa con el fenotipo de fragilidad.

Uno de los componentes clave de la fragilidad es la sarcopenia, una condición caracterizada por la pérdida de masa y función del músculo esquelético. La posibilidad de evaluar la masa muscular en atención primaria o al pie de la cama en un entorno hospitalario fue la idea principal detrás de este estudio. Las pautas actuales para el diagnóstico de sarcopenia del Grupo de trabajo europeo revisado sobre sarcopenia en personas mayores (EWGSOP2) recomiendan DXA y BIA para evaluar la masa muscular. Sin embargo, la disminución de la masa muscular y la fuerza no se produce al mismo ritmo. Goodpaster y colaboradores demostraron que en los ancianos que viven en la comunidad existe una mayor pérdida de fuerza muscular que de masa muscular.

Se cree que los cambios relacionados con la edad se deben a la arquitectura y composición muscular, y no solo al tamaño muscular, y pueden explicar la pérdida de fuerza muscular en esta población. DXA y BIA no pueden evaluar la composición muscular. La RM y la TC se consideran como pruebas de referencia. Sin embargo, estas técnicas no son prácticas para uso clínico debido a los precios elevados, la accesibilidad, la portabilidad y la radiación ionizante.

La ecografía puede superar estas limitaciones ya que puede evaluar no solo el tamaño sino también la composición muscular. Los cambios en la composición muscular se pueden observar como un aumento de la ecointensidad debido a la acumulación de tejido adiposo y fibroso intramuscular. Además, el cuádriceps femoral es un músculo penado, donde las fibras musculares se unen en ángulo a su tendón. Este ángulo se puede medir por ecografía y está disminuido en los músculos sarcopénicos.

Los parámetros que tienen un buen rendimiento técnico (precisión y exactitud) y clínico (sensibilidad y especificidad) son biomarcadores de imagen adecuados para uso clínico. Estos podrían tener una ventaja importante sobre la evaluación clásica del fenotipo de fragilidad que incluye parámetros subjetivos como la sensación de agotamiento. De hecho, se encontró que el efecto pronóstico independiente de cada criterio de fragilidad mostró diferencias importantes en la predicción de discapacidad crónica, hospitalización y muerte. Aquí es donde la ecografía muscular podría tener un mayor impacto clínico. Los parámetros ecográficos se pueden medir objetivamente en pacientes ambulatorios asintomáticos, así como en pacientes hospitalizados, y los valores se pueden comparar a lo largo del tiempo. De esta forma se puede evaluar cuantitativamente la presencia de fragilidad, la evolución en el tiempo o la efectividad de una potencial intervención terapéutica. La implementación de ecografía muscular podría facilitar las decisiones clínicas y el manejo de pacientes frágiles en la práctica diaria.

Mostramos que los parámetros ecográficos evaluados en nuestro estudio tenían un buen desempeño como biomarcadores de imagen. Primero, los valores medidos son similares a otros estudios y por lo tanto parecen ser válidos. A continuación, los parámetros mostraron una alta precisión con un error de medición relativamente bajo. Además, varios parámetros también mostraron una buena precisión en el entorno clínico y se comportaron igual o mejor que la fuerza muscular y la velocidad de la marcha.

El grosor muscular, el área y la ecointensidad tuvieron una alta precisión. Los ángulos penados mostraron una menor precisión con hasta un 21 % de imágenes excluidas (no cumplían con los criterios de calidad de imagen). Otros estudios informaron una alta precisión para las mediciones del grosor y el área muscular en adultos mayores con menor precisión para las mediciones de ecointensidad y ángulo penado. Encontramos los errores estándar de medición de 0,04 a 0,1 cm para espesores musculares, 0,3 cm^2 para el área, 1,5 a 1,9 A.U para ecointensidad y 0,9 a 1,6° para ángulos penados. Por lo tanto, estos parámetros son sensibles a cambios en el grosor y el área del músculo tan pequeños como 1 mm y 3 mm2 respectivamente.

Los ángulos penados en contracción fueron generalmente más altos que los ángulos en reposo y hubo diferencias significativas entre los grupos. Sin embargo, nótese que hubo mayores diferencias entre los ángulos en reposo y en contracción para el grupo control de individuos jóvenes mientras que para otros grupos esta diferencia fue mucho menor. Si consideramos que el error estándar de medición para el recto femoral fue de 0,9° y 1,1° en reposo y en contracción respectivamente, resulta obvio que cuanto menor es el ángulo, más difícil es medir cambios reales entre ángulos en reposo y en contracción. Además, este parámetro requería la

contracción voluntaria del cuádriceps y una parte importante de los pacientes no pudo mantener la contracción máxima durante el tiempo suficiente o presentó fasciculaciones que disminuyeron la calidad de la imagen. Consideramos que la utilidad de este parámetro es bastante limitada en pacientes frágiles.

Se encontraron correlaciones significativas entre la fuerza y el grosor muscular de todas las cabezas del cuádriceps, con la correlación más fuerte para el vasto medial. La ecointensidad mostró una correlación negativa con la fuerza muscular.

En cuanto a la velocidad de la marcha, hubo correlaciones con el tamaño muscular (correlación más fuerte con el área del recto femoral, sin embargo, no hubo correlaciones significativas con la ecointensidad de ninguna de las cabezas del cuádriceps.

Curiosamente, hubo pocas o ninguna correlación entre los parámetros ecográficos y los parámetros de actividad física obtenidos con el cuestionario. Estos parámetros demostraron ser poco fiables. Esto nuevamente cuestiona la importancia que se debe dar a todos los parámetros subjetivos al diagnosticar a una persona como 'frágil' o 'no frágil'.

Nuestro estudio confirma que los parámetros ecográficos que evalúan el cuádriceps femoral son útiles en la detección de pacientes frágiles, con valores de AUC para el área del recto femoral y grosor muscular. Además, mostramos correlaciones de múltiples parámetros ecográficos con el fenotipo de fragilidad. Los parámetros que denotaban sarcopenia - grosor muscular bajo, área baja y ángulos penados bajos, así como ecointensidad alta, se correlacionaron con la fragilidad. La correlación más fuerte se encontró para el área del recto femoral.

Se encontraron correlaciones débiles pero significativas entre los parámetros ecográficos y varias comorbilidades con la mayoría de los parámetros ecográficos (>10) correlacionados con osteoartritis, fracturas/osteoporosis, pérdida visual, hipertensión y obesidad, y menos parámetros (5-10) correlacionados con diabetes mellitus, neoplasia maligna previa, hiperlipidemia, EPOC, hipoacusia y depresión. Se cree que la sarcopenia y estas enfermedades comparten factores de riesgo comunes en las personas mayores: inactividad física, inflamación y desnutrición/obesidad; de hecho, se encontró que la sarcopenia es muy prevalente en pacientes con enfermedades cardiovasculares, demencia, diabetes mellitus y problemas respiratorios. Otros estudios relacionan la sarcopenia con un mayor riesgo de caídas. Encontramos una correlación inversa entre el área del recto femoral y el número de caídas en los últimos seis meses. Parece que la baja masa muscular, añadida al deterioro sensorial, pone a estos individuos en un mayor riesgo de caídas, lo que a su vez conduce a una actividad física limitada y

una disminución funcional y, en última instancia, aumenta el riesgo de institucionalización, morbilidad y mortalidad. Este fue el único resultado (outcome) que estudiamos.

El concepto de validación biológica de las características de imagen se está convirtiendo en una parte esencial de la traducción de los parámetros radiológicos a la práctica clínica. Seguimos esta idea con el objetivo de explorar el sustrato biológico de nuestros parámetros ecográficos.

Los niveles de creatinina se correlacionaron positivamente con el grosor del vasto medial. Los niveles de creatinina en suero son proporcionales a la masa muscular lo que explicaría este hallazgo. Sin embargo, no encontramos correlaciones significativas entre los niveles de creatinina y el grosor muscular de otras cabezas de cuádriceps ni con el fenotipo de fragilidad. Aparte de la masa muscular, existen varios factores que influyen en los niveles de creatinina (como la función renal y la ingesta) que podrían explicar la falta de esta correlación.

Aunque los niveles de albúmina por sí solos no mostraron ninguna correlación con la masa muscular ni con la fragilidad, los niveles de proteínas séricas mostraron una correlación positiva con el área del recto femoral y una correlación negativa con el fenotipo de fragilidad. Otros estudios informaron una asociación entre las concentraciones bajas de albúmina y la sarcopenia y encontraron que la albúmina baja puede aumentar el riesgo de desarrollar sarcopenia.

Encontramos que los niveles más altos de glucosa basal se correlacionaron con un bajo grosor muscular y un área baja del recto femoral. Además, la glucosa tuvo una correlación positiva con el fenotipo de fragilidad. Una revisión sistemática de 2020 informó que los pacientes con diabetes mellitus tipo 2 (DM2) tenían un mayor riesgo de sarcopenia. Varios estudios encontraron una correlación positiva entre la resistencia a la insulina y la fragilidad. Se propusieron varios mecanismos fisiopatológicos para explicar esta correlación. La insulina tiene efectos anabólicos sobre el músculo esquelético, regulando la síntesis de proteínas y el transporte de glucosa y mejorando el metabolismo muscular. Estas funciones se ven alteradas por la resistencia a la insulina presente en pacientes con DM2. La resistencia a la insulina disminuye la síntesis de proteínas y promueve la degradación de proteínas.

Los niveles de hemoglobina tuvieron una correlación positiva con el grosor muscular del vasto medial y una correlación negativa con la ecointensidad del recto femoral y el grosor de la grasa superficial. Un estudio del 2015 mostró una correlación entre la baja masa muscular medida con DXA y la anemia en hombres coreanos de edad avanzada. El estudio InCHIANTI también informó una asociación entre niveles bajos de hemoglobina con menor densidad muscular y masa muscular medida por TC. La razón de esta asociación podría ser la menor oxigenación del

músculo esquelético en la anemia. Además, como los pacientes anémicos pueden experimentar más fatiga, a menudo tienden a tener un estilo de vida más sedentario con menos actividad física y, por lo tanto, tienen menos masa muscular y una acumulación de grasa subcutánea, aunque no encontramos una relación directa entre la masa muscular y la actividad física autoinformada en nuestra población de estudio.

No hubo correlaciones significativas entre el volumen muscular y la tasa de filtración glomerular (TFG). Sin embargo, hubo correlaciones con los parámetros de la arquitectura muscular. Los ángulos penados del vasto externo en reposo y en así como el recto femoral en contracción mostraron correlaciones positivas con la TFG. Hubo una correlación negativa entre la TFG y el fenotipo de fragilidad. Un estudio coreano de 2020 informó la relación entre la obesidad sarcopénica y la disminución de la TFG en mujeres posmenopáusicas. La sarcopenia se encuentra con frecuencia en pacientes con enfermedad renal crónica y se debe al balance proteico negativo causado por múltiples factores que promueven el catabolismo proteico y disminuyen la síntesis de proteínas.

No encontramos correlaciones significativas entre la vitamina D y el volumen muscular ni con el fenotipo de fragilidad para nuestra población de estudio. Los niveles bajos de vitamina D están asociados con la osteoporosis y la sarcopenia entre los adultos mayores, lo que a su vez aumenta el riesgo de caídas. Esta asociación puede deberse a los efectos sobre el metabolismo de la célula muscular. Los resultados del estudio Newcastle 85+ informaron asociaciones entre niveles bajos de vitamina D y poca fuerza muscular en personas mayores. Otro estudio encontró una asociación entre los niveles bajos de vitamina D y la fragilidad incidente en una cohorte prospectiva de mujeres mayores; sin embargo, esta asociación dejó de ser significativa después de ajustar por enfermedades cardiometabólicas. En cuanto a nuestros resultados, creemos que diferentes poblaciones de estudio, la cantidad de exposición al sol y las variaciones estacionales en los niveles de vitamina D podrían haber contribuido a nuestros hallazgos. Además, no preguntamos sobre la ingesta de suplementos vitamínicos, lo que también podría haber interferido con los resultados.

Hubo una correlación positiva entre los niveles de IGF-1 y el volumen muscular, medido como el área del recto femoral y el grosor muscular del recto femoral. Estos hallazgos pueden explicarse por el papel que juega IGF-1 en la homeostasis muscular. Tiene un efecto anabólico sobre el tejido muscular, es decir, estimula la producción muscular y activa la hipertrofia celular, e inhibe la degradación de proteínas musculares. Por otro lado, la ecointensidad del recto femoral tuvo una correlación negativa con los niveles de IGF-1. La ecointensidad es una medida ecográfica de

la calidad muscular; los niveles más altos indican infiltración de grasa intramuscular y están asociados con la pérdida de masa muscular funcional, lo que podría explicar este hallazgo. Además, los niveles plasmáticos de IGF-1 fueron significativamente más bajos en el grupo frágil en comparación con los controles. Varios estudios relacionan los niveles bajos de IGF-1 con el rendimiento físico, la sarcopenia y la fragilidad. También encontramos una correlación negativa entre los niveles circulantes de IGF-1 y el fenotipo de fragilidad.

Con respecto a los marcadores inflamatorios, hubo correlaciones significativas de varias citoquinas con parámetros ecográficos, así como con fragilidad, pero la dirección de esas correlaciones fue generalmente opuesta a la de la literatura publicada. Es decir, encontramos correlaciones positivas entre el grosor del músculo vasto intermedio y lateral con los niveles circulantes de IL-6. No hubo correlaciones entre los parámetros ecográficos musculares y el TNF-α. En la literatura, las concentraciones más altas de IL-6 y TNF-α se asociaron con baja masa muscular y fuerza en personas mayores sanas. Por otro lado, los estudios también han mostrado concentraciones más altas de citoquinas proinflamatorias IL-6, TNF-α y CRP en pacientes frágiles. No encontramos esta correlación con el fenotipo de fragilidad en nuestro grupo de estudio. Estas moléculas de señalización también juegan un papel en otros procesos y esta puede ser la razón por la que no hemos encontrado resultados similares. En cuanto a las otras citoquinas proinflamatorias, la tendencia general fue similar.

La interpretación de estos hallazgos resulta ser compleja. La literatura publicada se centra principalmente en IL-6, TNF-α y CRP como marcadores de inflamación y concluye que la inflamación juega un papel importante en la patogénesis de la fragilidad. Cabe mencionar que además de ser una citoquina proinflamatoria, la IL-6 también se conoce como mioquina, ya que es producida por los miocitos durante el ejercicio y un aumento transitorio de sus niveles promueve la hipertrofia muscular. Contrariamente a esto, en el Framingham Heart Study, un aumento en los niveles de IL-6 predijo sarcopenia de dos años en mujeres mayores. Creemos que las características particulares de nuestra población de estudio, así como el pequeño tamaño de la muestra, podrían ser los principales contribuyentes para nuestros hallazgos. Por lo tanto, aunque varias citoquinas mostraron correlaciones con la masa muscular y el fenotipo de fragilidad, debido a la dirección de estas correlaciones, no confiamos en extraer conclusiones definitivas sobre su papel en la sarcopenia, ni recomendarlas como biomarcadores independientes para el diagnóstico de fragilidad.

Modelos de fragilidad.

En primer lugar, valoramos la influencia de la masa y calidad muscular evaluada por ecografía sobre la fragilidad en nuestra población de estudio. Para ello, exploramos combinaciones de parámetros ecográficos ajustados con parámetros funcionales y características físicas, mostrando el mejor modelo de análisis de regresión una tasa de predicción del 91,9%. El tamaño muscular (medido como grosor y área), así como la fuerza muscular, tuvieron la mayor influencia en la fragilidad dentro de este modelo, mientras que los parámetros de la arquitectura muscular tuvieron una contribución menor en el diagnóstico de la fragilidad. Este hallazgo es interesante ya que se cree que los cambios en la arquitectura muscular ocurren antes que la pérdida de volumen muscular en la evolución de la sarcopenia, y siguiendo esta idea, se esperaba que los ángulos penados y la ecointensidad mostraran una mayor influencia en la fragilidad dentro de los modelos. Creemos que la técnica y la adquisición de parámetros ecográficos podrían ser parcialmente responsables de esto. El grosor y el área muscular parecen ser parámetros más robustos con menor error de medición, al menos para el cuádriceps femoral. Sería interesante explorar la contribución de otros grupos musculares (la pierna o cara posterior del muslo) utilizando el mismo protocolo ecográfico para confirmar este hallazgo. Otro hallazgo curioso es que los modelos de fragilidad no dependían de la velocidad de la marcha sino de la masa y la fuerza muscular. Otros estudios encontraron que la marcha lenta era un fuerte predictor de discapacidad y caídas. En proyectos futuros, se podrían valorar otros parámetros funcionales (Timed up and go, Short Physical Performance Battery, etc.) y compararlos con los parámetros ecográficos.

Aunque muchos pacientes frágiles presentan sarcopenia, el síndrome de fragilidad debe entenderse como una entidad multidimensional que implica disfunción musculoesquelética combinada con senescencia endocrina e inflamación crónica que vuelve a la persona vulnerable a factores estresantes externos. Por lo tanto, consideramos que no existe un parámetro 'mejor' que lo describa, más bien, podría haber varias combinaciones de parámetros que pueden identificar a pacientes frágiles e individuos en riesgo de desarrollar fragilidad. Exploramos las asociaciones de los parámetros sanguíneos con la masa muscular y la fragilidad y utilizamos el concepto de combinaciones de parámetros bioquímicos para desarrollar modelos integrados. Estos modelos tienen en cuenta la presencia de baja masa muscular medida por el grosor muscular o área del recto femoral (mejores parámetros ecográficos), el bajo rendimiento físico medido por la fuerza muscular y la velocidad de la marcha, así como el desequilibrio de varios factores bioquímicos, hormonas y citoquinas inflamatorias.

Varios modelos mostraron índices de predicción >90 %, lo que demuestra que, incluso con un número limitado de parámetros, se pueden construir modelos precisos y eficientes para diagnosticar la fragilidad. En todos los modelos, el aumento de la masa muscular (grosor muscular y área del recto femoral) disminuyó las probabilidades de fragilidad de 2,5 a más de 300 veces. Este hallazgo respalda la idea de que la actividad física es un componente importante en la prevención de la fragilidad. Otros estudios han demostrado un aumento del área muscular medida por TC después de una intervención de ejercicio en pacientes frágiles, así como un aumento de la fuerza muscular. Además, todos los modelos que incluyeron el sexo como variable mostraron que las mujeres tenían mayores probabilidades de fragilidad, lo que también se informa en otros estudios. Este es un hallazgo esperado, ya que las mujeres en promedio tienen menos masa muscular que los hombres a cualquier edad, por lo tanto, la sarcopenia las pone en mayor riesgo de cruzar el umbral de masa muscular crítica necesaria para la movilidad y la vida independiente. Esto, junto con una mayor longevidad en comparación con los hombres, explica por qué es más probable que las mujeres necesiten institucionalización en sus últimos años de vida.

Buscamos modelos que usaran parámetros bioquímicos generales preferiblemente sobre citocinas, ya que creemos que es más probable que se acepten para un uso clínico generalizado. El modelo que utiliza el grosor muscular del recto femoral en combinación con los niveles basales de glucosa y las proteínas séricas podría ser un candidato aceptable para uso clínico.

Hasta donde sabemos, este es el primer estudio que vincula diferentes parámetros de imagen, bioquímicos y físicos para obtener herramientas cuantitativas que podrían usarse para la detección y, potencialmente, para el seguimiento de pacientes con síndrome de fragilidad. Sin embargo, se necesitan estudios longitudinales en una población más amplia para validar la eficacia de estos modelos en la predicción de resultados adversos como hospitalización, discapacidad y mortalidad.

Habiendo explorado todas las cabezas del cuádriceps, consideramos que el recto femoral podría ser el mejor candidato para evaluar la sarcopenia en el contexto del síndrome de fragilidad.

CONCLUSIONES

En base a los resultados obtenidos, hemos llegado a las siguientes conclusiones:

1. La ecografía muscular es útil para evaluar el tamaño y la arquitectura muscular en el contexto del síndrome de fragilidad, con varios parámetros que muestran una alta precisión y exactitud con un bajo margen de error.

2. Entre todas las cabezas del músculo cuádriceps, el recto femoral es el mejor sitio para la evaluación ecográfica de la sarcopenia.

3. El área y el grosor del recto femoral tienen un buen poder de discriminación para la fragilidad y son comparables con parámetros funcionales como la fuerza muscular y la velocidad de la marcha.

4. La ecografía muscular es factible en la práctica clínica diaria, ya que supone la medición de solo uno o dos parámetros, lo que requiere tiempo y entrenamiento mínimo.

5. Los parámetros de ultrasonido muscular no tienen asociación con los parámetros de actividad física autoinformados

6. Los parámetros de imagen por ecografía muestran correlaciones con varios parámetros bioquímicos que se alteran en pacientes frágiles, como la creatinina, las proteínas séricas, la glucosa, la hemoglobina, la tasa de filtración glomerular y el IGF-1.

7. Los modelos de fragilidad que combinan ecografía muscular y parámetros bioquímicos tienen un buen rendimiento diagnóstico en la identificación de individuos en riesgo de fragilidad con hasta un 95% de precisión. La disminución del tamaño muscular aumenta las probabilidades de fragilidad en todos los modelos

8. El modelo de fragilidad que aplica el grosor muscular del recto femoral, los niveles basales de glucosa y las proteínas séricas podría usarse en la práctica clínica debido a la simplicidad de la medición ecográfica y la disponibilidad de parámetros bioquímicos de una analítica rutinaria

INTRODUCTION

1.1 Ageing.

Ageing is a normal physiological process that consists of increased catabolism with the degeneration of organs and their function. Successful ageing means the ability to live independently, move without the support of others and preserve intellectual capacity for daily living (Sieber et al, 2017).

The number of old people is rising around the world, both in developed and developing regions (UN Dept. of Economic and Social Affairs, World population prospects, 2022). According to the World Health Organisation, in 2020 the world's population of people aged 60 and older was one billion and by 2050 this number will double (2.1 billion). This shift in the demographic profile is due to a steady increase in life expectancy over the last fifty years (figure 1.1).

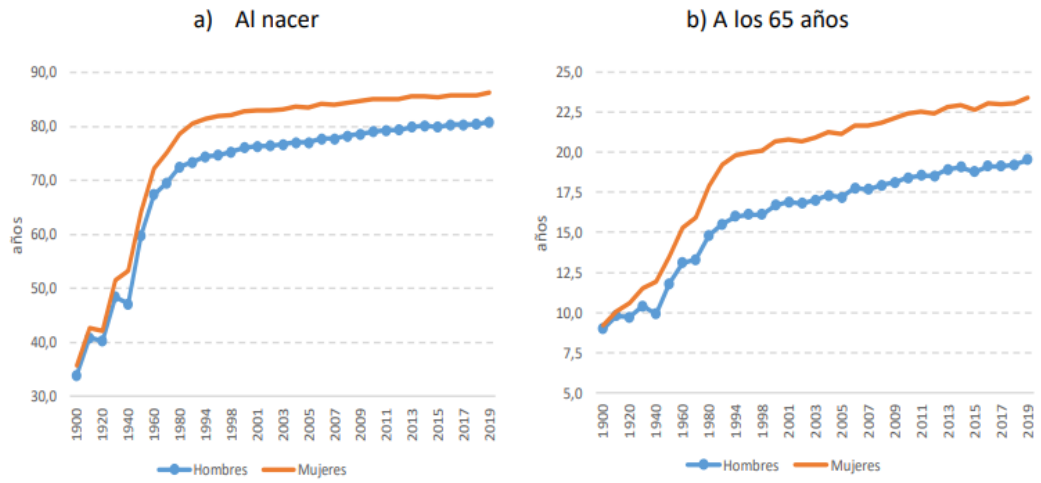

Figure 1.1 Life expectancy in Spain (1900-2019), a) at birth and b) at 65 years. Source: Fedea 2021, (https://documentos.fedea.net/pubs/eee/eee2021-07.pdf)

However, there is little evidence that this increased longevity is paired with an extended period of good health (Beard et al, 2016). In fact, there is an increase in comorbidities and disabilities associated with old age, which raises demands for long-term assistance and support (Congressional Budget Office, 2013) and increases the overall costs of health care. Modern healthcare systems are faced with the challenge to provide diagnosis and adequate management for this rising number of old people in order to improve their quality of life and

extend the disability-free period during old age. In this regard, frailty syndrome has special importance.

1.2 Frailty.

Frailty is defined as a clinical syndrome of increased vulnerability to outside stressors which can lead to adverse health outcomes and death (Morley et al, 2013). This syndrome is characterized by an accelerated decline in functional reserves, where patients are susceptible to seemingly minor events (for example an infection or new medication) which can result in serious worsening of health with extended periods of recovery and repercussions on the overall level of function. The adverse outcomes associated with frailty include falls, disability, hospitalisation, and mortality (Fried et al, 2001). The estimated prevalence of frail individuals older than 65 years in European countries ranges from 5.8% to 27.3% (Santos-Eggimann et al, 2009).

It is important to note that frailty is not a definitive state but rather a spectrum, where individuals may present a pre-frail phase where they function well but are at higher risk of developing severe frailty. Likewise, it was demonstrated that frailty can be partly reversible with adequate intervention programs (Cameron et al, 2013, Ng et al, 2015). Therefore, it is important to diagnose frail and non-disabled individuals and treat them to prevent dependency (Morley et al, 2013).

- Frailty phenotype

Initial efforts towards recognising frailty as an independent clinical entity were performed by Fried and colleagues (2001), who suggested that frailty is related to but different from disability and comorbidity. They developed a ´frailty phenotype´ evaluation for identifying frailty in community-dwelling older adults which includes assessment of five criteria: unintentional weight loss, feeling of exhaustion, weakness, slow walking speed, and low physical activity. Individuals presenting three or more criteria are diagnosed as frail, and people presenting one or two criteria are considered at risk of frailty.

Table 1.1 Frailty criteria by Fried and colleagues	
Weight loss	>4.5 kg/year
Exaustion	Self reported
Weakness	Grip strength (lowest 20%)
Slowness	Walking time/4.6 m (slowest 20%)
Low physical activity	Kcal/week (lowest 20%)
Diagnosis of frailty	3 or more criteria met
Diagnosis of pre-frailty	1 or 2 criteria met

Table 1.1 Frailty criteria developed by Fried et al. (2001)

The most common positive criteria were found to be weakness (54%) and slow gait speed (43%) (Rothman et al, 2008). Both these parameters are associated with accelerated muscle decline in old age.

1.3 Sarcopenia.

Sarcopenia is a term that refers to muscle wasting, and it is defined as age-related loss of skeletal muscle mass and strength which increases the risk of disability, poor quality of life, dependency, and death (Cruz-Jentoft et al, 2010). The updated European consensus on the definition of sarcopenia from 2019 (Cruz-Jentoft et al, 2019) proposes the use of the SARC-F questionnaire and low muscle strength as parameters for identifying sarcopenia, following the diagnostic confirmation by the existence of low muscle quantity or quality and use of physical performance tests for quantifying the severity of sarcopenia. The proposed cut-off points for diagnosis of sarcopenia are appendicular muscle mass (ASM, kg) per height (m^2) <7 kg/m^2 for men and <5.5 kg/m^2 for women; grip strength of <27 kg for men and <16 kg for women and gait speed ≤0.8 m/s (Cruz-Jentoft et al 2019).

The skeletal muscle is involved in locomotion and is the second largest store of energy in our body. It enables standing up from the chair, reaching for objects, preparing food, and performing personal hygiene. These simple tasks are those that ensure independence for daily living and when a frail person experiences a stressor event, the ability to perform these tasks is reduced. Additionally, during these events body mobilizes muscle proteins that are used for energy, synthesis of acute phase proteins, and the immune response (Attaix et al, 2005). This

leads to muscle wasting and further depletion of protein depots which impairs the aging organism to recover from stress, and ultimately increases the risk of immobility and falls.

Muscle homeostasis is regulated by the neuroendocrine and immune systems and the overall muscle mass depends on the balance between protein synthesis and breakdown. This balance is also affected by physical activity and nutritional status. Muscle wasting is a multi-factorial process that results from decreased protein synthesis, increased proteolysis, or both processes (Attaix et al, 2005). In sarcopenia, there is atrophy of type 2 muscle fibers, a decrease in the number of motor units as well as a decline in the number of α-motoneurons (Muscaritoli et al, 2010). Multiple endogenous and exogenous factors are believed to contribute to its development (figure 1.2).

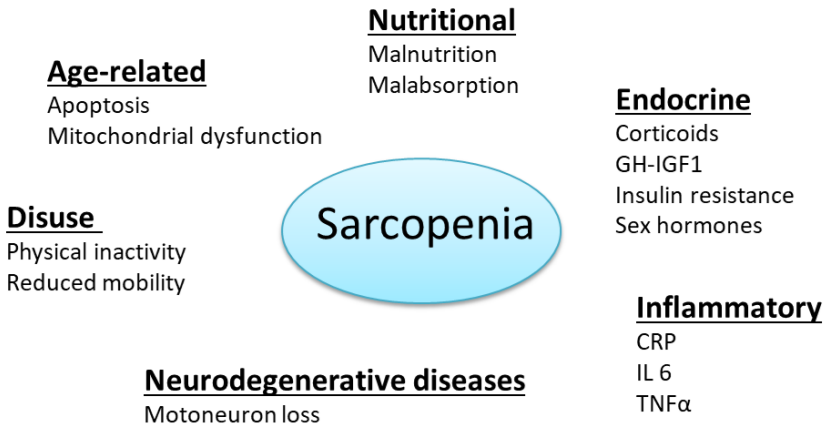

Figure 1.2 Factors potentially leading to sarcopenia.

1.3.1 The role of muscle architecture in sarcopenia

The definition of sarcopenia includes both muscle mass and strength since the relationship between them is not linear. There seems to be a faster decline in muscle strength than muscle mass in the community-dwelling old population (Goodpaster et al, 2006). Additionally, there are regional differences in the rate of muscle decline, with the loss of muscle mass in lower limbs more than twice the rate of loss in upper limbs (Janssen et al, 2000). This may be due to decreased use (less walking) as well as greater loss of motor units in the legs than in the arms (Narici and Maffulli, 2010).

This disparity between muscle mass and strength can be attributed to muscle architecture changes and not only a reduction in muscle volume (Narici and Maffulli, 2010). Muscle

architecture refers to the spatial arrangement of the muscle fibres and it determines its force and excursion capability (Mitchell et al, 2012). Most locomotor muscles are pennate muscles, where fibres are oriented at an angle to the tendon. This is an evolutionary adaptation for muscles that require the generation of large forces since it allows the packing of as much contractile tissue as possible along the tendon aponeuroses (figure 1.3). Muscle architecture is responsible for the force-generating potential. Muscle force depends on the number of sarcomeres in parallel, i.e., on muscle cross-sectional area, while shortening capability (velocity) depends on the number of sarcomeres in series, i.e., on fibre length. Due to the architecture of pennate muscles, anatomical cross-sectional area (ACSA) underrepresents the true muscle volume; therefore, the physiological cross-sectional area (PCSA) is calculated taking into account fibre angles. For fusiform muscles, due to the parallel orientation of the fibres (and angles at 0°), ACSA and PCSA are the same. Fusiform muscles have higher contractile velocity while pennate muscles produce higher force for the same muscle length.

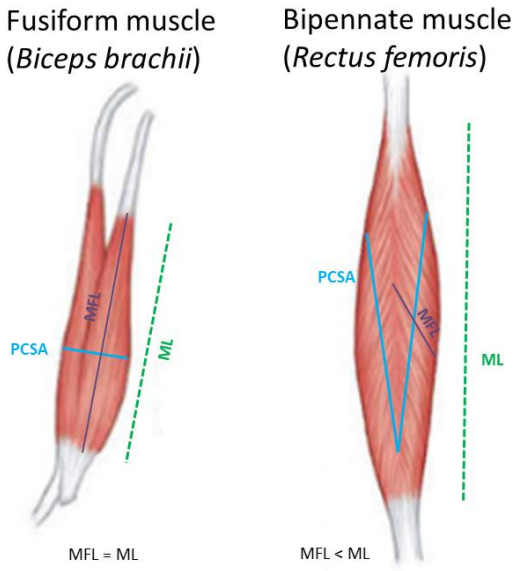

Figure 1.3 Illustrations of fusiform and pennate muscles. In fusiform muscles, muscle fibres run parallel to the muscle´s force-generating axis. In pennate muscles, muscle fibres run at a fixed angle relative to the force-generating axis. PCSA-physiological cross-sectional area, MFL-muscle fascicle length, ML-muscle length

Muscle architecture is dynamic and can change with training or immobility. Changes in muscle architecture with ageing include a decrease in pennate angles and cross-sectional area as a reflection of a loss of sarcomeres in parallel and consequent loss of muscle force-generating potential (Narici and Maffulli, 2010).

This loss of muscle tissue is frequently accompanied by intramuscular fat infiltration, known as myosteatosis (Taaffe et al, 2009). There is an association between greater fat infiltration assessed by computed tomography and lower muscle strength (Goodpaster et al, 2001). Moreover, it was found that greater fat infiltration was a predictor of mobility limitations (Visser et al, 2005). Sarcopenic obesity is a condition where age-dependent muscle loss and obesity appear together. It was shown that functional impairment is higher in sarcopenic obesity than in either sarcopenia or obesity alone (Rolland et al, 2009).

1.3.2. Sarcopenia and frailty phenotype – are they the same?

The relationship between frailty and sarcopenia is not yet fully defined. Indeed, frailty phenotype (Fried et al, 2001) and sarcopenia show overlap in diagnostic criteria (grip strength, gait speed) as well as treatment options (protein intake, supplementation of vitamin D, physical exercise) (Cruz-Jentoft et al, 2019). Additionally, both frailty and sarcopenia share clinical outcomes and some authors consider sarcopenia as a physical manifestation of frailty (Cesari et al, 2014, Landi et al, 2015). This makes sense since muscle decline is at the root of many of the negative health outcomes of frailty; in fact, physical function impairment is a common factor in both conditions (Cesari et al, 2014). Some authors propose the recognition of physical frailty and sarcopenia as a distinct entity (Cesari et al, 2017). Nevertheless, other authors consider that frailty syndrome is a much broader concept that includes a decline in multiple physiological systems that result in consequences not only on physical but on cognitive and social levels as well (Cruz-Jentoft et al, 2019). We are inclined to agree with the latter opinion – although sarcopenia is an important component of frailty syndrome; we consider these entities as different from each other.

1.4 Pathophysiology of frailty.

An understanding of the underlying processes that lead to frailty is needed for identifying possible biomarkers for its diagnosis and eventually, for developing treatment options. The pathophysiology of frailty is complex and multifactorial, it is hypothesized that molecular pathways governed by cellular senescence with DNA damage, oxidative stress, and mitochondrial decline lead to neuroendocrine dysregulation and chronic inflammation (Walston et al, 2006). These endocrine and inflammatory factors affect muscle metabolism and contribute

to the development of sarcopenia, as well as a decline in immune and cognitive functions and energy metabolism.

- Hormone dysregulation

  Multiple hormonal dysregulations are evident in the ageing process. Hypothalamic-pituitary axis is the main regulator of the ageing process and frailty. Deficits in the regulation of glucocorticoid secretion, insulin-like growth factor (IGF) signalling, and androgen production have been associated with ageing and frailty. The effects of these hormonal changes on frailty may be due to muscle decline, appetite changes, or activation of inflammatory pathways (Walston et al, 2006). Additionally, vitamin D and insulin resistance might also play role in the pathogenesis of frailty (Clegg and Hassan-Smith, 2018).

- Chronic low-grade inflammation

  Chronic inflammation seems to be connected both with frailty and sarcopenia. Immunosenescence denotes immune dysregulation that accompanies ageing and is characterised by an increase of pro-inflammatory cytokines and a reduction of anti-inflammatory cytokines which results in chronic low-grade inflammation (Michaud et al, 2013). This is different from acute inflammation which is beneficial to the host since it helps in pathogen removal and tissue repair (Furman et al, 2019). Chronic inflammation in old people is thought to be caused by cellular senescence and the development of senescence-associated secretory phenotype (SASP), where cells secrete pro-inflammatory cytokines, chemokines, and other pro-inflammatory molecules (Zhu et al, 2014). These factors can promote frailty through the effect on the musculoskeletal and endocrine systems, anaemia, cardiovascular diseases, and nutritional dysregulation. Elevated inflammatory mediators have inverse associations with haemoglobin concentration, IGF-1, and albumin levels as well as levels of micronutrients and vitamins (Chen et al, 2014).

  This pro-inflammatory state is characterized by the increase in pro-inflammatory cytokines such as interleukin-6 (IL-6), IL-1β and tumour necrosis factor-α (TNF-α) as well as C-reactive protein (CRP) and a decrease in anti-inflammatory cytokines such as IL-10 (Wilson et al, 2017). Interleukin-6 is involved in various somatic functions and has been identified as a regulating factor of the SASP (Zhu et al, 2014). Various studies report that

increased IL-6 levels correlate with frailty (table 1.2). TNF-α is another cytokine that is responsible for multiple pathways in the body and its increased expression is also associated with SASP (Kim et al, 2018). Studies show both positive and negative correlations with frailty (table 1.2). The list of most investigated cytokines in the frailty context is presented in table 1.2.

Cytokine	Primary activity	Correlation with frailty	Study
IL-6	acute phase response, B cell proliferation, synergistic with IL-1 and TNF	proportional	McKechnie et al, 2021; Hsu et al, 2019; Nascimento et al, 2018; Collerton et al, 2012; Buigues et al, 2020; Furtado et al, 2020 (in saliva); Liu et al, 2016, Tembo et al, 2021; Hubbard et al, 2008; Leng et al, 2009; Lai et al, 2014; Barzilay et al, 2007
		inversely proportional	no published data
		no correlation	Hammami et al, 2020, Alberro et al, 2021; Baylis et al, 2013
TNF-α	pro-inflammatory response, cytotoxic activity	proportional	Hammami et al, 2020; Nascimento et al, 2018; Collerton et al, 2012, Furtado et al, 2020
		inversely proportional	Marzetti et al, 2019 (in men)
		no correlation	Hsu et al, 2019; Buigues et al, 2020; Alberro et al, 2021; Lai et al, 2014
IL-8	pro-inflammatory, chemoattractant for neutrophils and T cells	proportional	Hsu et al, 2019; Hammami et al, 2020; Buigues et al, 2020
		inversely proportional	Marzetti et al, 2019
IL-1β	acute phase response, inflammation and fever	proportional	Furtado et al, 2020 (in saliva)
		no correlation	Hsu et al, 2019; Nascimento et al, 2018; Buigues et al, 2020; Baylis et al, 2013
IFN-γ	promotes cell mediated immunity, antiviral effects	proportional	Mohamad et al, 2018
		inversely proportional	Marzetti et al, 2019 (in men)
		no correlation	Furtado et al, 2020
IL-10	antibody production, supresses cellular immunity, inhibits the synthesis of IFN-γ and TNF-α	proportional	Furtado et al, 2020
		no correlation	Hsu et al, 2019; Nascimento et al, 2018; Baylis et al, 2013; Su et al, 2017
IL-17	pro-inflammatory activities similar to IL-1 and TNF-α, autoimmunity	inversely proportional	Marzetti et al, 2019 (men)
		no correlation	Hsu et al, 2019
IL-12p70	promotes cell mediated immune functions, IFN production	inversely proportional	Compté et al, 2013
IL-4	anti-inflammatory, inhibition of monokine production, B cell proliferation	no correlation	Hsu et al, 2019
IL-7	T and B lymphopoiesis	no correlation	Hsu et al, 2019
IL-13	IL-4 like activities	no correlation	Hsu et al, 2019

Abbreviations: IL-interleukin, TNF-tumor necrosis factor, IFN-interferon

Table 1.2 circulating cytokines and their relationship with frailty according to published literature

1.5 Biomarkers of frailty.

The clinical diagnosis of frailty relies on Fried´s operational definition based on five criteria (table 1.1) and it is the most commonly used method for identifying prefrail and frail individuals in the clinical setting (Buta et al, 2015). Although it is an extensively validated and useful tool up to date, it has some limitations in clinical practice. For example, it has a limited ability to predict

progression from a robust or prefrail to a frail state (Saedi et al, 2019). Additionally, some of the frailty criteria are self-reported and can hinder the assessment in various clinical scenarios (for example, in patients with cognitive impairment or depression). The overview of different frailty assessment tools is available in table 1.3.

Frailty assessment tool	Type of assessment	Components	Classification
Fried Frailty Phenotype	Mixed	5 criteria (handgrip strength, gait speed, unintetional weigth loss, exaustion and physical acivity level)	0: robust; 1-2: prefrail; ≥3: frail
FRAIL scale	Subjective	5 criteria (fatigue, resistance, ambulation, illnesses, weight loss)	0: robust; 1-2: prefrail; ≥3: frail
Edmonton Frail Scale	Mixed	9 domains (cognition, general health state, functional independence, emotional support, medication use, nutrition, mood, continence, and functional performance)	0–4: no frailty, 5–6: apparently vulnerable, 7–8: mild frailty, 9–10: moderate frailty, >11: severe frailty
Rockwood Frailty Index	Subjective	36 items (selected from the ICPC-coded, includes symptoms, diseases, functional impairments and social problems).	ratio between deficits present within the total of 36 deficits. (Cut-off 0,08); >0,08 Frail, <0.08 robust
Comprehensive geriatric assessment	Mixed	Global functionality, functional systems 'cognition, mood, mobility, and communication', major physiological systems, medication use, past history and contextual factors 'socio-family, environmental and caregiver assessment'	classifies the subject in one of the 10 clinical-functional strata ≥4: frail
Cumulative deficit approach (Puts model)	Mixed	Body weight, peak expiratory flow, cognition, presence of a vision problem a hearing problem or urinary incontinence—low mastery, depressive symptoms, and comorbidity	0: robust; 1-2: prefrail; ≥3: frail

Table 1.3 Overview of selected tools for assessing frailty. Adapted from Andrade et al., 2021

It is worth noting that frailty is often accompanied by various comorbidities that contribute to increased mortality. In fact, in some individuals, the development of frailty may be determined by multimorbidity rather than ageing itself. This contributes further to the phenotypic heterogeneity of this syndrome and hinders the development of clinical interventions for its treatment.

Therefore, there is great interest in developing objectively measured biomarkers for the identification of individuals at risk of frailty. This has proven to be a challenging task, largely due to multisystem involvement, complex pathophysiology, and overlap with different comorbidities.

There is a wide array of potential biomarkers being investigated:

1.5.1. Circulating markers

- Serum markers (haemoglobin, albumin, creatinine, glomerular filtration rate) and hormonal changes (DHEA, testosterone, vitamin D, IGF-1). These markers are generally associated with age-related decline and were studied in a frailty context. For example, various studies report correlations between lower haemoglobin levels and frailty in old people (Steinmeyer et al, 2020, Pires Corona et al, 2015, Lee et al, 2021). Furthermore, low albumin levels are an independent risk factor for frailty in type 2 diabetes mellitus patients (Yanagita et al, 2020). Likewise, low vitamin D levels are associated with an increased risk of frailty (Ju et al, 2018), and low levels of IGF-1 are associated with sarcopenia and frailty (Payette et al 2003, Doi et al 2018).

- Inflammatory markers – most studies have investigated CRP, IL-6, and TNF-α reporting positive and negative associations (summarized in table 1.2), however, there is interest in including more cytokines in biomarker panels (Cardoso et al, 2018).

- Products of oxidative damage - protein carbonyls were reported to be a predictor of walking disability (Semba et al, 2007).

However, these circulating markers can assess only individual features of the syndrome. Additionally, most of these biomarkers are weak predictors of disease progression (from prefrail to frail) or do not show an association with the outcomes (Saedi et al, 2019).

It is becoming clear that the search for a single best biomarker may not be an appropriate strategy and instead, a multidimensional approach could render better tools for detecting subclinical cases, diagnosing clinically manifested frailty, monitoring the evolution and response to eventual therapeutic interventions (Calvani et al, 2015). Recent studies are moving in this direction and investigating the multi-marker approach using blood-based biomarkers (Cardoso et al, 2018, Wennberg et al, 2021) or blood and muscle mass (measured by Dual-energy X-ray absorptiometry) parameters (Calvani et al 2021).

1.5.2. The current method for assessing sarcopenia

European Working Group on Sarcopenia (Cruz-Jentoft et al, 2019) proposes the use of the following techniques for assessing sarcopenia:

- **Muscle strength** – measured by a hand-held dynamometer. There is a moderate correlation between grip strength and strength in other muscle groups so a hand dynamometer can be used instead of more complex techniques for reliable assessment of muscle strength in clinical practice.
- **Muscle mass** – Dual-energy X-ray absorptiometry (DXA) is the standard method of assessing muscle mass; it can provide total body lean mass as well as appendicular muscle mass measurements. Bioelectrical impedance (BIA) is another method of estimating skeletal muscle mass based on whole-body electrical conductivity. The equipment is portable and affordable but lacks standardisation for different populations. Both methods can be influenced by hydration status.
- **Physical performance** – measured by gait speed, the Short Physical Performance Battery (SPPB), and Timed-Up and Go test (TUG). Gait speed is recommended for clinical practice as a quick and reliable method of assessing sarcopenia.

1.5.3. Imaging markers

Low muscle strength is predictive of immobilisation, physical disability, and increased mortality (Newman et al, 2006). However, active muscle strength and performance testing in elderly patients in clinical practice is often limited by several factors, for example, immobilisation of the patient, pain, acute illness, surgical interventions, or cognitive impairments. This prompted interest in the evaluation of quantifiable features from medical images and the development of imaging biomarkers that correlate with muscle strength. **Quantitative imaging biomarker (QIB)** is an objectively measured characteristic derived from in vivo images as an indicator of normal biological processes, pathogenic processes, or response to a therapeutic intervention (Sullivan et al, 2015). In other words, a biomarker should be able to diagnose, and track changes over time and help the clinical and therapeutic decision-making process (Cesari et al, 2012).

Several criteria need to be met to consider a QIB candidate for clinical use. On one hand, QIBs need to show good technical performance - good precision with a low margin of error as well as concordance with the reference value. Table 1.4 summarises these concepts. On the other hand, clinical validation should be determined – clinical usefulness (benefit to a subject in terms of outcomes) and clinical performance (sensitivity and specificity) (Sullivan et al, 2015).

Table 1.4 Technical and clinical performance of quantitative imaging biomarkers	
Precision	The closeness of agreement between measured quantity values obtained by means of replicate measurements of the same or similar experimetal units with specified conditions. Repeatability and reproducibility are types of precision
Bias	An estimate of a systematic measurement error. Bias is the difference between the mean of measurements of an object and its true value. For in vivo imaging estimation of bias is not possible. Therefore the assessment of bias is made by selecting patients to represent the whole spectrum of clinical characteristics (such as age) and by performing two or more replicats for each of measurand levels (as measured according to a reference method)
Reference value	The mean of replicates from reference method. Reference method is a methodology that has exact and clear description of the necessary conditions and procedures that provide accurate and precise laboratory data for it to be used to assess the validity of other laboratory methods.

Adapted from Metrology standards for Quantitative imaging biomarkers, Sullivan et al, 2015, doi: 10.1148/radiol.2015142202.

Table 1.4 Technical and clinical performance of quantitative imaging biomarkers

1.6 Imaging of sarcopenia – the role of ultrasound.

The earliest notions of muscle architecture and arrangement come from cadaveric studies. The obvious shortcoming of these studies is the inability to correlate anatomy with functional properties and muscle strength. Advancement in imaging techniques has allowed this assessment in vivo. MRI and CT are considered ´gold standard´ imaging techniques for muscle assessment, however, due to elevated cost, lack of availability and portability as well as ionising radiation (CT) use in primary care is limited.

MRI as well as ultrasound can measure both muscle volume and its architectural properties. There is high concordance between ultrasound and MRI for assessing muscle mass in healthy individuals (Worsley et al, 2014) (figure 1.4). MRI has a larger field of view but ultrasound can scan muscle in real-time and record dynamic changes during contraction (Franchi et al, 2018).

B-Mode ultrasound analyses echo waves that penetrate the body and reflect from structures with different acoustic impedance (lowest for air and highest for bone). The reflection coefficient depends on the acoustic impedances at the interface between two tissues and the angle at which an echo wave hits the structure of interest (Franchi et al, 2018). Skeletal muscle is hypoechoic (dark) on ultrasound due to high water content. The perimysial connective tissue appears brighter (hyperechoic) and gives muscles a characteristic dotted appearance in the

transverse plane (also referred to as starry sky appearance). Figure 1.4 shows MRI and ultrasound images of the thigh, *rectus femoris*, and *vastus intermedius* are seen as dark dotted areas on ultrasound. On the longitudinal plane, this perimysial connective tissue corresponds to white lines that are oriented at an angle to the muscle aponeurosis and give it a striated appearance (figure 1.5). This allows direct assessment of architecture by measuring muscle fascicles and the angle of insertion onto the aponeurosis (pennate angle). This architecture can be assessed at rest and during dynamic contraction, where muscle area and pennate angles increase (figure 1.6). Additionally, the presence of intramuscular fat infiltration is seen as hyperechoic or brighter than normal muscle (figure 1.7)

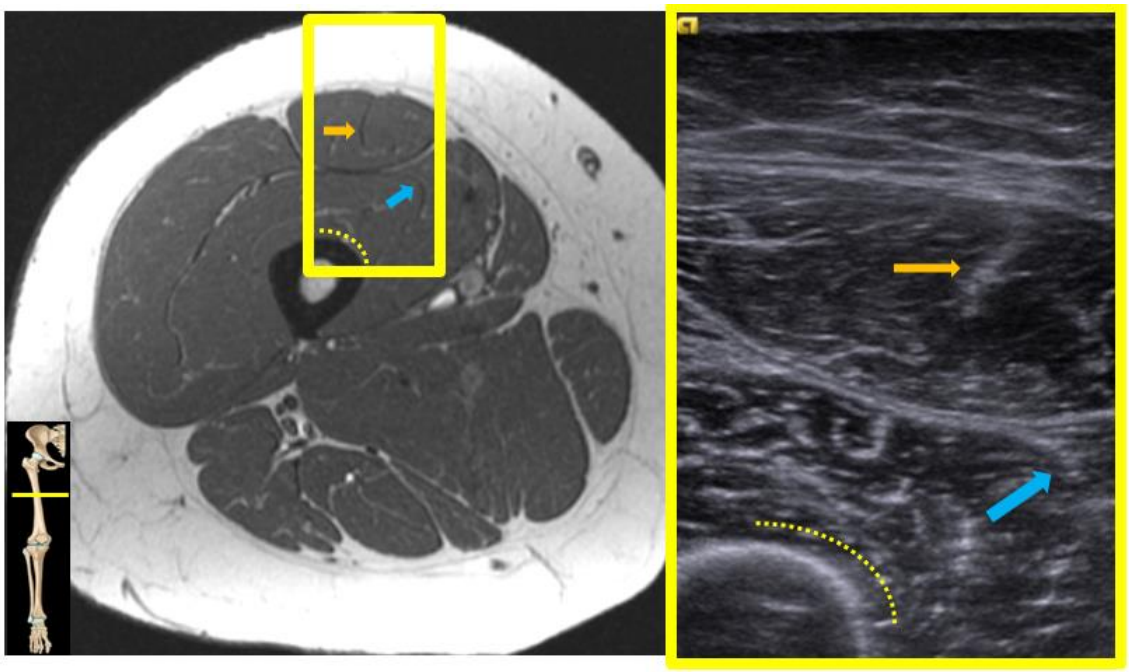

Figure 1.4 On the left, axial T1-weighted MRI image of the right mid-thigh and on the right, an ultrasound image of a section of anterior thigh (bordered in yellow), centred over rectus femoris and vastus intermedius muscles, shows comparability between the two imaging techniques. Arrows and dotted lines indicate the same anatomical features (orange arrow-central tendón of rectus femoris, blue arrow aponeurosis of vastus intermedius, dotted line-femur)

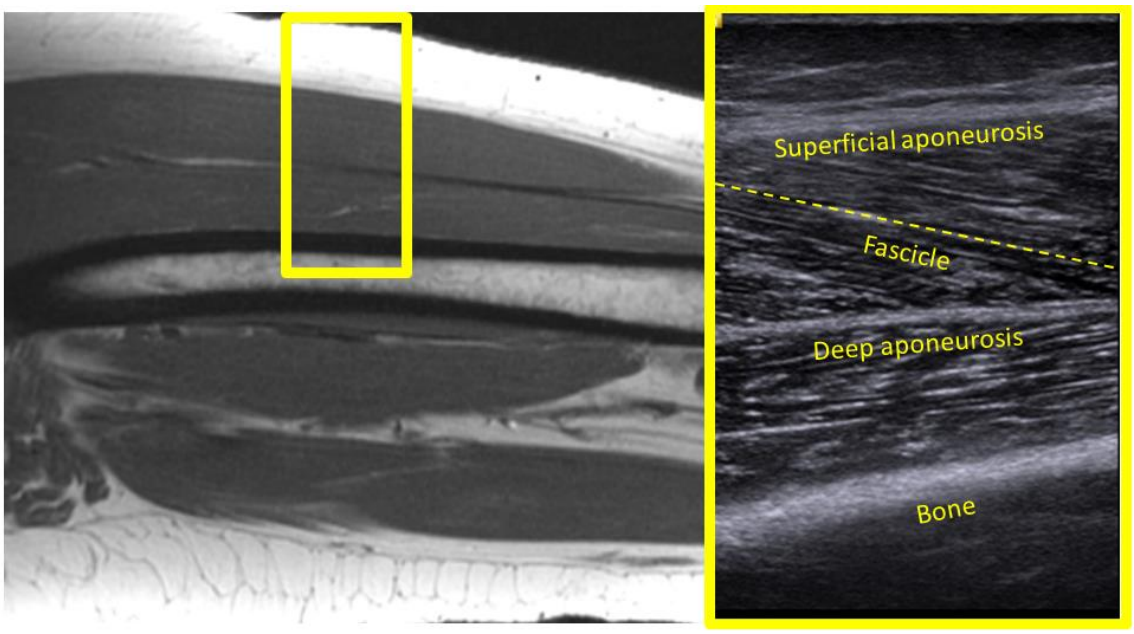

Figure 1.5 On the left, sagittal T1-weighted MRI image of the right mid-thigh. On the right, the ultrasound image shows the section (bordered in yellow) of the rectus femoris and vastus intermedius muscles in the longitudinal plane. Note pennate architecture is clearly visible in ultrasound with fascicles attaching at an angle to the aponeurosis

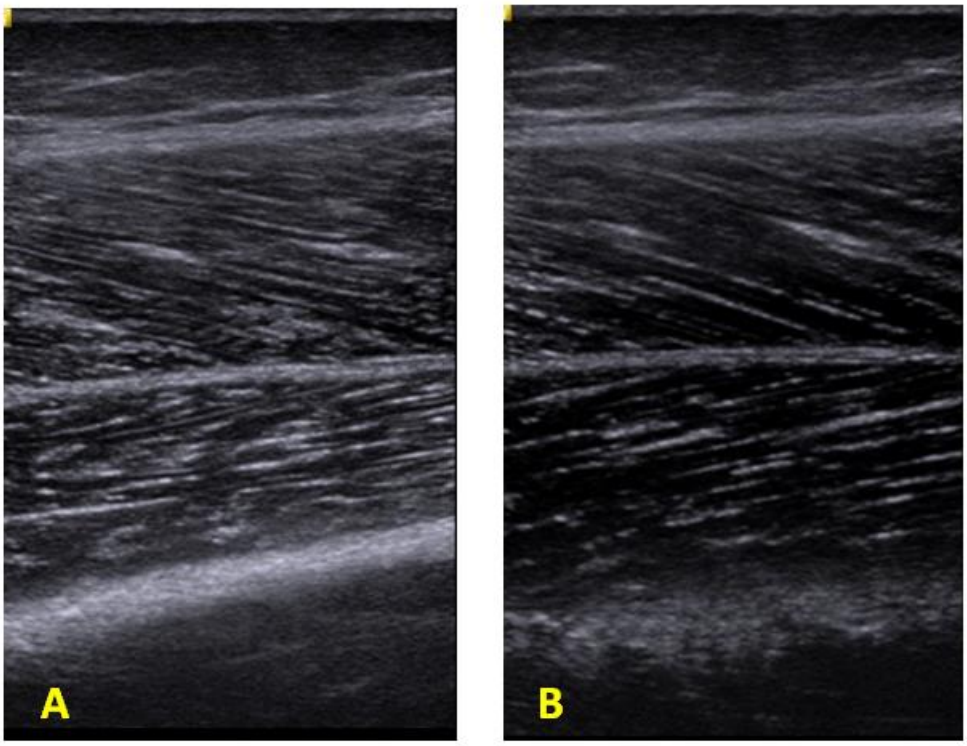

Figure 1.6 Longitudinal images of rectus femoris and vastus intermedius muscles at rest (A) and during dynamic contraction (B). Note that muscle thickness and pennate angles increase in image B.

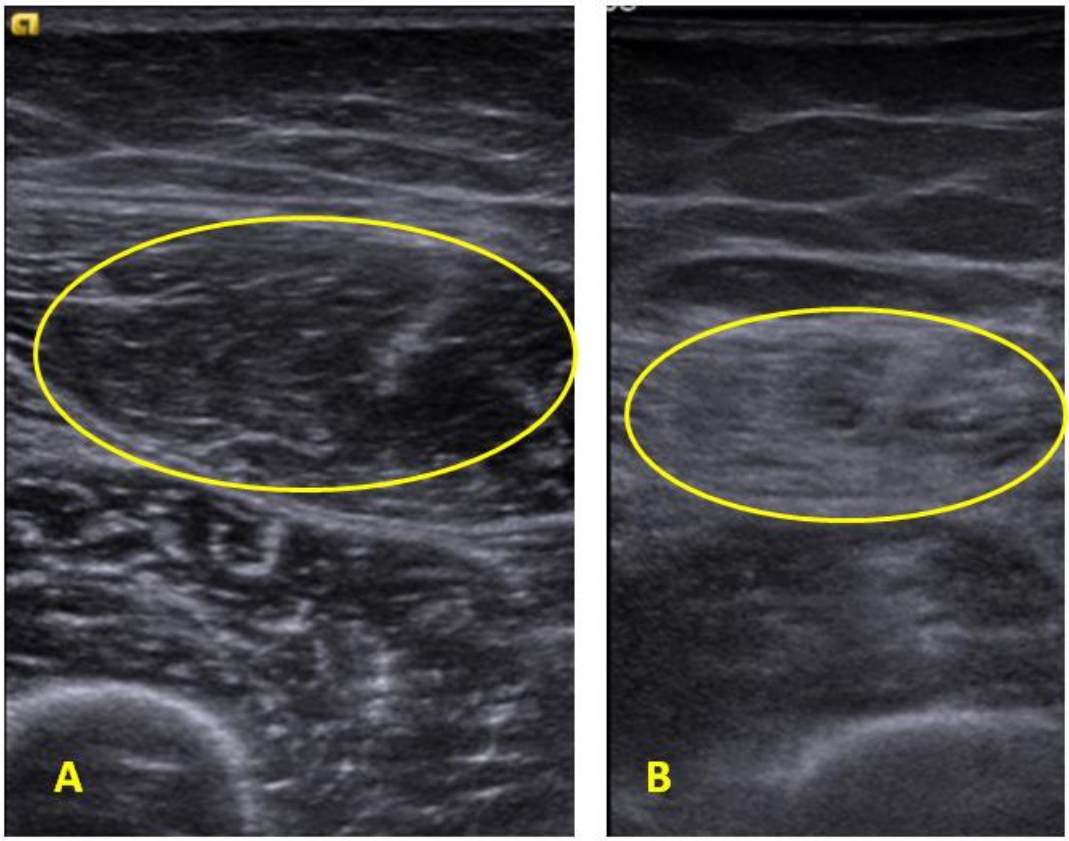

Figure 1.7 Transverse images of rectus femoris (yellow oval) of two different individuals showing normal muscle (A) and severe fat infiltration (B)

In order to assess sarcopenia by ultrasound in a clinical setting, some considerations should be taken into account:

1 The anatomic site of measurement

As stated before, with age there is greater muscle loss for the lower than upper limbs. This means that the same patient may have some muscles affected by sarcopenia and others not (Abe et al, 2011). Studies of Japanese people from 20 to 95 years old showed that there is a faster decline in muscle thickness of the anterior than the posterior compartment of the thigh (Abe et al, 2011). Given that sarcopenia in lower limb muscles should have a greater impact on mobility, muscle thickness of quadriceps femoris could be an early biomarker of sarcopenia. However, a link between muscle thickness of quadriceps femoris and gait speed could not be established (Abe et al, 2012), rather the authors found a correlation with a zigzag walk, which is not a standardised measurement of physical performance. Additionally, the local architecture of the quadriceps heads is different, and some muscle heads are better predictors of knee extension force than other heads (Ando et al, 2015).

This could mean that architectural changes in some quadriceps heads may have a greater impact on functional outcomes in sarcopenic patients.

2 Scanning technique

In order to obtain standardised and comparable measurements in the clinical setting, apart from fixing anatomical landmarks, care should be taken in performing the ultrasound technique regarding probe orientation relative to the body surface and level of pressure exerted since this can alter tissue dimensions and echointensity (Harris-Love et al, 2014).
Studies report comparable results using both linear and curved array probes for measuring the cross-sectional area of the muscle (Warner et al, 2008, Mandal et al, 2016).

3 Ultrasound parameters

Five different parameters can be obtained by ultrasound for the assessment of sarcopenia. Most studies report the measurement of muscle thickness and cross-sectional area for assessing muscle quantity. Muscle thickness is measured as the perpendicular line that joins the superficial and deep aponeurosis of the muscle. The measurement ought to be performed on the thickest portion of the muscle in order to obtain comparable values. Likewise, the cross-sectional area is the area of the muscle traced at its thickest portion.

On the other hand, echointensity, pennate angle, and fascicle length are used for assessing muscle quality. Echointensity (EI) refers to the mean pixel intensity in a defined region of interest. These values are expressed in arbitrary units with a range from 0 (the darkest) to 255 (the brightest). The overall value is the sum of contractile and non-contractile tissue (fat and fibrous tissue) within the said region. Lower EI indicates superior muscle quality (figure 1.7) (Young et al, 2016). Pennate angle (PA) is the angle of insertion of muscle fascicle to its aponeurosis (figure 1.6). This angle varies along the muscle length and is dependent on joint position and the degree of muscle contraction. Fascicle length can be traced from insertions on superficial and deep aponeuroses. For quadriceps muscle, fascicle length is greater than the field of view of standard probes which requires using specialized probes with a larger field of view or applying trigonometric equations to calculate this value (Miron Mombiela et al, 2020).
The use of contrast-enhanced ultrasound for the assessment of muscle vascularization and elastography is in the initial phase of the investigation and seems to have limited applicability in clinical practice (Mirón Mombiela et al, 2020). The strengths and limitations of each parameter are summarised in table 1.5.

	Ultrasound parameter	Anatomic site of assessment	Strengths	Limitations	Level of evidence*
Muscle quantity	Muscle thickness	All compartments (most studies on quadriceps femoris)	Simple and reproducible. Good correlation with gold standard imaging techniques	Fixed anatomic landmarks needed for site-specific measurement. Results depend on pressure applied to the probe. Site-specific sarcopenia may bias the results	Level 2
	Cross sectional area	Lower limbs (mostly rectus femoris muscle head)	Simple and reproducible. Good correlation with gold standard imaging techniques. Both linear and curved array probes can be used	Fixed anatomic landmarks needed for site-specific measurement. Assessment technique not completely standardized. May not be appropriate for pennate muscles	Level 2
Muscle quality	Echointensity	All compartments (mostly quadriceps femoris)	Gives information about the amount of fibrotic changes and fatty infiltration. Good correlation with muscle strength and function. Better intra-rater than interrater correlation	Absolute values of echointensity are not comparable between studies. Software for analysis needid (several available for free). Assesment technique not standardized. Influenced by technical parameters (gain, focus, frequency) and tissue thickness	Level 2
	Pennate angle	Lower limbs (mostly gastrocnemius medialis)	Gives information about muscle structure and strength generation capacity	Specific training for operator needed. Requires patient collaboration. Results are influenced by joint position and degree of muscle contraction. Correlation with functional parameters still unclear	Level 3
	Fascicle length	Lower limbs (mostly gastrocnemius medialis)	Gives information about muscle structure and strength generation capacity	Specific training for operator needed. Requires use of non standard transducers (with extended field of view) or calculation from other parameters using trigonometric equations. No studies that compare this parameter with clinical outcomes	Level 3

*Based on the Oxford Centre for Evidence-Based Medicine 2011 Levels of Evidence. OCEBM Levels of Evidence Working Group

Table 1.5 Ultrasound parameters for assessing sarcopenia. Table adapted from Miron Mombiela et al, 2020

Additionally, some studies reported measurements of muscle activity with ultrasound, where pennate angles increased during isometric contraction for various muscle groups of the upper and lower limb as well as oblique abdominal muscles (Hodges et al, 2003).

1.7 The challenge.

In frail individuals, the ageing process is accelerated which leads to disability, increased morbidity, and eventually death. Frailty is preventable and partially reversible if diagnosed early enough (Puts et al, 2017), therefore, there is special interest in developing biomarkers for the identification of individuals at risk of frailty in order to implement timely interventions and

reduce poor outcomes. In this regard, the development of quantitative biomarkers for the diagnosis of frailty is of paramount importance.

Up to date, there is no specific quantitative biomarker for diagnosis of frailty although many circulating and imaging parameters are being investigated. A good biomarker needs to be accessible, cost-effective as well as precise, and reliable. Over the last few years, the concept of biomarker panels rather than single biomarkers is gaining more momentum (Cardoso et al, 2018; Wennberg et al, 2021; Calvani et al, 2021).

Although various ultrasound parameters are being investigated, there is no clear evidence whether muscle size or muscle quality parameters or a combination of both show better performance in diagnosing frail patients. Additionally, the lack of standardised protocols for performing muscle ultrasound in elderly patients with sarcopenia can decrease the reliability and reproducibility of the results and showed to be a significant limitation for the clinical implementation. There are no clear guidelines for the muscle group that should be studied, for scanning technique (patient position and probe placement) nor parameters acquired (Ticinesi et al, 2017).

Moreover, no studies investigated the combination of circulating and imaging parameters for diagnosing frailty. This is important since imaging findings should be backed with biological data in order to understand histologic and molecular profiles of the visual parameters (Tomaszewski and Gillies, 2021).

Although muscle ultrasound does not form part of current protocols for diagnosing sarcopenia, this technique could be useful in the clinical setting as it can measure changes in muscle volume, composition, and architecture (Ticinesi et al, 2017). In fact, ultrasound is already used in clinical practice for other muscle-related pathologies such as neuromuscular disorders (Pillen and van Alfen, 2011). Additionally, the European Geriatric Medicine Society recently proposed a consensus protocol for using ultrasound for muscle mass assessments (Perkisas et al, 2021).

Therefore, we assumed that ultrasound imaging can be used reliably for assessing sarcopenia provided that appropriate protocol was applied, the operator was trained in performing the exam, and that the protocol with a combination of ultrasound parameters that assess both muscle mass and quality could distinguish community-dwelling individuals at risk of frailty. Additionally, we hypothesized that the combination of ultrasound and circulating parameters would render a good quantitative tool for diagnosing patients at risk of frailty in the clinical setting.

OBJECTIVES AND HYPOTHESIS

Work hypothesis: a combination of muscle ultrasound and biochemical parameters offers good diagnostic performance in detecting patients at risk of frailty

General objective – identify the best imaging and biochemical biomarkers for diagnosing subjects at risk of frailty.

Specific objectives:

- Assess the properties of muscle ultrasound parameters (accuracy and precision) as potential clinical biomarkers in opportunistic screening and baseline evaluation of frailty patients.
- Evaluate the feasibility of using muscle size and architecture parameters obtained by ultrasound in a clinical setting.
- Correlate muscle ultrasound parameters with physical parameters (physical activity, gait speed, and muscle strength measured with a hand dynamometer) as well as biochemical parameters.
- Assess the diagnostic performance of muscle ultrasound and biochemical parameters in distinguishing subjects at risk of frailty from non-frail individuals and determine the best frailty models.

MATERIALS AND METHODS

3.1 Materials.

The present study was carried out in the Radiology and Clinical Analysis departments of the General University Hospital of Valencia (CHGUV) and the Physiology department of the University of Valencia.

For the ultrasound exams and functional measurements:

- Ultrasound machine (Model Acuson S2000, Siemens, Munich, Germany)
- Electronic programs for the citation, image archiving (Impax, Agfa HealthCare, Belgium), and patient control (Connect Hall, Connectall Systems S.L, Spain)
- Handheld digital dynamometer (Trailite Steiner, TL-LSC100 Coesfeld, Germany)
- Digital balance (SECA model 803, 150kg capacity)
- Chronometer (Samsung Galaxy Smartphone).

For the laboratory analysis:

- Clinical chemistry analyser (AU 5400, Beckman Coulter, USA)
- Immunoassay analyser (UniCel DxI 800 Access, Beckman Coulter, USA)
- Flow cytometry analyser (xMAP Luminex 100, Luminex Corporation, USA)
- High-performance liquid chromatography (HPLC) system (Dionex Ultimate 3000, Thermo Fisher Scientific, USA)

Figure 3.1 HPLC equipment for the determination of MDA levels

3.2 Study Design and Setting.

This was a prospective experimental study performed in an outpatient clinical setting. The project was a collaboration between the Radiology and Clinical Analysis departments of CHGUV and the Physiology department of the University of Valencia.

The experimental part of the study included muscle ultrasound and blood tests. The ultrasounds were performed at the Radiology Department of CHGUV. After the image acquisition, a muscle strength measurement was performed. Then the patient was instructed to walk at a normal pace the distance of 4.6 metres previously marked on the floor in the hall outside the ultrasound booth, and the walking time was recorded. We proceeded to the height and weight measurements and study questionnaires (available in the Annex as STUDY QUESTIONNAIRE). This data was used to determine frailty phenotype (Fried et al, 2001) as a reference method. Frailty phenotype was chosen for comparability with other studies since it is the most widely used technique for assessing frail patients in the clinical setting (Buta et al, 2015). Medical histories were acquired retrospectively from electronic history viewer (PANGEA, Grupo de Informática Medica BET, UPV).

For the patients who accepted the blood test the electronic appointment for blood extraction was issued on the day of the ultrasound exam. Blood extraction was carried out at the Clinical Analysis Department of CHGUV after 8 hours of fasting, per usual protocol. Blood samples were processed as soon as possible, always within the hour of the extraction. The biochemical analysis was carried out on the same day. Additionally, 4 vials of plasma and serum per patient were stored at -80°C at the Biobank of CHGUV for the oxidative stress, hormone, and cytokine analysis. The extraction protocol is available in the Annex. Once all the patients were examined, these samples were sent for the respective analyses – oxidative stress analysis was carried out at the University of Valencia, and hormone and cytokine panels were performed at the Clinical Analysis department of CHGUV.

3.3 Study Subjects.

The study was conducted on humans after obtaining the approval of the ethics committee of the CHGUV. Each patient gave written informed consent for ultrasound or ultrasound and blood test before entering the study (available in the Annex as INFORMED CONSENT).

The inclusion criteria for the experimental group were:

- age 60 and above,
- ability to walk independently (including with the help of a cane/walker),
- access to the medical history.

The exclusion criteria:

- neuromuscular disorders or acute or chronic diseases that would alter the muscle architecture or interfere with measuring grip strength using a hand dynamometer,
- oncologic patients undergoing chemo or radiotherapy (oncologic patients in remission were included in the study),
- institutionalised patients or patients unable to get to the research centre using their means of transportation,
- severe dementia that would influence the patient's ability to understand the informed consent and the study questionnaire.

Healthy subjects between 20 and 59 years were invited to participate as the control group since there is a peak in muscle thickness measured by ultrasound between these ages (Arts et al, 2007).

Patients were referred from primary care (Centro de Salud Fuensanta) and recruited from the ultrasound exams for unrelated pathologies (ex. abdominal and thyroid exams) carried out by the main researcher from June to October of 2017.

For calculating the sample size an online calculator was used (https://riskcalc.org/samplesize/). We used data from our previous study due to similarities in socio-demographic characteristics - the prevalence of frailty was 29% among patients older than 60 years (Mirón Mombiela et al, 2017). With a type I error rate (α) of 0.05 and an absolute error of precision (d) of 10%, the study sample was calculated for n=80.

A total of 163 patients were invited to the study, of which 140 accepted to participate (figure 3.2). Muscle ultrasounds were performed on 140 individuals. At the time of the ultrasound exam, the main researcher was blinded for medical histories and frailty parameters of the participants. This way the selection bias was reduced and random sampling of the general geriatric population of the area was possible. Of 140 ultrasounds performed 128 subjects met the inclusion and exclusion criteria and were included in the study. Of all the enrolled patients 72 accepted to donate blood for the testing. There were a total of 62 samples processed.

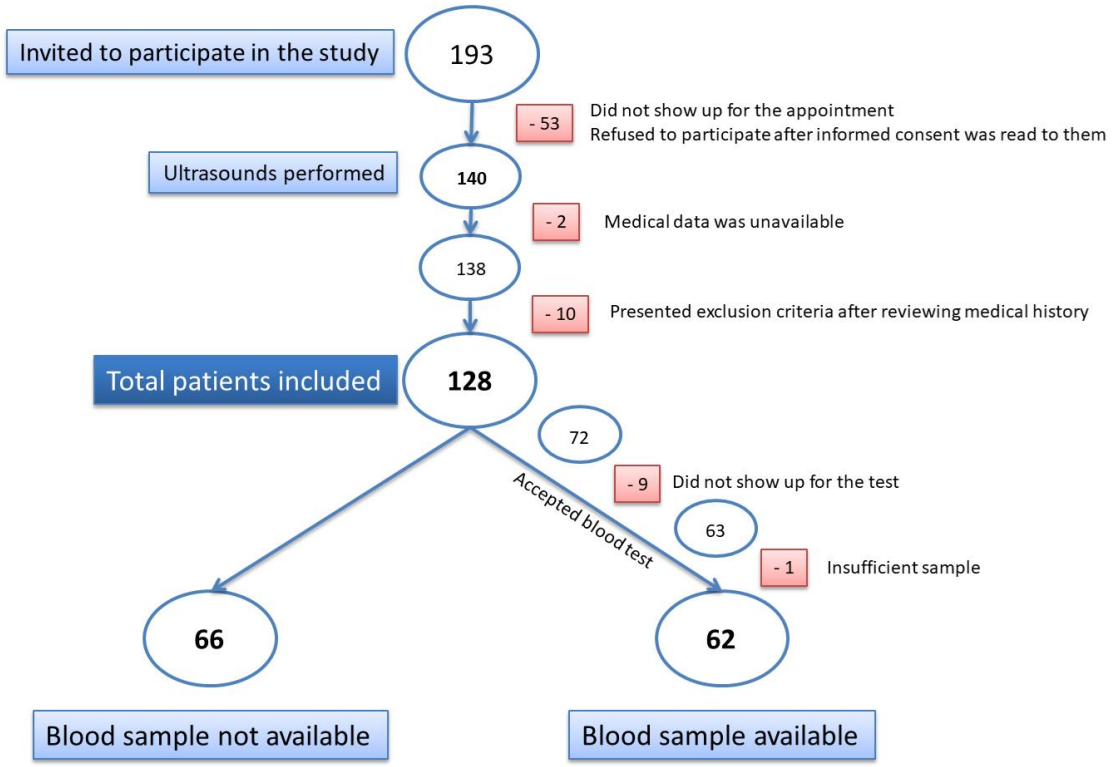

Figure 3.2 Flow chart of study participants

3.4 Methods of Measurement.

3.4.1 Muscle ultrasound

A small pilot study was conducted in order to calibrate the ultrasound machine and verify the protocol. Test ultrasounds were performed on 5 healthy young subjects in order to determine the anatomical site (the anterior compartment of the thigh was chosen over other areas due to size and accessibility), view planes (axial/sagittal views), and possible parameters (from our previous work and available literature we planned to measure muscle thickness and echointensity. We tested if it was possible to capture images for assessing pennate angles at rest and in contraction, more specifically, whether the subjects could perform the maximum contraction of the quadriceps at the request and maintain the contraction steady long enough to obtain three images for the analysis, figure 3.3). Additionally, the optimal settings of gain and focus were tested, and a musculoskeletal pre-set was chosen to provide the best contrast resolution between muscle and connective tissue and ensure comparability between images. Total exam time was also estimated at this point in order to schedule the patients more efficiently.

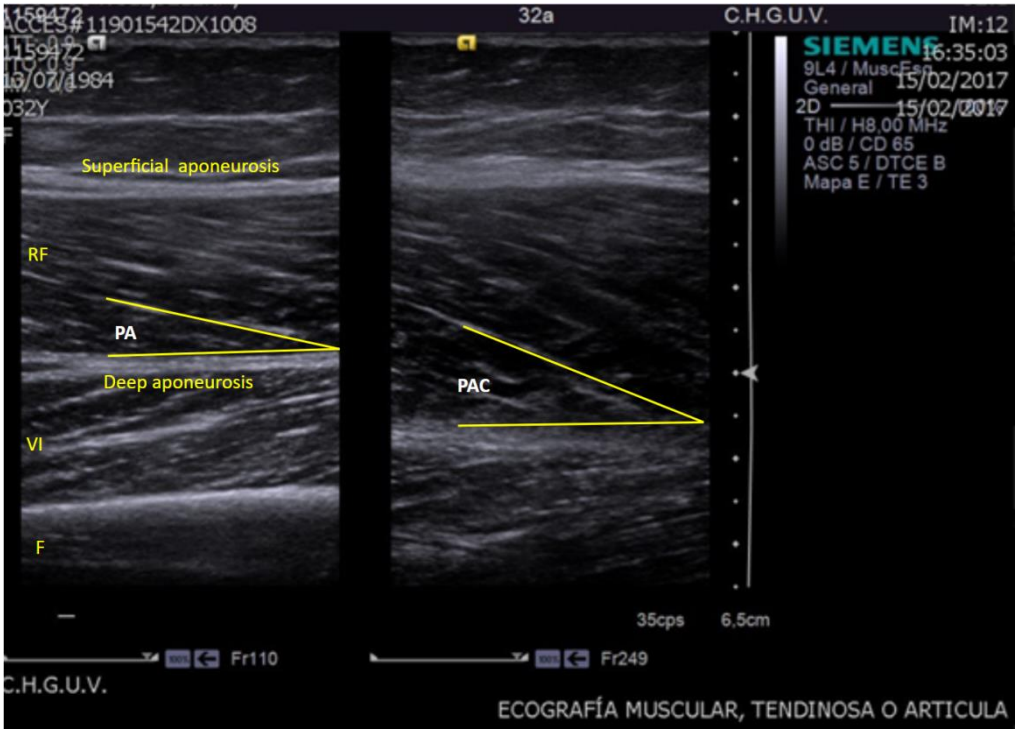

Figure 3.3 Test ultrasound of rectus femoris muscle at rest (image on the left) and in contraction (image on the right). Note the increase of the angle between the deep aponeurosis and muscle fibers. RF – rectus femoris, VI – vastus intermedius, F – femur, PA – pennate angle, PAC – pennate angle in contraction

The tissues of the anterior compartment of the right thigh were scanned using ultrasound in B mode with a 4-9 MHz linear transducer in musculoskeletal pre-set. The patients were placed in the supine position and the images were taken applying an abundant quantity of contact gel and with minimal pressure with the probe during the exam in order to avoid tissue distortion.

All four heads of the *quadriceps femoris* muscle were scanned (Blazevich et al, 2006; Ando et al, 2016). The first set of images was taken at the midpoint between the anterior superior iliac spine and the lateral femoral condyle in transverse and longitudinal planes and was used to assess *rectus femoris* and *vastus intermedius* muscle heads (Figure 3.4 A – anterior view). Then, with the probe held in a longitudinal position, the patient was instructed to contract the quadriceps muscle and hold steady for a few moments and the images in contraction were taken. From this point, the probe was positioned laterally at the same level (Figure 3.4 B – lateral view) in order to include the *vastus lateralis* muscle head. The scans were also performed in transverse and longitudinal planes at rest following imaging in contraction. Finally, the probe was positioned medially and slightly distally (Figure 3.4 C – medial view) and the *vastus medialis* head was scanned in both planes (longitudinal and transversal) at rest and during contraction.

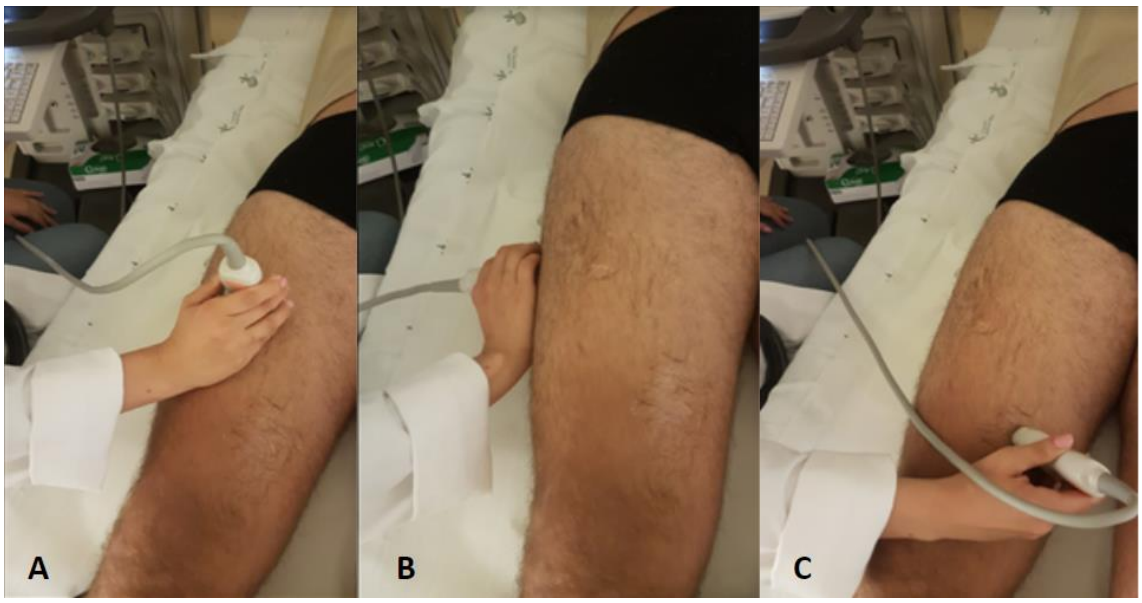

Figure 3.4 Probe placement – A) anterior view (rectus femoris and vastus intermedius heads), B) lateral view (vastus lateralis head) and C) medial view (vastus medialis head)

Finally, a convex transducer was used to obtain a sufficient field of view and include the cross-sectional image of the *rectus femoris* muscle head in order to trace the total area at its widest point (Narici, 1989). For this, images were taken in the anterior view (Figure 3.4 A). Figures 3.5 and 3.6 show examples of ultrasound images in transverse and longitudinal planes.

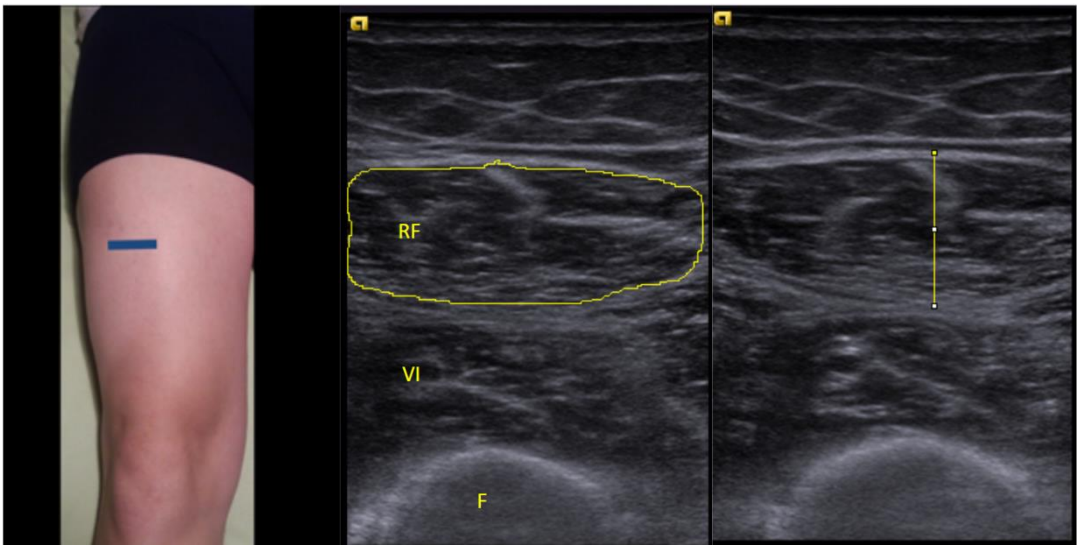

Figure 3.5 Ultrasound probe placement – the transverse plane of rectus femoris muscle, examples of measurements of echointensity (selected area in the middle image) and muscle thickness (distance at the widest portion of muscle belly, image on the right)

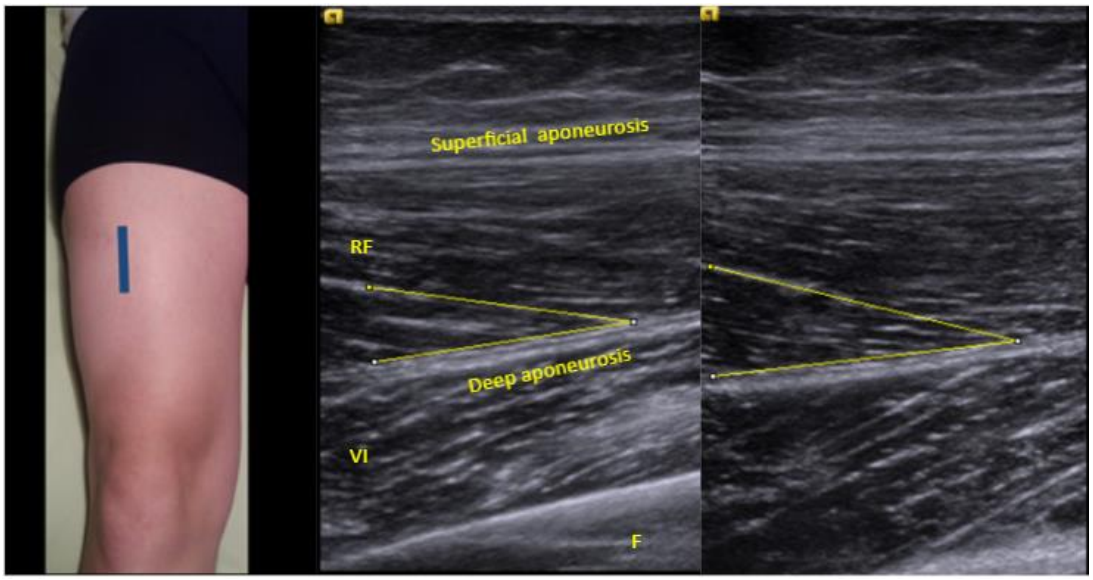

Figure 3.6 Ultrasound probe placement – the longitudinal plane of rectus femoris muscle, examples of measurements of pennate angles at rest (middle image) and in contraction (image on the right)

Each image was acquired three times for statistical analysis. A total of 30 images per patient were stored in the Picture Archiving and Communication System (PACS) of the hospital; there were nine images per each view – anterior view in the transverse plane (3 images), the longitudinal plane at rest (3 images), the longitudinal plane in contraction (3 images); lateral view in the transverse plane, the longitudinal plane at rest and in contraction (total of 9 images, 3 per plane), as well as medial view (9 images). Finally, there were 3 images in the anterior transverse view with the convex transducer.

After each exam, a radiological report was written and saved in medical history. A template was used for efficiency (available in the Annex as RADIOLOGY REPORT).

The images were processed using ImageJ for Windows, 64-bit version (National Institute of Health, USA), free software available at https://imagej.nih.gov/ij/download.html. Each image was calibrated (Set Scale tool) before measuring. Echointensity (EI) and muscle thickness (MT) were measured from the images taken in the transverse plane and the mean value of the three measurements (one measurement per image) was used for the statistical analysis. For the echointensity, a manual ROI (Caresio et al, 2015) was traced including most of the muscle visible in the image and avoiding aponeurosis and bone. Additionally, for comparison reasons, echointensity was measured in the longitudinal plane applying the same manual ROI method. Muscle thickness was measured from transverse images as the maximum distance between the two aponeuroses, using a ruler tool, and the mean value was used for the analysis. Examples of

EI and MT measurements are shown in figure 3.7. Pennate angles (PA) were measured from longitudinal images at rest and in contraction using an angle tool. Clearly visible fascicle was chosen and the angle was traced between the fascicle and its insertion in the deep aponeurosis (figure 3.8). Images from patients who did not comply with the contraction request (unable to contract the muscle at the request or maintain the contraction/presented muscle fasciculations etc.) were annotated at the time of the imaging and were not taken into account for the results. Additionally, the superficial fat thickness was measured from all the images in the transverse plane (fat distribution differs among the scanning landmarks) as the distance between the skin and the superficial aponeurosis. Finally, the rectus femoris cross-sectional area was measured from the images taken with the convex transducer (Hammond et al, 2014) using manual ROI. Parameters were measured once from each of the three respective images whenever possible. In cases where one of the images was suboptimal (partially blurry, no visible attachment of the fascicle to the aponeurosis, etc), the measurement was taken twice from the optimal image of the same view.

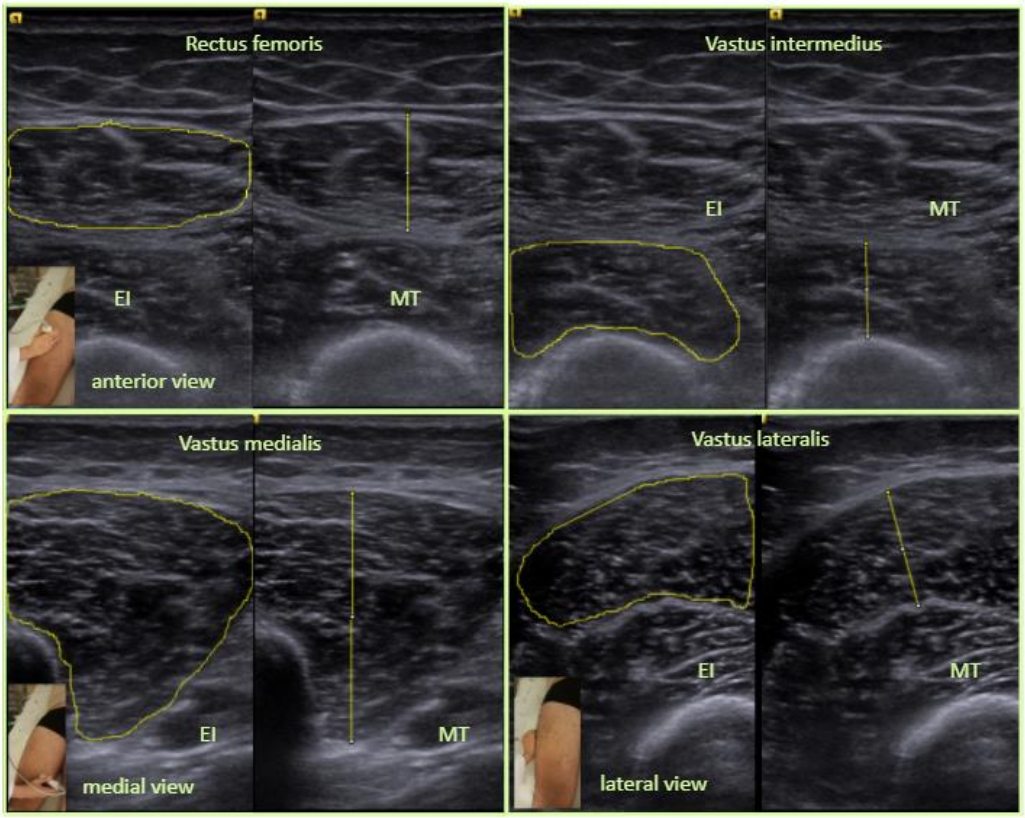

Figure 3.7 contains images in the transverse plane of all four quadriceps heads and shows examples of echointensity (EI) and muscle thickness (MT) measurements. Note that rectus femoris and vastus intermedius are measured from the same image.

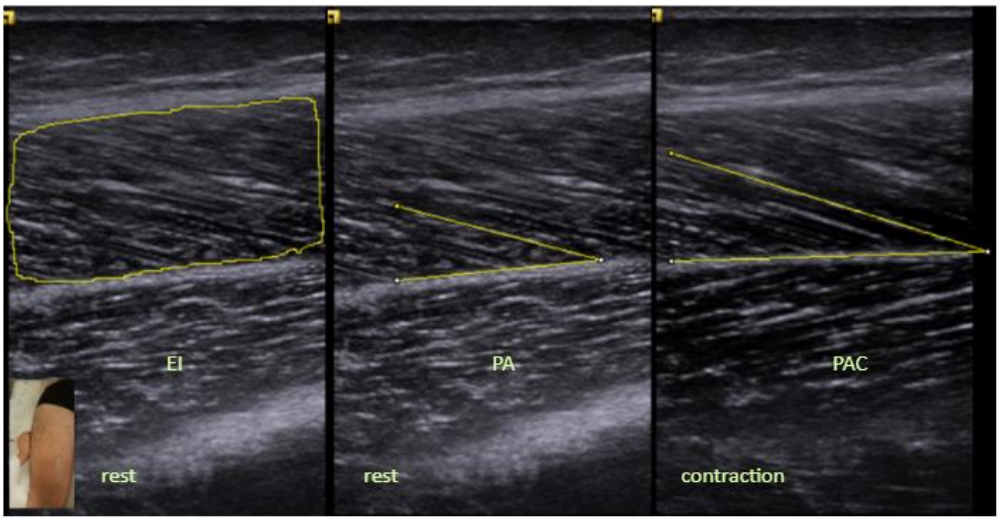

Figure 3.8 Example of measurements of echointensity (EI) and pennate angles at rest (PA) and in contraction (PAC) of vastus lateralis muscle. Images are taken in lateral view, longitudinal plane at rest, and contraction. Note that the pennate angle increases with contraction.

3.4.2. Muscle strength measurement

The grip strength of the dominant hand was measured using a digital hand dynamometer (Tralite, TL-LSC100). Patients were seated and held the dynamometer with the elbow flexed at a 90° angle and the wrist in a neutral position (figure 3.9). Previously it was explained that the test consisted of making as much pressure as possible (as opposed to holding for the longest time). Patients had three attempts for maximal pressure for 5 seconds with 30 seconds of rest between them. During the test, patients were encouraged to try their best. Values were expressed in kg. The mean of the three measurements was used for the analysis.

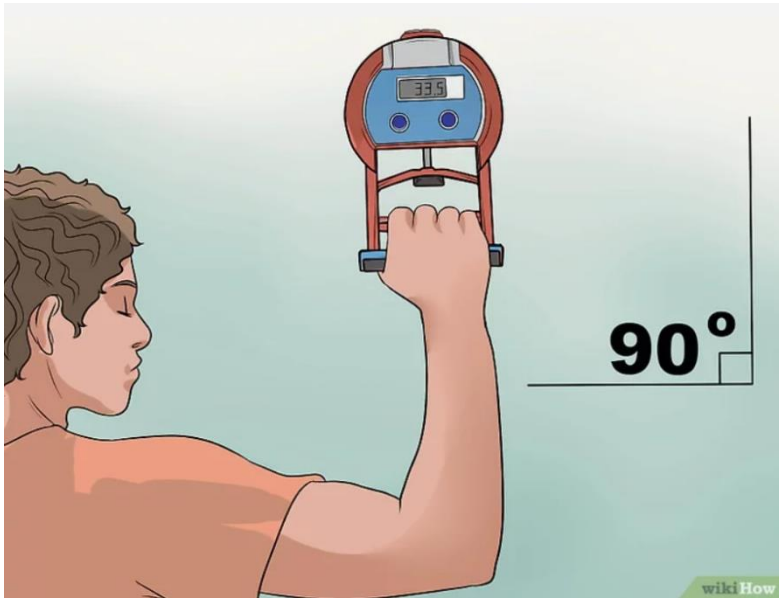

Figure 3.9. Illustration of muscle strength measurement with a hand dynamometer. Image downloaded from wikihow.com

3.4.3. Walking speed measurement

A distance of 4.6-meter was marked on the floor of the corridor outside the ultrasound booth. Patients were instructed to walk at a normal pace without rushing, as would they normally walk on the street, and were allowed to use their usual walking aids (cane, walker). The starting point was located 0.5 m away from the start line in order to avoid reaction time biases and the patient was encouraged to walk until fully crossing the end mark. Walking time was measured with a Smartphone chronometer application.

3.4.4. Study questionnaire

- Epidemiological and anthropometric data

This section included general epidemiological data (date of birth, sex, age) and height and weight measurements. A measuring tape was placed on the wall of the ultrasound booth, subjects were instructed to stand barefoot straight against the wall with their feet together. A ruler was placed at the top of the patient's head and the measurement was read from the tape. The value was expressed in metres. The weight was determined afterward, instructing patients to step barefoot on the scale. The scale was calibrated before each ultrasound session. The value was expressed in kilograms. Body mass index was calculated for each patient using the formula: BMI = weight (kg)/height $(m)^2$.

- Medical history and risk factors

Medical histories were reviewed to determine the presence of associated diseases (hypertension, hyperlipidemia, diabetes mellitus, chronic obstructive pulmonary disease (COPD), hearing and visual impairment, previous stroke/transitory ischaemic attack (TIA), congestive heart failure, heart disease, myocardial infarction, renal disease, osteoarthritis, anxiety/depression, osteoporotic fractures, hepatopathy, dementia, connective tissue disease, previous malignancy with proven remission, peripheral vascular disease, and peptic ulcer. Additionally, patients were screened for Parkinson's disease, hemiplegia, and active malignancy and excluded from the study if positive due to association with secondary sarcopenia (exclusion criteria): three patients had active malignancy at the time of the ultrasound, two had Parkinson's disease and none had hemiplegia.

Risk factors (smoking, alcohol abuse, and obesity) were recorded. Patients were asked about the number of falls in the last 6 months. (Landi et al, 2012). Additionally, a number of primary care visits, emergency room visits, and hospitalizations in the last 6 months were also recorded (Beaudart et al, 2017).

3.4.5. Frailty phenotype

Frailty criteria proposed by Fried and colleagues (Fried et al, 2001) were used for determining frailty phenotype. These criteria assess unintentional weight loss, exhaustion, low physical activity, slow walking speed, and muscle weakness. The Frailty criteria chart is available in the Annex as FRIED'S FRAILTY CRITERIA CHART.

Appetite and weight loss – this information was obtained by asking the following question: did you lose more than 4.5 kg unintentionally in the last year?

Exhaustion – a positive answer to one or both statements – I feel that everything I did in the last 3-4 days was a great effort/I feel the lack of energy to do the things I normally like doing.

Low physical activity – walking less than 2.30h/week for men or less than 2h/week for women.

Slow walking speed – speed lower than predetermined values according to sex and height of the subject.

Muscle weakness – values lower than predetermined according to BMI and sex of the subject.

Each positive criterion was scored with one point. The final score was a sum of the five criteria. According to the number of points, the subjects were classified to:

Robust – 0 points,

Pre-frail – 1 or 2 points,

Frail – 3-5 points.

3.4.6. IPAQ

This section was based on the International Physical Activity Questionnaire (IPAQ) (2016). (Retrieved from https://sites.google.com/site/ theipaq/ in May of 2017). Patients were asked to recall and quantify their physical activities in the last seven days. The questions included vigorous and moderate physical activities, walking, and time spent sitting (Figure 3.10). This questionnaire was chosen in order to have standardised and comparable data with other international studies (Craig et al., 2003).

IPAQ-E		
1	Durante los últimos 7 días, ¿en cuántos realizó actividades físicas intensas tales como levantar pesos pesados, cavar, hacer ejercicios aeróbicos o andar rápido en bicicleta?	
2	Habitualmente, ¿cuánto tiempo en total dedicó a una actividad física intensa en uno de esos días? Indique cuantos minutos por día.	
3	Durante los últimos 7 días, ¿en cuántos días hizo actividades físicas moderadas tales como transportar pesos livianos, o andar en bicicleta a velocidad regular? No incluya caminar	
4	Habitualmente, ¿cuánto tiempo en total dedicó a una actividad física moderada en uno de esos días? Indique cuantos minutos por día.	
5	Durante los últimos 7 días, ¿caminó por lo menos 10 minutos seguidos?	
6	Habitualmente, ¿cuánto tiempo en total dedicó a caminar en uno de esos días? Indique cuantos minutos por día.	
7	Durante los últimos 7 días, ¿cuánto tiempo pasó sentado durante un día hábil? Indique cuantos minutos por día.	

Figure 3.10 International Physical Activity Questionnaire in Spanish.

3.4.7. Biochemical analysis

General biochemical and immunochemical analysis

Blood was drawn after at least 8 hours of fasting. The extraction was carried out in a tube with EDTA anticoagulant for the complete blood count and in a tube without additives for the rest of the parameters. After extracting the sample without additives, the clot was retracted and the tube was centrifuged at 2000 g for 10 minutes at room temperature. The list of the analytes and corresponding procedures is detailed in table 3.1.

	Table 3.1 General biochemical and immunochemical analysis		
	Analyte	Procedure	Equipment
Hemogram	Leucocytes	Impedance	DXH-800, Beckman Coulter
	Leucocyte formula	Flow cytometry	DXH-800, Beckman Coulter
	RBC	Impedance	DXH-800, Beckman Coulter
	HGB	Spectrophotometry	DXH-800, Beckman Coulter
	HCT	Mathematical calculation	DXH-800, Beckman Coulter
	MCV	Mathematical calculation	DXH-800, Beckman Coulter
	MCH	Mathematical calculation	DXH-800, Beckman Coulter
	MCHC	Mathematical calculation	DXH-800, Beckman Coulter
	Platelets	Impedance	DXH-800, Beckman Coulter
Proteins	Proteins	Coluorimetry	AU 5800, Beckman Coulter
	CRP	Immunoturbidimetry	AU 5800, Beckman Coulter
	Albumin	Coluorimetry	AU 5800, Beckman Coulter
	Glucose	Enzymatic UV method	AU 5800, Beckman Coulter
Renal function	Urea	Kinetic UV method	AU 5800, Beckman Coulter
	Creatinine	Kinetic colourimetry	AU 5800, Beckman Coulter
	Glomerular filtration rate	Calculation	AU 5800, Beckman Coulter
Bone	Calcium	Coluorimetry	AU 5800, Beckman Coulter
	Phosphorus	Coluorimetry	AU 5800, Beckman Coulter
Liver	ALT	Kinetic UV method	AU 5800, Beckman Coulter
	ALP	Kinetic UV method	AU 5800, Beckman Coulter
Ions	Chlorine	Ion-selective electrode	AU 5800, Beckman Coulter
	Potassium	Ion-selective electrode	AU 5800, Beckman Coulter
	Sodium	Ion-selective electrode	AU 5800, Beckman Coulter
Lipid metabolism	Total cholesterol	Enzymatic colourimetry	AU 5800, Beckman Coulter
	Triglycerides	Enzymatic colourimetry	AU 5800, Beckman Coulter
	HDL cholesterol	Enzymatic colourimetry	AU 5800, Beckman Coulter
	LDL cholesterol	Enzymatic colourimetry	AU 5800, Beckman Coulter
CV risk	CPK	Kinetic UV method	AU 5800, Beckman Coulter
	Homocysteine	Turbidimetry	ACL TOP 700, Werfen
Iron mtb	Ferritin	Immunoturbidimetry	AU 5800, Beckman Coulter
	Iron	Coluorimetry	AU 5800, Beckman Coulter
	TS	Immunoturbidimetry	AU 5800, Beckman Coulter
	Vitamin D	Chemiluminescence	DXI 800, Beckman Coulter
Hormones	Cortisol	Chemiluminescence	DXI 800, Beckman Coulter
	Insulin	Chemiluminescence	DXI 800, Beckman Coulter
	PTH	Chemiluminescence	DXI 800, Beckman Coulter
	TSH	Chemiluminescence	DXI 800, Beckman Coulter
	IGF-1	Chemiluminescence	Liaison XL, Diasorin

Abbreviations: RBC - red blood cells, HGB - hemoglobin, HCT - hematocrit, MCV - mean corpuscular volume, MCH - mean corpuscular hemoglobin, MCHC - mean corpuscular hemoglobin concentration, ALT - alanine aminotransferase, ALP - alkaline phosphatase, HDL - high-density lipoprotein, LDL - low-density lipoprotein, CPK - creatine phosphokinase, TS - transferrin saturation, CRP- C-reactive protein, PTH - parathormone, TSH - thyroid stimulating hormone, IGF 1 - Insulin-like growth factor 1

Table 3.1 General biochemical and immunochemical analysis

Oxidative stress analysis

Plasma sample was used for the determination of Malondialdehyde (MDA) and protein carbonylation.

a) Oxidative stress in lipids

Malondialdehyde (MDA) is a result of the lipid peroxidation of polyunsaturated fatty acids, mainly from the cell membranes, which are degraded by reactive O2 species. High-performance liquid chromatography (HPLC) was used for this determination. Chromatography is a physical separation method in which the components that need to be separated are distributed between two phases, the stationary phase (column of silica or alumina particles) and the mobile phase, which in this case is liquid and acts as a sample carrier. The chromatographic separation in HPLC is the result of the specific interactions of the sample molecules in both phases. MDA [$CH_2(CHO)_2$] is a very reactive compound, its molecule is small (molecular weight of 72.0636 g/mol) and it is volatile, all of which makes its measurement very difficult. Therefore, before measurement sample derivatization needed to be performed using thiobarbituric acid (TBA). The method described by Wong and colleagues was used (Wong et al, 1987), in which a molecule of MDA reacts with 2 molecules of thiobarbituric acid (TBA) producing an adduct that is a pink chromogen with an absorption maximum between λ= 532-535 nm. The results obtained were expressed in micromolarity (μM) equivalent to nanomoles/mL (nm/mL). The procedure description is available in Annex as DETERMINATION OF MDA IN PLASMA.

b) Oxidative stress in proteins

The Protein Assay Kit based on the Lowry method (Lowry et al, 1951) was used for this analysis, which is a colorimetric method for the quantitative assessment of proteins in plasma. Lowry's reagent, included in the kit, contains sodium dodecyl sulfate (SDS), which facilitates the dissolution of partially insoluble proteins, and alkaline cupric tartrate, which binds proteins. Folin's reagent, also included in the kit, contains phenol, which interacts with tartrate and gives rise to a blue-colored compound (heteropolymolybdenum Blue). The colour intensity of this compound is proportional to the protein concentration, according to the Lambert-Beer law. The concentration of the unknown sample was determined graphically by plotting the absorbance against known concentrations of our internal standard, bovine serum albumin (BSA). This procedure is detailed in Annex as DETERMINATION OF PLASMA PROTEINS BY LOWRY.

For the determination of carbonylated proteins, the Western blotting or immunoblotting method was applied, using the OxyBlot protein oxidation detection Kit. Electrophoresis was carried out in gels with a polyacrylamide matrix (PAGE), under denaturing conditions, in order to separate proteins by their molecular weight. For this, the combination of a denaturing detergent (SDS) and a reducing agent (β-mercaptoethanol) was used. The densitometry of the bands was determined using the ImageJ software (NIH, USA). As a loading control, membranes were

stained with Ponceau red. The densitometry of the membrane was calculated as a ratio: densitometry of protein carbonylation/densitometry of the membrane stained with Ponceau red, expressing the result as arbitrary units of oxidised proteins. The procedure is available in Annex as PROTEIN CARBONYLATION.

Cytokine analysis

Pro and anti-inflammatory cytokines were assessed in plasma samples using xMAP Luminex technology. A commercial Luminex assay kit (MILLIPLEX MAP HSTCMAG-28SK-16plex) was used for detection and quantification of following cytokines: ITAC, Fractalkine, IFN-γ, IL-10, MIP-3α, IL-12p70, IL-13, IL-17a, IL-1β, IL-2, IL-4, IL-23, IL-6, IL-7, IL- 8, TNF-α.

This technology is a bead-based immunoassay, colour coded beads are dyed with a graded mixture of two fluorophores (red and infrared) in different concentrations in order to create up to 100 different regions on the fluorescent spectrum enabling measurement of up to 100 analytes in one sample.

The technique is based on the ELISA sandwich test and consists of the following steps:

1. Each bead is precoated with a cytokine-specific antibody (capture antibody). The sample is added to the mixture of beads and the antibodies bind to the cytokines of interest.
2. The specific biotinylated antibody is added (detection antibody), and it forms an antibody-antigen sandwich with the cytokine.
3. Phycoerythrin (PE)-conjugated streptavidin is added (reporter dye). It binds to biotinylated antibodies. This provides the bead with an additional fluorescent emission signature when it binds to the cytokine of interest.
4. Beads are read on a dual-laser flow-based detection instrument. Red laser (635 nm) excites both the red and infrared dyes and enables detection of the type of bead (identifies the cytokine of interest). Green laser (525 nm) excites the reporter dye bound to the antigen-antibody complex (quantifies the amount of cytokine bound to the bead).

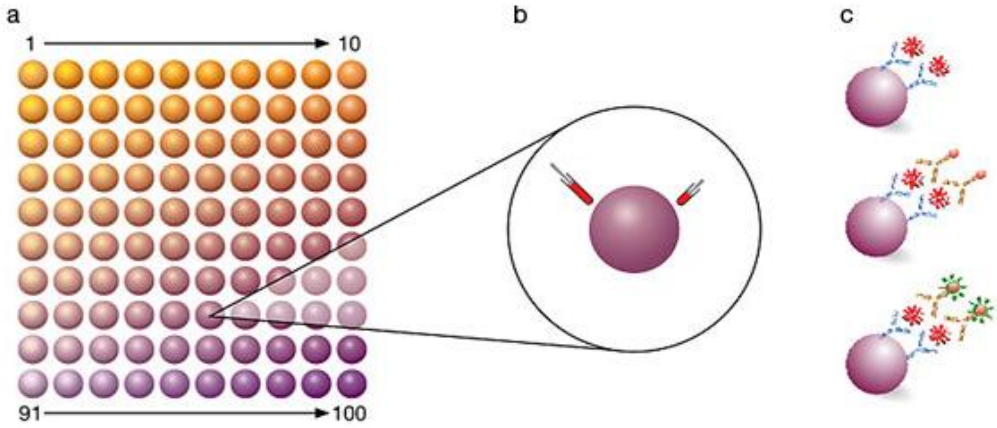

Figure 3.11. Luminex assay principle: a.b. there are up to 100 different regions based on different proportions of red and infrared fluorophores. c. cytokine binds to capture antibody; biotinylated (detection) antibody is added, and it forms a sandwich with the cytokine; PE-conjugated streptavidin (reporter dye) is added, and it binds to detection antibody. Image downloaded from https://www.bio-rad.com/es-es/applications-technologies/multiplex-immunoassays

The samples were processed on a 96-well plate. Reagents for standards and quality controls were provided in the kit and prepared as instructed in technical guidelines. The overnight protocol was used following the instructions detailed in the guidelines and the plate was read on a flow cytometry instrument (protocol available in Annex as LUMINEX PROTOCOL). A report for each analyte was created including standard curves, mean fluorescence of the beads vs background, bead count, recovery percentages, and concentrations of the analytes. Data were acquired and analysed using xPonent 3.1 software.

3.4.8. Statistical analysis

Statistical analysis was performed using SPSS software, version 22.0 for Windows (IBM, SPSS Inc.). All continuous variables were presented as means ± standard deviations while ordinal variables were presented as quantity and percentages. The distribution of the continuous variables was assessed with the Kolmogorov-Smirnov normality test. For assessing differences between sexes t-student test was used for the variables with a normal distribution (parametric variables) and the Mann-Whitney test for non-parametric variables. The differences of study variables according to frailty phenotype were evaluated using the ANOVA test for parametric variables followed by the Bonferroni post-hoc test, whereas the Kruskal-Wallis test was used for non-parametric variables.

Correlation analysis was performed to assess the relationships among physical characteristics, ultrasound, and biochemical parameters. Spearman's coefficient (rho) was used for continuous

variables and Kendall´s tau was used for ordinal variables. The strength of correlation was arbitrarily divided into three categories – weak, moderate and strong, and interpreted as weak for values r<0.399, moderate for values r from 0.400 to 0.699, and strong for values r>0.700.

The accuracy of ultrasound parameters was tested using areas under the receiver operating characteristic (ROC) curve. Frailty phenotype was divided into the non-frail group (controls and robust group) and at-risk group (pre-frail and frail) based on the different behaviour of these two populations observed in our previous work (Mirón Mombiela et al, 2021). The values were classified as poor for ≤0.70, acceptable for 0.71-0.80, excellent for 0.81-0.90, and outstanding for 0.91-1.00 (Hosmer and Lemeshow, 2000). The precision of the measurement technique was also tested using the intraclass correlation coefficients (ICC) and Bland-Altman Limits of Agreement. The ICC values were classified as poor for values ≤0.50, moderate for 0.51-0.75, good for 0.75-0.90, and excellent for 0.91-1.00 (Koo and Li, 2016).

Stepwise logistic regression analysis was performed with ultrasound and biochemical parameters adjusted with physical characteristics to determine the best predictive models for frailty. The frailty phenotype was used as a dependent variable, creating two groups: non-frail and at-risk groups. Robust patients and young controls were assigned to the non-frail group, and pre-frail and frail patients were assigned to the at-risk group. In order to avoid using independent variables with high correlation among them, which would introduce errors in the regression models (inflation of variance and changes in the signs and confidence intervals (Ryan, 2009)) a test for multicollinearity was performed using the Variance Inflation Factor (VIF). Generally, VIF >5 or >10 suggests multicollinearity (Chatterjee and Simonoff, 2013), whereas VIF = 1 indicates a complete absence of multicollinearity. The independent variables selected for each model had VIF <2.5. The level of influence of the independent variables on frailty was expressed by odds ratios. Values >1 increase the odds while values between 0 and 1 decrease the odds of frailty. In order to compare these ratios, the values <1 were converted using the formula 1/OR.

Due to multiple tests performed on our data, there is an increased rate of false positive results. For all the data analysed we obtained 1901 p values. Benjamini and Hochberg's formula was used to assess false discovery rates (FDR) and provide reasonable estimates for truly significant data. The p values were ranked in ascending order and then adjusted p-values (or q-values) were calculated using the formula FDR = PvalCount * Pval / PvalRank. For the selected q-value of 0.05, we should expect to have 10 false positives out of 206 positive results.

Statistical significance was defined as p<0.05.

RESULTS

4.1 Baseline characteristics.

The sample consisted of 128 patients, of which 66 were females (51%) and 62 males (49%). Table 4.1 shows physical characteristics (age, weight, height, BMI, muscle strength, and gait speed) and physical activity questionnaire parameters (IPAQ) according to sex. The sample was homogeneous regarding age, BMI, gait speed, physical activity, and walking. There were significant differences between sexes in weight, height, muscle strength, intense and moderate physical activity, and time spent seated during the day.

Table 4.1 Baseline characteristics according to sex

	Sex	Female (N=66)	Male (N=62)	Total (N=128)	Statistical test
	Variable (unit)	Mean ± SD	Mean ± SD	Mean ± SD	p
Physical characteristics	***Age (years)***	62 ± 15	62 ± 20	62 ± 17	*0,810**
	Weight (kg)	70.3 ± 14.8	80 ± 14	75 ± 15.1	*<0.001*
	Height (m)	1.57 ± 0.08	1.71 ± 0.09	1.64 ± 0.11	*<0.001**
	BMI (kg/m2)	28.55 ± 5.60	27.36 ± 4.05	27.97 ± 4.93	*0.175*
	Muscle strength (kg)	19.64 ± 6.21	33.34 ± 10.03	26.33 ± 10.75	*<0.001**
	Gait speed (s)	4.4 ± 2	4 ± 1.2	4.2 ± 1.6	*0,534**
IPAQ	***Physical activity (h/week)***	9.3 ± 7	10.7 ± 11.5	10 ± 9.5	*0,864**
	IPA (min/day)	3 ± 11	15 ± 44	9 ± 32	*0,046**
	MPA (min/day)	75 ± 85	45 ± 55	61 ± 73	*0,026**
	Walking (min/day)	81 ± 60	92 ± 99	86 ± 81	*0,982**
	Seated (min/day)	250 ± 137	308 ± 141	279 ± 142	*0,021**

Abbreviations: IPA - intense physical activity, MPA - moderate physical activity, SD - standard deviation

* non parametric test

Table 4.1 Baseline characteristics according to sex

There were 36 controls (28%), 22 robust (17%), 53 prefrail (41%), and 17 frail patients (13%). Physical characteristics (age, weight, height, BMI, muscle strength, and gait speed) and IPAQ parameters that included weekly physical activity, daily intense and moderate physical activity, daily walking, and seated time according to frailty phenotype are represented in table 4.2. There were significant differences between groups in age, height, BMI, muscle strength, gait speed, physical activity, intense physical activity, and walking. There were no significant differences in weight, moderate physical activity, and time spent seated. Finally, the sample was homogeneously distributed among groups regarding sex. The table includes the number of

positive frailty criteria, based on which the patients were assigned to a corresponding group. Frailty criteria were also applied in the control group for comparison.

Table 4.2 Baseline characteristics according to frailty phenotype							
	Frailty Phenotype	Control (N=36)	Robust (N=22)	Prefrail (N=53)	Frail (N=17)	Total (N=128)	Statistical test
	Variable (unit)	Mean ± SD	Mean ± SD	Mean ± SD	Mean ± SD	Mean ± SD	*p*
Physical characteristics	***Age (years)***	37 ± 8	66 ± 8	73 ± 8	74 ± 6	62 ± 17	*<0.001**
	Weight (kg)	76.3 ± 18.4	75.3 ± 12.4	75 ± 13.9	72 ± 15.2	75 ± 15.1	*0.819*
	Height (m)	1.72 ± 0.11	1.64 ± 0.09	1.61 ± 0.09	1.56 ± 0.08	1.64 ± 0.11	*<0.001**
	BMI (kg/m2)	25.61 ± 4.71	28.09 ± 4.01	29.06 ± 4.93	29.43 ± 5.05	27.97 ± 4.93	*0.005*
	Muscle strength (kg)	32.16 ± 11.38	32.55 ± 9.50	22.28 ± 8.44	18.90 ± 6.59	26.33 ± 10.75	*<0.001**
	Gait speed (s)	3.5 ± 0.8	3.7 ± 0.5	4.2 ± 1.7	6.4 ± 2.1	4.2 ± 1.6	*<0.001**
IPAQ	***Physical activity (h/week)***	13.3 ± 14.9	10.8 ± 4.8	8.9 ± 6.1	5.4 ± 4.7	10 ± 9.5	*0,010**
	IPA (min/day)	29 ± 55	4 ± 15	1 ± 8	0 ± 0	9 ± 32	*<0.001**
	MPA (min/day)	56 ± 64	62 ± 98	67 ± 71	50 ± 62	61 ± 73	*0,727**
	Walking (min/day)	117 ± 128	93 ± 41	76 ± 53	46 ± 40	86 ± 81	*0,007**
	Seated (min/day)	298 ± 154	255 ± 141	266 ± 128	307 ± 158	279 ± 142	*0,600**
Sex	**Female**	17	9	28	12	66	*0.287**
	Male	19	13	25	5	62	
Frailty criteria	**0**	26	22	0	0	48	*<0.001**
	1	7	0	24	0	32	
	2	3	0	29	0	32	
	3	0	0	0	13	13	
	4	0	0	0	3	3	
	5	0	0	0	1	1	

Abbreviations: IPA - intense physical activity, MPA - moderate physical activity, SD - standard deviation

* non parametric test

Table 4.2 Baseline characteristics according to frailty phenotype

4.2 Comorbidities.

Comorbidities were assessed according to sex and frailty phenotype.

Table 4.3 shows the distribution of comorbidities, risk factors, and use of the healthcare system according to sex. Most of the parameters were homogeneous except for COPD and alcohol abuse which were more frequent in men, and anxiety/depression and osteoporotic fractures which were more common in women.

Table 4.3. Comorbidities and risk factors according to sex					
	Sex	Female (N=66)	Male (N=62)	Total (N=128)	Statistical test*
	Variable	N (%)	N (%)	N (%)	p
Associated diseases	**Hypertension**	32 (48.5)	37 (59.7)	69 (53.9)	*0.204*
	Hyperlipidemia	37 (56.1)	35 (56.5)	72 (56.3)	*0.964*
	Diabetes Mellitus	13 (19.7)	15 (24.2)	28 (21.9)	*0.539*
	COPD	0 (0)	10 (16.1)	10 (7.8)	*0.001*
	Hearing impairment	10 (15.2)	9 (14.5)	19 (14.8)	*0.920*
	Visual impairment	24 (36.4)	20 (32.3)	44 (34.4)	*0.625*
	Previous stroke/TIA	5 (7.6)	6 (9.7)	11 (8.6)	*0.672*
	Congestive heart failure	5 (7.6)	3 (4.8)	8 (6.3)	*0.523*
	Heart disease	9 (13.6)	12 (19.4)	21 (16.4)	*0.383*
	Myocardial infarction	1 (1.5)	4 (6.5)	5 (3.9)	*0.150*
	Renal disease	6 (9.1)	5 (8.1)	11 (8.6)	*0.836*
	Arthritis/Osteoarthritis	26 (39.4)	16 (25.8)	42 (32.8)	*0.102*
	Anxiety/depression	27 (40.9)	10 (16.1)	37 (28.9)	*0.002*
	Osteoporotic fractures	21 (31.8)	0 (0)	21 (16.4)	*<0.001*
	Hepatopathy	1 (1.5)	1 (1.6)	2 (1.6)	*0.964*
	Dementia	7 (10.6)	4 (6.5)	11 (8.6)	*0.402*
	Connective tissue disease	6 (9.1)	10 (16.1)	16 (12.5)	*0.229*
	Previous malignancy**	10 (15.2)	9 (14.5)	19 (14.8)	*0.920*
	Peripheral vascular disease	2 (3)	3 (4.8)	5 (3.9)	*0.598*
	Peptic ulcer	4 (6.1)	4 (6.5)	8 (6.3)	*0.927*
Risk factors	**Smoking**	10 (15.2)	14 (22.6)	24 (18.8)	*0.282*
	Alcohol abuse	0 (0)	13 (21)	13 (10.2)	*<0.001*
	Falls	22 (33.3)	12 (19.4)	34 26.6)	*0.074*
	Obesity	26 (39.4)	16 (25.8)	42 (32.8)	*0.102*
Healthcare system use	***Primary care visits (N)***	1.7 ± 2	1.4 ± 1.7	1.5 ± 1.9	*0.448*
	ER visits (N)	0.4 ± 0.8	0.3 ± 0.7	0.4 ± 0.8	*0.918*
	Hospitalizations (N)	0.1 ± 0.3	0.1 ± 0.2	0.1 ± 0.3	*0.614*

Abbreviations: COPD - chronic obstructive pulmonary disease, TIA - transitory ischemic attack, ER - emergency room, N - number, **proven remission, no active treatment.

* non parametric test used for all the variables

Table 4.3 Comorbidities and risk factors according to sex

The distribution of comorbidities, risk factors, and healthcare system use according to frailty phenotype is represented in table 4.4, showing significant differences between groups for hypertension, hyperlipidemia, diabetes mellitus, hearing and visual impairment, congestive heart failure and heart disease, osteoarthritis, anxiety/depression, osteoporotic fractures, dementia, previous malignancy, falls and primary care visits.

Table 4.4 Comorbidities and risk factors according to frailty phenotype						
	Frailty Phenotype	Control (N=36)	Robust (N=22)	Prefrail (N=53)	Frail (N=17)	Statistical Test*
	Variable	N (%)	N (%)	N (%)	N (%)	p
Associated diseases	**Hypertension**	2 (5.6)	12 (54.5)	44 (83)	11 (64.7)	*<0.001*
	Hyperlipidemia	3 (8.3)	14 (63.6)	40 (75.5)	15 (88.2)	*<0.001*
	Diabetes Mellitus	0 (0)	2 (9)	20 (37.7)	6 (35.3)	*<0.001*
	COPD	0 (0)	2 (9)	6 (11.3)	2 (11.8)	*0.224*
	Hearing impairment	0 (0)	4 (18.2)	11 (20.8)	4 (23.5)	*0.030*
	Visual impairment	0 (0)	5 (22.7)	27 (50.9)	12 (70.6)	*<0.001*
	Previous stroke/TIA	0 (0)	2 (9)	8 (15.1)	1 (5.9)	*0.094*
	Congestive heart failure	0 (0)	0 (0)	5 (9.4)	3 (17.6)	*0.036*
	Heart disease	1 (2.8)	5 (22.7)	10 (18.9)	5 (29.4)	*0.049*
	Myocardial infarction	0 (0)	1 (4.5)	3 (5.7)	1 (5.9)	*0.552*
	Renal disease	0 (0)	2 (9)	8 (15.1)	1 (5.9)	*0.094*
	Arthritis/Osteoarthritis	1 (2.8)	9 (40.9)	23 (43.4)	9 (52.9)	*<0.001*
	Anxiety/depression	1 (2.8)	4 (18.2)	21 (39.6)	11 (64.7)	*<0.001*
	Osteoporotic fractures	1 (2.8)	3 (13.6)	10 (18.9)	7 (41.2)	*0.005*
	Hepatopathy	0 (0)	0 (0)	1 (1.9)	1 (5.9)	*0.389*
	Dementia	0 (0)	0 (0)	7 (13.2)	4 (23.5)	*0.008*
	Connective tissue disease	1 (2.8)	4 (18.2)	8 (15.1)	3 (17.6)	*0.212*
	Previous malignancy**	0 (0)	4 (18.2)	12 (22.6)	3 (17.6)	*0.028*
	Peripheral vascular disease	0 (0)	3 (13.6)	2 (3.8)	0 (0)	*0.052*
	Peptic ulcer	0 (0)	1 (4.5)	6 (11.3)	1 (5.9)	*0.184*
Risk factors	**Smoking**	9 (25)	7 (31.8)	7 (13.2)	1 (5.9)	*0.098*
	Alcohol abuse	1 (2.8)	4 (18.2)	4 (7.5)	4 (23.5)	*0.059*
	Falls	2 (5.6)	5 (22.7)	22 (41.5)	5 (29.4)	*0.002*
	Obesity	7 (19.4)	8 (36.4)	20 (37.7)	7 (41.2)	*0.244*
Healthcare system use	***Primary care visits (N)***	0.6 ± 1	1.4 ± 1.7	1.8 ± 1.9	2.7 ± 2.2	*<0.001*
	ER visits (N)	0.2 ± 0.5	0.4 ± 0.7	0.4 ± 0.7	0.7 ± 1.3	*0.296*
	Hospitalizations (N)	0 ± 0.2	0.1 ± 0.2	0 ± 0.1	0.2 ± 0.5	*0.308*

Abbreviations: COPD - chronic obstructive pulmonary disease, TIA - transitory ischemic attack, ER - emergency room, N - number, **proven remission, no active treatment.

* non parametric test used for all the variables

Table 4.4 Comorbidities and risk factors according to frailty phenotype

4.3 Ultrasound parameters.

Table 4.5 summarizes ultrasound parameters for all heads of the *quadriceps femoris* muscle according to sex. There were significant differences between sexes in almost all parameters except pennate angles for *rectus femoris, vastus intermedius,* and *vastus lateralis* heads as well as muscle thickness of *vastus lateralis* head.

Table 4.5 Ultrasound parameters according to sex					
Muscle	Sex	Female (N=66)	Male (N=62)	Total (N=128)	Statistical Test
	Variable (unit)	Mean ± SD	Mean ± SD	Mean ± SD	p
Rectus femoris	**SFT (cm)**	1.54 ± 0.61	0.72 ± 0.32	1.14 ± 0.64	*<0.001**
	MT (cm)	1.47 ± 0.40	1.62 ± 0.42	1.54 ± 0.41	*0.044*
	AREA (cm²)	5.91 ± 2.64	7.02 ± 2.86	6.45 ± 2.80	*0,023**
	EI Tr (AU)	66.27 ± 16.66	51.61 ± 16.69	59.17 ± 18.16	*<0.001**
	EI L (AU)	64.15 ± 16.91	49.13 ± 16.10	56.88 ± 18.10	*<0.001*
	PA (°)	13.20 ± 3.11	12.17 ± 2.94	12.69 ± 3.06	*0.061*
	PAC (°)	13.76 ± 3.56	13.22 ± 3.44	13.48 ± 3.50	*0,572**
Vastus intermedius	**MT (cm)**	1.32 ± 0.43	1.50 ± 0.47	1.41 ± 0.46	*0,035**
	EI Tr (AU)	57.80 ± 18.51	44.51± 17.87	51.42 ± 19.32	*<0.001*
	EI L (AU)	60.12 ± 19.08	47.50 ± 19.28	54.06 ± 20.12	*<0.001*
	PA (°)	14.60 ± 3.53	14.49 ± 3.54	14.55 ± 3.52	*0,770**
	PAC (°)	16.07 ± 3.97	16.67 ± 4.15	16.38 ± 4.05	*0.452*
Vastus medialis	**SFT (cm)**	1.33 ± 0.52	0.65 ± 0.31	1.00 ± 0.55	*<0.001**
	MT (cm)	3.69 ± 0.61	4.07 ± 0.61	3.87 ± 0.64	*<0.001**
	EI Tr (AU)	59.35 ± 14.49	49.45 ± 15.42	54.56 ± 15.70	*<0.001**
	EI L (AU)	67.03 ± 16.26	52.73 ± 15.25	60.10 ± 17.28	*<0.001**
	PA (°)	18.20 ± 3.67	20.07 ± 4.53	19.13 ± 4.21	*0.013*
	PAC (°)	21.24 ± 4.63	24.17 ± 5.70	22.67 ± 5.36	*0.002*
Vastus lateralis	**SFT (cm)**	1.43 ± 0.70	0.50 ± 0.28	0.98 ± 0.71	*<0.001**
	MT (cm)	1.80 ± 0.37	1.89 ± 0.33	1.84 ± 0.35	*0.146*
	EI Tr (AU)	59.37 ± 15.28	47.89 ± 16.76	53.81 ± 16.96	*<0.001*
	EI L (AU)	60.47 ± 15.79	51.68 ± 17.32	56.21 ± 17.06	*0.003*
	PA (°)	15.93 ± 3.37	16.12 ± 3.26	16.02 ± 3.31	*0,747**
	PAC (°)	16.26 ± 3.14	16.82 ± 3.83	16.54 ± 3.49	*0.367*

Abbreviations: SFT - superficial fat thickness, MT - muscle thickness, EI - echointensity, Tr - transversal plane, L - longitudinal plane, PA - pennate angle, PAC pennate angle in contraction, AU - arbitrary units

* non parametric test

Table 4.5 Ultrasound parameters according to sex

Ultrasound parameters according to frailty phenotype are summarized in table 4.6. There were significant differences between groups for all the parameters of the *rectus femoris* muscle. Muscle thickness of all *quadriceps* heads showed significant differences between groups. As for the echointensity, there were significant differences between groups for the *rectus femoris* head, whereas *vastus intermedius*, *vastus medialis,* and *vastus lateralis* heads did not show differences between groups. Pennate angles at rest and in contraction showed significant differences between groups for all muscle heads except *vastus medialis* at rest.

Table 4.6 Ultrasound parameters according to frailty phenotype						
Muscle	Frailty Phenotype	Control (N=36)	Robust (N=22)	Prefrail (N=53)	Frail (N=17)	Statistical Test
	Variable (unit)	Mean ± SD	Mean ± SD	Mean ± SD	Mean ± SD	p
Rectus femoris	**SFT (cm)**	1.16 ± 0.57	0.82 ± 0.49	1.22 ± 0.68	1.29 ± 0.73	*0,031**
	MT (cm)	1.91 ± 0.35	1.56 ± 0.36	1.38 ± 0.34	1.27 ± 0.28	*<0.001*
	AREA (cm²)	9.23 ± 2.70	6.54 ± 2.08	5.06 ± 1.87	4.75 ± 1.48	*<0.001**
	EI Tr (AU)	49.43 ± 17.82	61.89 ± 20.04	62.00 ± 15.60	67.46 ± 16.82	*0,001**
	EI L (AU)	48.76 ± 16.80	58.54 ± 20.24	59.75 ± 16.94	62.97 ± 17.15	*0.012*
	PA (°)	14.10 ± 2.75	12.54 ± 2.96	11.89 ± 2.92	12.24 ± 3.49	*0.008*
	PAC (°)	15.48 ± 3.68	13.22 ± 3.62	12.20 ± 2.82	13.13 ± 2.67	*0,002**
Vastus intermedius	**MT (cm)**	1.65 ± 0.50	1.40 ± 0.38	1.26 ± 0.39	1.36 ± 0.49	*0,002**
	EI Tr (AU)	52.42 ± 17.45	53.45 ± 19.64	50.84 ± 19.71	48.43 ± 22.60	*0.854*
	EI L (AU)	55.31 ± 19.24	55.95 ± 20.37	53.97 ± 19.74	49.24 ± 23.66	*0.732*
	PA (°)	15.48 ± 3.05	14.31 ± 3.82	13.62 ± 3.63	15.31 ± 3.50	*0,038**
	PAC (°)	19.40 ± 3.29	15.47 ± 3.20	14.80 ± 3.92	14.31 ± 2.79	*<0.001*
Vastus medialis	**SFT (cm)**	1.02 ± 0.47	0.80 ± 0.50	1.03 ± 0.61	1.10 ± 0.53	*0,144**
	MT (cm)	4.40 ± 0.64	3.78 ± 0.60	3.70 ± 0.48	3.44 ± 0.45	*<0.001**
	EI Tr (AU)	52.78 ± 16.19	57.17 ± 18.59	53.91 ± 14.48	56.96 ± 14.94	*0,867**
	EI L (AU)	56.67 ± 17.02	58.88 ± 17.25	61.77 ± 17.03	63.76 ± 18.75	*0,536**
	PA (°)	20.18 ± 4.34	18.44 ± 3.43	18.72 ± 4.54	19.13 ± 3.69	*0.359*
	PAC (°)	24.73 ± 5.70	21.00 ± 3.66	22.31 ± 5.51	21.46 ± 5.04	*0.035*
Vastus lateralis	**SFT (cm)**	1.02 ± 0.62	0.75 ± 0.59	0.99 ± 0.69	1.19 ± 0.99	*0,217**
	MT (cm)	2.10 ± 0.37	1.77 ± 0.28	1.75 ± 0.30	1.66 ± 0.26	*<0.001*
	EI Tr (AU)	47.99 ± 15.69	53.88 ± 19.39	56.18 ± 17.26	58.67 ± 12.74	*0.081*
	EI L (AU)	49.23 ± 15.00	59.41 ± 19.10	57.34 ± 17.12	63.32 ± 14.35	*0.017*
	PA (°)	18.24 ± 3.27	15.72 ± 3.06	14.87 ± 2.60	15.18 ± 3.52	*<0.001**
	PAC (°)	18.32 ± 3.04	16.46 ± 3.73	15.36 ± 3.18	16.53 ± 3.73	*0.001*

Abbreviations: SFT - superficial fat thickness, MT - muscle thickness, EI - echointensity, Tr - transversal plane, L - longitudinal plane, PA - pennate angle, PAC pennate angle in contraction, AU - arbitrary units

* non parametric test

Table 4.6 Ultrasound parameters according to frailty phenotype

Post-hoc analysis of statistically significant variables with normal distribution showed the following (table 4.6):

- There were differences in muscle thickness of *rectus femoris* and *vastus lateralis* as well as the pennate angle in the contraction of *vastus intermedius* between controls and all three experimental groups. No differences in these parameters were noted between robust, prefrail, and frail individuals.
- Echointesity of *rectus femoris* measured in the longitudinal plane was different between the control and prefrail group as well as the control and frail group. No differences were found between the robust and prefrail nor the robust and frail group.
- The pennate angle of the *rectus femoris* was different between the control and prefrail groups. There were no differences between the rest of the groups.

- There was a significant difference in pennate angle in the contraction of *vastus medialis* between groups, but in post hoc analysis there was no significant difference (p=0.058 for control and robust group)
- The echointensity of *vastus lateralis* in the longitudinal plane was different between the control and frail group. No differences were found between the rest of the groups.
- There were significant differences in pennate angle in the contraction of *vastus lateralis* between the control and prefrail group, but no differences were shown between the robust and prefrail nor the robust and frail group.

Table 4.6A Post-hoc analysis of ultrasound parameters according to frality phenotype

Variable	Group	Control	Robust	Prefrail	Frail
MT RF	Control		0.001	0.000	0.000
	Robust	0.001		0.237	0.057
	Prefrail	0.000	0.237		1.000
	Frail	0.000	0.057	1.000	
EI L RF	Control		0.249	0.026	0.041
	Robust	0.249		1.000	1.000
	Prefrail	0.026	1.000		1.000
	Frail	0.041	1.000	1.000	
PA RF	Control		0.311	0.004	0.282
	Robust	0.311		1.000	1.000
	Prefrail	0.004	1.000		1.000
	Frail	0.282	1.000	1.000	
PAC VM	Control		0.058	0.214	0.238
	Robust	0.058		1.000	1.000
	Prefrail	0.214	1.000		1.000
	Frail	0.238	1.000	1.000	
PAC VI	Control		0.001	0.000	0.001
	Robust	0.001		1.000	1.000
	Prefrail	0.000	1.000		1.000
	Frail	0.001	1.000	1.000	
MT VL	Control		0.001	0.000	0.000
	Robust	0.001		1.000	1.000
	Prefrail	0.000	1.000		1.000
	Frail	0.000	1.000	1.000	
EI L VL	Control		0.150	0.152	0.027
	Robust	0.150		1.000	1.000
	Prefrail	0.152	1.000		1.000
	Frail	0.027	1.000	1.000	
PAC VL	Control		0.241	0.000	0.442
	Robust	0.241		1.000	1.000
	Prefrail	0.000	1.000		1.000
	Frail	0.442	1.000	1.000	

Abbreviations: MT - muscle thickness, EI L - echointensity in longitudinal plane, PA - pennate angle, PAC - pennate angle in contraction, RF - rectus femoris, VM - vastus medialis, VI - vastus intermedius, VL - vastus lateralis

cells in yellow represent significant difference between groups (p<0.05)

Table 4.6A Post-hoc analysis of ultrasound parameters according to frailty phenotype

4.4 Biochemical analyses.

A total of 61 blood samples were analysed. There were 34 female (56%) and 27 male (44%) individuals. There were 18 (29%) subjects assigned to the control group and 8 (13%) robust, 26 (43%) prefrail, and 9 (15%) frail patients. General blood analysis was performed as well as hormone status. Additionally, oxidative stress parameters were assessed.

Table 4.7 shows biochemical parameters (hemogram, proteins, glucose metabolism, renal and liver function, bone metabolism, ions, lipid metabolism, cardiovascular risk parameters, iron metabolism) and hormones (TSH, PTH, cortisol, insulin, IGF-1) according to sex.

There were differences between sexes in red blood cell parameters (RBC count, haemoglobin, haematocrit, MCH, MCHC), platelets, creatinine, phosphorus, total cholesterol, HDL, LDL, ferritin, and TS. Groups were homogeneous according to hormone levels.

Table 4.7 Biochemical parameters and hormones according to sex					
	Sex	Female (N=34)	Male (N=27)	Total (N=61)	Statistical Test
	Variable (unit) [reference value]	Mean ± SD	Mean ± SD	Mean ± SD	p
Hemogram	**Leucocytes** (10^3/µL) [3.8-10.8]	6.76 ± 1.55	6.84 ± 1.59	6.80 ± 1.56	*0.853*
	Neutrophils (10^3/µL) [40.0-75.0]	3.64 ± 1.14	3.86 ± 1.21	3.74 ± 1.17	*0,384**
	Lymphocytes (10^3/µL) [20.0-45.0]	2.34 ± 0.90	2.04 ± 0.50	2.20 ± 0.76	*0,171**
	RBC (10^6/µL) [4.7-6.0]	4.50 ± 0.39	4.77 ± 0.50	4.62 ± 0.46	*0.018*
	HGB (g/dL) [13.5-18.0]	13.62 ± 1.05	14.83 ± 1.30	14.16 ± 1.31	*0.000*
	HCT (%) [42.0-52.0]	40.45 ± 3.09	43.46 ± 3.94	41.81 ± 3.78	*0.001*
	MCV (fL) [78.0-100.0]	90.03 ± 4.04	91.34 ± 5.72	90.62 ± 4.87	*0.293*
	MCH (pg) [27.0-31.0]	30.31 ± 1.49	31.19 ± 2.11	30.70 ± 1.83	*0,015**
	MCHC (g/dL) [32.0-36.0]	33.66 ± 0.77	34.12 ± 0.79	33.87 ± 0.81	*0.025*
	Platelets (10^3/µL) [135.0-350.0]	234.15 ± 54.41	205.78 ± 46.01	221.34 ± 52.35	*0.033*
Proteins	**Proteins** (g/dL) [6.6-8.3]	6.80 ± 0.39	6.90 ± 0.52	6.85 ± 0.45	*0.405*
	CRP (mg/L) [0.0-0.5]	0.39 ± 0.43	0.38 ± 0.45	0.39 ± 0.43	*0,689**
	Albumin (g/dL) [3.4-5.4]	4.17 ± 0.40	4.20 ± 0.34	4.19 ± 0.37	*0,589**
	Glucose (mg/dL) [74.0-100.0]	106.94 ± 28.64	105.11 ± 22.70	106.11 ± 25.93	*0,921**
Renal function	**Urea** (mg/dL) [17.0-43.0]	33.74 ± 9.29	37.04 ± 7.45	35.23 ± 8.60	*0.134*
	Creatinine (mg/dL) [0.67-1.17]	0.71 ± 0.18	0.85 ± 0.15	0.78 ± 0.18	*0.001*
	Glomerular filtration rate (mL/min/1.73m²)	82.40 ± 12.98	83.42 ± 9.56	82.86 ± 11.48	*0,639**
Bone metabolism	**Calcium** (mg/dL) [8.8-10.6]	9.50 ± 0.31	9.54 ± 0.38	9.52 ± 0.34	*0.633*
	Phosphorus (mg/dL) [2.5-4.5]	3.50 ± 0.47	3.21 ± 0.57	3.37 ± 0.53	*0.032*
Liver function	**ALT** (U/L) [10.0-45.0]	22.59 ± 16.92	20.46 ± 6.78	21.63 ± 13.28	*0,547**
	ALP (U/L) [30.0-120.0]	81.32 ± 26.03	69.32 ± 17.82	75.90 ± 23.31	*0,082**
Ions	**Chlorine** (mEq/L) [98.0-106.0]	103.15 ± 2.66	103.39 ± 2.86	103.26 ± 2.73	*0.728*
	Potassium (mEq/L) [3.5-5.1]	4.39 ± 0.28	4.45 ± 0.34	4.42 ± 0.31	*0.429*
	Sodium (mEq/L) [136.0-146.0]	139.5 ± 2.43	139.64 ± 1.75	139.56 ± 2.13	*0,828**
Lipid metabolism	**Total cholesterol** (mg/dL) [100.0-200.0]	206.70 ± 34.31	177.57 ± 31.76	193.55 ± 36.02	*0.001*
	Triglycerides (mg/dL) [50.0-150.0]	132.50 ± 81.38	132.46 ± 62.73	132.48 ± 72.97	*0,641**
	HDL cholesterol (mg/dL) [40.0-200.0]	58.32 ± 17.44	48.36 ± 11.35	53.82 ± 15.70	*0,027**
	LDL cholesterol (mg/dL) [0.0-130.0]	123.88 ± 29.05	104.82 ± 22.36	115.27 ± 27.74	*0.006*
Cardiovascular risk	**CPK** (U/ml) [24.0-171.0]	142.35 ± 179.11	102.11 ± 42.71	124.18 ± 136.27	*0,983**
	Total cholesterol/HDL	3.80 ± 1.11	3.83 ± 0.98	3.81 ± 1.04	*0,453**
	Homocysteine (mmol/L) [4.3-11.1]	10.38 ± 3.12	11.88 ± 4.28	11.06 ± 3.73	*0,090**
Iron metabolism	**Ferritin** (ng/mL) [20.0-250.0]	91.09 ± 91.68	190.96 ± 171.99	136.19 ± 141.95	*0,001**
	Iron (µg/dL) [70.0-180.0]	81.68 ± 26.16	93.32 ± 32.34	86.93 ± 29.45	*0.122*
	TS (%) [25.0-50.0]	25.31 ± 9.08	31.15 ± 10.98	27.95 ± 10.32	*0.025*
	Vitamin D (ng/mL) [30.0-100.0]	26.68 ± 14.97	24.19 ± 7.74	25.56 ± 12.22	*0,783**
Hormones	**Cortisol** (µg/dL) [5.0-25.0]	11.80 ± 2.84	10.99 ± 2.99	11.44 ± 2.91	*0.283*
	Insulin (µIU/mL) [2.6-24.9]	9.00 ± 7.85	9.16 ± 9.12	9.07 ± 8.36	*0,420**
	PTH (pg/mL) [10.0-55.0]	50.56 ± 25.70	37.89 ± 16.66	44.95 ± 22.89	*0,074**
	TSH (mIU/L) [0.37-4.7]	2.34 ± 1.21	1.99 ± 0.87	2.18 ± 1.08	*0,369**
	IGF-1 (ng/ml) [sex/age dependent**]	115.35 ± 39.03	124.84 ± 70.58	119.62 ± 55.18	*0,829**

Abbreviations: N - number, SD - standard deviation, RBC - red blood cells, HGB - hemoglobin, HCT - hematocrit, MCV - mean corpuscular volume, MCH - mean corpuscular hemoglobin, MCHC - mean corpuscular hemoglobin concentration, ALT - alanine aminotransferase, ALP - alkaline phosphatase, HDL - high-density lipoprotein, LDL - low-density lipoprotein, CPK - creatine phosphokinase, TS - transferrin saturation, CRP- C-reactive protein, PTH - parathormone, TSH - thyroid stimulating hormone, IGF-1 - Insulin-like growth factor 1, IU - international units

* non parametric test

** values available in annex table 4.7A

Table 4.7 Biochemical parameters and hormones according to sex

Table 4.8 summarizes biochemical parameters and hormones according to frailty phenotype.

There were significant differences between groups in MCV and MCH levels, proteins, glucose, urea, glomerular filtration rate, potassium, sodium, homocysteine, albumin, PTH, and IGF-1.

Table 4.8 Biochemical parameters and hormones according to frailty phenotype						
	Frailty phenotype	Control (N=18)	Robust (N=8)	Prefrail (N=26)	Frail (N=9)	Statistical Test
	Variable (unit) [reference value]	Mean ± SD	Mean ± SD	Mean ± SD	Mean ± SD	p
Hemogram	**Leucocytes** (10^3/µL) [3.8-10.8]	6.27 ± 1.52	6.98 ± 1.35	7.00 ± 1.50	7.10 ± 1.96	*0.410*
	Neutrophils (10^3/µL) [40.0-75.0]	3.30 ± 1.12	3.64 ± 1.06	4.10 ± 1.18	3.62 ± 1.13	*0.176**
	Lymphocytes (10^3/µL) [20.0-45.0]	2.23 ± 0.59	2.48 ± 0.47	2.03 ± 0.62	2.43 ± 1.40	*0.137**
	RBC (10^6/µL) [4.7-6.0]	4.79 ± 0.52	4.62 ± 0.36	4.61 ± 0.33	4.33 ± 0.63	*0.102*
	HGB (g/dL) [13.5-18.0]	14.22 ± 1.33	14.48 ± 1.16	14.37 ± 1.31	13.17 ± 1.08	*0.093*
	HCT (%) [42.0-52.0]	41.72 ± 3.88	42.31 ± 2.79	42.60 ± 3.92	39.18 ± 3.21	*0.127*
	MCV (fL) [78.0-100.0]	87.27 ± 2.63	91.66 ± 3.38	92.23 ± 3.98	91.59 ± 8.28	*0.005*
	MCH (pg) [27.0-31.0]	29.74 ± 1.19	31.31 ± 1.36	31.13 ± 1.48	30.80 ± 3.29	*0.015**
	MCHC (g/dL) [32.0-36.0]	34.07 ± 0.87	34.15 ± 0.74	33.74 ± 0.72	33.59 ± 0.91	*0.278*
	Platelets (10^3/µL) [135.0-350.0]	238.72 ± 58.00	239.13 ± 52.82	206.30 ± 48.68	215.89 ± 42.60	*0.155*
Proteins	**Proteins** (g/dL) [6.6-8.3]	7.14 ± 0.50	6.83 ± 0.40	6.66 ± 0.35	6.82 ± 0.41	*0.004*
	CRP (mg/L) [0.0-0.5]	0.27 ± 0.34	0.26 ± 0.26	0.47 ± 0.49	0.49 ± 0.52	*0.338**
	Albumin (g/dL) [3.4-5.4]	4.36 ± 0.34	4.23 ± 0.67	4.07 ± 0.27	4.16 ± 0.26	*0.032**
	Glucose (mg/dL) [74.0-100.0]	85.61 ± 10.66	107.13 ± 18.15	117.56 ± 28.04	111.89 ± 24.84	*<0.001**
Renal function	**Urea** (mg/dL) [17.0-43.0]	32.33 ± 8.35	36.79 ± 7.09	38.25 ± 8.36	30.61 ± 8.31	*0.037*
	Creatinine (mg/dL) [0.67-1.17]	0.77 ± 0.13	0.78 ± 0.19	0.80 ± 0.20	0.70 ± 0.21	*0.512*
	Glomerular filtration rate (mL/min/1.73m²)	88.95 ± 3.11	84.40 ± 9.96	78.25 ± 13.66	83.13 ± 11.60	*0.009**
Bone metabolism	**Calcium** (mg/dL) [8.8-10.6]	9.67 ± 0.30	9.46 ± 0.40	9.42 ± 0.36	9.54 ± 0.26	*0.121*
	Phosphorus (mg/dL) [2.5-4.5]	3.41 ± 0.56	3.50 ± 0.49	3.27 ± 0.53	3.44 ± 0.59	*0.669*
Liver function	**ALT** (U/L) [10.0-45.0]	19.11 ± 4.78	34.13 ± 29.20	20.00 ± 9.11	20.44 ± 9.99	*0.177**
	ALP (U/L) [30.0-120.0]	69.00 ± 19.06	81.88 ± 34.59	77.63 ± 22.11	79.22 ± 23.84	*0.568**
Ions	**Chlorine** (mEq/L) [98.0-106.0]	101.94 ± 2.34	104.50 ± 2.83	103.81 ± 2.94	103.11 ± 1.96	*0.069*
	Potassium (mEq/L) [3.5-5.1]	4.27 ± 0.25	4.60 ± 0.33	4.50 ± 0.33	4.32 ± 0.14	*0.015*
	Sodium (mEq/L) [136.0-146.0]	138.17 ± 2.75	140.00 ± 1.20	140.33 ± 1.73	139.67 ± 1.00	*0.017**
Lipid metabolism	**Total cholesterol** (mg/dL) [100.0-200.0]	190.78 ± 24.92	205.63 ± 34.59	191.11 ± 40.68	195.67 ± 44.26	*0.771*
	Triglycerides (mg/dL) [50.0-150.0]	103.67 ± 68.34	132.75 ± 76.49	152.85 ± 76.45	128.78 ± 57.28	*0.071**
	HDL cholesterol (mg/dL) [40.0-200.0]	55.78 ± 15.36	61.88 ± 19.90	49.44 ± 11.50	55.89 ± 21.44	*0.323**
	LDL cholesterol (mg/dL) [0.0-130.0]	114.33 ± 20.27	117.25 ± 27.87	115.78 ± 31.39	113.89 ± 33.18	*0.993*
Cardiovascular risk	**CPK** (U/ml) [24.0-171.0]	194.22 ± 235.11	100.00 ± 21.67	96.15 ± 44.86	89.67 ± 39.67	*0.151**
	Total cholesterol/HDL	3.67 ± 1.13	3.56 ± 1.10	4.00 ± 1.02	3.76 ± 0.95	*0.475**
	Homocysteine (mmol/L) [4.3-11.1]	9.02 ± 2.60	11.48 ± 2.40	12.34 ± 4.43	10.91 ± 2.84	*0.016**
Iron metabolism	**Ferritin** (ng/mL) [20.0-250.0]	143.67 ± 193.75	188.63 ± 168.30	131.48 ± 104.86	88.78 ± 88.74	*0.314**
	Iron (µg/dL) [70.0-180.0]	91.17 ± 34.05	84.25 ± 16.92	87.37 ± 31.27	79.56 ± 24.75	*0.807*
	TS (%) [25.0-50.0]	28.37 ± 10.77	26.65 ± 6.06	29.02 ± 11.12	25.06 ± 10.81	*0.773*
	Vitamin D (ng/mL) [30.0-100.0]	25.41 ± 7.18	28.20 ± 9.50	25.64 ± 16.18	23.27 ± 9.27	*0.355**
Hormones	**Cortisol** (µg/dL) [5.0-25.0]	11.71 ± 3.47	11.96 ± 2.98	10.81 ± 2.25	12.27 ± 3.43	*0.514*
	Insulin (µIU/mL) [2.6-24.9]	6.79 ± 4.73	6.44 ± 3.92	10.21 ± 10.04	12.69 ± 10.53	*0.295**
	PTH (pg/mL) [10.0-55.0]	33.44 ± 13.81	42.00 ± 23.74	51.81 ± 25.63	50.78 ± 21.90	*0.039**
	TSH (mIU/L) [0.37-4.7]	2.12 ± 0.85	2.43 ± 1.01	2.09 ± 0.76	2.37 ± 2.09	*0.701**
	IGF-1 (ng/ml) [sex/age dependent**]	165.76 ± 64.11	115.89 ± 49.34	99.88 ± 28.98	83.69 ± 42.80	*<0.001**

Abbreviations: N - number, SD - standard deviation, RBC - red blood cells, HGB - hemoglobin, HCT - hematocrit, MCV - mean corpuscular volume, MCH - mean corpuscular hemoglobin, MCHC - mean corpuscular hemoglobin concentration, ALT - alanine aminotransferase, ALP - alkaline phosphatase, HDL - high-density lipoprotein, LDL - low-density lipoprotein, CPK - creatine phosphokinase, TS - transferrin saturation, CRP- C-reactive protein, PTH - parathormone, TSH - thyroid stimulating hormone, IGF 1 - Insulin-like growth factor 1, IU - international units

* non parametric test

** values available in annex table 4.7A

Table 4.8 Biochemical parameters and hormones according to frailty phenotype

Table 4.9 shows cytokines (ITAC, fractalkine, IFN-γ, IL-10, MIP-3a, IL-12p70, IL-13, IL-17a, IL-1b, IL-2, IL-4, IL-23, IL-6, IL-7, IL-8, and TNF-α) and oxidative stress parameters (MDA and oxidized proteins) according to sex.

Both sexes were homogeneous for all the parameters except for MIP-3a.

As to oxidative stress parameters, there were significant differences in levels of oxidized proteins.

Table 4.9 Cytokines and oxidative stress parameters according to sex

	Sex	Female (N=34)	Male (N=27)	Total (N=61)	Statistical Test
	Variable (unit) [reference intervals**]	Mean ± SD	Mean ± SD	Mean ± SD	p
Cytokines	**ITAC** (pg/mL) [17.67-78.02]	37.94 ± 13.39	38.66 ± 17.31	38.26 ± 15.12	*0,794**
	Fractalkine (pg/mL) [63.80-492.43]	240.68 ± 102.98	209.03 ± 98.56	226.67 ± 101.45	*0.229*
	IFN-γ (pg/mL) [3.51-61.61]	22.10 ± 15.44	21.70 ± 12.47	21.93 ± 14.09	*0,760**
	IL-10 (pg/mL) [0.12-38.87]	10.11 ± 5.93	10.37 ± 10.04	10.22 ± 7.94	*0,495**
	MIP-3a (pg/mL) [4.81-64.21]	22.80 ± 12.80	28.35 ± 13.27	25.26 ± 13.20	*0,043**
	IL-12p70 (pg/mL) [0.0-20.27]	3.65 ± 1.96	4.82 ± 5.51	4.17 ± 3.95	*0,942**
	IL-13 (pg/mL) [0.0-23.5]	6.02 ± 4.43	4.86 ± 5.47	5.51 ± 4.91	*0,115**
	IL-17a (pg/mL) [2.58-55.26]	20.47 ± 13.82	21.79 ± 13.91	21.05 ± 13.76	*0,611**
	IL-1β (pg/mL) [0.06-4.46]	0.83 ± 0.53	1.15 ± 1.19	0.97 ± 0.89	*0,392**
	IL-2 (pg/mL) [0.50-13.82]	4.38 ± 2.27	5.68 ± 3.73	4.95 ± 3.05	*0,199**
	IL-4 (pg/mL) [0.0-52.02]	9.99 ± 13.19	8.84 ± 8.91	9.48 ± 11.42	*0,777**
	IL-23 (pg/mL) [20.31-843.68]	327.41 ± 232.69	277.39 ± 256.11	305.27 ± 242.55	*0,251**
	IL-6 (pg/mL) [0.35-8.88]	2.88 ± 1.90	3.46 ± 2.25	3.13 ± 2.06	*0,376**
	IL-7 (pg/mL) [0.70-16.27]	9.43 ± 3.90	8.77 ± 4.33	9.14 ± 4.07	*0.532*
	IL-8 (pg/mL) [3.57-44.44]	11.40 ± 8.55	13.84 ± 10.03	12.48 ± 9.23	*0,096**
	TNF-α (pg/mL) [4.64-15.43]	8.38 ± 2.42	9.17 ± 2.51	8.73 ± 2.47	*0,110**
Oxidative stress	**MDA** (μM)	1.63 ± 0.50	1.81 ± 0.63	1.71 ± 0.57	*0,213**
	Protox (A.U.)	113.44 ± 67.11	77.53 ± 42.59	97.22 ± 59.70	*0,017**

Abbreviations: ITAC - interferon-inducible T-cell alpha chemoattractant, IFNγ - interferon gamma, IL - interleukin, MIP - Macrophage Inflammatory Protein, TNFα - Tumour Necrosis Factor Alpha, MDA - malondialdehyde, Protox - oxidized proteins, N - number, A.U. - arbitrary units

* non parametric test

** estimated intervals, calculated from control group as 2.5th and 97.5th percentiles

Table 4.9 Cytokines and oxidative stress parameters according to sex

Cytokines according to frailty phenotype are summarized in table 4.10.

Significant differences between groups were found for the levels of IFN-γ, MIP-3a, IL-12p70, IL-13, IL-17a, IL-1b, IL-2, IL-4, IL-7, and IL-8. There were no differences in levels of ITAC, fractalkine, IL-10, IL-23, IL-6, and TNF-α.

Note that there were no differences between groups in oxidative stress parameters.

Table 4.10 Cytokines and oxidative stress parameters according to frailty phenotype						
	Frailty Phenotype	Control (N=18)	Robust (N=8)	Prefrail (N=26)	Frail (N=9)	Statistical Test
	Variable (unit) [reference intervals**]	Mean ± SD	Mean ± SD	Mean ± SD	Mean ± SD	p
Cytokines	**ITAC** (pg/mL) [17.67-78.02]	37.67 ± 16.99	39.49 ± 16.14	37.45 ± 15.44	40.69 ± 10.79	*0.753**
	Fractalkine (pg/mL) [63.80-492.43]	257.21 ± 61.25	235.20 ± 120.81	195.42 ± 96.49	248.30 ± 146.58	*0.208*
	IFN-γ (pg/mL) [3.51-61.61]	32.78 ± 16.52	22.53 ± 12.92	13.52 ± 6.14	23.96 ± 12.05	*<0.001**
	IL-10 (pg/mL) [0.12-38.87]	13.14 ± 10.36	10.74 ± 9.19	7.90 ± 5.41	10.65 ± 6.49	*0.196**
	MIP-3a (pg/mL) [4.81-64.21]	31.73 ± 16.78	30.79 ± 13.80	18.20 ± 6.63	27.78 ± 10.50	*0.002**
	IL-12p70 (pg/mL) [0.0-20.27]	5.69 ± 3.42	6.72 ± 8.20	2.71 ± 1.73	3.04 ± 2.00	*0.004**
	IL-13 (pg/mL) [0.0-23.5]	7.76 ± 5.27	3.25 ± 3.24	4.28 ± 3.06	6.55 ± 7.80	*0.044**
	IL-17a (pg/mL) [2.58-55.26]	30.67 ± 14.62	23.03 ± 16.06	13.37 ± 7.45	22.25 ± 12.71	*0.002**
	IL-1β (pg/mL) [0.06-4.46]	1.52 ± 1.29	1.03 ± 0.62	0.61 ± 0.39	0.87 ± 0.70	*0.002**
	IL-2 (pg/mL) [0.50-13.82]	6.35 ± 2.41	6.29 ± 4.46	3.69 ± 2.61	4.60 ± 2.69	*0.005**
	IL-4 (pg/mL) [0.0-52.02]	14.85 ± 13.79	7.33 ± 3.53	5.32 ± 7.28	12.65 ± 16.14	*0.010**
	IL-23 (pg/mL) [20.31-843.68]	365.82 ± 223.71	277.19 ± 244.42	280.80 ± 266.35	279.82 ± 221.78	*0.309**
	IL-6 (pg/mL) [0.35-8.88]	3.86 ± 2.31	3.55 ± 3.14	2.54 ± 1.40	3.03 ± 1.82	*0.336**
	IL-7 (pg/mL) [0.70-16.27]	11.29 ± 3.46	9.53 ± 4.30	7.54 ± 3.40	9.12 ± 5.26	*0.023*
	IL-8 (pg/mL) [3.57-44.44]	7.58 ± 1.95	14.68 ± 4.82	16.25 ± 12.17	9.45 ± 5.74	*0.004**
	TNF-α (pg/mL) [4.64-15.43]	8.22 ± 2.21	8.90 ± 1.45	8.69 ± 2.88	9.72 ± 2.39	*0.407**
Oxidative stress	**MDA** (μM)	1.84 ± 0.68	1.71 ± 0.49	1.74 ± 0.55	1.38 ± 0.28	*0.314**
	Protox (A.U.)	81.35 ± 35.63	84.10 ± 30.44	102.37 ± 74.53	125.21 ± 62.46	*0.438**

Abbreviations: ITAC - interferon-inducible T-cell alpha chemoattractant, IFNγ - interferon gamma, IL - interleukin, MIP - Macrophage Inflammatory Protein, TNFα - Tumour Necrosis Factor Alpha, MDA - malondialdehyde, Protox - oxidized proteins, N - number, A.U. - arbitrary units

* non parametric test

** estimated intervals, calculated from control group as 2.5th and 97.5th percentiles

Table 4.10 Cytokines and oxidative stress parameters according to frailty phenotype

4.5 Correlations.

Correlation analysis of all the variables of the study was performed in order to assess possible relationships among ultrasound, physical and biochemical parameters. These parameters were then selected and used in the regression analysis in order to determine their predictive value for frailty.

4.5.1. Frailty phenotype and baseline characteristics

Table 4.11 shows correlations between frailty phenotype and baseline characteristics. Statistically significant correlations are in yellow for p values <0.01 and in green for p<0.05. Cells in white represent non-significant correlation coefficients. Frailty phenotype showed a strong positive correlation with age (r=0.760), and a moderate positive correlation with gait speed and primary care visits (r=0.624 and 0.410 respectively). There was a moderate negative correlation between frailty phenotype and muscle strength (r=-0.614) and intense physical activity (r=-0.472) while there was a weak negative correlation for physical activity and walking (r= -0.229 and -0.252 respectively). A strong positive correlation was found between height and muscle

strength (r=0.704) and there was a moderate positive correlation between sex and muscle strength (r=0.678). The rest of the correlations are shown in table 4.11.

Table 4.11 Correlations of frailty phenotype and baseline characteristics (N = 128)

	Frailty phenotype	Sex	Weight	Height	BMI
Frailty phenotype	-	-.136	-.052	-,482**	,278**
Age	,760**	.021	-.012	-,381**	,250**
Gait speed	,624**	-.055	.026	-,283**	,210*
Muscle strenght	-,614**	,678**	,317**	,704**	-165
Primary care visits	,410**	-.067	-.085	-,275**	.106
ER visits	.159	-.009	.000	-.144	.117
Hospitalizations	.081	.045	-.011	-.045	.056
Physical activity	-,229**	.015	-.060	.017	-.142
IPA	-,472**	,178*	.041	,357**	-,224*
MPA	-.015	-,199*	.011	-.051	.031
Walking	-,252**	.002	-.051	.016	-.130
Seated	.003	,205*	,227*	,179*	.094
**The correlation is significant at the 0.01 level (bilateral).					
*The correlation is significant at the 0.05 level (bilateral).					

Abbreviations: BMI - body mass index, ER - emergency room, IPA - intense physical activity, MPA - moderate physical activity

Rho of Spearman used for statistical analysis

Table 4.11 Correlations of frailty phenotype and baseline characteristics

4.5.2. Ultrasound and functional parameters

The correlations of frailty phenotype with ultrasound and functional parameters are shown in table 4.12. There was a moderate inverse correlation between frailty phenotype and the area of the *rectus femoris* muscle head (r=-0.612). Frailty phenotype showed a moderate negative correlation with muscle thickness of *rectus femoris, vastus medialis,* and *vastus lateralis* heads (r=-0.563, -0.483, and -0.403 respectively), and weak negative correlation with *vastus intermedius* head (r=-0.292). There was also a moderate negative correlation between frailty phenotype and the pennate angle of *vastus intermedius* in contraction (r=-0.476), as well as a weak negative correlation with the pennate angle of *rectus femoris* and *vastus lateralis* muscle heads at rest and in contraction. A weak positive correlation was found for frailty phenotype and echointensity of *rectus femoris* and *vastus lateralis* muscles (data shown in the table for echointensity measured both in transverse and longitudinal planes).

On the other hand, moderate positive correlations were shown between muscle strength and area of *rectus femoris*, as well as muscle thickness of *vastus medialis* head (r=0.425 and 0.474 respectively). Other quadriceps heads showed a weak positive correlation with muscle strength

(for *rectus femoris* r=0.378, *vastus intermedius* r=0.299, and for *vastus lateralis* r=0.339). Inversely, there were negative correlations between muscle strength and echointensity, moderate for *rectus femoris* (r=-0.451) and weak for *vastus medialis* and *vastus lateralis* heads (r=-0.380 and – 0.382 respectively).

Weak inverse correlations were found between gait speed (represented as walking time in seconds) and muscle thickness of *rectus femoris*, *vastus medialis,* and *vastus lateralis* heads (r=-0.260, -0.280, and -0.323), area of *rectus femoris* (r=-0.334), as well as with pennate angle in the contraction of *rectus femoris* and *vastus intermedius* heads and pennate angles of *vastus lateralis* at rest and contracted. There were no correlations between gait speed and echointensity of any quadriceps heads.

Note the poor to no correlation between ultrasound parameters and self-reported physical activity parameters.

Table 4.12 Correlations of frailty phenotype with functional and ultrasound parameters (N = 128)								
	Frailty Phenotype	Gait speed	MS	Physical activity	IPA	MPA	Walking	Seated
MT RF	-,563**	-,260**	,378**	-.025	,219*	-.046	-.004	,182*
EI Tr RF	,336**	.101	-,451**	-.077	-.117	.048	-.069	-.030
EI LRF	,283**	.087	-,439**	.006	-.056	.022	.021	-.057
PA RF	-,281**	-.172	.082	-.010	.152	-.019	-.033	.004
PAC RF	-,309**	-,209*	,202*	-.073	.181	-.020	-.049	.099
MT VI	-,292**	-.162	,299**	-.030	.146	.036	-.019	,222*
EI Tr VI	-.079	-.137	-,227*	-.041	.091	-.043	-.019	-.001
EI LVI	-.082	-.100	-,245**	-.097	.099	-.063	-.076	.012
PA VI	-.175	-.101	.112	-.066	,224*	-.145	-.056	.157
PAC VI	-,476**	-,252**	,279**	-.080	,299**	-.001	-.069	.102
MT VM	-,483**	-,280**	,474**	.064	,219*	.050	.080	,188*
EI Tr VM	.047	-.114	-,253**	.014	-.032	-.044	.031	-.120
EI L VM	.131	-.086	-,380**	-.049	.010	-.051	-.034	-.108
PA VM	-.086	-.084	,290**	-.035	-.046	-.028	-.044	.165
PAC VM	-,176*	-.077	,364**	-.083	.084	-.004	-.076	,203*
MT VL	-,403**	-,246**	,339**	.049	,189*	.009	.070	.155
EI Tr VL	,236**	.076	-,382**	-.039	-.033	.041	-.044	.001
EI L VL	,263**	.033	-,281**	-.059	-.082	-.043	-.054	-.009
PA VL	-,386**	-,323**	,277**	-.160	,291**	.049	-.150	.104
PAC VL	-,308**	-,214*	,291**	-.091	,197*	,177*	-.084	.148
AREA RF	-,612**	-,334**	,425**	-.024	,385**	.000	-.006	.158
**The correlation is significant at the 0.01 level (bilateral).								
*The correlation is significant at the 0.05 level (bilateral).								

Abbreviations: MT - muscle thickness, EI - echointensity, Tr - transversal plane, L - longitudinal plane, PA - pennate angle, PAC pennate angle in contraction, RF - rectus femoris, VI - vastus intermedius, VM - vastus medialis, VL - vastus lateralis, MS - muscle strength, IPA - intense physical activity, MPA - moderate physical activity

Rho of Spearman used for statistical analysis

Table 4.12 Correlations of frailty phenotype with functional and ultrasound parameters

4.5.3. Comorbidities and ultrasound parameters

Correlations of comorbidities with ultrasound parameters were assessed, showing generally weak or no significant correlation. Comorbidities that showed correlation to 10 or more of 24 ultrasound parameters are represented in table 4.13: hypertension (10/24), visual loss (11/24), osteoarthritis (14/24), fractures/osteoporosis (14/24), falls (10/24) and obesity (11/24). Hypertension showed weak negative correlations to the area of the *rectus femoris* and pennate angle of *vastus lateralis*, r=-0.340 and -0.329 respectively as well as the pennate angle in contraction (r=-0.308) and muscle thickness of *rectus femoris* (r=-0.303). There were weak positive correlations between fractures/osteoporosis and obesity and superficial fat thickness of *rectus femoris*, r=0.302 and 0.306 respectively, as well as the superficial fat thickness of *vastus medialis*, r=0.311 and 0.302 respectively. The rest of the correlations are shown in table 4.13.

Diabetes mellitus and previous malignancy correlated to 7/24 and 6/24 parameters respectively. Hyperlipidemia, COPD, hearing loss, and anxiety/depression all had significant correlations to 5 of 24 parameters. Previous stroke, congestive heart failure, myocardial infarction, dementia, and alcohol abuse showed weak correlations to 4 of 24 ultrasound parameters. Connective tissue disease and peptic ulcer showed a correlation to 2/24 ultrasound parameters. Heart disease and peripheral vascular disease had a weak correlation to 1 of 24 ultrasound parameters. Finally, renal disease, hepatopathy, and smoking did not show a correlation to any of the ultrasound parameters assessed (0/24). A full table of comorbidities is available in annex table 4A. Note weak negative correlations between falls and the area of rectus femoris, muscle thickness of rectus femoris, vastus medialis y lateralis as well as the pennate angle in the contraction of rectus femoris and vastus medialis. Also, there were weak positive correlations between obesity and echointensity of all quadriceps heads as well as superficial fat thickness.

Table 4.13 Correlations of comorbidities with ultrasound parameters (N = 128)

	Hypertension	Visual Loss	Osteoarthritis	Fractures/ Osteoporosis	Falls	Obesity
SFT RF	-.054	.004	.090	,302**	.139	,306**
MT RF	-,303**	-,281**	-,216**	-,159*	-,148*	.004
EI Tr RF	.087	,152*	,279**	,271**	.133	,213**
EI LRF	.059	,151*	,288**	,209**	.122	,202**
PA RF	-,197**	-,177*	-.133	-.033	-.139	-.044
PAC RF	-,242**	-,218**	-,159*	-.055	-,173*	-.132
MT VI	-,164*	-,179*	-.107	-.091	-.083	,165*
EI Tr VI	-.112	-.074	.091	,174*	.107	,207**
EI LVI	-.101	-.046	.113	,157*	,144*	,238**
PA VI	-.148	-.021	-,173*	-.010	-.099	-.040
PAC VI	-,308**	-,257**	-,277**	-.065	-,273**	-.143
SFT VM	-.100	-.041	.095	,311**	,151*	,302**
MT VM	-,198**	-,276**	-,175*	-,230**	-,158*	-.011
EI Tr VM	-.049	-.037	.072	.118	.109	.046
EI L VM	-.010	.074	,226**	,189**	.098	,152*
PA VM	-.060	-.086	-.138	-,146*	-.069	.046
PAC VM	-.095	-.112	-,200**	-,162*	-,159*	.064
SFT VL	-.103	-.029	.074	,262**	.123	,230**
MT VL	-,197**	-,247**	-.101	-,176*	-,150*	.081
EI Tr VL	.075	.127	,243**	,255**	,150*	,231**
EI L VL	.124	.138	,224**	,224**	.121	,204**
PA VL	-,329**	-,207**	-,266**	-.126	-.104	.018
PAC VL	-,202**	-,210**	-,149*	-.094	-.069	-.028
AREA RF	-,340**	-,295**	-,241**	-,213**	-,206**	-.050

**The correlation is significant at the 0.01 level (bilateral).

*The correlation is significant at the 0.05 level (bilateral).

Abbreviations: MT - muscle thickness, EI - echointensity, PA - pennate angle, PAC pennate angle in contraction, RF - rectus femoris, VI - vastus intermedius, VM - vastus medialis, VL - vastus lateralis

Kendall's τ used for statistical analysis

Table 4.13 Correlations of comorbidities with ultrasound parameters

4.5.4. Ultrasound and biochemical parameters

Correlations between ultrasound and biochemical parameters (table 4.14), hormone levels (table 4.15), cytokines, and oxidative stress (table 4.16) were assessed. Correlations with frailty phenotype were added for each table.

Muscle thickness of all *quadriceps* heads as well as pennate angles of *vastus intermedius* and *lateralis* showed significant correlations with biochemical parameters and cytokine levels, while echointensity showed mostly no correlation with either of the blood parameters assessed. Pennate angles of *rectus femoris* and *vastus medialis* heads also did not have significant correlations with blood parameters.

For visibility purposes, ultrasound and biochemical parameters with the largest number of significant correlations per row/column were selected and shown in table 4.14. A full table of biochemical and ultrasound parameters is available in annex table 4B.

Moderate negative correlations were found between the superficial fat thickness of *vastus lateralis* and hemoglobin, ferritin, and creatinine levels (r=-0.467, -0.468, and -0.414 respectively). There was a moderate negative correlation between the area of the *rectus femoris* and MCV and MCH (r=-0.450 and -0.402 respectively). There was a moderate negative correlation between MCHC level and superficial fat thickness of *rectus femoris* and *vastus medialis*, r=-0.425 and -0.441 respectively. A moderate positive correlation was found between muscle thickness of *vastus medialis* and creatinine levels (r=0.439). There was a moderate positive correlation between the echointensity of *vastus lateralis* and total and LDL cholesterol levels, r=0.410 and 0.416 respectively. Finally, MCV and glucose showed a moderate positive correlation with frailty phenotype, r=0.428 and 0.564 respectively (data available in annex table 4B).

The rest of the correlations between ultrasound and biochemical parameters are shown in table 4.14.

Table 4.14. Correlations of ultrasound and biochemical parameters (N= 61)																	
	SFT RF	MT RF	EI LRF	PAC RF	MT VI	EI Tr VI	SFT VM	MT VM	PA VM	SFT VL	MT VL	EI Tr VL	EI L VL	PA VL	PAC VL	AREA RF	Frailty phenotype
RBC	-.267*	0.188	-.349**	-0.135	0.153	-0.148	-.267*	.361**	.292*	-.327**	0.179	-.262*	-.283*	0.172	.253*	.346**	-.328**
HGB	-.359**	0.017	-.318*	-.303*	-0.050	-0.125	-.367**	.289*	0.191	-.467**	0.003	-0.190	-0.235	-0.086	0.141	0.101	-0.186
HCT	-.289*	0.025	-.294*	-0.237	-0.008	-0.089	-.262*	.318*	0.170	-.414**	0.035	-0.176	-0.247	-0.029	0.125	0.123	-0.183
MCV	-0.140	-.310*	0.141	-0.103	-0.134	-0.011	-0.094	-0.182	-0.184	-0.159	-.346**	0.159	0.103	-.318*	-0.157	-.450**	,428**
MCH	-.392**	-.276*	0.020	-0.244	-0.212	-0.120	-.368**	-0.159	-0.142	-.360**	-.320*	0.072	0.065	-.354**	-0.132	-.402**	,308*
MCHC	-.425**	0.038	-0.216	-.298*	-0.211	-0.165	-.441**	-0.001	-0.011	-.292*	-0.109	-0.075	-0.039	-0.162	0.082	0.002	-0.185
Platelets	.320*	0.200	0.153	0.201	-0.014	.313*	.343**	0.032	-0.053	.388**	-0.094	0.189	0.100	0.080	0.185	0.172	-0.234
Proteins	0.116	0.218	-.255*	0.153	0.170	0.063	0.120	0.223	0.187	0.104	0.128	-0.224	-.297*	0.144	.390**	.296*	-.319*
Creatinine	-.319*	0.187	-0.220	-.282*	0.220	-0.161	-.271*	.439**	0.049	-.443**	0.186	-0.237	-0.207	-0.084	0.050	0.130	-0.055
ALT	-0.048	0.182	-0.174	-0.100	.327**	-0.029	0.004	.293*	.422**	-0.007	-0.041	-0.051	-0.052	0.137	0.245	0.114	-0.068
ALP	.271*	-0.022	0.186	-0.044	0.141	0.216	.367**	-0.094	-0.013	0.197	-0.010	.268*	0.164	-0.057	-0.075	-0.051	0.162
Total cholesterol	0.196	0.078	0.226	0.142	0.054	.251*	0.196	-0.051	.336**	0.118	-0.071	.336**	.410**	0.032	-0.038	0.038	-0.048
Triglycerides	-0.005	-0.044	0.041	-0.185	.271*	-0.130	0.064	0.106	.295*	-0.097	-0.006	0.110	0.116	0.020	0.073	-0.044	,276*
HDL cholesterol	0.089	0.104	0.016	0.148	-0.195	.275*	0.070	-0.110	-0.109	0.235	-0.191	0.157	0.097	-0.036	-0.045	0.087	-0.139
LDL cholesterol	0.219	0.004	.310*	0.163	0.013	.253*	0.189	-0.126	.320*	0.100	0.012	.316*	.416**	-0.020	-0.110	-0.032	-0.063
CPK	-0.131	0.099	-.309*	-0.152	-0.172	-0.028	-0.150	0.060	0.109	-0.112	0.041	-0.243	-0.213	0.087	0.083	0.190	-,289*
Ferritin	-.361**	0.047	-0.091	-0.159	0.176	-0.062	-0.232	0.217	.263*	-.468**	0.015	-0.066	-0.047	-0.116	0.044	-0.027	-0.047
TS	-0.221	-0.158	-0.250	-.423**	-0.104	-.303*	-0.192	0.125	0.044	-.305*	0.063	-0.118	-0.179	-0.009	0.201	-0.147	-0.036
CRP	.331**	0.041	0.201	0.123	0.223	-0.015	.366**	0.036	0.094	0.224	-0.105	0.244	0.246	-0.047	0.079	-0.035	0.225
**The correlation is significant at the 0.01 level (bilateral).																	
*The correlation is significant at the 0.05 level (bilateral).																	

Abbreviations: MT - muscle thickness, EI - echointensity, PA - pennate angle, PAC pennate angle in contraction, RF - rectus femoris, VI - vastus intermedius, VM - vastus medialis, VL - vastus lateralis, RBC - red blood cells, HGB - hemoglobin, HCT - hematocrit, MCV - mean corpuscular volume, MCH - mean corpuscular hemoglobin, MCHC - mean corpuscular hemoglobin concentration, ALT - alanine aminotransferase, ALP - alkaline phosphatase, HDL - high-density lipoprotein, LDL - low-density lipoprotein, CPK - creatine phosphokinase, TS - transferrin saturation, CRP- C-reactive protein

Rho of Spearman used for statistical analysis

Table 4.14 Correlations of ultrasound and biochemical parameters

Table 4.15 summarizes correlations between ultrasound parameters and hormone levels. A full table of these parameters is available in annex table 4C.

Insulin-like growth factor 1 had a positive moderate correlation with the area of *rectus femoris* and frailty phenotype (r=0.510 and 0.582 respectively), and a weak negative correlation with echointensity of *rectus femoris*, r=-0.378. There were also weak positive correlations with muscle thickness of *rectus femoris* and *vastus medialis* heads (r=0.374 and 0.356 respectively), as well as with pennate angle in the contraction of *vastus intermedius*, r=0.352. Parathormone showed a weak positive correlation with frailty phenotype, r=0.352, and a weak negative correlation with the pennate angle of *vastus lateralis*, r=-0.302. Cortisol, insulin, and thyroid stimulating hormone mostly had no significant correlations with ultrasound parameters.

Table 4.15. Correlations of ultrasound parameters and hormones (N= 61)									
	MT RF	EI Tr RF	EI LRF	PAC VI	MT VM	PA VM	PA VL	AREA RF	Frailty phenotype
Cortisol	0.161	0.077	0.124	0.022	0.101	0.118	.257*	0.049	-.103
Insulin	-0.039	0.045	0.038	-0.004	0.022	.285*	-0.020	-0.012	.236
PTH	-0.155	0.234	0.252	-0.085	-0.175	-0.003	-.302*	-0.192	,352**
IGF 1	.374**	-.378**	-.299*	.352*	.356**	-0.144	.268*	.510**	-,582**
TSH	0.008	0.181	0.154	-0.159	0.023	0.102	0.129	0.023	-.112
**The correlation is significant at the 0.01 level (bilateral).									
*The correlation is significant at the 0.05 level (bilateral).									

Abbreviations: MT - muscle thickness, EI - echointensity, PA - pennate angle, PAC pennate angle in contraction, RF - rectus femoris, VI - vastus intermedius, VM - vastus medialis, VL - vastus lateralis, PTH - parathormone, TSH - thyroid stimulating hormone, IGF 1 - Insulin-like growth factor 1

Rho of Spearman used for statistical analysis

Table 4.15 Correlations of ultrasound parameters and hormones

Table 4.16 shows correlations between ultrasound parameters and cytokine and oxidative stress levels.

IL-8 had a moderate inverse correlation with the pennate angle of *vastus intermedius* at rest and in contraction (r=-0.470 and -0.425 respectively), as well as weak negative correlations with muscle thickness of *rectus femoris*, *vastus intermedius,* and *vastus lateralis* and pennate angle of *vastus lateralis* at rest and in contraction, data are shown in the table 4.16.

There were moderate to weak positive correlations between muscle thickness of various quadriceps heads and pennate angles of *vastus lateralis* and *intermedius* with fractalkine, IFN-γ, IL-10, MIP-3a, IL-12p70, IL-13, IL-17a, IL-1β, IL-2, IL-4, IL-6 and IL-7, values shown in the table 4.16.

ITAC, IL-23, and TNF-α as well as oxidative stress parameters mostly had no significant correlations with ultrasound parameters.

IL-12p70 and IL-1β had a moderate negative correlation with frailty phenotype, r= -0.418 and -0.410 respectively. IFN-γ, MIP-3a, IL-17a, IL-2, IL-4, and IL-7 all showed weak negative correlations with frailty phenotype, values shown in table 4.16. Note that neither IL-6 nor TNF-α had a significant correlation with frailty in our study.

A full table of these parameters is available in annex table 4D.

Table 4.16. Correlations of ultrasound parameters and cytokines and oxidative stress parameters (N= 61)															
	SFT RF	MT RF	PA RF	MT VI	PA VI	PAC VI	SFT VM	MT VM	SFT VL	MT VL	EI Tr VL	PA VL	PAC VL	AREA RF	Frailty phenotype
ITAC	0.036	-0.153	0.025	-0.016	0.079	0.087	-0.023	-0.034	-0.030	-0.152	0.114	-0.052	-0.063	-0.198	.072
Fractalkine	0.220	.259*	0.243	.369**	.302*	.290*	.261*	0.242	0.152	.260*	0.083	.424**	.285*	-0.012	-.216
IFNγ	0.074	.318*	0.147	.397**	.312*	.401**	0.062	.271*	0.107	.294*	-0.018	.358**	.370**	0.242	-,367**
IL10	0.231	0.186	0.005	.386**	.276*	0.148	0.186	0.061	0.184	0.235	0.204	0.249	.282*	0.056	-.179
MIP3a	-0.068	0.167	-0.035	.426**	.390**	.399**	-0.058	.278*	-0.088	.256*	-0.043	.262*	.399**	.272*	-,252*
IL12p70	0.122	0.249	0.011	.289*	0.199	0.261	0.126	0.232	0.160	.306*	0.076	.330*	.327*	0.162	-,418**
IL13	.340**	0.156	.284*	0.138	0.160	0.246	0.247	0.093	.312*	.296*	0.110	.269*	.255*	0.043	-.211
IL17a	0.084	0.225	0.139	.369**	.299*	.434**	0.062	0.240	0.086	.263*	0.036	.353**	.418**	0.216	-,344**
IL1b	0.037	.408**	0.086	.293*	0.219	0.184	0.061	0.230	0.077	0.215	-0.014	.377**	.331**	.296*	-,410**
IL2	-0.005	.352**	0.099	.428**	0.247	0.234	-0.018	.336**	0.058	0.212	0.025	.302*	.345**	0.245	-,360**
IL4	0.183	.288*	0.196	.313*	0.176	0.259	0.141	0.241	0.205	0.071	0.189	.292*	.328*	0.173	-,308*
IL23	.308*	0.237	0.140	0.169	0.260	0.091	.307*	0.203	0.239	0.195	0.077	0.215	.272*	-0.025	-.207
IL6	0.172	0.119	-0.061	.340**	0.184	0.169	0.130	0.176	0.120	.267*	.297*	0.244	0.168	0.167	-.174
IL7	0.170	.296*	.339**	.315*	.306*	.294*	0.242	0.184	0.124	0.247	.258*	.337**	0.229	0.023	-,293*
IL8	-0.236	-.279*	-0.232	-.297*	-.470**	-.425**	-0.243	-0.233	-0.177	-.297*	0.099	-.316*	-.353**	-0.159	.198
TNFα	-0.176	-0.035	-0.029	0.078	0.011	0.093	-0.189	0.117	-.293*	0.101	-0.025	-0.148	0.033	-0.098	.140
MDA	-0.178	0.030	-0.023	-0.088	-0.062	-0.049	-0.139	.268*	-.315*	0.119	-0.114	0.046	0.070	0.108	-.178
Protox	0.246	-0.020	.268*	-0.194	0.102	-0.052	0.246	-0.148	.294*	-0.049	-0.004	0.079	0.097	-0.096	.179
**The correlation is significant at the 0.01 level (bilateral).															
*The correlation is significant at the 0.05 level (bilateral).															

Abbreviations: MT - muscle thickness, EI - echointensity, PA - pennate angle, PAC pennate angle in contraction, RF - rectus femoris, VI - vastus intermedius, VM - vastus medialis, VL - vastus lateralis, ITAC - interferon-inducible T-cell alpha chemoattractant, IFNγ - interferon gamma, IL - interleukin, MIP - Macrophage Inflammatory Protein, TNFα - Tumour Necrosis Factor Alpha, MDA - malondialdehyde, Protox - oxidized proteins

Rho of Spearman used for statistical analysis

Table 4.16 Correlations of ultrasound parameters and cytokines and oxidative stress parameters

4.6 Performance of ultrasound parameters as potential imaging biomarkers.

In order to assess the performance of the ultrasound parameters as imaging biomarkers and their clinical usefulness we tested them for accuracy and precision.

4.6.1 Accuracy of the ultrasound parameters

To determine the accuracy or discriminative power of the ultrasound parameters, areas under the receiver operating characteristic (ROC) curve were analysed. Frailty phenotype was divided into non-frail (controls and robust group) and at-risk group (prefrail and frail groups). Physical characteristics parameters (muscle strength, gait speed, and physical activity) were added for comparison.

Table 4.17. AUC of ultrasound and functional parameters							
Muscle	Variable	AUC	95% CI	Cut-off value	Sensitivity*	Specificity*	p
Rectus femoris	**MT**	0.793	0.714 - 0.871	1.72 cm	0.871	0.621	*<0.001*
	AREA	0.838	0.766 - 0.910	6.72 cm²	0.857	0.741	*<0.001*
	EI	0.661	0.563 - 0.758	53.10 AU	0.671	0.586	*0.002*
	PA	0.652	0.555 - 0.748	12.5°	0.636	0.621	*0.004*
	PAC	0.675	0.577 - 0.774	13.41°	0.638	0.596	*0.001*
Vastus intermedius	**MT**	0.670	0.577 - 0.763	1.32 cm	0.629	0.638	*0.001*
	EI	0.396	0.255 - 0.538	-	-	-	*0.166*
	PA	0.608	0.501 - 0.715	14.04°	0.611	0.593	*0.052*
	PAC	0.726	0.629 - 0.822	16.83°	0.720	0.667	*<0.001*
Vastus medialis	**MT**	0.731	0.642 - 0.819	3.89 cm	0.714	0.569	*<0.001*
	EI	0.464	0.314 - 0.613	-	-	-	*0.628*
	PA	0.506	0.354 - 0.658	-	-	-	*0.939*
	PAC	0.536	0.386 - 0. 685	-	-	-	*0.641*
Vastus lateralis	**MT**	0.686	0.594 - 0.779	1.87 cm	0.686	0.603	*<0.001*
	EI	0.606	0.506 - 0.706	52.35 AU	0.629	0.621	*0.039*
	PA	0.705	0.613 - 0.796	16.58°	0.721	0.603	*<0.001*
	PAC	0.680	0.586 - 0.773	16.34°	0.681	0.638	*0.001*
Variables for comparison	**Muscle strength**	0.802	0.727 - 0.877	28.1 kg	0.814	0.579	*<0.001*
	Gait speed	0.748	0.661 - 0.834	3.55 s	0.686	0.793	*<0.001*
	Physical activity	0.618	0.520 - 0.716	7.88 h/week	0.614	0.552	*0.022*

Abbreviations: MT - muscle thickness, EI - echointensity, Tr - transversal, L - longitudinal, PA - pennate angle, PAC pennate angle in contraction, CI - confidence interval, AU - arbitrary units

* Sensitivity and specificity represented for the given cut-off value

The AUC values were classified poor for values ≤0.70, acceptable for 0.71-0.80, excellent for 0.81-0.90 and outstanding for 0.91-1.00.

Table 4.17 AUC of ultrasound and functional parameters

Table 4.17 shows areas under the curve with confidence intervals and sensitivities and specificities for the selected cut-off values. When selecting cut-off values, higher sensitivity was prioritized since the test is meant to be diagnostic (screening for frailty), although it might include more false positive cases (lower specificity). The area of the *rectus femoris* and muscle thickness of the *rectus femoris* showed excellent (AUC=0.838) and acceptable (AUC =0.793) discriminative power respectively. The area of the *rectus femoris* performed better than muscle strength. The rest of the parameters performed poorly to acceptably.

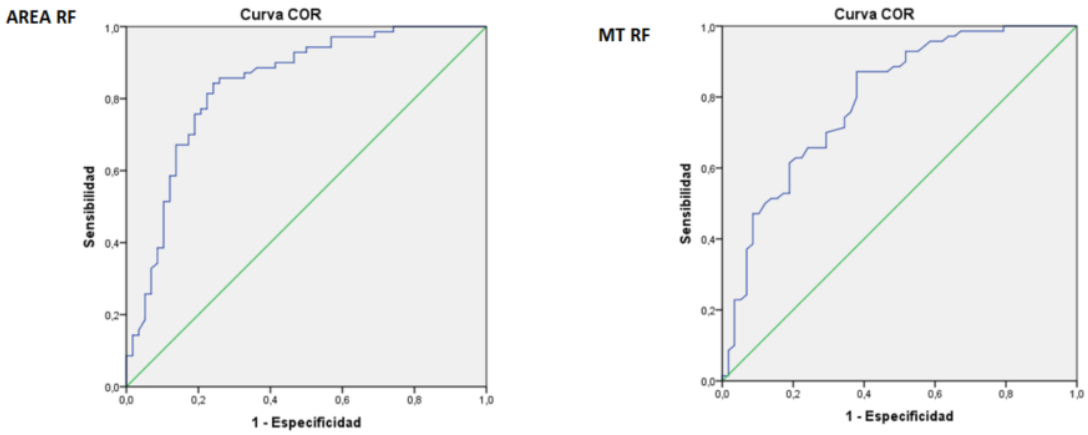

Figure 4.1 shows ROC curves for the area and muscle thickness of the rectus femoris. For the cut-off value of 6.72 cm^2 of the area of rectus femoris, there is 86% sensitivity and 74% specificity for detecting frailty. For the cut-off value of 1.72 cm of the muscle thickness of the rectus femoris, there is 87% sensitivity and 62% specificity for detecting frailty.

4.6.2. The precision of the ultrasound parameters

We tested the precision of our measurement technique by assessing the intraclass correlation coefficients (ICC) and Bland-Altman Limits of Agreement.

Table 4.18. Intraclass correlation coefficients (ICC) of the ultrasound parameters

Muscle	Variable	ICC	95% CI	p	Excluded N(%)
Rectus femoris	**MT**	0.991	0.987 - 0.993	<0.001	0 (0)
	AREA	0.987	0.983 - 0.990	<0.001	0 (0)
	EI	0.993	0.990 - 0.995	<0.001	0 (0)
	PA	0.909	0.878 - 0.934	<0.001	5 (3.9)
	PAC	0.902	0.866 - 0.930	<0.001	16 (12.5)
Vastus intermedius	**MT**	0.991	0.987 - 0.993	<0.001	0 (0)
	EI	0.991	0.988 - 0.993	<0.001	1 (0.8)
	PA	0.882	0.838 - 0.916	<0.001	20 (15.6)
	PAC	0.914	0.880 - 0.940	<0.001	28 (21.9)
Vastus medialis	**MT**	0.975	0.967 - 0.982	<0.001	0 (0)
	EI	0.988	0.984 - 0.991	<0.001	0 (0)
	PA	0.911	0.880 - 0.935	<0.001	4 (3.1)
	PAC	0.918	0.889 - 0.940	<0.001	5 (3.9)
Vastus lateralis	**MT**	0.978	0.971 - 0.984	<0.001	0 (0)
	EI	0.991	0.988 - 0.993	<0.001	0 (0)
	PA	0.756	0.672 - 0.822	<0.001	2 (1.6)
	PAC	0.918	0.889 - 0.940	<0.001	1 (0.8)

Abbreviations: MT - muscle thickness, EI - echointensity, PA - pennate angle, PAC pennate angle in contraction, CI - confidence interval

The ICC values were classified poor for values ≤0.50, moderate for 0.51-0.75, good for 0.75-0.90 and excellent for 0.91-1.00.

Table 4.18 Intraclass correlation coefficients (ICC) of the ultrasound parameters

We compared repeated measurements for each of the ultrasound parameters obtaining excellent ICC for most of them, except the pennate angle of *vastus intermedius* and *vastus lateralis* muscles, which showed good ICC (table 4.18). Note that the pennate angles for all muscle heads had slightly worse coefficients than the rest of the parameters, and had also an elevated number of missing data (values could not be measured).

Most of the parameters had high repeatability (or low error of measurement), as shown in table 4.19, cells in white. Additionally, we compared echointensities in transverse and longitudinal planes for all the muscle heads. The data showed the presence of systematic bias (cells marked green) for all these measurements. Systematic bias was also found for muscle thickness, echointensity measured in the longitudinal plane and pennate angle of *rectus femoris*, pennate angles of *vastus intermedius,* and echointensity in the transverse plane of *vastus medialis*. On the other hand, the pennate angle in the contraction of *vastus intermedius* and the pennate angle of *vastus medialis* showed proportional bias (cells marked orange).

Table 4.19. Bland-Altman limits of agreement of ultrasound parameters					
Muscle	Variable	T-test*	Mean difference (± 95% CI of LoA)	SEM	Regression analysis**
Rectus femoris	MT	0.038	NA	0,04 cm	NA
	AREA	0.244	-0.08 ± 1.51	0,32 cm²	0.626
	EI Tr	0.195	-0.45 ± 7.64	1,52 A.U.	0.345
	EI L	0.036	NA	1,51 A.U.	NA
	EI Tr vs EI L	<0.001	NA	-	NA
	PA	0.037	NA	0,92°	NA
	PAC	0.591	0.13 ± 5.26	1,10°	0.619
Vastus intermedius	MT	0.677	-0.00 ± 0.24	0,04 cm	0.980
	EI Tr	0.128	-0.58 ± 8.36	1,83 A.U.	0.320
	EI L	0.196	-0.49 ± 8.33	1,91 A.U.	0.882
	EI Tr vs EI L	<0.001	NA	-	NA
	PA	0.025	NA	1,21°	NA
	PAC	0.983	-0.01 ± 7.42	1,19°	0.028
Vastus medialis	MT	0.780	-0.01 ± 0.54	0,10 cm	0.404
	EI Tr	0.002	NA	1,72 A.U.	NA
	EI L	0.236	-0.37 ± 6.82	1,89 A.U.	0.875
	EI Tr vs EI L	<0.001	NA	-	NA
	PA	0.661	0.12 ± 5.86	1,26°	0.048
	PAC	0.938	-0.03 ± 8.3	1,53°	0.755
Vastus lateralis	MT	0.858	0.00 ± 0.26	0,05 cm	0.253
	EI Tr	0.590	-0.17 ± 7.03	1,61 A.U.	0.682
	EI L	0.281	-0.27 ± 5.49	1,62 A.U.	0.777
	EI Tr vs EI L	<0.001	NA	-	NA
	PA	0.184	-0.30 ± 4.94	1,64°	0.789
	PAC	0.909	0.02 ± 4.77	1,00°	0.876

Abbreviations: MT - muscle thickness, EI - echointensity, Tr - transversal plane, L - longitudinal plane, PA - pennate angle, PAC pennate angle in contraction, CI - confidence interval, LoA - limits of agreement, SEM - standard error of measurement (calculated as SEM = SD$\sqrt{1}$-ICC)

* T-test was used to determine the presence of systematic bias. P value <0.05 indicates the presence of systematic bias

** Linear regression was used to determine the presence of proportional bias. P value <0.05 indicates the presence of proportional bias

Table 4.19 Bland-Altman limits of agreement of ultrasound parameters

4.7 Frailty models with logistic regression analysis.

Stepwise logistic regression analysis was performed using ultrasound and biochemical parameters and physical characteristics to estimate their diagnostic power for frailty. Multiple predictive models were developed using different ultrasound parameters (muscle thickness, echointensity, pennate angles, and area of the *rectus femoris*) adjusted with biochemical parameters (general biochemical parameters, panel of cytokines and hormones) and with the physical characteristics (gait speed, muscle strength, sex, BMI).

4.7.1. Ultrasound parameters and physical characteristics

Different ultrasound parameters were tested in order to establish the best predictive models. We assumed that the parameters with the highest AUC (AUC>0.7, table 4.17), muscle thicknesses as well as the parameters measured for *rectus femoris* (parameters that showed significant differences between groups, table 4.6) would perform superiorly over echointensity and pennate angles or over other *quadriceps* heads (table 4.6). These models showed predictions from 76 to 82.5% and when adjusted with physical characteristics, the predictions scored up to 89%. However, the only ultrasound parameter that influenced significantly the dependent variable was the area of *rectus femoris* (models shown in annex tables 4E, 4F, and 4G).

We also tested various combinations of ultrasound parameters, the correct predictions ranged from 62.5 to 79%. When adjusted with physical characteristics, the correct prediction of the overall models ranged from 80.8 to 91.9%. The best model is represented in table 4.20.

The tables include the dependent variable (frailty phenotype), the independent variables used in different steps (represented with a different colour), and their respective statistics - Wald test with statistical significance and odds ratios). If the value p is <0.05, the variable contributes significantly to the model. Odds ratios (OR) are standardized values that make it possible to compare the level of influence of the independent variables on frailty (dependent variable) within the model. The tables include the statistical significance (p) of the blocks and the model ($\chi 2$ tests), Nagelkerke's R2 test that represents the variance (the variation of the dependent variable that can be explained with the model) as well as the percentage of correctly classified cases (correct prediction).

Table 4.20 Logistic regression analysis model BEST US						
	Ultrasound parameters			Adjustment with physical characteristics		
	Wald	p	OR	Wald	p	OR
Frailty phenotype (constant)	.805	.370	1.175			
AREA RF	21.706	.000	.561	14.432	.000	.513
SFT RF	1.846	.174	1.787	.766	.381	.472
MT VL	4.165	.041	.183	2.501	.114	.169
MT VM	5.118	.024	.313	3.840	.050	.239
PAC VM	2.030	.154	1.069	4.412	.036	1.165
EI VL	.576	.448	.987	1.348	.246	.976
BMI				4.905	.027	1.217
Sex				6.065	.014	.071
Muscle strength				12.304	.000	.788
Gait speed				2.364	.124	1.738
Block χ^2 (df)				36,704 (4), p<0.001		
Model χ^2 (df)	64,447 (6), p<0.001			101,152 (10), p<0.001		
Nagelkerke R^2	.542			.745		
Correct prediction	79.0			91.9		

Sample size=128; Abreviations: RF - rectus femoris, VL - vastus lateralis, VM - vastus medialis, SFT - superficial fat thickness, MT - muscle thickness, EI - echointensity, BMI - body mass index.

Table 4.20 Logistic regression analysis model BEST US

The logistic regression analysis model BEST US (table 4.20) was statistically significant in the first step (χ^2 (5) = 64.447, p<0.001). The model explained 54.2% of the variance of frailty phenotype and classified correctly 79% of the cases. When adjusted for physical characteristics, the block and model were statistically significant (p<0.001). The model explained 74.5% of the variance of frailty phenotype and classified correctly 91.9% of the cases. Area of *rectus femoris* (p<0.001), muscle thickness of *vastus medialis* (p=0.05), pennate angle in the contraction of *vastus medialis* (p=0.036), BMI (p=0.027), sex (p=0.014) and muscle strength (p<0.001) contributed significantly to the final model. Muscle thickness of *vastus lateralis* was significant only in the first step whereas the superficial fat thickness of *rectus femoris* and echointensity of *vastus lateralis* did not influence significantly frailty (the dependent variable). An increase in one square centimetre of the area of *rectus femoris,* and maintaining all the rest of the variables constant, decreases the odds of frailty 1.95 times. An increase in one centimetre of muscle thickness of *vastus medialis* decreases the odds of frailty 4.18 times. An increase in one degree of pennate angle in the contraction of *vastus medialis* increases the odds of frailty 1.16 times. An increase in one kg of muscle strength decreases the odds of frailty 1.27 times and an increase in one unit of BMI increases the odds of frailty 1.22 times. Finally, the odds of frailty were 14.08 times greater in women than in men.

4.7.2. Ultrasound and biochemical parameters with physical characteristics

The models using the area of *rectus femoris* or muscle thickness of *rectus femoris* (as the parameters with the highest AUC, table 4.17) were constructed. Different biochemical parameters were tested, namely the ones that showed significant differences among frailty groups (table 4.8). The parameters that had p<0.01 tended to perform better in the predictive models. Cytokines and hormones that showed correlations with frailty phenotype were also chosen for the analysis (tables 4.15 and 4.16).

These parameters were then adjusted with physical characteristics (BMI, sex, gait speed, and muscle strength). Since the sample size for this analysis was n=61, we decided to use up to 6 variables for each model. The best models are displayed in tables 4.21, 4.22, and 4.23.

Logistic regression model BIO 1

Table 4.21 Logistic regression analysis model BIO 1									
	Ultrasound parameters			Adjustment with biochemical parameters			Adjustment with physical characteristics		
	Wald	p	OR	Wald	p	OR	Wald	p	OR
Frailty phenotype (constant)	1.599	.206	1.385						
MT RF	15.584	.000	.011	10.557	.001	.010	4.445	.035	.003
GLUCOSE				5.830	.016	1.063	2.730	.098	1.068
PROTEINS				4.581	.032	.115	5.262	.022	.007
BMI							.317	.573	0.915
Gait speed							3.958	.047	8.869
Muscle strength							3.967	.046	.790
Block χ^2 (df)				18.354 (2) p<0.001			15.464 (3) p=0.001		
Model χ^2 (df)	26.632 (1) p<0.001			44.987 (3) p<0.001			60.452 (6) p<0.001		
Nagelkerke R^2	.470			.694			.838		
Correct prediction	75.8			87.1			93.5		

Sample size=61; Abreviations: MT RF - muscle thicknes of rectus femoris, BMI - body mass index.

Table 4.21 Logistic regression analysis model BIO 1

Logistic regression analysis model BIO 1 (table 4.21) features muscle thickness of rectus femoris combined with the best general biochemical parameters. The model was significant in the first step (p<0.001), it explained 47% of the variance of frailty phenotype predicting correctly 75.8% of the cases. When adjusted with biochemical parameters, the block and the model remained significant (p<0.001), the model explained 69.4% of the variance and the correct prediction was 87.1%. Finally, when adjusted with physical characteristics, the block and the model were significant (p<0.001), the model explained 83.8% of the variance and correctly predicted 93.5% of the cases. Muscle thickness of *rectus femoris* (p=0.035), proteins (p=0.022), gait speed (p=0.047), and muscle strength (p=0.046) contributed significantly to the final model. Glucose was significant in the second step (p=0.016) and did not reach statistical significance in the final

step. An increase in one centimetre of muscle thickness of the *rectus femoris* and maintaining all the rest of the variables constant decreases the odds of frailty 333 times. An increase in one unit of proteins decreases the odds of frailty 143 times. An increase in one second of walking time (decrease in gait speed) increases the odds of frailty 8.87 times. An increase in one kg of muscle strength decreases the odds of frailty 1.26 times.

Logistic regression model BIO 2

Table 4.22 Logistic regression analysis model BIO 2									
	Ultrasound parameters			Adjustment with biochemical parameters			Adjustment with physical characteristics		
	Wald	p	OR	Wald	p	OR	Wald	p	OR
Frailty phenotype (constant)	1.318	.251	1.346						
AREA RF	14.613	.000	.508	11.459	.001	.536	5.010	.025	.372
MIP3a				4.452	.035	.933	6.471	.011	.856
IL 1b				3.881	.049	.237	3.901	.048	.081
BMI							4.651	.031	1.667
Sex							5.355	.021	.0002
Muscle strength							5.667	.017	0.626
Block χ^2 (df)				12,186 (2) p=0,002			25,695 (3) p<0,001		
Model χ^2 (df)	25,976 (1) p<0,001			38,163 (3) p<0,001			63,858 (6) p<0,001		
Nagelkerke R^2	.466			.625			.872		
Correct prediction	80.3			80.3			95.1		

Sample size=61; Abreviations: RF - rectus femoris, MIP - Macrophage Inflammatory Protein, IL - interleukin, BMI - body mass index.

Table 4.22 Logistic regression analysis model BIO 2

For the model BIO 2 (table 4.22) the parameters chosen were MIP-3a and IL-1β. Both parameters showed correlations with the area of rectus femoris as well as with the frailty phenotype (table 4.16). The model was significant in all three steps (p<0.001). The first step explained 46.6% of the variance predicting correctly 80.3% of the cases. When adjusted with biochemical parameters and physical characteristics, the model explained 87.2% of the variance and predicted correctly 95.1% of the cases. For each square centimetre increase of the area of *rectus femoris* and maintaining all the rest of the variables constant, the odds of frailty decrease 2.69 times. An increase in one unit of MIP-3a decreases the odds of frailty 1.17 times. An increase in one unit of IL-1β decreases the odds of frailty 12.34 times. An increase in one unit of BMI increases the odds of frailty 1.67 times. An increase in one kilogram of muscle strength decreases the odds of frailty 1.6 times. The odds of frailty were 5000 times higher in women.

Logistic regression model BIO 3

Table 4.23 Logistic regression analysis model BIO 3									
	Ultrasound parameters			Adjustment with biochemical parameters			Adjustment with physical characteristics		
	Wald	p	OR	Wald	p	OR	Wald	p	OR
Frailty phenotype (constant)	1.060	.303	1.308						
MT RF	14.743	.000	.012	7.498	.006	.026	4.713	.030	.017
IGF 1				4.335	.037	.978	3.052	.081	.977
IFN γ				5.502	.019	.920	5.809	.016	.890
Gait speed							1.241	.265	2.092
Muscle strength							4.739	.029	.848
Block χ^2 (df)				16.860 (2) p<0.001			12,885 (2) p=0,002		
Model χ^2 (df)	24.751 (1) p<0,001			41.612 (3) p<0,001			54.497 (5) p<0,001		
Nagelkerke R^2	.453			.671			.801		
Correct prediction	75.0			83.3			93.3		

Sample size=61; Abreviations: MT RF - muscle thicknes of rectus femoris, IGF 1 - insulin-like growth factor 1, IFN γ - interferon gamma.

Table 4.23 Logistic regression analysis model BIO 3

The model BIO 3, shown in table 4.23, displays IGF-1 and IFN-γ, both parameters had a significant correlation with frailty phenotype (tables 4.15 and 4.16). The model was significant in all three steps (p<0.001). The first step explained 45.3% of the variance predicting correctly 75% of the cases. When adjusted with biochemical parameters, the model explained 67.1% of the variance and predicted correctly 83.3% of the cases. In the final step, when adjusted with physical characteristics, the model explained 80.1% of the variance and predicted correctly 93.3% of the cases. Muscle thickness of *rectus femoris* (p=0.030), IFN-γ (p=0.016) and muscle strength (p=0.029) contributed significantly to the final model. IGF-1 was significant in second step (p=0.037), and when adjusted with physical characteristics, it did not reach statistical significance (p=0.08). A decrease in one centimetre of muscle thickness of the *rectus femoris* increases the odds of frailty 58.8 times. An increase in one unit of IFN-γ decreases the odds of frailty 1.12 times. An increase in one kg of muscle strength decreases the odds of frailty 1.18 times.

Models BIO 4 (muscle thickness of *rectus femoris*, MCV, and proteins) and BIO 5 (area of *rectus femoris*, IL-12, and IL-17) are shown in annex tables 4H and 4I, with a correct prediction of 91.9% and 91.8% respectively. The rest of the models had an overall prediction below 90% and are not shown.

DISCUSSION

Muscle ultrasound exams were performed on a population of community-dwelling seniors. We then conducted a questionnaire and measured walking speed and hand grip strength to classify our subjects according to frailty phenotype criteria (Fried et al, 2001). Blood samples were drawn for general biochemical analysis, hormones, cytokines, and oxidative stress parameters. Ultrasound images were processed and twenty-four ultrasound-based parameters were extracted for further analysis. On one hand, we aimed to validate the ultrasound parameters for accuracy and precision as imaging biomarkers and evaluate their potential for clinical use, and on the other, to explore biological substrates for imaging findings. Furthermore, this wide array of parameters enabled us to create logistic regression models that combine different imaging, physical and biochemical parameters for quantitative diagnosis of frailty.

Several methods have been used for measuring frailty based on clinical criteria, including frailty phenotype and the accumulated deficits approach. Although very useful, these techniques still rely on various subjective parameters and lack standardised evaluation in various clinical scenarios.

Self-reported information confers important data for any medical assessment, however, in this setting, it might have low accuracy since many patients suffer from cognitive impairment. The development of quantitative tools for the assessment of frailty could be an important step toward improving the management of these patients as it would give the opportunity for universal administration, with more reliable identification of patients at risk, permitting timely interventions, and thus hopefully delaying adverse outcomes and death. Therefore, the search for objective screening tools is gaining more importance in recent years with an ongoing investigation into many circulating and imaging biomarkers that could be used for this purpose. However, there is a gap between investigation and translation to clinical practice. Many of the parameters are limited to the research setting, have low cost-efficiency that imparis the widespread administration, show insufficient discriminative power, or lack associations with relevant outcomes (Saedi et al, 2019). Clinicians seek for a brief, easy-to-administer screening tool with high sensitivity for detecting frailty (Huisingh-Scheetz et al, 2019). We consider that muscle ultrasound may be a step toward bridging this gap.

The results of this study confirm that muscle ultrasound could be used in outpatients as a screening method and it is possible to diagnose subjects at risk of frailty with up to 95% accuracy

using frailty models that combine ultrasound and biochemical parameters. Several important findings support this result (mentioned in continuation and commented on later in the text):

1. We showed that muscle ultrasound can be a useful tool for assessing muscle volume and architecture in the context of frailty syndrome, with high precision and accuracy (tables 4.17 and 4.18) and could be considered as a valid alternative to current standard methods for evaluation of muscle mass in a clinical setting (Cruz-Jentoft et al, 2018). Muscle ultrasound parameters alone such as area of rectus femoris and muscle thickness of rectus femoris were able to identify low muscle size and had good discriminative power for frailty with AUC of 0.84 (95% CI 0.77-0.91) and 0.79 (95% CI 0.71-0.87) respectively (table 4.17) and were comparable to muscle strength, AUC= 0.80 (95% CI 0.73-0.88) and gait speed, AUC=0.74 (95% CI 0.67-0.83). The sensitivity for detecting frailty was 87% and 86% for the muscle thickness and area of the rectus femoris respectively (with cut-off values of 1.72 cm for muscle thickness and 6.72 cm^2 for the area of the rectus femoris).
2. The logistic regression analysis models demonstrated that the frailty prediction rate of muscle architecture parameters alone ranged from 76.5% to 82.5%, and when adjusted with physical characteristics, the models classified correctly up to 91.9% of the cases (table 4.20).
3. The combination of muscle architecture and biochemical parameters adjusted with physical characteristics showed very good performance and predicted frailty in up to 95% of the cases (tables 4.21-4.23, annex tables 4H and 4I). Both decreases in muscle thickness and area of rectus femoris as hallmarks of sarcopenia increased the odds of frailty in all the models displayed. Various biochemical parameters, cytokines, and hormones showed significant correlations with frailty phenotype (tables 4.14 to 4.16) and were used for the regression analysis.
4. Muscle size had positive correlations both with muscle strength and gait speed, while muscle quality was associated with muscle strength but not with gait speed. There were no correlations between ultrasound parameters and physical activity (self-reported).
5. Various biochemical analytes showed correlations with ultrasound parameters as well as with frailty phenotype. There were positive correlations between muscle size and haemoglobin levels. Higher basal glucose levels correlated with low muscle thickness and area of rectus femoris as well as frailty phenotype. IGF-1 showed a positive correlation with muscle size and a negative correlation with frailty phenotype.

5.1 Why ultrasound?

One of the key components of frailty is sarcopenia, a condition characterised by loss of skeletal muscle mass and function (Santilli et al, 2014). The possibility of assessing muscle mass in primary care or at the bedside in a hospital environment was the main idea behind this study. Current guidelines for the diagnosis of sarcopenia by the revised European Working Group on Sarcopenia in Older People (EWGSOP2) recommend DXA and BIA for assessing muscle mass (Cruz-Jentoft et al, 2018). However, the decline in muscle mass and strength does not occur at the same rate. Goodpaster and colleagues (2006) showed in community-dwelling old people that there is a greater loss of muscle strength than mass.

It is believed that age-related changes in muscle architecture and composition rather than just muscle size can explain the loss of muscle strength in this population (Narici and Maffulli, 2010). DXA and BIA cannot assess muscle composition. MRI and CT are considered gold standards in this regard, where muscle attenuation by CT or various MRI sequences (diffusion tensor imaging, Dixon, spectroscopy, etc) can be used (Perkisas et al, 2018). Although superior, these techniques are not practical for clinical use due to costs, accessibility, portability, and ionising radiation.

Ultrasound can overcome these limitations. Apart from reliably assessing muscle size by measuring muscle thickness and area (Nijholt et al, 2017), ultrasound can assess muscle composition as well. Changes in muscle composition can be observed as increased echointensity due to the accumulation of intramuscular adipose and fibrous tissue (Pillen et al, 2008). Additionally, the quadriceps femoris is a pennate muscle, where muscle fibres attach at an angle to its tendon, the degree of this angle reflects the sarcomeres in parallel and it is proportional to muscle force-generating potential. This angle can be measured by ultrasound, and it is decreased in sarcopenic muscles (Narici and Maffulli, 2010).

We chose to work with community dwelling seniors (as opposed to hospitalised patients) in order to assess the feasibility of ultrasound in primary care. Since there was no recommended ultrasound protocol in this setting, we performed literature research on available techniques and parameters and developed our own protocol based on our previous experience (Miron Mombiela et al, 2020), managing technical challenges and cross-checking the intra- and inter-rater reliabilities (unpublished data). We decided to perform the ultrasound on the anterior compartment of the thigh for two reasons. On one hand, the investigation showed that there is a greater loss of muscle mass in the lower than upper limbs and anterior than posterior thigh (Janssen et al, 2000; Abe et al, 2011). On the other hand, the *quadriceps* is a large muscle and it gives enough room to identify important morphological features, permitting the operator to

train the technique and measure parameters even in severely sarcopenic individuals that may be encountered in clinical practice. As for the parameters, apart from measuring muscle size (muscle thickness and area), we also aimed at assessing muscle architecture (echointensity and pennate angles). Note that the pennate angle is not a constant value, and it changes depending on joint angle and degree of muscle contraction. It was found that pennate angles of *vastus lateralis* increase during voluntary contraction in young healthy individuals (Oliveira et al, 2017). We wanted to explore if this measurement could be used in the clinical setting with frail patients and if it would reflect the contractile potential of sarcopenic muscle.

Parameters that have good technical (precision and accuracy) and clinical performance (sensitivity and specificity) are suitable imaging biomarkers for clinical use (Sullivan et al. 2015). These could have an important advantage over classical frailty phenotype assessment which includes self-reported parameters such as the feeling of exhaustion. In fact, it was found that the independent prognostic effect of each frailty criterion showed important differences in predicting chronic disability, hospitalisation, and death (Rothman et al, 2008). This is where muscle ultrasound could have a greater clinical impact. Ultrasound parameters can be objectively measured in asymptomatic outpatients as well as in acute settings and values can be compared over time. This way the presence of frailty, evolution in time, or effectiveness of potential therapeutic intervention can be quantitatively assessed. The implementation of muscle ultrasound exams could facilitate clinical decisions and management of frail patients in day-to-day practice.

5.2 Technical and clinical performance of ultrasound parameters.

We showed that the ultrasound parameters assessed in our study had a good performance as imaging biomarkers. First, the values measured are like other studies and thus seem to be valid (Strasser et al, 2013, Chauhan et al, 2013, Alegre et al, 2006, Mirón Mombiela et al, 2017). Next, the parameters showed high precision with a relatively low error of measurement. Moreover, various parameters also showed good accuracy in the clinical setting and performed equal to or better than muscle strength and gait speed.

There are several findings to support this: average muscle thickness of *rectus femoris* of 1.91 ± 0.35 cm in healthy controls versus 1.27 ± 0.28 cm in frail patients (table 4.6) is comparable to the study of Strasser et al. (2013), who reported muscle thickness in young subjects to be 1.81 ± 0.4 cm and in old subjects 1.35 ± 0.19 cm. Other *quadriceps* heads had similar thicknesses compared to this study (table 5.1). On the other hand, we measured pennate angles generally higher (18.2 ± 3.3° vs 14.7 ± 2.5° for *vastus lateralis* in healthy controls) and echointensities

lower (49 ± 18 A.U vs 101.9 ± 14 A.U for *rectus femoris* in healthy controls) compared to Strasser´s study. Other studies report the pennate angle of *vastus lateralis* in young healthy controls to be 15.1 ± 3.81° (Chauhan et al, 2013) and 16.2 ± 3.2° (Alegre et al.2006). Mirón Mombiela et al. (2017) show the echointensity of *rectus femoris* to be 60 ± 20 A.U. for healthy controls. We believe these variations are due to site measurement and probe orientation for pennate angles and different machines and gain settings for echointensity.

Table 5.1 Examples of ultrasound parameter measurements in healthy controls						
	MT RF	MT VI	MT VL	PA VL	EI RF	EI VL
Our study	1.91 ± 0.35 cm	1.65 ± 0.50 cm	2.10 ± 0.37 cm	18.2 ± 3.3°	49 ± 18 A.U	48 ± 15.69 A.U
Strasser et al, 2013	1.81 ± 0.4 cm	1.71 ± 0.44 cm	2.26 ± 0.38 cm	14.7 ± 2.5°	101.9 ± 14 A.U	96.2 ± 14.9 A.U
Chauhan et al, 2013				15.1 ± 3.81°		
Alegre et al, 2006				16.2 ± 3.2°		
Miron Mombiela et al, 2017					60 ± 20 A.U	

Abbreviations: MT - muscle thickness, PA - pennate angle, EI - echointensity, RF - rectus femoris muscle, VI - vastus intermedius muscle, VL - vastus lateralis muscle

Table 5.1 Examples of ultrasound parameter measurements in healthy controls

Muscle thickness, cross-sectional area, and echointensity had high precision (ICC 0.97-0.99, table 4.18). Pennate angles showed lower precision (ICC 0.76-0.90) with up to 21% of excluded images (did not meet image quality criteria). Other studies reported high precision for muscle thickness and area measurements in older adults (Strasser et al, 2013, Scanlon et al, 2014, Welch et al 2018) with lower precision for echointensity and pennate angle measurements (Strasser et al, 2013). We found systematic bias in measuring muscle thickness, echointensity, and pennate angle of *rectus femoris* as well as echointensity of *vastus medialis* and pennate angle of *vastus intermedius* (table 4.19). Probe placement and the amount of pressure applied as well as the interpretation of the images may have contributed to this finding (König et al, 2014). We found the standard errors of measurement from 0.04 to 0.1 cm for muscle thicknesses, 0.3 cm^2 for the area, 1.5 to 1.9 A.U for echointensity, and 0.9 to 1.6° for pennate angles (table 4.19). Therefore, all the changes greater than the limits of error can be interpreted as muscle architecture changes (Denegar et al 1993). In other words, these parameters are sensitive to changes in muscle thickness and area as small as 1 mm and 3 mm^2 respectively.

Echointensity showed lower accuracy in detecting frailty compared to muscle thickness and area, with AUC for *rectus femoris* and *vastus lateralis* ranging from 0.60 to 0.66 (95%CI 0.51-0.76). Our previous cohort showed similar results, AUC 0.69 (95%CI 0.59-0.78) (Miron Mombiela et al, 2021).

Pennate angles in contraction were generally higher than angles at rest, and there were significant differences among groups (table 4.6). However, notice there were greater differences

between angles at rest and in contraction for the control group of young individuals whereas for other groups this difference was much smaller, for example, the pennate angle of *rectus femoris* at rest in the prefrail group was 11.9 ± 2.9° and in contraction 12.2 ± 2.8°.

If we consider that the standard error of measurement (table 4.19) for *rectus femoris* was 0.9° and 1.1° at rest and in contraction respectively, it becomes obvious that the smaller the angle is, the more difficult it gets to measure true changes between angles at rest and in contraction. Additionally, this parameter was not easily obtained as it required voluntary contraction of the *quadriceps* muscle and a significant portion of patients were not able to sustain maximal contraction long enough or presented fasciculations which decreased image quality and resulted in the exclusion of up to 21% of the images (table 4.18). We are uncertain if this finding is entirely due to architectural changes in sarcopenic muscle and the inability to recruit all existing fibres in an efficient contraction manner or if some patients had difficulty achieving contraction lying in a supine position and would maybe perform better sitting and extending the leg at request. We presented all data for this parameter, but we acknowledge that its usefulness is rather limited in frail patients and various technical improvements need to be implemented before considering its inclusion in clinical protocols.

Various muscle architecture parameters have already been validated for accuracy compared to gold-standard imaging techniques, finding very good agreement between ultrasound and magnetic resonance for muscle thickness and subcutaneous fat thickness of the anterior thigh (Mechelli et al, 2019, Betz et al 2021) and average agreement for muscle cross-sectional area of *vastus lateralis* (Betz et al, 2021). There were strong correlations between intramuscular fat assessed by MRI and muscle echointensity (Young et al, 2015). Watanabe and colleagues (2018) reported moderate associations between echointensity and muscle attenuation assessed by CT. We did not perform validation tests with other imaging techniques which is one of the limitations of the present study.

5.3 Ultrasound parameters and functional capacity.

Muscle size and quality contribute to its functional capacity. We showed associations between muscle size and composition with muscle strength. There were significant correlations between muscle strength and muscle thicknesses of all *quadriceps* heads, with the strongest correlation for *vastus medialis* ($r=0.474$, $p<0.01$). Echointensity showed a negative correlation with muscle strength (for *rectus femoris* $r=-0.451$, $p<0.05$). Other studies also reported correlations between muscle strength and echointensity (Miron Mombiela et al, 2017, Watanabe et al, 2013, Fukumoto et al, 2012).

As for gait speed, there were correlations with muscle size (strongest correlation with the area of *rectus femoris*, r=-0.334, p<0.01), however, there were no significant correlations with echointensity of any of the quadriceps heads. Some studies reported correlations between the echointensity of *rectus femoris* and gait speed (Rech et al, 2014) while others found no correlation neither for limb or spine muscles (Yoshiko et al, 2018). The pennate angle of *vastus lateralis* showed a correlation with gait speed (r=-0.323, p<0.01). Correlations between gait speed and pennate angle of *vastus lateralis* (Aubertin-Leheudre et al, 2019) as well as *gastrocnemius medialis* (Zhu et al, 2019) were reported in previous studies.

Interestingly, there were few to no correlations between ultrasound parameters and self-reported physical activity parameters (table 4.12). These parameters proved to be highly unreliable. We believe that patients tended to overestimate the amount of daily physical activity and were not objective when reporting walking and rest times. This again raises concerns about the significance that should be given to all self-reported, subjective parameters when diagnosing a person as ´frail´ or ´non-frail´.

5.4 Ultrasound parameters and frailty.

Our study confirms that ultrasound parameters assessing *quadriceps femoris* muscle are clinically useful in detecting frail patients, with AUC values for the area of *rectus femoris* 0.84 (0.77-0.91) and muscle thickness 0.79 (0.71-0.87). Moreover, we showed correlations of multiple ultrasound parameters with frailty phenotype (table 4.12). Parameters that denoted sarcopenia, namely low muscle thickness, low area, and low pennate angles as well as high echointensity were all correlated with frailty. The strongest correlation was found for the area of *rectus femoris*, r=-0.612, p<0.01.

Frailty often overlaps with comorbidities in old patients; in fact, some studies showed that 82% of frail patients had comorbidities (Wong et al, 2010). We registered comorbidities as a part of the integral assessment of our study population and correlated this data with ultrasound parameters. There were generally weak but significant correlations between ultrasound parameters and various comorbidities with the most ultrasound parameters (>10) associated with osteoarthritis, fractures/osteoporosis, visual loss, hypertension, and obesity (table 4.13), and fewer parameters (5-10) associated with diabetes mellitus, previous malignancy, hyperlipidemia, COPD, hearing loss and depression (annex table 4A). It is believed that sarcopenia and these diseases share common risk factors in old people – physical inactivity, inflammation, and malnutrition/obesity, in fact, it was found that sarcopenia is highly prevalent

in patients with cardiovascular disease, dementia, diabetes mellitus, and respiratory disease (Pacifico et al, 2020). Other studies link sarcopenia with an increased risk of falls (Beaudart et al, 2017). We found an inverse correlation between the area of the *rectus femoris* and the number of falls in the last six months (table 4.13). It seems that low muscle mass, probably aided by sensory impairment, puts these individuals at higher risk of falls which in turn leads to limited physical activity and functional decline and ultimately increases the risk of institutionalisation, morbidity, and mortality. This was the only outcome we studied.

5.5 The biological meaning of imaging parameters.

The concept of biological validation of imaging features is becoming an essential part of translating radiologic imaging data to clinical practice. With the development of new technologies where automated processing of a high volume of data extracted from radiologic images is used for the identification of clinically relevant parameters, there is a problem of overfitting the models. Since it is exclusively data-driven, this method alone cannot explain the biological meaning of the observed relationships within these models. That is why it is important to correlate image-based models to biological parameters (Tomaszewski and Gillies, 2021). The most obvious application of this concept is in oncologic radiology – image features (shape, density, presence of marginal spiculations, etc.) are correlated with histologic and genomic parameters of cancer to understand the microscopic characteristics of the visual findings (Mirón Mombiela et al, 2022; Shui et al, 2020).

Although we did not use automated machine learning platforms, it can be argued that there is a certain analogy with the concept of studying multiple imaging parameters in the process of developing ultrasound biomarkers for frailty. We followed this idea aiming to explore the biological substrate of our ultrasound parameters. We also wanted to see if the diagnostic performance can be improved and if we could reach a better understanding of underlying factors involving ultrasound-based parameters.

We performed correlation analysis and compared our results to the available literature. There were several interesting findings we would like to comment on.

General biochemical parameters: As for muscle-related parameters, creatinine levels were positively correlated with muscle thickness of *vastus medialis* ($r=0.439$, $p<0.01$). Creatinine levels in serum are proportional to muscle mass (Keshaviah et al, 1994) which would explain this finding. However, we found no significant correlations between creatinine levels and muscle

thickness of other *quadriceps* heads nor with frailty phenotype. Apart from muscle mass, various factors influence creatinine levels (such as renal function and dietary intake) which could explain the lack of this correlation.

Although albumin levels alone did not show any statistically significant correlation with muscle mass nor with frailty, serum protein levels showed a positive correlation with the area of *rectus femoris* ($r=0.296$, $p<0.05$) and a negative correlation with frailty phenotype ($r=-0.319$, $p<0.05$). Other studies reported an association between low albumin concentrations and sarcopenia (Baumgartner et al, 1996) and found that low albumin may increase the risk of developing sarcopenia (Visser et al, 2005). Serum proteins consist of albumin (56%), globulins (40%), and other proteins in much lower concentrations; therefore, the variations of its levels are expected to be dependent on one of the two major components.

We found that higher basal glucose levels correlated with low muscle thickness and area of *rectus femoris* ($r=-0.307$ and -0.297 respectively, $p<0.05$). Also, glucose had a positive correlation with the frailty phenotype ($r=0.564$, $p<0.01$). A systematic review from 2020 (Anagnostis et al.) reported that patients with type 2 diabetes mellitus (DM2) had an increased risk of sarcopenia. Various studies found a positive correlation between insulin resistance and frailty (Perez-Tasigchana et al, 2017, Barzilay et al, 2007). Several pathophysiological mechanisms were proposed to explain this correlation. Insulin has anabolic effects on skeletal muscle, regulating protein synthesis and glucose transport and improving muscle metabolism. These functions are impaired by insulin resistance present in patients with DM2. Insulin resistance decreases protein synthesis and promotes protein degradation (Pereira et al, 2007). Additionally, chronic hyperglycaemia causes the accumulation of advanced glycosylation end-products (AGEs) which can promote oxidative stress, inflammatory cytokines, and the breakdown of muscle proteins (Mori et al, 2019). Other authors argue that macrovascular complications of DM2 could lead to peripheral arterial disease and in turn cause a decrease in muscle mass, strength, and performance (Dziubek et al, 2015). Another entity important in this context is sarcopenic obesity, a condition where insulin resistance, obesity, and sarcopenia coexist in the same individuals (Cleasby et al, 2016). In these patients high intramuscular fat accumulation and visceral adiposity promote insulin resistance and impair muscle glucose uptake with the consequent decrease in intracellular energy production, which affects muscle quantity and quality. This lower muscle mass in turn favours insulin resistance creating a vicious circle.

Haemoglobin levels had a positive correlation with muscle thickness of *vastus medialis* ($r=0.289$, $p<0.05$) and a negative correlation with echointensity of *rectus femoris* ($r=-0.318$, $p<0.05$) and

superficial fat thickness (r=-467, p<0.01). A study by Moon et al (2015) showed a correlation between low muscle mass measured with DXA and anaemia in Korean elderly men. InCHIANTI study (Cesari et al, 2004) also reported an association between low haemoglobin levels with lower muscle density and muscle mass measured by CT. The reason for this association could be the lower oxygenation of skeletal muscle in anaemia (Dodd et al, 1993). Additionally, as anaemic patients may experience more fatigue, they often tend to have a more sedentary lifestyle with less physical activity and therefore have less muscle mass and more superficial fat accumulation (Cesari et al, 2004), although, we did not find a direct association between muscle mass and self-reported physical activity in our study population.

There were no significant correlations between muscle volume and glomerular filtration rate (GFR). However, there were correlations with muscle architecture parameters. Pennate angles of *vastus lateralis* at rest and in contraction (r=0.396, p<0.01 and r=0.256, p<0.05 respectively), as well as rectus femoris in contraction (r=0.348, p<0.05), showed positive correlations with GFR. There was a negative correlation between GFR and frailty phenotype (r=-0.330, p<0.01). A Korean study from 2020 (Hong et al) reported the relationship between sarcopenic obesity and decreased GFR in postmenopausal women. Sarcopenia is frequently found in patients with chronic kidney disease, and it is due to negative protein balance caused by multiple factors that promote protein catabolism and decrease protein synthesis (Sabatino et al, 2021).

We found no significant correlations between vitamin D and muscle volume nor with frailty phenotype for our study population. Vitamin D decreases with age mainly due to reduced sun exposure, altered skin response to UV radiation, and decreased renal function (de Jongh et al, 2017). Low levels of vitamin D are associated with osteoporosis and sarcopenia among older adults, which in turn increases the risk of falls (Bischoff-Ferrari et al, 2009). This association may be due to effects on muscle cell metabolism (Wassner et al, 1983). Results from Newcastle 85+ study reported associations between low vitamin D levels (<10 ng/mL) and low muscle strength in old people (Granic et al, 2017). A cross-sectional study showed associations between low vitamin D levels (<20 ng/mL) and low muscle mass measured by DXA in a frail elderly population from the Netherlands (Tieland et al, 2013). Another study found an association between low vitamin D levels (<10 ng/mL) and incident frailty in a prospective cohort of old women; however, this association was no longer significant after adjusting for cardiometabolic diseases (Buta et al, 2017). As for our results, we believe different study populations, the amount of sun exposure as well as seasonal variations in vitamin D levels could have contributed to our findings. Additionally, we did not inquire about any vitamin supplement intake, which could have also interfered with the results. As for the role of vitamin D supplementation in preventing frailty, a

recent randomised trial on over 25000 individuals showed vitamin D3 supplementation did not affect the incidence of frailty when compared with a placebo (Orkaby et al, 2022).

Hormones: We demonstrated the correlation between IGF-1 and muscle mass and composition. There was a positive correlation between IGF-1 levels and muscle volume, measured as the area of the *rectus femoris* ($r=0.510$, $p<0.01$) and the muscle thickness of the *rectus femoris* ($r=0.374$, $p<0.05$). These findings can be explained by the role that IGF-1 plays in muscle homeostasis. It has an anabolic effect on muscle tissue, namely, it stimulates muscle production and activates cell hypertrophy, and inhibits muscle protein degradation. On the other hand, the echointensity of *rectus femoris* had a negative correlation with IGF-1 levels ($r=-0.378$, $p<0.01$). Echointensity is an ultrasound measure of muscle quality; higher levels indicate intramuscular fat infiltration and are associated with loss of functional muscle mass, which could explain this finding. Additionally, plasma levels of IGF-1 were significantly lower in the frail group compared to controls (table 4.8). Various studies link low levels of IGF-1 with physical performance (van Nieuwport et al 2018), sarcopenia, and frailty (Payette et al 2003, Doi et al 2018). We also found a negative correlation between circulating IGF-1 levels and frailty phenotype ($r=-0.582$, $p<0.01$).

Regarding inflammatory markers, there were significant correlations of various cytokines with ultrasound parameters as well as frailty, but the direction of those correlations was generally opposite to that in published literature. Namely, we found positive correlations between muscle thickness of *vastus intermedius* and *lateralis* with circulating levels of IL-6. There were no correlations between muscle ultrasound parameters and TNF-α (table 4.16). In literature higher concentrations of IL-6 and TNF-α were associated with low muscle mass and strength in healthy old people (Visser et al, 2002). Anker and colleagues (1999) reported that increased cytokine levels (TNF-α and IL-6) had a negative correlation with muscle mass in patients with chronic heart failure and cachexia. On the other hand, studies have also shown higher concentrations of pro-inflammatory cytokines IL-6, TNF-α as well as CRP in frail patients (Hubbard et al, 2009, Collerton et al, 2012). We did not find this correlation with frailty phenotype in our study group (tables 4.14 and 4.16). These signalling molecules also play a role in other processes and this can be the reason why we have not found similar results. As for the other pro-inflammatory cytokines, the general trend was similar. For example, IL-1β had a positive correlation with muscle thickness of *rectus femoris* and *vastus intermedius*, IFN-γ showed positive correlations with the muscle mass of all *quadriceps* heads and pennate angles of *vastus intermedius* and

lateralis, and both parameters had a negative correlation with frailty phenotype. On the other hand, IL-8 did show a negative correlation with muscle thickness of *rectus femoris*, *vastus intermedius*, and *lateralis* and pennate angles of *vastus intermedius* and *lateralis*, but had no significant correlation with frailty phenotype (table 4.16). Other studies reported a weak association between IL-8 levels and frailty in community-dwelling older men (Hsu et al., 2017) and increased serum IL-8 in older frail adults (Hammami et al, 2020). The levels of anti-inflammatory cytokine IL-10 had positive correlations with muscle thickness of *vastus intermedius*, however, there were no significant correlations with frailty. Various studies have reported no correlations between circulating IL-10 and frailty phenotype (Hsu et al., 2017, Su et al., 2017).

The interpretation of these findings proves to be somewhat challenging. Published literature mainly focuses on IL-6, TNF-α, and CRP as the markers of inflammation and concludes that inflammation plays an important role in the pathogenesis of frailty (McKechnie et al, 2021, Hammami et al, 2020, Cheng et al, 2022). It is worth mentioning that apart from being a pro-inflammatory cytokine, IL-6 is also referred to as myokine, as it is produced by myocytes during exercise, and a transient increase in its levels promotes muscle hypertrophy (Serrano et al, 2007). Contrary to this, in the Framingham Heart Study, an increase in IL-6 levels predicted two-year sarcopenia in older women (Payette et al, 2003). Rather than theorising about the relationship between muscle hypertrophy or the possible beneficial effect of inflammation on muscle mass and its protective role in frailty, and especially since our patients were not subjected to physical exercise before blood tests, we are inclined to believe that particular characteristics of our study population, as well as small sample size, could be the main contributors for our findings. Table 4.10 shows differences in cytokine levels divided according to frailty phenotype. Note the trend of generally lower levels of most of the parameters in prefrail patients (which was the group with the largest N) regarding the control group of young individuals as well as robust and frail patients. Interestingly, if we look at the table of correlations for total lymphocyte count, which is a general marker of immune status (annex table 4B), there were no significant correlations with ultrasound parameters nor with the frailty phenotype for our study population. Due to the small sample size, we did not perform a subanalysis adjusting data for age, sex, or comorbidities to further investigate the possible cause of these correlations. Therefore, although various cytokines showed correlations with muscle mass as well as frailty phenotype, due to the direction of these correlations, we are not confident in extracting definitive conclusions regarding their role in sarcopenia, nor recommending them as independent biomarkers for diagnosing frailty.

The role of MIP-3α is unclear and has not been studied as an independent marker of sarcopenia or frailty. This chemokine has a pro-inflammatory effect and is involved in pathways of various inflammatory and autoimmune diseases, HIV as well as the metastatic spread of different cancers (Ranasinghe and Eri, 2018). In our study population, it had a weak negative correlation with frailty phenotype and we showed one regression model where it contributes to the diagnosis of frailty together with IL-1β.

Oxidative stress parameters: We did not find almost any correlations between oxidative stress parameters and muscle mass measured by ultrasound nor with oxidative stress and frailty phenotype in our study population. Previous studies did show a correlation between frailty and both MDA and protein carbonylation (Ingles et al, 2014). Again, we believe that the small sample size could be the main contributor to this finding.

5.6 Frailty models.

First, we explored the influence of muscle mass and quality assessed by ultrasound on frailty in our study population. For this purpose, we tested combinations of ultrasound parameters adjusted with functional parameters and physical characteristics, with the best regression analysis model showing a prediction rate of 91.9% (table 4.20; other models with lower prediction rates shown in annex tables 4E, 4F, and 4G). Muscle size (measured as thickness and area) as well as muscle strength had the strongest influence on frailty within this model while muscle architecture parameters had a minor contribution in diagnosing frailty.

This finding is interesting since it is believed that muscle architecture changes happen sooner than muscle volume loss in the evolution of sarcopenia (Narici and Maffulli, 2010), and following this idea, pennate angles and echointensity were expected to show greater influence on frailty within the models. We believe that the ultrasound technique and parameter acquisition could be partially responsible for this. Muscle thickness and area seem to be more robust parameters with lower measurement error, at least for *quadriceps* muscle. It would be interesting to explore the contribution of other muscle groups (lower leg or posterior thigh) using the same ultrasound protocol to confirm this finding.

Another curious finding is that the frailty models were not dependent on gait speed but rather on muscle mass and strength. Other studies found that slow gait speed was a strong predictor of

disability and falls (Rothman et al, 2008). In future projects, other functional parameters could be tested (Timed up and go, Short Physical Performance Battery, etc.) and compared to ultrasound parameters. Although ultrasound models showed good results in predicting frailty, we believe that the general downside of these models in the clinical setting is the use of multiple parameters measured from different sites which increments scanning time and introduces accumulated measurement error, which in turn does not improve dramatically the overall prediction rate within the models (combination of various ultrasound parameters showed correct prediction up to 82.5%, annex table 4G, area of *rectus femoris* alone showed 80.3%, table 4.22). Before implementing ultrasound exams in clinical practice, studies on a wider and more diverse population are needed in order to determine the cut-off values for low muscle mass and quality and to establish normal, adjusted for age, values both for men and women.

Although many frail patients present with sarcopenia, frailty syndrome should be understood as a multidimensional entity that involves musculoskeletal dysfunction paired with endocrine senescence and chronic inflammation which renders a person vulnerable to outside stressors (Morley et al, 2013). Therefore, we consider that there is no one ´best´ parameter describing it, rather, we outline there could be various combinations of parameters that can successfully identify frail patients and individuals at risk of developing frailty. Apart from sarcopenia, frailty has been associated with multiple biochemical, endocrine, and immune factors. A previous study by Mitnitski and colleagues (2015) reported that blood parameters that individually may have weak correlations with frailty and ageing, in combination showed a strong association with mortality. We explored the associations of blood parameters with muscle mass and frailty and used the concept of biochemical parameter combinations to develop integrated models. These models take into account the presence of low muscle mass measured by muscle thickness or area of *rectus femoris* (best ultrasound parameters), low physical performance measured by muscle strength and walking speed as well as imbalance of various biochemical factors, namely hormones such as IGF-1, inflammatory cytokines as well as general biochemical parameters.

We are aware that the small sample size is an important limitation of this analysis, therefore we performed multiple sets of regression analysis using no more than six variables per set in order to decrease the probability of overfitting the models.

Various models showed prediction rates >90% (tables 4.21-4.23, annex tables 4H and 4I) proving the point that even with a limited number of selected parameters accurate and efficient models for diagnosing frailty can be constructed. Note that in all models increase in muscle mass (muscle thickness as well as area of *rectus femoris*) decreased the odds of frailty from 2.5 to

over 300 times. This finding supports the idea that physical activity is an important component in preventing frailty. Other studies have shown an increase in muscle cross-sectional area measured by CT after exercise intervention in frail patients (Cadore et al, 2013) as well as an increase in muscle power and performance (Hruda et al, 2003). Also, all the models that included sex as a variable showed that women had greater odds of frailty which is also reported in other studies (Fried et al, 2001). This is an expected finding since women on average have less muscle mass than men at any given age (Janssen et al, 2000), therefore sarcopenia places them at greater risk of crossing the threshold of critical muscle mass needed for mobility and independent living. This, paired with higher longevity compared to men, explains why women are more likely to need institutionalisation in their last years of life (Narici and Maffulli, 2010).

We searched for models using general biochemical parameters preferably over cytokines since we believe these are more likely to be accepted for widespread clinical use (if the parameter acquisition was cheaper or the parameter was already available from general blood analysis performed routinely for different pathology). The model that uses muscle thickness of the *rectus femoris* in combination with basal glucose levels and serum proteins (table 4.21) could be an acceptable candidate for clinical use. It showed a prediction rate of 93.5 %. An increase in muscle thickness of *rectus femoris*, muscle strength, as well as protein levels, decreases the odds of frailty while a decrease in gait speed increases the odds of frailty in this model.

To our knowledge, this is the first study to link different imaging, biochemical and physical parameters in order to obtain quantitative tools that could be used for screening and potentially for monitoring patients with frailty syndrome. However, longitudinal studies on a wider population are needed to validate these models for efficacy in predicting adverse outcomes such as hospitalisation, disability, and mortality. If the models show to be useful in clinical practice, they could be applied not only to outpatients as screening for frailty but also to acutely ill patients at admission for assessing the muscle reserves, probability of complications, and the likelihood of recuperation.

5.7 Are the ultrasound parameters good biomarkers for frailty?

Having explored all quadriceps muscle heads, we consider that the *rectus femoris* is the best candidate for assessing sarcopenia in the context of frailty syndrome. It is reasonably large, the most superficial structure that is readily visible with ultrasound in patients lying in a supine position. Measuring muscle thicknesses and areas requires minimal training and has high

accuracy with a low margin of error which gives these parameters an advantage in the clinical setting. They could be used for monitoring, especially in patients acutely ill, patients in ICU, or in cases where using a hand dynamometer is not viable, like in patients with severe arthritis (Gellhorn et al, 2018).

Echointensities and pennate angles of muscle fibres at rest and in contraction do not contribute significantly as individual parameters to the overall diagnostic performance. We believe that these parameters are not easily standardised nor reasonably reproducible in the clinical setting. However, they could be used in combination for investigational purposes as good predictors of sarcopenia.

5.8 Limitations and final remarks

These results should be interpreted in light of various limitations:

- The study had a cross-sectional study design; therefore a causal relationship between ultrasound and biochemical parameters with frailty phenotype cannot be determined. Longitudinal studies are needed to confirm the associations between these parameters and clinically relevant outcomes such as disability and death.
- Our study group consisted of Spaniards and therefore cannot be extrapolated to other populations which may vary in anthropomorphic features, lifestyle, and dietary habits, all of which can influence muscle ultrasound parameters.
- We did not collect data about protein intake or non-prescribed vitamin supplementation, which may have interfered with the interpretation of the correlations with corresponding biochemical parameters and frailty.
- The sample size for biochemical analysis was small, possibly explaining the lack of statistical significance of various parameters as well as the direction of correlations for cytokines and ultrasound parameters regarding previous literature.
- We did not perform a comparison between ultrasound and gold-standard imaging techniques (MRI and CT) to validate the parameters for accuracy.
- The influence of different ultrasound machines on ultrasound parameters was not assessed.
- There might have been a selection bias – very old patients and subjects with poor general health tended to refuse participation in the study or blood testing due to their condition, which may have led to the underrepresentation of the frail group.

In summary, the results of this study show that muscle ultrasound is useful in the clinical setting for screening individuals at risk of frailty using newly developed protocol for this purpose. Patients from primary care without frailty referrals were tested, showing that muscle ultrasound is feasible in this setting and takes no more than a couple of minutes with sufficient training. Additionally, scanning all muscle heads of *quadriceps femoris* for both muscle quantity and quality parameters provided us with sufficient data in order to select the most relevant features of sarcopenic muscle and apply them in frailty models.

We found that various ultrasound parameters can measure correctly and precisely architectural changes in sarcopenic muscle and here we show that they can be used in combination to detect frailty with a high prediction rate. Additionally, we prove that there are various combinations of ultrasound and biochemical parameters used within regression models that show very good prediction rates, emphasising that there should be more than one system taken into consideration when developing quantitative models for the assessment of frailty syndrome. These findings advance knowledge and contribute to further characterisation of the relationship between imaging parameters and underlying biochemical processes in the context of frailty.

We understand the time constraints of busy primary care practice, therefore, we would like to point out that it is sufficient to measure only one or two ultrasound parameters (for example, muscle thickness and area of *rectus femoris*) which require a minimum amount of time and training. This could have an important clinical impact since ultrasound is a widely available and relatively cheap technology that would allow for widespread administration on virtually any population. The benefits of screening community-dwelling seniors lie in detecting pre-frail individuals and applying timely intervention (Huisingh-Scheetz et al, 2019) where treatment could have a greater effect and prevent future disability.

CONCLUSIONS

Based on the results obtained, we can draw the following conclusions:

1. Muscle ultrasound is useful for assessing muscle size and architecture in the context of frailty syndrome, with various parameters showing high precision and accuracy with a low margin of error.
2. Among all quadriceps muscle heads *rectus femoris* is the best site for ultrasound assessment of sarcopenia.
3. The area and muscle thickness of the *rectus femoris* have good discriminative power for detecting frailty and are comparable to functional parameters such as muscle strength and gait speed.
4. Muscle ultrasound is feasible in busy clinical practice as it requires measurement of only one or two parameters, with a minimum amount of time and training
5. Ultrasound imaging parameters follow underlying processes that characterise frailty and show correlations with various biochemical parameters that are altered in frail patients, such as creatinine, serum proteins, glucose, haemoglobin, glomerular filtration rate, and IGF-1.
6. Frailty models that combine muscle ultrasound and biochemical parameters have a good diagnostic performance in identifying individuals at risk of frailty with up to 95% of accuracy. A decrease in muscle size increases the odds of frailty in all the models.
7. A frailty model that applies muscle thickness of *rectus femoris*, basal glucose levels, and serum proteins could be used in clinical practice due to the simplicity of ultrasound measurement and the availability of biochemical parameters from routine blood analysis.

BIBLIOGRAPHY

Abe T, Ogawa M, Loenneke JP, Thiebaud RS, Loftin M, Mitsukawa N. Relationship between site-specific loss of thigh muscle and gait performance in women: the HIREGASAKI study. Arch Gerontol Geriatr. 2012 Sep-Oct;55(2):e21-5. doi: 10.1016/j.archger.2012.06.009.

Abe T, Sakamaki M, Yasuda T, Bemben MG, Kondo M, Kawakami Y, Fukunaga T. Age-related, site-specific muscle loss in 1507 Japanese men and women aged 20 to 95 years. J Sports Sci Med. 2011 Mar 1;10(1):145-50.

Alberro, A., Iribarren-Lopez, A., Sáenz-Cuesta, M. et al. Inflammaging markers characteristic of advanced age show similar levels with frailty and dependency. Sci Rep 11, 4358 (2021). Doi:10.1038/s41598-021-83991-7.

Alegre, L. M., Jiménez, F., Gonzalo-Orden, J. M., Martín-Acero, R., & Aguado, X. (2006). Effects of dynamic resistance training on fascicle lengthand isometric strength. Journal of Sports Sciences, 24(5), 501–508. doi:10.1080/02640410500189322

Anagnostis P, Gkekas NK, Achilla C, Pananastasiou G, Taouxidou P, Mitsiou M, Kenanidis E, Potoupnis M, Tsiridis E, Goulis DG. Type 2 Diabetes Mellitus is Associated with Increased Risk of Sarcopenia: A Systematic Review and Meta-analysis. Calcif Tissue Int. 2020 Nov;107(5):453-463. doi: 10.1007/s00223-020-00742

Ando R, Nosaka K, Inami T, et al. Difference in fascicle behaviors between superficial and deep quadriceps muscles during isometric contractions. Muscle Nerve. 2016;53(5):797-802. doi: 10.1002/mus.24905

Ando R, Saito A, Umemura Y, Akima H. Local architecture of the vastus intermedius is a better predictor of knee extension force than that of the other quadriceps femoris muscle heads. Clin Physiol Funct Imaging. 2015 Sep;35(5):376-82. doi: 10.1111/cpf.12173.

Andrade LEL, New York BSAC, Gonçalves RSDSA, Fernandes SGG, Maciel ÁCC. Mapping instruments for assessing and stratifying frailty among community-dwelling older people: a scoping review. BMJ Open. 2021 Dec 22;11(12):e052301. doi: 10.1136/bmjopen-2021-052301.

Anker SD, Ponikowski PP, Clark AL, Leyva F, Rauchhaus M, Kemp M, Teixeira MM, Hellewell PG, Hooper J, Poole-Wilson PA, Coats AJ. Cytokines and neurohormones relating to body composition alterations in the wasting syndrome of chronic heart failure. Eur Heart J. 1999 May;20(9):683-93. doi: 10.1053/euhj.1998.1446.

Arts IM, Pillen S, Overeem S, Schelhaas HJ, Zwarts MJ. Rise and fall of skeletal muscle size over the entire life span. J Am Geriatr Soc. 2007;55(7):1150-1152. doi: JGS1228

Attaix D, Mosoni L, Dardevet D, Combaret L, Mirand PP, & Grizard J (2005). Altered responses in skeletal muscle protein turnover during aging in anabolic and catabolic periods. The International Journal of Biochemistry & Cell Biology, 37(10), 1962–1973. doi:10.1016/j.biocel.2005.04.009

Aubertin-Leheudre, M., Martel, D., Narici, M., & Bonnefoy, M. (2019). The usefulness of muscle architecture assessed with ultrasound to identify hospitalized older adults with physical decline. Experimental Gerontology, 125, 110678. doi:10.1016/j.exger.2019.110678

Barzilay JI, Blaum C, Moore T, Xue QL, Hirsch CH, Walston JD, Fried LP. Insulin resistance and inflammation as precursors of frailty: the Cardiovascular Health Study. Arch Intern Med. 2007 Apr 9;167(7):635-41. doi: 10.1001/archinte.167.7.635.

Barzilay, J. I. (2007). Insulin Resistance and Inflammation as Precursors of Frailty. Archives of Internal Medicine, 167(7), 635. doi:10.1001/archinte.167.7.635

Baumgartner RN, Koehler KM, Romero L, Garry PJ. Serum albumin is associated with skeletal muscle in elderly men and women. Am J Clin Nutr. 1996 Oct;64(4):552-8. doi: 10.1093/ajcn/64.4.552.

Baylis D, Bartlett DB, Syddall HE, Ntani G, Gale CR, Cooper C, Lord JM, Sayer AA. Immune-endocrine biomarkers as predictors of frailty and mortality: a 10-year longitudinal study in community-dwelling older people. Age (Dordr). 2013 Jun;35(3):963-71. doi: 10.1007/s11357-012-9396-8.

Beard, J. R., Officer, A., de Carvalho, I. A., Sadana, R., Pot, A. M., Michel, J.-P., … Chatterji, S. (2016). The World report on ageing and health: a policy framework for healthy ageing. The Lancet, 387(10033), 2145–2154. doi:10.1016/s0140-6736(15)00516-4

Beaudart C, Zaaria M, Pasleau F, Reginster J, Bruyère O. Health outcomes of sarcopenia: A systematic review and meta-analysis. PloS one. 2017;12(1):e0169548. doi: 10.1371/journal.pone.0169548.

Beaudart C, Zaaria M, Pasleau F, Reginster JY, Bruyère O. Health Outcomes of Sarcopenia: A Systematic Review and Meta-Analysis. PLoS One. 2017 Jan 17;12(1):e0169548. doi: 10.1371/journal.pone.0169548.

Benjamini, Y., & Hochberg, Y. (1995). Controlling the False Discovery Rate: A Practical and Powerful Approach to Multiple Testing. Journal of the Royal Statistical Society. Series B (Methodological), 57(1), 289–300. http://www.jstor.org/stable/2346101

Betz TM, Wehrstein M, Preisner F, Bendszus M, Friedmann-Bette B. Reliability and validity of a standardised ultrasound examination protocol to quantify vastus lateralis muscle. J Rehabil Med. 2021 Jul 6;53(7):jrm00212. doi: 10.2340/16501977-2854.

Bischoff-Ferrari HA, Dawson-Hughes B, Staehelin HB, Orav JE, Stuck AE, Theiler R, Wong JB, Egli A, Kiel DP, Henschkowski J. Fall prevention with supplemental and active forms of vitamin D: a meta-analysis of randomised controlled trials. BMJ. 2009 Oct 1;339:b3692. doi: 10.1136/bmj.b3692.

Blazevich AJ, Gill ND, Zhou S. Intra- and intermuscular variation in human quadriceps femoris architecture assessed in vivo. J Anat. 2006;209(3):289-310. doi: JOA619

Buigues C, Navarro-Martínez R, Sánchez-Martínez V, Serrano-Carrascosa M, Rubio-Briones J, Cauli O. Interleukin-6 and Lymphocyte Count Associated and Predicted the Progression of Frailty Syndrome in Prostate Cancer Patients Undergoing Antiandrogen Therapy. Cancers (Basel). 2020 Jun 29;12(7):1716. doi: 10.3390/cancers12071716.

Buta B, Choudhury PP, Xue QL, Chaves P, Bandeen-Roche K, Shardell M, Semba RD, Walston J, Michos ED, Appel LJ, McAdams-DeMarco M, Gross A, Yasar S, Ferrucci L, Fried LP, Kalyani RR. The Association of Vitamin D Deficiency and Incident Frailty in Older Women: The Role of Cardiometabolic Diseases. J Am Geriatr Soc. 2017 Mar;65(3):619-624. doi: 10.1111/jgs.14677.

Buta BJ, Walston JD, Godino JG, Park M, Kalyani RR, Xue QL, Bandeen-Roche K, Varadhan R. Frailty assessment instruments: Systematic characterization of the uses and contexts of highly-cited instruments. Ageing Res Rev. 2016 Mar;26:53-61. doi: 10.1016/j.arr.2015.12.003.

Cadore EL, Casas-Herrero A, Zambom-Ferraresi F, Idoate F, Millor N, Gómez M, Rodriguez-Mañas L, Izquierdo M. Multicomponent exercises including muscle power training enhance muscle mass, power output, and functional outcomes in institutionalized frail nonagenarians. Age (Dordr). 2014 Apr;36(2):773-85. doi: 10.1007/s11357-013-9586-z.

Calvani R, Marini F, Cesari M, Tosato M, Anker SD, von Haehling S, Miller RR, Bernabei R, Landi F, Marzetti E; SPRINTT consortium. Biomarkers for physical frailty and sarcopenia: state of the science and future developments. J Cachexia Sarcopenia Muscle. 2015 Dec;6(4):278-86. doi: 10.1002/jcsm.12051.

Calvani R, Picca A, Marini F, Biancolillo A, Gervasoni J, Persichilli S, Primiano A, Coelho-Junior HJ, Cesari M, Bossola M, Urbani A, Onder G, Landi F, Bernabei R, Marzetti E. Identification of biomarkers for physical frailty and sarcopenia through a new multi-marker approach: results from the BIOSPHERE study. Geroscience. 2021 Apr;43(2):727-740. doi: 10.1007/s11357-020-00197-x.

Cameron ID, Fairhall N, Langron C, Lockwood K, Monaghan N, Aggar C, Sherrington C, Lord SR, Kurrle SE. A multifactorial interdisciplinary intervention reduces frailty in older people: randomized trial. BMC Med. 2013 Mar 11;11:65. doi: 10.1186/1741-7015-11-65.

Cardoso AL, Fernandes A, Aguilar-Pimentel JA, de Angelis MH, Guedes JR, Brito MA, Ortolano S, Pani G, Athanasopoulou S, Gonos ES, Schosserer M, Grillari J, Peterson P, Tuna BG, Dogan S, Meyer A, van Os R, Trendelenburg AU. Towards frailty biomarkers: Candidates from genes and pathways regulated in aging and age-related diseases. Ageing Res Rev. 2018 Nov;47:214-277. doi: 10.1016/j.arr.2018.07.004.

Caresio C, Molinari F, Emanuel G, Minetto MA. Muscle echo intensity: Reliability and conditioning factors. Clin Physiol Funct Imaging. 2015;35(5):393-403. doi: 10.1111/cpf.12175

Cesari M, Fielding RA, Pahor M, Goodpaster B, Hellerstein M, van Kan GA, Anker SD, Rutkove S, Vrijbloed JW, Isaac M, Rolland Y, M'rini C, Aubertin-Leheudre M, Cedarbaum JM, Zamboni M, Sieber CC, Laurent D, Evans WJ, Roubenoff R, Morley JE, Vellas B; International Working Group on Sarcopenia. Biomarkers of sarcopenia in clinical trials-recommendations from the International Working Group on Sarcopenia. J Cachexia Sarcopenia Muscle. 2012 Sep;3(3):181-90. doi: 10.1007/s13539-012-0078-2.

Cesari M, Landi F, Calvani R, Cherubini A, Di Bari M, Kortebein P, Del Signore S, Le Lain R, Vellas B, Pahor M, Roubenoff R, Bernabei R, Marzetti E; SPRINTT Consortium. Rationale for a

preliminary operational definition of physical frailty and sarcopenia in the SPRINTT trial. Aging Clin Exp Res. 2017 Feb;29(1):81-88. doi: 10.1007/s40520-016-0716-1.

Cesari M, Landi F, Vellas B, Bernabei R, Marzetti E. Sarcopenia and physical frailty: two sides of the same coin. Front Aging Neurosci. 2014 Jul 28;6:192. doi: 10.3389/fnagi.2014.00192.

Cesari M, Penninx B, Lauretani F, Russo CR, Carter C, Bandinelli S, Atkinson H, Onder G, Pahor M, Ferrucci L, Hemoglobin Levels and Skeletal Muscle: Results From the InCHIANTI Study, The Journals of Gerontology, 2004, 59(3), M249–M254, doi:10.1093/gerona/59.3.M249

Chatterjee S., Simonoff J. S. (2013). Handbook of regression analysis. New York, NY: Wiley.

Chauhan B, Hamzeh MA, Cuesta-Vargas AI. Prediction of muscular architecture of the rectus femoris and vastus lateralis from EMG during isometric contractions in soccer players. Springerplus. 2013 Oct 18;2:548. doi: 10.1186/2193-1801-2-548.

Chen X, Mao G, Leng SX. Frailty syndrome: an overview. Clin Interv Aging. 2014 Mar 19;9:433-41. doi: 10.2147/CIA.S45300.

Cheng Z, He D, Li J, Wu Q, Liu Z, Zhu Y. C-reactive protein and white blood cell are associated with frailty progression: a longitudinal study. Immun Ageing. 2022 Jun 3;19(1):29. doi: 10.1186/s12979-022-00280-1.

Cleasby ME, Jamieson PM, Atherton PJ. Insulin resistance and sarcopenia: mechanistic links between common co-morbidities. J Endocrinol. 2016 May;229(2):R67-81. doi: 10.1530/JOE-15-0533.

Clegg A, Hassan-Smith Z. Frailty and the endocrine system. Lancet Diabetes Endocrinol. 2018 Sep;6(9):743-752. doi: 10.1016/S2213-8587(18)30110-4.

Collerton J, Martin-Ruiz C, Davies K, Hilkens CM, Isaacs J, Kolenda C, Parker C, Dunn M, Catt M, Jagger C, von Zglinicki T, Kirkwood TB. Frailty and the role of inflammation, immunosenescence and cellular ageing in the very old: cross-sectional findings from the Newcastle 85+ Study. Mech Ageing Dev. 2012 Jun;133(6):456-66. doi: 10.1016/j.mad.2012.05.005.

Collerton J, Martin-Ruiz C, Davies K, Hilkens CM, Isaacs J, Kolenda C, Parker C, Dunn M, Catt M, Jagger C, von Zglinicki T, Kirkwood TB. Frailty and the role of inflammation, immunosenescence and cellular ageing in the very old: cross-sectional findings from the Newcastle 85+ Study. Mech Ageing Dev. 2012 Jun;133(6):456-66. doi: 10.1016/j.mad.2012.05.005.

Compté N, Zouaoui Boudjeltia K, Vanhaeverbeek M, De Breucker S, Tassignon J, Trelcat A, Pepersack T, Goriely S. Frailty in old age is associated with decreased interleukin-12/23 production in response to toll-like receptor ligation. PLoS One. 2013 Jun 5;8(6):e65325. doi: 10.1371/journal.pone.0065325.

Congressional Budget Office. Rising demand for long-term services and supports for elderly people. Washington, DC: Congressional Budget Office; 2013. Available at https://www.cbo.gov/publication/44363

Craig CL, Marshall AL, Sjöström M, et al. International physical activity questionnaire: 12-country reliability and validity. Med Sci Sports Exerc. 2003;35(8):1381-1395. doi: 10.1249/01.MSS.0000078924.61453.FB

Cruz-Jentoft AJ, Baeyens JP, Bauer JM et al. Sarcopenia: European consensus on definition and diagnosis: report of the European working group on sarcopenia in older people. Age Ageing 2010; 39: 412–23.

Cruz-Jentoft AJ, Bahat G, Bauer J, Boirie Y, Bruyère O, Cederholm T, Cooper C, Landi F, Rolland Y, Sayer AA, Schneider SM, Sieber CC, Topinkova E, Vandewoude M, Visser M, Zamboni M; Writing Group for the European Working Group on Sarcopenia in Older People 2 (EWGSOP2), and the Extended Group for EWGSOP2. Sarcopenia: revised European consensus on definition and diagnosis. Age Ageing. 2019 Jan 1;48(1):16-31. doi: 10.1093/ageing/afy169.

Cruz-Jentoft AJ, Bahat G, Bauer J, Boirie Y, Bruyère O, Cederholm T, Cooper C, Landi F, Rolland Y, Sayer AA, Schneider SM, Sieber CC, Topinkova E, Vandewoude M, Visser M, Zamboni M; Writing Group for the European Working Group on Sarcopenia in Older People 2 (EWGSOP2), and the Extended Group for EWGSOP2. Sarcopenia: revised European consensus on definition and diagnosis. Age Ageing. 2019 Jan 1;48(1):16-31. doi: 10.1093/ageing/afy169.

de Jongh RT, van Schoor NM, Lips P. Changes in vitamin D endocrinology during aging in adults. Mol Cell Endocrinol. 2017 Sep 15;453:144-150. doi: 10.1016/j.mce.2017.06.005.

Denegar, C. R., & Ball, D. W. (1993). Assessing Reliability and Precision of Measurement: An Introduction to Intraclass Correlation and Standard Error of Measurement, Journal of Sport Rehabilitation, 2(1), 35-42.

Dodd SL, Powers SK, Brooks E, Crawford MP. Effects of reduced O2 delivery with anemia, hypoxia, or ischemia on peak VO2 and force in skeletal muscle. J Appl Physiol (1985). 1993 Jan;74(1):186-91. doi: 10.1152/jappl.1993.74.1.186.

Doi T, Makizako H, Tsutsumimoto K, Hotta R, Nakakubo S, Makino K, Suzuki T, Shimada H. Association between Insulin-Like Growth Factor-1 and Frailty among Older Adults. J Nutr Health Aging. 2018;22(1):68-72. doi: 10.1007/s12603-017-0916-1.

DW Hosmer, S Lemeshow Applied Logistic Regression, 2nd Ed. Chapter 5, John Wiley and Sons, New York, NY (2000), pp. 160-164

Dziubek W, Bulińska K, Stefańska M, Woźniewski M, Kropielnicka K, Jasiński T, Jasiński R, Pilch U, Dąbrowska G, Skórkowska-Telichowska K, Wojcieszczyk-Latos J, Kałka D, Janus A, Zywar K, Paszkowski R, Szuba A. Peripheral arterial disease decreases muscle torque and functional walking capacity in elderly. Maturitas. 2015 Aug;81(4):480-6. doi: 10.1016/j.maturitas.2015.06.001.

Franchi MV, Raiteri BJ, Longo S, Sinha S, Narici MV, Csapo R. Muscle Architecture Assessment: Strengths, Shortcomings and New Frontiers of in Vivo Imaging Techniques. Ultrasound Med Biol. 2018 Dec;44(12):2492-2504. doi: 10.1016/j.ultrasmedbio.2018.07.010.

Fried LP, Tangen CM, Walston J, Newman AB, Hirsch C, Gottdiener J, Seeman T, Tracy R, Kop WJ, Burke G, McBurnie MA; Cardiovascular Health Study Collaborative Research Group. Frailty in older adults: evidence for a phenotype. J Gerontol A Biol Sci Med Sci. 2001 Mar;56(3):M146-56. doi: 10.1093/gerona/56.3.m146.

Fukumoto Y, Ikezoe T, Yamada Y, Tsukagoshi R, Nakamura M, Mori N, Kimura M, Ichihashi N. Skeletal muscle quality assessed from echo intensity is associated with muscle strength of middle-aged and elderly persons. Eur J Appl Physiol. 2012 Apr;112(4):1519-25. doi: 10.1007/s00421-011-2099-5.

Furman D, Campisi J, Verdin E, Carrera-Bastos P, Targ S, Franceschi C, Ferrucci L, Gilroy DW, Fasano A, Miller GW, Miller AH, Mantovani A, Weyand CM, Barzilai N, Goronzy JJ, Rando TA, Effros RB, Lucia A, Kleinstreuer N, Slavich GM. Chronic inflammation in the etiology of disease across the life span. Nat Med. 2019 Dec;25(12):1822-1832. doi: 10.1038/s41591-019-0675-0.

Furtado GE, Uba Chupel M, Minuzzi L, Patrício M, Loureiro M, Bandelow S, Hogervorst E, Ferreira JP, Teixeira AM. Exploring the potential of salivary and blood immune biomarkers to elucidate physical frailty in institutionalized older women. Exp Gerontol. 2020 Jan;129:110759. doi: 10.1016/j.exger.2019.110759.

Gellhorn, A.C., Stumph, J.M., Zikry, H.E. et al. Ultrasound measures of muscle thickness may be superior to strength testing in adults with knee osteoarthritis: a cross-sectional study. BMC Musculoskelet Disord 19, 350 (2018). doi:10.1186/s12891-018-2267-4

Goodpaster BH, Carlson CL, Visser M, Kelley DE, Scherzinger A, Harris TB, Stamm E, Newman AB. Attenuation of skeletal muscle and strength in the elderly: The Health ABC Study. J Appl Physiol (1985). 2001 Jun;90(6):2157-65. doi: 10.1152/jappl.2001.90.6.2157.

Goodpaster BH, Park SW, Harris TB, Kritchevsky SB, Nevitt M, Schwartz AV, Simonsick EM, Tylavsky FA, Visser M, Newman AB. The loss of skeletal muscle strength, mass, and quality in older adults: the health, aging and body composition study. J Gerontol A Biol Sci Med Sci. 2006 Oct;61(10):1059-64. doi: 10.1093/gerona/61.10.1059.

Granic A, Hill TR, Davies K, Jagger C, Adamson A, Siervo M, Kirkwood TB, Mathers JC, Sayer AA. Vitamin D Status, Muscle Strength and Physical Performance Decline in Very Old Adults: A Prospective Study. Nutrients. 2017 Apr 13;9(4):379. doi: 10.3390/nu9040379.

Hammami S, Ghzaiel I, Hammouda S, Sakly N, Hammami M, Zarrouk A. Evaluation of pro-inflammatory cytokines in frail Tunisian older adults. PLoS One. 2020 Nov 9;15(11):e0242152. doi: 10.1371/journal.pone.0242152.

Hammond K, Mampilly J, Laghi FA, Goyal A, Collins EG, McBurney C, Jubran A, Tobin MJ. Validity and reliability of rectus femoris ultrasound measurements: Comparison of curved-array and linear-array transducers. J Rehabil Res Dev. 2014;51(7):1155-64. doi: 10.1682/JRRD.2013.08.0187.

Harris-Love MO, Monfaredi R, Ismail C, Blackman MR, Cleary K. Quantitative ultrasound: measurement considerations for the assessment of muscular dystrophy and sarcopenia. Front Aging Neurosci. 2014 Jul 14;6:172. doi: 10.3389/fnagi.2014.00172.

Hodges PW, Pengel LH, Herbert RD, Gandevia SC. Measurement of muscle contraction with ultrasound imaging. Muscle Nerve. 2003 Jun;27(6):682-92. doi: 10.1002/mus.10375.

Hong C, Baek JY, Lee JW, Lee JH, Lee K, Park TJ, Kim J. Relationship between Decreased Estimated Glomerular Filtration Rate and Sarcopenic Obesity among Postmenopausal Women: Korea National Health and Nutrition Examination Survey (2008-2011). Korean J Fam Med. 2020 Sep;41(5):332-338. doi: 10.4082/kjfm.19.0032.

Hruda KV, Hicks AL, McCartney N. Training for muscle power in older adults: effects on functional abilities. Can J Appl Physiol. 2003 Apr;28(2):178-89. doi: 10.1139/h03-014.

Hsu B, Hirani V, Cumming RG, Naganathan V, Blyth FM, Wright FC, Waite LM, Seibel MJ, Handelsman DJ, Le Couteur DG. Cross-Sectional and Longitudinal Relationships Between Inflammatory Biomarkers and Frailty in Community-dwelling Older Men: The Concord Health and Ageing in Men Project. J Gerontol A Biol Sci Med Sci. 2019 May 16;74(6):835-841. doi: 10.1093/gerona/glx142.

Hsu, B., Hirani, V., Cumming, R. G., Naganathan, V., Blyth, F. M., Wright, F. C., … Le Couteur, D. G. (2017). Cross-Sectional and Longitudinal Relationships Between Inflammatory Biomarkers and Frailty in Community-dwelling Older Men: The Concord Health and Ageing in Men Project. The Journals of Gerontology: Series A. doi:10.1093/gerona/glx142

Hubbard RE, O'Mahony MS, Calver BL, Woodhouse KW. Nutrition, inflammation, and leptin levels in aging and frailty. J Am Geriatr Soc. 2008 Feb;56(2):279-84. doi: 10.1111/j.1532-5415.2007.01548.x.

Hubbard RE, O'Mahony MS, Savva GM, Calver BL, Woodhouse KW. Inflammation and frailty measures in older people. J Cell Mol Med. 2009;13(9B):3103-3109. doi:10.1111/j.1582-4934.2009.00733.x

Huisingh-Scheetz M, Martinchek M, Becker Y, Ferguson MK, Thompson K. Translating Frailty Research Into Clinical Practice: Insights From the Successful Aging and Frailty Evaluation Clinic. J Am Med Dir Assoc. 2019 Jun;20(6):672-678. doi: 10.1016/j.jamda.2018.12.002.

Inglés M, Gambini J, Carnicero JA, García-García FJ, Rodríguez-Mañas L, Olaso-González G, Dromant M, Borrás C, Viña J. Oxidative stress is related to frailty, not to age or sex, in a geriatric population: lipid and protein oxidation as biomarkers of frailty. J Am Geriatr Soc. 2014 Jul;62(7):1324-8. doi: 10.1111/jgs.12876.

Janssen I, Heymsfield SB, Wang ZM, Ross R. Skeletal muscle mass and distribution in 468 men and women aged 18-88 yr. J Appl Physiol (1985). 2000 Jul;89(1):81-8. doi: 10.1152/jappl.2000.89.1.81

Ju SY, Lee JY, Kim DH. Low 25-hydroxyvitamin D levels and the risk of frailty syndrome: a systematic review and dose-response meta-analysis. BMC Geriatr. 2018 Sep 4;18(1):206. doi: 10.1186/s12877-018-0904-2.

Keshaviah PR, Nolph KD, Moore HL, Prowant B, Emerson PF, Meyer M, Twardowski ZJ, Khanna R, Ponferrada L, Collins A. Lean body mass estimation by creatinine kinetics. J Am Soc Nephrol. 1994 Jan;4(7):1475-85. doi: 10.1681/ASN.V471475.

Kim SJ, Mehta HH, Wan J, Kuehnemann C, Chen J, Hu JF, Hoffman AR, Cohen P. Mitochondrial peptides modulate mitochondrial function during cellular senescence. Aging (Albany NY). 2018 Jun 10;10(6):1239-1256. doi: 10.18632/aging.101463.

König N, Cassel M, Intziegianni K, Mayer F. Inter-rater reliability and measurement error of sonographic muscle architecture assessments. J Ultrasound Med. 2014 May;33(5):769-77. doi: 10.7863/ultra.33.5.769.

Koo TK, Li MY. A Guideline of Selecting and Reporting Intraclass Correlation Coefficients for Reliability Research. J Chiropr Med. 2016 Jun;15(2):155-63. doi: 10.1016/j.jcm.2016.02.012.

Lai HY, Chang HT, Lee YL, Hwang SJ. Association between inflammatory markers and frailty in institutionalized older men. Maturitas. 2014 Nov;79(3):329-33. doi: 10.1016/j.maturitas.2014.07.014.

Landi F, Liperoti R, Russo A, et al. Sarcopenia as a risk factor for falls in elderly individuals: Results from the ilSIRENTE study. Clin Nutr. 2012;31(5):652-658. doi: S0261-5614(12)00036-2

Landi F, Calvani R, Cesari M, Tosato M, Martone AM, Bernabei R, Onder G, Marzetti E. Sarcopenia as the Biological Substrate of Physical Frailty. Clin Geriatr Med. 2015 Aug;31(3):367-74. doi: 10.1016/j.cger.2015.04.005.

Lee CT, Chen MZ, Yip CYC, Yap ES, Lee SY, Merchant RA. Prevalence of Anemia and Its Association with Frailty, Physical Function and Cognition in Community-Dwelling Older Adults: Findings from the HOPE Study. J Nutr Health Aging. 2021;25(5):679-687. doi: 10.1007/s12603-021-1625-3.

Leng SX, Xue QL, Tian J, Huang Y, Yeh SH, Fried LP. Associations of neutrophil and monocyte counts with frailty in community-dwelling disabled older women: results from the Women's Health and Aging Studies I. Exp Gerontol. 2009 Aug;44(8):511-6. doi: 10.1016/j.exger.2009.05.005.

Liu CK, Lyass A, Larson MG, Massaro JM, Wang N, D'Agostino RB Sr, Benjamin EJ, Murabito JM. Biomarkers of oxidative stress are associated with frailty: the Framingham Offspring Study. Age (Dordr). 2016 Feb;38(1):1. doi: 10.1007/s11357-015-9864-z.

Lowry OH, Rosebrough NJ, Farr AL, Randall RJ. Protein measurement with the Folin phenol reagent. J Biol Chem. 1951 Nov;193(1):265-75.

Mandal S, Suh E, Thompson A, Connolly B, Ramsay M, Harding R, Puthucheary Z, Moxham J, Hart N. Comparative study of linear and curvilinear ultrasound probes to assess quadriceps rectus femoris muscle mass in healthy subjects and in patients with chronic respiratory disease. BMJ Open Respir Res. 2016 Jan 12;3(1):e000103. doi: 10.1136/bmjresp-2015-000103.

Marzetti E, Picca A, Marini F, Biancolillo A, Coelho-Junior HJ, Gervasoni J, Bossola M, Cesari M, Onder G, Landi F, Bernabei R, Calvani R. Inflammatory signatures in older persons with physical frailty and sarcopenia: The frailty "cytokinome" at its core. Exp Gerontol. 2019 Jul 15;122:129-138. doi: 10.1016/j.exger.2019.04.019.

McKechnie DGJ, Papacosta AO, Lennon LT, Ramsay SE, Whincup PH, Wannamethee SG. Associations between inflammation, cardiovascular biomarkers and incident frailty: the British Regional Heart Study. Age Ageing. 2021 Nov 10;50(6):1979-1987. doi: 10.1093/ageing/afab143.

Mechelli F, Arendt-Nielsen L, Stokes M, Agyapong-Badu S. Validity of Ultrasound Imaging Versus Magnetic Resonance Imaging for Measuring Anterior Thigh Muscle, Subcutaneous Fat, and Fascia Thickness. Methods Protoc. 2019 Jul 10;2(3):58. doi: 10.3390/mps2030058.

Michaud M, Balardy L, Moulis G, Gaudin C, Peyrot C, Vellas B, Cesari M, Nourhashemi F. Proinflammatory cytokines, aging, and age-related diseases. J Am Med Dir Assoc. 2013 Dec;14(12):877-82. doi: 10.1016/j.jamda.2013.05.009.

Mirón Mombiela R, Arildskov AR, Bruun FJ, Hasselbalch LH, Holst KB, Rasmussen SH, Borrás C. What Genetics Can Do for Oncological Imaging: A Systematic Review of the Genetic Validation Data Used in Radiomics Studies. Int J Mol Sci. 2022 Jun 10;23(12):6504. doi: 10.3390/ijms23126504.

Mirón Mombiela R, Facal de Castro F, Moreno P, Borras C. Ultrasonic Echo Intensity as a New Noninvasive In Vivo Biomarker of Frailty. J Am Geriatr Soc. 2017 Dec;65(12):2685-2690. doi: 10.1111/jgs.15002.

Mirón Mombiela R, Vucetic J, Monllor P, Cárdenas-Herrán JS, Taltavull de La Paz P, Borrás C. Diagnostic Performance of Muscle Echo Intensity and Fractal Dimension for the Detection of Frailty Phenotype. Ultrason Imaging. 2021 Nov;43(6):337-352. doi: 10.1177/01617346211029656.

Mirón Mombiela R, Vucetic J, Rossi F, Tagliafico AS. Ultrasound Biomarkers for Sarcopenia: What Can We Tell So Far? Semin Musculoskelet Radiol. 2020 Apr;24(2):181-193. doi: 10.1055/s-0039-3402745.

Mitchell WK, Williams J, Atherton P, Larvin M, Lund J, Narici M. Sarcopenia, dynapenia, and the impact of advancing age on human skeletal muscle size and strength; a quantitative review. Front Physiol. 2012 Jul 11;3:260. doi: 10.3389/fphys.2012.00260.

Mitnitski A, Collerton J, Martin-Ruiz C, Jagger C, von Zglinicki T, Rockwood K, Kirkwood TB. Age-related frailty and its association with biological markers of ageing. BMC Med. 2015 Jul 13;13:161. doi: 10.1186/s12916-015-0400-x.

Mohamad M, Ebeid S, Shawky Khater M, Alsadany M. Interferon- Gamma- Inducible Guanosine Triphosphate Cyclohydrolase 1 (GTP-CH1) Pathway Is Associated with Frailty in Egyptian Elderly. Rep Biochem Mol Biol. 2018 Oct;7(1):52-58.

Moon JH, Kong MH, Kim HJ. Relationship between low muscle mass and anemia in Korean elderly men: Using the Korea National Health and Nutrition Examination Survey (KNHANES IV–V), J Clin Gerontology and Geriatrics, 2015; 6(4), 115–119. doi:10.1016/j.jcgg.2015.03.007

Mori H, Kuroda A, Ishizu M, Ohishi M, Takashi Y, Otsuka Y, Taniguchi S, Tamaki M, Kurahashi K, Yoshida S, Endo I, Aihara KI, Funaki M, Akehi Y, Matsuhisa M. Association of accumulated advanced glycation end-products with a high prevalence of sarcopenia and dynapenia in patients with type 2 diabetes. J Diabetes Investig. 2019 Sep;10(5):1332-1340. doi: 10.1111/jdi.13014.

Morley, J. E., Vellas, B., Abellan van Kan, G., Anker, S. D., Bauer, J. M., Bernabei, R., … Walston, J. (2013). Frailty Consensus: A Call to Action. Journal of the American Medical Directors Association, 14(6), 392–397. doi:10.1016/j.jamda.2013.03.022

Muscaritoli, M., Anker, S. D., Argilés, J., Aversa, Z., Bauer, J. M., Biolo, G., … Sieber, C. C. (2010). Consensus definition of sarcopenia, cachexia and pre-cachexia: Joint document elaborated by Special Interest Groups (SIG) “cachexia-anorexia in chronic wasting diseases” and “nutrition in geriatrics.” Clinical Nutrition, 29(2), 154–159. doi:10.1016/j.clnu.2009.12.004

Narici MV, Maffulli N. Sarcopenia: characteristics, mechanisms and functional significance. Br Med Bull. 2010;95:139-59. doi: 10.1093/bmb/ldq008.

Narici MV, Roi GS, Landoni L, Minetti AE, Cerretelli P. Changes in force, cross-sectional area and neural activation during strength training and detraining of the human quadriceps. Eur J Appl Physiol Occup Physiol. 1989;59(4):310-319. doi: 10.1007/BF02388334

Nascimento CMC, Zazzetta MS, Gomes GAO, Orlandi FS, Gramani-Say K, Vasilceac FA, Gratão ACM, Pavarini SCI, Cominetti MR. Higher levels of tumor necrosis factor β are associated with frailty in socially vulnerable community-dwelling older adults. BMC Geriatr. 2018 Nov 6;18(1):268. doi: 10.1186/s12877-018-0961-6.

Newman AB, Kupelian V, Visser M, Simonsick EM, Goodpaster BH, Kritchevsky SB, et al. Strength, but not muscle mass, is associated with mortality in the Health, Aging and Body Composition Study cohort. J Gerontol A Biol Sci Med Sci. 2006;61:72–77.

Ng TP, Feng L, Nyunt MS, Feng L, Niti M, Tan BY, Chan G, Khoo SA, Chan SM, Yap P, Yap KB. Nutritional, Physical, Cognitive, and Combination Interventions and Frailty Reversal Among Older Adults: A Randomized Controlled Trial. Am J Med. 2015 Nov;128(11):1225-1236.e1. doi: 10.1016/j.amjmed.2015.06.017.

Nijholt W, Scafoglieri A, Jager-Wittenaar H, Hobbelen JSM, van der Schans CP. The reliability and validity of ultrasound to quantify muscles in older adults: a systematic review. J Cachexia Sarcopenia Muscle. 2017 Oct;8(5):702-712. doi: 10.1002/jcsm.12210

Oliveira, F. T. M. de, Oliveira, C. G. de, & Farinatti, P. (2017). Pennation angle of vastus laterallis during isometric contractions performed at two knee angles. Fisioterapia Em Movimento, 30(suppl 1), 75–83. doi:10.1590/1980-5918.030.s01.ao07

Orkaby AR, Dushkes R, Ward R, Djousse L, Buring JE, Lee IM, Cook NR, LeBoff MS, Okereke OI, Copeland T, Manson JE. Effect of Vitamin D3 and Omega-3 Fatty Acid Supplementation on Risk of Frailty: An Ancillary Study of a Randomized Clinical Trial. JAMA Netw Open. 2022 Sep 1;5(9):e2231206. doi: 10.1001/jamanetworkopen.2022.31206.

Pacifico, J., Geerlings, M. A. J., Reijnierse, E. M., Phassouliotis, C., Lim, W. K., & Maier, A. B. (2019). Prevalence of sarcopenia as a comorbid disease: A systematic review and meta-analysis. Experimental Gerontology, 110801. doi:10.1016/j.exger.2019.110801

Payette, Hã©., Roubenoff, R., Jacques, P. F., Dinarello, C. A., Wilson, P. W. F., Abad, L. W., & Harris, T. (2003). Insulin-Like Growth Factor-1 and Interleukin 6 Predict Sarcopenia in Very Old

Community-Living Men and Women: The Framingham Heart Study. Journal of the American Geriatrics Society, 51(9), 1237–1243. doi:10.1046/j.1532-5415.2003.51407.x

Pereira, S., Marliss, E. B., Morais, J. A., Chevalier, S., & Gougeon, R. (2007). Insulin Resistance of Protein Metabolism in Type 2 Diabetes. Diabetes, 57(1), 56–63. doi:10.2337/db07-0887

Pérez-Tasigchana RF, León-Muñoz LM, Lopez-Garcia E, Gutierrez-Fisac JL, Laclaustra M, Rodríguez-Artalejo F, Guallar-Castillón P. Metabolic syndrome and insulin resistance are associated with frailty in older adults: a prospective cohort study. Age Ageing. 2017 Sep 1;46(5):807-812. doi: 10.1093/ageing/afx023.

Perkisas S, Baudry S, Bauer J, Beckwée D, De Cock AM, Hobbelen H, Jager-Wittenaar H, Kasiukiewicz A, Landi F, Marco E, Merello A, Piotrowicz K, Sanchez E, Sanchez-Rodriguez D, Scafoglieri A, Cruz-Jentoft A, Vandewoude M. Application of ultrasound for muscle assessment in sarcopenia: towards standardized measurements. Eur Geriatr Med. 2018 Dec;9(6):739-757. doi: 10.1007/s41999-018-0104-9.

Perkisas S, Bastijns S, Baudry S, Bauer J, Beaudart C, Beckwée D, Cruz-Jentoft A, Gasowski J, Hobbelen H, Jager-Wittenaar H, Kasiukiewicz A, Landi F, Małek M, Marco E, Martone AM, de Miguel AM, Piotrowicz K, Sanchez E, Sanchez-Rodriguez D, Scafoglieri A, Vandewoude M, Verhoeven V, Wojszel ZB, De Cock AM. Application of ultrasound for muscle assessment in sarcopenia: 2020 SARCUS update. Eur Geriatr Med. 2021 Feb;12(1):45-59. doi: 10.1007/s41999-020-00433-9.

Pillen S, Tak RO, Zwarts MJ, Lammens MM, Verrijp KN, Arts IM, van der Laak JA, Hoogerbrugge PM, van Engelen BG, Verrips A. Skeletal muscle ultrasound: correlation between fibrous tissue and echo intensity. Ultrasound Med Biol. 2009 Mar;35(3):443-6. doi: 10.1016/j.ultrasmedbio.2008.09.016.

Pillen S, van Alfen N. Skeletal muscle ultrasound. Neurol Res. 2011 Dec;33(10):1016-24. doi: 10.1179/1743132811Y.0000000010.

Pires Corona L, Drumond Andrade FC, de Oliveira Duarte YA, Lebrao ML. The Relationship between Anemia, Hemoglobin Concentration and Frailty in Brazilian Older Adults. J Nutr Health Aging. 2015 Nov;19(9):935-40. doi: 10.1007/s12603-015-0502-3.

Puts MTE, Toubasi S, Andrew MK, Ashe MC, Ploeg J, Atkinson E, Ayala AP, Roy A, Rodríguez Monforte M, Bergman H, McGilton K. Interventions to prevent or reduce the level of frailty in

community-dwelling older adults: a scoping review of the literature and international policies. Age Ageing. 2017 May 1;46(3):383-392. doi: 10.1093/ageing/afw247.

Ranasinghe R, Eri R. Pleiotropic Immune Functions of Chemokine Receptor 6 in Health and Disease. Medicines (Basel). 2018 Jul 2;5(3):69. doi: 10.3390/medicines5030069.

Rech A, Radaelli R, Goltz FR, da Rosa LH, Schneider CD, Pinto RS. Echo intensity is negatively associated with functional capacity in older women. Age (Dordr). 2014;36(5):9708. doi: 10.1007/s11357-014-9708-2.

Rockwood K, Song X, MacKnight C, Bergman H, Hogan DB, McDowell I, Mitnitski A. A global clinical measure of fitness and frailty in elderly people. CMAJ. 2005 Aug 30;173(5):489-95. doi: 10.1503/cmaj.050051.

Rolland Y, Lauwers-Cances V, Cristini C, Abellan van Kan G, Janssen I, Morley JE, Vellas B. Difficulties with physical function associated with obesity, sarcopenia, and sarcopenic-obesity in community-dwelling elderly women: the EPIDOS (EPIDemiologie de l'OSteoporose) Study. Am J Clin Nutr. 2009 Jun;89(6):1895-900. doi: 10.3945/ajcn.2008.26950.

Rothman MD, Leo-Summers L, Gill TM. Prognostic significance of potential frailty criteria. J Am Geriatr Soc. 2008 Dec;56(12):2211-16. doi: 10.1111/j.1532-5415.2008.02008.x.

Ryan TP. Modern regression methods. 2. ed. ed. Hoboken, NJ: Wiley; 2009.

Sabatino A, Cuppari L, Stenvinkel P, Lindholm B, Avesani CM. Sarcopenia in chronic kidney disease: what have we learned so far? J Nephrol. 2021 Aug;34(4):1347-1372. doi: 10.1007/s40620-020-00840-y.

Saedi AA, Feehan J, Phu S, Duque G. Current and emerging biomarkers of frailty in the elderly. Clin Interv Aging. 2019 Feb 19;14:389-398. doi: 10.2147/CIA.S168687.

Santilli V, Bernetti A, Mangone M, Paoloni M. Clinical definition of sarcopenia. Clin Cases Miner Bone Metab. 2014 Sep;11(3):177-80.

Santos-Eggimann B, Cuénoud P, Spagnoli J, Junod J. Prevalence of frailty in middle-aged and older community-dwelling Europeans living in 10 countries. J Gerontol A Biol Sci Med Sci. 2009 Jun;64(6):675-81. doi: 10.1093/gerona/glp012.

Scanlon, T.C., Fragala, M.S., Stout, J.R., Emerson, N.S., Beyer, K.S., Oliveira, L.P. and Hoffman, J.R. (2014), Muscle architecture and strength: Adaptations to short-term resistance training in older adults. Muscle Nerve, 49: 584-592. doi:10.1002/mus.23969

Semba RD, Ferrucci L, Sun K, Walston J, Varadhan R, Guralnik JM, Fried LP. Oxidative stress and severe walking disability among older women. Am J Med. 2007 Dec;120(12):1084-9. doi: 10.1016/j.amjmed.2007.07.028.

Serrano, A. L., Baeza-Raja, B., Perdiguero, E., Jardí, M., & Muñoz-Cánoves, P. (2008). Interleukin-6 Is an Essential Regulator of Satellite Cell-Mediated Skeletal Muscle Hypertrophy. Cell Metabolism, 7(1), 33–44. doi:10.1016/j.cmet.2007.11.011

Shui L., Ren H., Yang X., Li J., Chen Z., Yi C., Zhu H., Shui P. The Era of Radiogenomics in Precision Medicine: An Emerging Approach to Support Diagnosis, Treatment Decisions, and Prognostication in Oncology. Front. Oncol. 2020;10:570465. doi: 10.3389/fonc.2020.570465.

Sieber, C. C. (2017). Frailty – From concept to clinical practice. Experimental Gerontology, 87, 160–167. doi:10.1016/j.exger.2016.05.004

Steinmeyer Z, Delpierre C, Soriano G, Steinmeyer A, Ysebaert L, Balardy L, Sourdet S. Hemoglobin concentration; a pathway to frailty. BMC Geriatr. 2020 Jun 11;20(1):202. doi: 10.1186/s12877-020-01597-6.

Stock MS, Whitson M, Burton AM, Dawson NT, Sobolewski EJ, Thompson BJ. Echo Intensity Versus Muscle Function Correlations in Older Adults are Influenced by Subcutaneous Fat Thickness. Ultrasound Med Biol. 2018 Aug;44(8):1597-1605. doi: 10.1016/j.ultrasmedbio.2018.04.009.

Strasser EM, Draskovits T, Praschak M, Quittan M, Graf A. Association between ultrasound measurements of muscle thickness, pennation angle, echogenicity and skeletal muscle strength in the elderly. Age (Dordr). 2013 Dec;35(6):2377-88. doi: 10.1007/s11357-013-9517-z.

Su, L., Hao, Q.-K., Liu, S., & Dong, B.-R. (2017). Monocytes Related Inflammatory Biomarkers are Associated With Frailty Syndrome. International Journal of Gerontology, 11(4), 225–229. doi:10.1016/j.ijge.2017.08.004

Sullivan DC, Obuchowski NA, Kessler LG, Raunig DL, Gatsonis C, Huang EP, Kondratovich M, McShane LM, Reeves AP, Barboriak DP, Guimaraes AR, Wahl RL; RSNA-QIBA Metrology Working

Group. Metrology Standards for Quantitative Imaging Biomarkers. Radiology. 2015 Dec;277(3):813-25. doi: 10.1148/radiol.2015142202.

Taaffe DR, Henwood TR, Nalls MA, Walker DG, Lang TF, Harris TB. Alterations in muscle attenuation following detraining and retraining in resistance-trained older adults. Gerontology. 2009;55(2):217-23. doi: 10.1159/000182084.

Tembo MC, Holloway-Kew KL, Bortolasci CC, Brennan-Olsen SL, Williams LJ, Kotowicz MA, Pasco JA. Association between serum interleukin-6 and frailty in older men: cross-sectional data. Eur Geriatr Med. 2021 Aug;12(4):887-892. doi: 10.1007/s41999-021-00490-8.

Ticinesi A, Meschi T, Narici MV, Lauretani F, Maggio M. Muscle Ultrasound and Sarcopenia in Older Individuals: A Clinical Perspective. J Am Med Dir Assoc. 2017 Apr 1;18(4):290-300. doi: 10.1016/j.jamda.2016.11.013.

Tieland, M., Brouwer-Brolsma, E. M., Nienaber-Rousseau, C., van Loon, L. J. C., & De Groot, L. C. P. G. M. (2013). Low vitamin D status is associated with reduced muscle mass and impaired physical performance in frail elderly people. European Journal of Clinical Nutrition, 67(10), 1050–1055. doi:10.1038/ejcn.2013.144

Tomaszewski MR, Gillies RJ. The Biological Meaning of Radiomic Features. Radiology. 2021 May;299(2):E256. doi: 10.1148/radiol.2021219005. Erratum for: Radiology. 2021 Mar;298(3):505-516.

United Nations, Department of Economic and Social Affairs, Population Division (2022). World Population Prospects 2022, Online Edition. Available at https://population.un.org/wpp/

van Nieuwpoort IC, Vlot MC, Schaap LA, Lips P, Drent ML. The relationship between serum IGF-1, handgrip strength, physical performance and falls in elderly men and women. Eur J Endocrinol. 2018 Aug;179(2):73-84. doi: 10.1530/EJE-18-0076.

Visser M, Kritchevsky SB, Newman AB, Goodpaster BH, Tylavsky FA, Nevitt MC, Harris TB. Lower serum albumin concentration and change in muscle mass: the Health, Aging and Body Composition Study. Am J Clin Nutr. 2005 Sep;82(3):531-7. doi: 10.1093/ajcn.82.3.531.

Visser M, Pahor M, Taaffe DR, Goodpaster BH, Simonsick EM, Newman AB, Nevitt M, Harris TB. Relationship of interleukin-6 and tumor necrosis factor-alpha with muscle mass and muscle strength in elderly men and women: the Health ABC Study. J Gerontol A Biol Sci Med Sci. 2002 May;57(5):M326-32. doi: 10.1093/gerona/57.5.m326.

Visser, M., Goodpaster, B. H., Kritchevsky, S. B., Newman, A. B., Nevitt, M., … Rubin, S. M. (2005). Muscle Mass, Muscle Strength, and Muscle Fat Infiltration as Predictors of Incident Mobility Limitations in Well-Functioning Older Persons. The Journals of Gerontology Series A: Biological Sciences and Medical Sciences, 60(3), 324–333. doi:10.1093/gerona/60.3.324

Walston, J., Hadley, E. C., Ferrucci, L., Guralnik, J. M., Newman, A. B., Studenski, S. A., … Fried, L. P. (2006). Research Agenda for Frailty in Older Adults: Toward a Better Understanding of Physiology and Etiology: Summary from the American Geriatrics Society/National Institute on Aging Research Conference on Frailty in Older Adults. Journal of the American Geriatrics Society, 54(6), 991–1001. doi:10.1111/j.1532-5415.2006.00745.x

Warner MB, Cotton AM, Stokes MJ. Comparison of curvilinear and linear ultrasound imaging probes for measuring cross-sectional area and linear dimensions. J Med Eng Technol. 2008 Nov-Dec;32(6):498-504. doi: 10.1080/03091900701695533.

Wassner SJ, Li JB, Sperduto A, Norman ME. Vitamin D Deficiency, hypocalcemia, and increased skeletal muscle degradation in rats. J Clin Invest. 1983 Jul;72(1):102-12. doi: 10.1172/jci110947.

Watanabe Y, Ikenaga M, Yoshimura E, Yamada Y, Kimura M. Association between echo intensity and attenuation of skeletal muscle in young and older adults: a comparison between ultrasonography and computed tomography. Clin Interv Aging. 2018 Oct 2;13:1871-1878. doi: 10.2147/CIA.S173372.

Watanabe Y, Yamada Y, Fukumoto Y, Ishihara T, Yokoyama K, Yoshida T, Miyake M, Yamagata E, Kimura M. Echo intensity obtained from ultrasonography images reflecting muscle strength in elderly men. Clin Interv Aging. 2013;8:993-8. doi: 10.2147/CIA.S47263.

Welch D, Ndanyo LS, Brown S, Agyapong-Badu S, Warner M, Stokes M, Samuel D. Thigh muscle and subcutaneous tissue thickness measured using ultrasound imaging in older females living in extended care: a preliminary study. Aging Clin Exp Res. 2018 May;30(5):463-469. doi: 10.1007/s40520-017-0800-1.

Wennberg AM, Ding M, Ebeling M, Hammar N, Modig K. Blood-Based Biomarkers and Long-term Risk of Frailty-Experience From the Swedish AMORIS Cohort. J Gerontol A Biol Sci Med Sci. 2021 Aug 13;76(9):1643-1652. doi: 10.1093/gerona/glab137.

Wilson D, Jackson T, Sapey E, Lord JM. Frailty and sarcopenia: The potential role of an aged immune system. Ageing Res Rev. 2017 Jul;36:1-10. doi: 10.1016/j.arr.2017.01.006.

Wong CH, Weiss D, Sourial N, Karunananthan S, Quail JM, Wolfson C, Bergman H. Frailty and its association with disability and comorbidity in a community-dwelling sample of seniors in Montreal: a cross-sectional study. Aging Clin Exp Res. 2010 Feb;22(1):54-62. doi: 10.1007/BF03324816.

Worsley PR, Kitsell F, Samuel D, Stokes M. Validity of measuring distal vastus medialis muscle using rehabilitative ultrasound imaging versus magnetic resonance imaging. Man Ther. 2014 Jun;19(3):259-63. doi: 10.1016/j.math.2014.02.002.

Yanagita I, Fujihara Y, Iwaya C, Kitajima Y, Tajima M, Honda M, Teruya Y, Asakawa H, Ito T, Eda T, Yamaguchi N, Kayashima Y, Yoshimoto M, Harada M, Yoshimoto S, Aida E, Yanase T, Nawata H, Muta K. Low serum albumin, aspartate aminotransferase, and body mass are risk factors for frailty in elderly people with diabetes-a cross-sectional study. BMC Geriatr. 2020 Jun 9;20(1):200. doi: 10.1186/s12877-020-01601-z.

Yoshiko, A., Kaji, T., Sugiyama, H., Koike, T., Oshida, Y., & Akima, H. (2018). Muscle quality characteristics of muscles in the thigh, upper arm and lower back in elderly men and women. European Journal of Applied Physiology, 118(7), 1385–1395. doi:10.1007/s00421-018-3870-7

Young HJ, Jenkins NT, Zhao Q, Mccully KK. Measurement of intramuscular fat by muscle echo intensity. Muscle Nerve. 2015 Dec;52(6):963-71. doi: 10.1002/mus.24656.

Young HJ, Southern WM, Mccully KK. Comparisons of ultrasound-estimated intramuscular fat with fitness and health indicators. Muscle Nerve. 2016 Oct;54(4):743-9. doi: 10.1002/mus.25105.

Zhu S, Lin W, Chen S, Qi H, Wang S, Zhang A, Cai J, Lai B, Sheng Y, Ding G. The correlation of muscle thickness and pennation angle assessed by ultrasound with sarcopenia in elderly Chinese community dwellers. Clin Interv Aging. 2019 May 28;14:987-996. doi: 10.2147/CIA.S201777.

Zhu, Y., Armstrong, J. L., Tchkonia, T., & Kirkland, J. L. (2014). Cellular senescence and the senescent secretory phenotype in age-related chronic diseases. Current Opinion in Clinical Nutrition and Metabolic Care, 17(4), 324–328. doi:10.1097/mco.0000000000000065

ANNEX MATERIAL

ANNEX INFORMED CONSENT

IMPRESO DE INFORMACIÓN Y CONSENTIMIENTO INFORMADO DE LOS SUJETOS A INCLUIR EN EL PROYECTO DE INVESTIGACIÓN

TÍTULO: ***"Estudio de arquitectura muscular determinada por ecografía para el diagnóstico de fragilidad con correlación de marcadores clínicos, físicos y bioquímicos".***

INVESTIGADOR PRINCIPAL: Rebeca Mirón Mombiela

OBJETIVOS

El objetivo del presente estudio es determinar si los cambios en la arquitectura muscular por ecografía permite realizar el diagnóstico de la fragilidad en el adulto mayor y correlacionan con parámetros clínicos, físicos y biológicos conocidos de fragilidad.

DESCRIPCIÓN DEL ESTUDIO

Se le realizará una ecografía muscular del muslo donde se tomarán fotos para estudiar a posteriori la arquitectura muscular y también se tomarán medidas del grosor muscular y una estimación numérica de la cantidad de grasa contenida dentro del músculo. Al concluir la ecografía se le realizará una medición de fuerza muscular con un dinamómetro, se le medirá la altura y el peso corporal. Luego se le entregará un cuestionario para rellenar por usted con preguntas personales y generales (Ejemplo: edad, género, etc), seguido de preguntas en relación a su calidad de vida en el momento actual. Luego se le solicitará que camine 4 metros para evaluar la velocidad con la que camina. Y por último se volverá a repetir la ecografía pero en otro aparato.

Si usted tiene una analítica solicitada por su médico de cabecera pendiente, se le preguntará si está de acuerdo con donar un poco de sangre para realizar estudios diagnósticos y de investigación (ej.: oxidación de lípidos y proteínas, marcadores de inflamación, etc). Además deseamos saber si desea donar los sobrantes de las muestras tras su procesado, que serán almacenados en el Biobanco del Hospital general Universitario de Valencia y conservados formando parte de la colección asociada a este estudio. Si usted accede a ello en el momento que vaya al laboratorio se le extraerán 2 tubos adicionales de sangre para dichos análisis.

Si Ud. está de acuerdo, libremente firme el consentimiento de participación en este estudio que para este fin se ha añadido al final de este impreso.

RIESGOS Y BENEFICIOS

No existen riesgos asociados al uso de ecografía.
Con su participación en este estudio, usted va a ayudar a realizar el diagnóstico de síndrome de fragilidad del adulto mayor y a entender mejor el proceso de envejecimiento de las personas.

Según su condición clínica esta información podrá o no ser aprovechada en su propia salud.

PARTICIPACIÓN EN EL ESTUDIO

Su participación en este estudio es totalmente voluntaria y no recibirá remuneración alguna. Como paciente, el rechazo a participar no supondrá ninguna penalización o ni afectará en modo alguno a la calidad de la asistencia sanitaria que reciba.

CONFIDENCIALIDAD

Toda la información obtenida será confidencial, los datos recogidos se introducirán, por el Equipo investigador, en una base de datos para realizar el análisis estadístico pero su nombre no aparecerá en ningún documento del estudio, sólo se le asignará un número. En concreto, las muestras se identificarán con un número y se agruparan por patologías afines. En ningún caso se le identificará en las publicaciones que puedan realizarse con los resultados del estudio. Sin embargo, esta información podrá ser revisada por el Comité Ético de Investigación Clínica de este Hospital así como por organismos gubernamentales competentes.

El procedimiento de destrucción de las muestras será el mismo que se utiliza habitualmente con el resto de las muestras del Consorcio Hospital General Universitario de Valencia. Puede ejercer su derecho de acceso y rectificación de sus datos. También, si así lo desea, puede ser informado de los resultados del estudio

El estudio se realizará asegurando el cumplimiento de normas éticas y legales vigentes (Declaración de Helsinki).

Si tiene alguna duda o no entiende este texto consulte antes de firmar el documento con la Dra. Rebeca Mirón Mombiela con nº de teléfono +34 601 209 362 que es el médico responsable de esta investigación y le puede preguntar cualquier duda o problema que tenga relacionado con este estudio o consulte con sus familiares y, finalmente, si está de acuerdo firme este consentimiento. Se le entregará una copia.

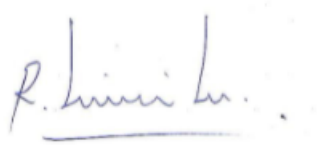

Fdo.: Rebeca Mirón Mombiela
Investigador Principal del Proyecto
Servicio de Radiodiagnóstico
Tel: +34 601 209 362

CONSENTIMIENTO DEL PACIENTE SUJETO DE ESTUDIO

Título del proyecto de investigación: ***"Estudio de arquitectura muscular determinada por ecografía para el diagnóstico de fragilidad con correlación de marcadores clínicos, físicos y bioquímicos "***

Yo, ……..……

He leído la hoja de información anterior.
He podido hacer preguntas sobre el estudio.
He recibido suficiente información sobre el estudio.

He hablado con ……..……

Comprendo que mi participación es voluntaria.
Comprendo que puedo retirarme del estudio:

- **Cuando quiera.**
- **Sin tener que dar explicaciones.**
- **Sin que esto repercuta en mis cuidados médicos.**

Consiento participar en el estudio de ecografía.

Doy mi consentimiento para que este material aparezca en informes y artículos de revista de publicaciones médicas.
Entiendo que:

- **Mi nombre no será publicado.**
- **El material no será utilizado para publicidad o embalaje.**
- **El material no será utilizado fuera de contexto.**

Firmado …….. **Fecha……..**

CONSENTIMIENTO DEL PACIENTE SUJETO DE ESTUDIO

Título del proyecto de investigación: ***"Estudio de arquitectura muscular determinada por ecografía para el diagnóstico de fragilidad con correlación de marcadores clínicos, físicos y bioquímicos "***

Yo, ……..……

He leído la hoja de información anterior.
He podido hacer preguntas sobre el estudio.
He recibido suficiente información sobre el estudio.

He hablado con ……..……

Comprendo que mi participación es voluntaria.
Comprendo que puedo retirarme del estudio:

- **Cuando quiera.**
- **Sin tener que dar explicaciones.**
- **Sin que esto repercuta en mis cuidados médicos.**

Consiento que se me realice la extracción de sangre para análisis bioquímicos.

Doy mi consentimiento para que este material aparezca en informes y artículos de revista de publicaciones médicas.
Entiendo que:

- **Mi nombre no será publicado.**
- **El material no será utilizado para publicidad o embalaje.**
- **El material no será utilizado fuera de contexto.**

-

Firmado …….. **Fecha……..**

CONSENTIMIENTO DEL PACIENTE SUJETO DE ESTUDIO

Título del proyecto de investigación: ***"Estudio de arquitectura muscular determinada por ecografía para el diagnóstico de fragilidad con correlación de marcadores clínicos, físicos y bioquímicos "***

Yo, ……..……

He leído la hoja de información anterior.
He podido hacer preguntas sobre el estudio.
He recibido suficiente información sobre el estudio.

He hablado con ……..……

Comprendo que mi participación es voluntaria.
Comprendo que puedo retirarme del estudio:

- **Cuando quiera.**
- **Sin tener que dar explicaciones.**
- **Sin que esto repercuta en mis cuidados médicos.**

Consiento la donación de sangre para estudios posteriores.

Doy mi consentimiento para que este material aparezca en informes y artículos de revista de publicaciones médicas.
Entiendo que:

- **Mi nombre no será publicado.**
- **El material no será utilizado para publicidad o embalaje.**
- **El material no será utilizado fuera de contexto.**

-

Firmado …….. **Fecha……..**

CONSENTIMIENTO DEL PACIENTE SUJETO DE ESTUDIO

Título del proyecto de investigación: ***"Estudio de arquitectura muscular determinada por ecografía para el diagnóstico de fragilidad con correlación de marcadores clínicos, físicos y bioquímicos "***

Yo, ……..……

He leído la hoja de información anterior.
He podido hacer preguntas sobre el estudio.
He recibido suficiente información sobre el estudio.

He hablado con ……..……

Comprendo que mi participación es voluntaria.
Comprendo que puedo retirarme del estudio:

- **Cuando quiera.**
- **Sin tener que dar explicaciones.**
- **Sin que esto repercuta en mis cuidados médicos.**

Consiento que los sobrantes de mi sangre pasen a formar parte del Biobanco HGUV.

Doy mi consentimiento para que este material aparezca en informes y artículos de revista de publicaciones médicas.
Entiendo que:

- **Mi nombre no será publicado.**
- **El material no será utilizado para publicidad o embalaje.**
- **El material no será utilizado fuera de contexto.**

-

Firmado …….. **Fecha……..**

Biobanco
Hospital General Universitario de Valencia

PROTOCOLOS DE EXTRACCIÓN DE DERIVADOS SANGUÍNEOS USADOS EN LA COLECCIÓN "FRAGILIDAD" DEL BIOBANCO HGUV

1. EXTRACCIÓN DE PLASMA

- Partimos de sangre total extraída por venopunción. Si la extracción ha sido correcta, la muestra no debe presentar coágulo. El tipo de tubo de extracción es el tubo lila, que usa como anticoagulante EDTA.
- Centrifugar la muestra de SP a 1500g durante 10' a temperatura ambiente. Después de la centrifugación encontraremos en el tubo 3 fases:
  - La fracción superior de color amarillo que corresponde al plasma.
  - La fase intermedia de color blanco, donde encontramos la capa leuco-plaquetaria.
  - La fracción inferior de color rojo oscuro que corresponde a los eritrocitos.
- Con una pipeta se aspira cuidadosamente el plasma (fase superior amarilla), se transfiere a un tubo de centrífuga convenientemente identificado.
- Centrifugar el plasma trasferido a 2500g durante 10' a temperatura ambiente.
- Transferir el sobrenadante en alícuotas de al menos 0.5ml a cada tubo de criopreservación y almacenar a -80ºC.

2. EXTRACCIÓN DE SUERO

El suero sanguíneo se obtiene de muestras de sangre periférica extraída por venopunción en tubos de extracción sanguínea secos, con gel o con partículas activadoras de la coagulación como aditivo.

- Una vez recibida la muestra en el laboratorio, **mantener el tubo de sangre en vertical** en una gradilla **para su coagulación durante 30'** contado desde el momento de la extracción.
- **Centrifugar** la muestra de SP a **2000g** a **RT**, durante **10'**. Después de la centrifugación encontraremos en el tubo 2 fases:
  - La fracción superior transparente y de color amarillo, que corresponde al suero.
  - La fracción inferior de color rojo oscuro, que corresponde a la sangre coagulada.
- Con la ayuda de una pipeta se aspira cuidadosamente el suero (fase superior amarilla) sin tocar la interfase y se transfieren **alícuotas de 0.5ml** a tubos de criopreservación y **almacenar a -80ºC**.

ANNEX RADIOLOGY REPORT

INFORME DE ECOGRAFÍA

ECOGRAFÍA MUSCULAR EXPERIMENTAL:

El paciente cumple con los criterios de inclusión y no cumple con ninguno de los de exclusión para participar en el estudio. Antes de iniciar la exploración se ha revisado y firmado el consentimiento informado para participar en el estudio: "Estudio de arquitectura muscular determinado por ecografía con correlación de marcadores de fragilidad clínicos, físicos y biológicos".

Se procede en modo B con transductor lineal de alta resolución a identificar en planos transversales los 2 vientres musculares del cuádriceps (recto femoral y vasto interno) derecho. Se procede a realizar tres mediciones del grosor muscular (GM) y del grosor del tejido graso subcutáneo (GG). Se identifica en plano longitudinal el recto femoral en reposo y se registran el penado en reposo (APR). Se solicita al paciente que realice una contracción voluntaria máxima del cuádriceps y se registra el ángulo penado en contracción (APC). Se repite la misma exploración en plano transversal y longitudinal para el vasto medial y vasto intermedio.

Utilizando el programa Image-J se obtiene el valor de ecointensidad (EI) y el área anatómica (AA) de las los vientres musculares en los cortes transversales.

Se concluye la exploración sin incidencias.

Firma Radiólogo: _____.

ANNEX FRIED'S FRAILTY CRITERIA CHART

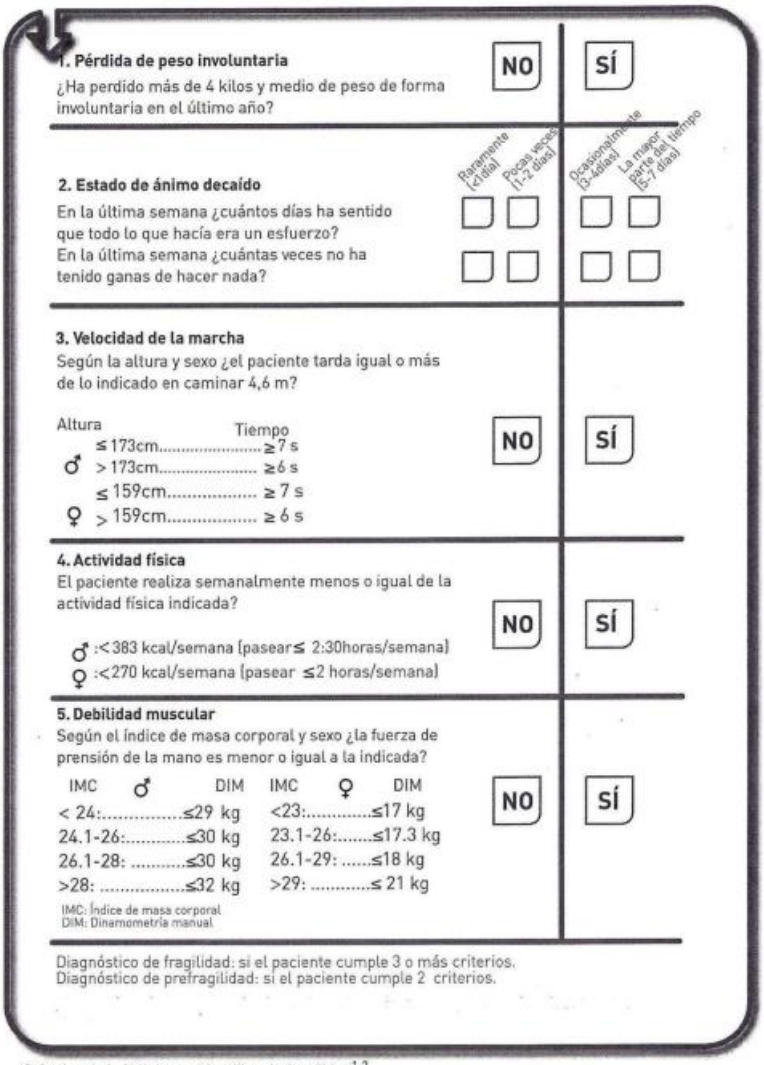

1. Pérdida de peso involuntaria

¿Ha perdido más de 4 kilos y medio de peso de forma involuntaria en el último año?

NO ☐ SÍ ☐

2. Estado de ánimo decaído

	Raramente (<1día)	Pocas veces (1-2 días)	Ocasionalmente (3-4días)	La mayor parte del tiempo (5-7 días)
En la última semana ¿cuántos días ha sentido que todo lo que hacía era un esfuerzo?	☐	☐	☐	☐
En la última semana ¿cuántas veces no ha tenido ganas de hacer nada?	☐	☐	☐	☐

3. Velocidad de la marcha

Según la altura y sexo ¿el paciente tarda igual o más de lo indicado en caminar 4,6 m?

Altura		Tiempo
♂	≤ 173cm	≥ 7 s
	> 173cm	≥ 6 s
♀	≤ 159cm	≥ 7 s
	> 159cm	≥ 6 s

NO ☐ SÍ ☐

4. Actividad física

El paciente realiza semanalmente menos o igual de la actividad física indicada?

♂ :< 383 kcal/semana (pasear≤ 2:30horas/semana)
♀ :<270 kcal/semana (pasear ≤2 horas/semana)

NO ☐ SÍ ☐

5. Debilidad muscular

Según el índice de masa corporal y sexo ¿la fuerza de prensión de la mano es menor o igual a la indicada?

IMC ♂	DIM	IMC ♀	DIM
< 24:	≤29 kg	<23:	≤17 kg
24.1-26:	≤30 kg	23.1-26:	≤17.3 kg
26.1-28:	≤30 kg	26.1-29:	≤18 kg
>28:	≤32 kg	>29:	≤ 21 kg

IMC: Índice de masa corporal
DIM: Dinamometría manual

NO ☐ SÍ ☐

Diagnóstico de fragilidad: si el paciente cumple 3 o más criterios.
Diagnóstico de prefragilidad: si el paciente cumple 2 criterios.

Criterios de L. Fried para identificar la fragilidad[1-2].

1- Fried L et al. "Frailty in Older Adults: Evidence for a Phenotype". J Gerontol A Biol Sci Med Sci 2001:56(3): M146–M156. **2-** Fried LP, Ferrucci L, Darer J, Williamson JD, Anderson G. "Untangling the concepts of disability, frailty, and comorbidity: implications for improved targeting and care". J Gerontol A Biol Sci Med Sci. 2004;59:255-63.

ANNEX STUDY QUESTIONNAIRE

CONFIDENCIAL

#Hx: _____ SIP: _____

CUESTIONARIO ELECTRÓNICO SOBRE GENERALIDADES DEL PARTICIPATE, HISTORIA CLÍNICA Y FACTORES DE RIESGO

TÍTULO DEL PROYECTO: "Estudio de arquitectura muscular determinada por ecografía para el diagnóstico de fragilidad con correlación de marcadores clínicos, físicos y bioquímicos"

SECCIÓN A: Datos generales sobre el paciente. A rellenar por el investigador.

Fecha de nacimiento		Edad actual (años):	
Género:		Peso (kgs):	
Estado Marital:		Altura (mts):	
Estado Social:		IMC:	
Vive solo:		Institucionalizado:	

SECCIÓN B: Preguntas a realizar sobre la historia clínica del paciente. En el caso de no poder responder la pregunta o de que el paciente no se acuerde, ante la duda se confirmará mediante la historia electrónica del paciente.

ANTECEDENTES PERSONALES					
Hipertensión	Si	No	Cáncer previo	Si	No
Hiperlipidemia	Si	No	Depresión o síndrome ansioso	Si	No
Diabetes Mellitus	Si	No	Demencia/Pérdida de la memoria	Si	No
Insuficiencia cardiaca	Si	No	Enfermedad de Parkinson	Si	No
Cardiopatía isquémica	Si	No	Insuficiencia renal	Si	No
Ictus previo	Si	No	Hepatopatía	Si	No
Enfermedad obstructiva crónica	Si	No	Problemas visuales recientes	Si	No
Artritis	Si	No	Problemas auditivos recientes	Si	No
Osteoporosis	Si	No		Si	No
Fracturas recientes	Si	No		Si	No
# de fracturas en los 6 meses previos			Índice de Charlson:		

FACTORES DE RIESGO				
# de caídas en los 6 meses previos		# de factores de riesgo para caídas		
# de visitas al médico de atención 1º		Obesidad	Si	No
# de visitas al servicio de urgencias:		Alcohólico	Si	No
# de admisiones hospitalarias		Fumador	Si	No

SECCIÓN C: Cuestionario sobre estado de fragilidad del paciente. Por favor dé la respuesta que mejor describa sus opiniones al investigador. Recuerde que no existen respuestas correctas ni incorrectas.

1. ¿Cómo ha sido mi apetito recientemente? Bueno Malo
2. He perdido más de 4 kg de peso en el último año. Sí No
3. Siento que todo lo que hago es un esfuerzo. Sí No
4. Tengo muy poca energía para realizar las cosas que yo quiero hacer. Sí No
5. Tiempo para caminar 4.6m (segundos) : _____
6. Fuerza muscular de mano dominante:

Total de criterios patológicos: _____ = Robusto ☐ Pre-Frágil ☐ Frágil ☐

IPAQ-E		
1	Durante los últimos 7 días, ¿en cuántos realizó actividades físicas intensas tales como levantar pesos pesados, cavar, hacer ejercicios aeróbicos o andar rápido en bicicleta?	
2	Habitualmente, ¿cuánto tiempo en total dedicó a una actividad física intensa en uno de esos días? Indique cuantos minutos por día.	
3	Durante los últimos 7 días, ¿en cuántos días hizo actividades físicas moderadas tales como transportar pesos livianos, o andar en bicicleta a velocidad regular? No incluya caminar	
4	Habitualmente, ¿cuánto tiempo en total dedicó a una actividad física moderada en uno de esos días? Indique cuantos minutos por día.	
5	Durante los últimos 7 días, ¿caminó por lo menos 10 minutos seguidos?	
6	Habitualmente, ¿cuánto tiempo en total dedicó a caminar en uno de esos días? Indique cuantos minutos por día.	
7	Durante los últimos 7 días, ¿cuánto tiempo pasó sentado durante un día hábil? Indique cuantos minutos por día.	

Gracias por su ayuda.

ANNEX DETERMINATION OF MDA IN PLASMA

CUANTIFICACIÓN DE MDA EN PLASMA

a) Preparación de los reactivos

- *Tampón acetato sódico anhidro 2 M, pH 3.5 con TBA 0.2%*: Para preparar 200 mL de tampón se toman 23,8 mL de ácido acético glacial (pureza 98%) y se le añaden a unos 120 mL de agua desionizada ("milli-Q"). Se ajusta el pH hasta 3,5 con hidróxido de sodio (NaOH) 10 M. A continuación, se añade a la solución 0,4 g de ácido tiobarbitúrico y se mantiene en agitación, a 50-60ºC, hasta la total disolución del TBA. Se comprueba que el pH se mantiene y, si no es así, se vuelve a ajustar. Finalmente, se enrasa el volumen a 200 mL y se guarda protegido de la luz a 4º C.

- *Tampón KH_2PO_4 50 mM, pH 6.8*: Para preparar 200 mL se pesan 1,36 g de KH_2PO_4 y se añaden a unos 120 mL de agua desionizada. A continuación, se ajusta el pH con KOH (1 M) hasta 6,8 y se enrasa con agua desionizada hasta alcanzar el volumen final. Posteriormente, se guarda a 4º C.

- *Tampón KH_2PO_4 50 mM, pH 3.5*: Para preparar 200 mL se pesan 1,36 g de KH_2PO_4 y se añaden a unos 120 mL de agua desionizada; se ajusta el pH con HCl (1 M) hasta 3,5 y se enrasa con agua desionizada hasta el volumen final. Se guarda también a 4º C.

b) Preparación de los patrones

La identificación y cuantificación del MDA de las muestras analizadas se lleva a cabo por medio de una recta de calibrado, la cual se prepara previamente con una solución comercial de MDA. Para ello se procede de la manera siguiente:

1. Se parte de una solución comercial de MDA-bis (dimetilacetal, PM: 164,2 g/mol, Merck) a concentración de 12,2 M. Haremos los cálculos para obtener una solución 100 mM que será nuestra solución de partida o solución madre (100 mM) luego haremos diluciones seriadas hasta obtener los puntos de la recta de calibrado. Para la solución inicial de 100 mM, diluiremos 8,2 µL de MDA 12,2 M en 991,8 µL de agua desionizada, alicuotaremos 25 µL en eppendorfs y congelaremos a -20ºC.

2. Partiendo de la solución madre de 100 mM haremos diluciones seriadas hasta obtener las concentraciones de MDA que queremos configuren nuestra recta patrón:
    - 10 mM dilución 1:2 y obtenemos una solución 5 mM
    - 5 mM dilución 1:100 obtenemos una solución 50 µM
    - 50 µM dilución 1:2 y obtenemos 1° punto de la recta 25 µM
    - 25 µM dilución 1:2 obtenemos solución 12,5 µM
    - 12,5 µM ó nmol/mL
    - 5 µM obtenida por dilución 1:5 de la solución 25 µM
    - 2,5 µM obtenida por dilución 1:2 de la solución 5 µM
    - 1,25 µM obtenida por dilución 1:2 de la solución 2,5 µM
    - 0,625 µM obtenida por dilución 1:2 de la solución 1,25 µM

Los puntos elegidos para nuestra recta patrón son: 25 µM – 12,5 µM – 5 µM – 2,5 µM – 1,25 µM – 0,625 µM además de un blanco que contendrá agua desionizada en lugar de muestra y que seguirá el mismo proceso de derivatización.

Tener en cuenta que para la preparación de cualquier recta de calibrado es de suma importancia la homogeneidad de las disoluciones, motivo por el cual es muy recomendable el uso de un vortex.

c) Procedimiento de derivatización

1. A 500 µL del tampón inicial (con TBA) se le añaden 20 µL de plasma.
2. La preparación se incuba durante 60 minutos a una temperatura de 95ºC. Es en este paso donde se produce la hidrólisis de los lipoperóxidos y la consiguiente liberación de moléculas de MDA, que se conjugan con dos moléculas de ácido tiobarbitúrico (TBA), por tanto, lo que se determina es el **aducto MDA-TBA_2** como índice de peroxidación lipídica.
3. Al sacarlas, las muestras deben mantenerse en hielo.
4. Añadir 500 µL del tampón de KH_2PO_4 (pH 6,8) a cada muestra. Agitar. Este paso es crítico ya que el aducto MDA-TBA_2 es inestable en el rango de pH neutro-básico, por lo que debe hacerse con rapidez.
5. Centrifugar durante 5 min. a 13000 g, a una temperatura de 4ºC.
6. A 200 µL del sobrenadante añadirle 200 µL del tampón KH_2PO_4 50 mM, pH 3,5 y agitar.
7. Tomar 200 µL y colocarlos en un vial para realizar el análisis por HPLC.

d) Preparación de las fases móviles para HPLC

Se trata de una elución "isocrática", donde la composición de la fase móvil es constante.

Como ya se ha dicho, es una cromatografía en "fase reversa", es decir, la fase estacionaria o columna es no polar (hidrocarburos adheridos a partículas de sílice) mientras que la fase móvil es polar, en nuestro caso está constituida por una solución salina KH_2PO_4 50 mM de pH 6,8 y acetonitrilo en proporción 73/18. Esto quiere decir que el tiempo de retención será mayor para las moléculas de naturaleza apolar, mientras que las moléculas de carácter polar eluyen más rápidamente y es sabido que el MDA es uno de los aldehídos más polares.

En el proceso cromatográfico hay dos fases: una fase de elución, que es el intervalo de tiempo donde eluirá nuestra molécula, y posteriormente una fase de lavado y equilibrado de la columna a fin de prepararla para el paso de la siguiente muestra.

- *Fase de lavado (Fase B):* está constituida por una mezcla de acetonitrilo/ agua desionizada al 70%, ambos de máxima pureza (agua desionizada tipo "milli-Q").

- *Fase de elución (Fase A):* La sal que contiene esta fase es KH_2PO_4 50 mM, pH 6,8. La relación es de 83/17 (KH_2PO_4 50 mM, pH 6,8/ acetonitrilo). El modo de preparación es el siguiente:

1. Pesar 13,6 g de KH_2PO_4 y disolverlos en unos 1800 mL de agua desionizada ("mili-Q").
2. Ajustar el pH de esta disolución a 6,8 con KOH 1 M.
3. Enrasar hasta 2000 mL.
4. Añadir 410 mL de acetonitrilo. Esta solución debe homogeneizarse bien.
5. La solución será filtrada con un kitasatos, mediante bomba de vacío y filtro de 0,22 micras (Millipore).

Antes de pasar por el HPLC, ambas fases deben desgasificarse por baño de ultrasonidos unos 20 minutos ya que las burbujas de aire suponen un serio problema en la HPLC.

e) Condiciones cromatográficas

- Flujo de las fases: 1 mL/min
- Detección en HPLC: se utilizó el detector UV a 532 nm.

-| Columna: C18 Hypersil GOLD, dimensiones 150 x 4,6 mm y 5 µm de partícula.

f) Método cromatográfico

Al ser un método isocrático, sólo se necesita programar el tiempo que va a estar pasando cada una de las fases líquidas correspondientes. Cada cromatograma conlleva unos 24 minutos y la secuencia de las fases móviles a través del HPLC es la que se muestra en la Figura 1:

Figura 1.Programación de la duración (minutos) de las Fases A y B, durante un cromatograma del análisis de Malondialdehído (MDA).

Una programación de muestras supone el repetir cada secuenciación anterior tantas veces como muestras y patrones se deseen analizar, de tal manera que se obtiene de cada muestra un cromatograma como el que se muestra en la siguiente figura (Figura 2).

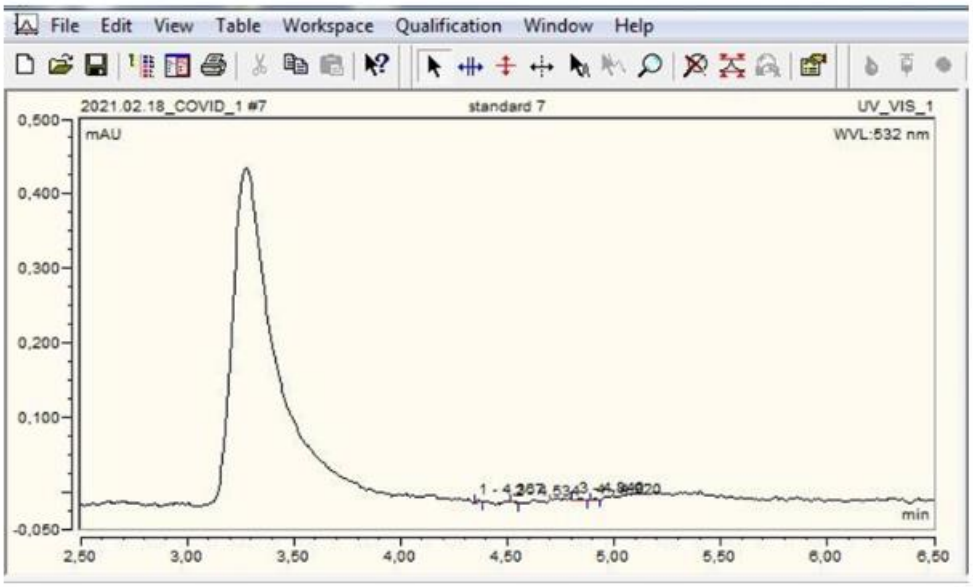

Figura 2. Cromatograma de una muestra problema.

ANNEX DETERMINATION OF PLASMA PROTEINS BY LOWRY

DETERMINACIÓN DE PROTEÍNAS POR LOWRY

a. Preparación de los reactivos

- *Reactivo Lowry:* Añadir 40 mL de agua desionizada al reactivo comercial *Lowry Reagent Powder*. A continuación, mezclar hasta disolver por completo. Guardar a temperatura ambiente.

- *Reactivo Folin:* Añadir 90 mL de agua desionizada a 18 mL de la solución *Folin & Ciocalteu Phenol Reagent* en una botella opaca y mezclar bien. Guardar a temperatura ambiente.

b. Preparación de la recta patrón

Dado que, como hemos mencionado anteriormente, la cuantificación de proteínas totales de las muestras analizadas se llevó a cabo gracias a una curva patrón, previamente al ensayo hubo que prepararla:

1. Preparar un concentrado de seroalbúmina bovina (BSA) (10 mg/mL): pesar 10 mg de BSA en un eppendorf y añadirle 1 mL de agua desionizada ("milli Q").
2. Realizar diferentes diluciones a partir de la solución anterior, para conseguir los siguientes puntos para nuestra recta patrón:
    - 5 mg/mL (diluir a la mitad la solución de 10 mg/mL).
    - 2.5 mg/mL (diluir a la mitad la solución anterior).
    - 1 mg/mL (diluir 1/10 la solución de 10 mg/mL).
    - 0.1 mg/mL (diluir 1/10 la solución anterior).
    - Blanco (sólo agua desionizada).

c. Protocolo

1. En un eppendorf pipetear 490 µL de agua desionizada y 10 µL de la muestra.
2. Añadir 500 µL del reactivo de Lowry e incubar 20 minutos en oscuridad.
3. Añadir 250 µL del reactivo de Folin Ciocalteu e incubar 30 minutos en oscuridad.
4. Medir la absorbancia a λ= 660 nm.

d. Cuantificación de los resultados

Para calcular las absorbancias de las diferentes muestras problema, se descartaron las llamadas "interferencias" (otros solventes o reactivos del sistema que absorben a la misma longitud de onda que dichas muestras). Para ello, se preparó una muestra que contenía todos los componentes del sistema menos aquel que se desea medir (muestra o patrón). Esta muestra se llama blanco y la absorbancia de éste debe restarse a las muestras problema y a los patrones, o bien, con el blanco se calibra el instrumento a absorbancia igual a 0, es decir, 100% de transmisión.

ΔAbs = Abs muestra o patrón – Abs blanco

El resultado se expresó en una gráfica de la absorbancia en función de la concentración (mg/mL). Si el sistema seguía la ley de Lambert-Beer, se obtenía una línea recta que pasaba

cerca del origen. A continuación, se determinó gráficamente la concentración de la muestra desconocida dibujando la absorbancia frente a concentraciones conocidas de nuestro patrón interno (BSA). Se escogió la parte lineal y se calculó la recta de regresión lineal que mejor se ajustaba y a ésta se interpolaron los datos de absorción de nuestras muestras de plasma (Figura 1).

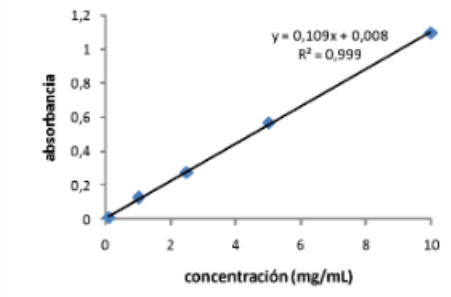

Figura 1. Ejemplo de recta patrón para la determinación de la concentración de proteínas en mg/mL en función de la absorbancia a λ= 660 nm.

DETERMINACIÓN DE CARBONILACIÓN PROTEICA EN PLASMA

a. Derivatización de las muestras

1. Añadir 5 µL de muestra a un eppendorf, o el volumen necesario para tener 20 µg de proteína. Si el volumen es inferior, ajustar a 5 µL con agua desionizada.
2. Añadir 5 µL de SDS al 12% p/v. En el caso de que el volumen de la muestra exceda los 5 µL, se corrige añadiendo menor volumen de SDS a mayor concentración.
3. Añadir 10 µL de 2,4-dinitrofenilhidrazina (DNPH) a cada muestra, que marcará los grupos carbonilo. También se prepararán muestras como controles negativos, a los que se añade solución de derivatización control.
4. Incubar a temperatura ambiente durante 15 minutos.
5. Añadir 7.5 µL de la solución de neutralización. Si no se había añadido un agente reductor a la muestra durante el homogenado, añadir 1-1.5 µL de β-mercaptoetanol.

b. Western blotting

1. Cargar las muestras en los geles: Se carga un volumen total por muestra de 28 µL en cada pocillo (15 pocillos en total), empleando geles discontinuos al 12.5% de Acrilamida (29:1 Acrilamida: Bisacrilamida) con un 0.1% de SDS.
2. Electroforesis (Figura 1): Se aplica un campo eléctrico de voltaje constante de 20 miliamperios (mA) durante al menos 2 horas en tampón Tris-Glicina (25 mM Tris, 200 mM Glicina, 0.1% SDS, pH 8.3).

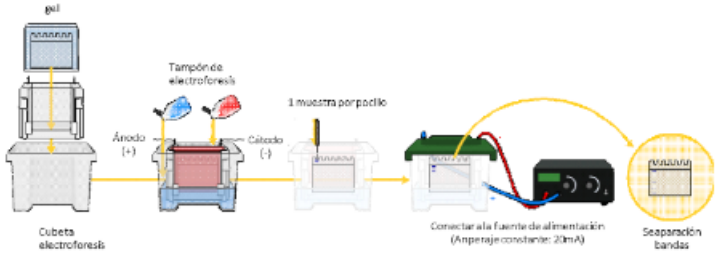

Figura 1. Esquema electroforesis SDS-PAGE

0. Transferencia: Una vez finalizado el desplazamiento electroforético, el gel se transfiere (*blotting*) a una membrana de PVDF (Schelider & Schuel, USA), mediante electrotransferencia en condiciones húmedas, por medio del sistema Mini-protean II (Bio-Rad, USA). El proceso se mantiene de forma que pasan 170 mA por cada membrana de la cual se hace transferencia, en tampón de transferencia (25 mM Tris, 192 mM Glicina, Metanol 20% v/v, pH 8.3).
1. Bloqueo: Tras la transferencia, las membranas se incuban 60 minutos a temperatura ambiente en tampón de bloqueo: 5% p/v de BSA, 0.1% Tween-20 en 1x PBS (PBS-T).
2. Lavados: Se realiza 1 lavado de 15 minutos y dos de 5 minutos con 10 mL de PBS-T.

3. Anticuerpo primario: Las membranas se incuban durante toda la noche a 4°C en agitación orbital, en tampón de anticuerpo primario (5% BSA, 0.1 % Tween-20 en 1x PBS) con una dilución de anticuerpo primario 1:150.
4. Lavados: Se repite el paso 5.
5. Las membranas son incubadas 60 minutos con el anticuerpo secundario conjugado con peroxidasa de rábano. El anticuerpo se disuelve en tampón de bloqueo a la concentración 1:300.
6. Lavados: Se repite el paso 5.
7. Revelado: La membrana se incuba 1-5 minutos con reactivo ECL (Amersham Pharmacia, USA) e inmediatamente se revela con un detector quimioluminiscente, mediante el programa *Image Gauge* V4.0 de FUJIFILM.

c. Cuantificación de los resultados

Las imágenes obtenidas fueron almacenadas en formato digital TIF para poder realizar la densitometría de las bandas, utilizando el programa "Image J". Como control de carga, se tiñeron las membranas con rojo Ponceau. Así, se calculó la densitometría de la membrana haciendo un ratio: densitometría de la carbonilación de proteínas/ densitometría de la membrana teñida con rojo Ponceau, expresándose el resultado como unidades arbitrarias de proteínas oxidadas.

ANNEX LUMINEX PROTOCOL

PREPARATION OF REAGENTS FOR IMMUNOASSAY

A. Preparation of Antibody-Immobilized Beads

If premixed beads are used, sonicate the premixed bead bottle 30 seconds and then vortex for 1 minute before use.

For individual vials of beads, sonicate each antibody-bead vial for 30 seconds; vortex for 1 minute. Add 70 µL from each antibody-bead vial to the Mixing Bottle and bring final volume to 3.5 mL with LBD. Vortex the mixed beads well. Unused portion may be stored at 2-8°C for up to one month. (Note: Due to the composition of magnetic beads, you may notice a slight color in the bead solution. This does not affect the performance of the beads or the kit.)

Example: When using 10 antibody-immobilized beads, add 70 µL from each of the 10 bead vials to the Mixing Bottle. Then add 2.8 mL LBD

B. Preparation of Serum Matrix

This step is required for serum or plasma samples only.

Add 1.0 mL deionized water to the bottle containing lyophilized serum matrix (Cat# MXHSM-7). Mix well. Allow at least 10 minutes for complete reconstitution. Add 3 mL Assay Buffer (Cat# L-ABIR) to the bottle for a final volume of 4 mL. Unused reconstituted matrix should be stored at ≤ -20°C for up to one month.

C. Preparation of Quality Controls

For serum and plasma samples, reconstitute Quality Control 1 (QC1) and Quality Control 2 (QC2) vials with **250 µL MXHSM-7**. **These are the Stock QC Vials.** Invert the Stock Vials several times to mix and vortex. Allow the vials to sit for 5-10 minutes. Label two tubes QC1 and QC2 and add 150 µL MXHSM-7 to each tube. Remove 50 µL from QC1 or QC2 Stock Vials and add to the 150 µL MXHSM-7 in the respective QC1 and QC2 tubes and vortex. **Use these one to four diluted QCs in the assay**. Unused portions may be stored at ≤ -20°C for up to one month.

For culture samples, substitute the appropriate sample media for the MXHSM-7 used for serum and plasma samples above.

D. Preparation of Wash Buffer

Bring the 10X Wash Buffer to room temperature and mix to bring all salts into solution. Dilute 60 mL of 10X Wash Buffer with 540 mL deionized water. Store the unused portion at 2-8°C for up to one month.

E. Preparation of Human High Sensitivity T Cell Standard

1.) For serum and plasma samples, reconstitute the Human High Sensitivity T Cell Standard with **250 µL MXHSM-7**. Invert the vial several times to mix. Vortex the vial for 10 seconds. Allow the vial to sit for 5-10 minutes. **This is the Stock Standard Vial NOT Standard 7.** Unused Standard may be stored at ≤ -20°C for up to one month.

2). Preparation of Working Standards

For serum and plasma samples, label seven polypropylene microfuge tubes as Standard 7, Standard 6, Standard 5, Standard 4, Standard 3, Standard 2 and Standard 1. Add 150 µL of MXHSM-7 to each of the seven tubes. Prepare serial dilutions by adding 50 µL of the Stock Standard to the Standard 7 tube, mix well and transfer 50 µL of the Standard 7 to the Standard 6 tube, mix well and transfer 50 µL of the Standard 6 tube to the Standard 5 tube, mix well and transfer 50 µL of the Standard 5 tube to the Standard 4 tube, mix well and transfer 50 µL of the Standard 4 tube to the Standard 3 tube, mix well and transfer 50 µL of the Standard 3 tube to the Standard 2 tube, mix well and transfer 50 µL of the Standard 2 tube to the Standard 1 tube and mix well. The 0 pg/mL standard (Background) will be MXHSM-7 or appropriate sample media.

Standard #	Volume of MXHSM-7 to Add	Volume of Standard to Add
Stock Standard	250 µL	0

Standard #	Volume of MXHSM-7 to Add	Volume of Standard to Add
Standard 7	150 µL	50 µL of Stock Standard
Standard 6	150 µL	50 µL of Standard 7
Standard 5	150 µL	50 µL of Standard 6
Standard 4	150 µL	50 µL of Standard 5
Standard 3	150 µL	50 µL of Standard 4
Standard 2	150 µL	50 µL of Standard 3
Standard 1	150 µL	50 µL of Standard 2

3). For other samples (tissue culture, cell culture etc.) substitute the appropriate media for the MXHSM-7 used for serum and plasma samples above.

Preparation of Standards

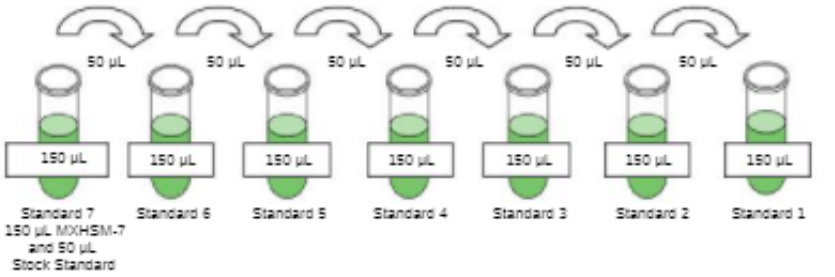

Standard	ITAC, IL-10 (pg/mL)	GM-CSF (pg/mL)	Fractalkine (pg/mL)	IFNγ, MIP-3α (pg/mL)
Standard 1	1.46	1.22	18.3	0.61
Standard 2	5.86	4.88	73.2	2.44
Standard 3	23.4	19.5	293.0	9.8
Standard 4	93.8	78.1	1,171.9	39
Standard 5	375	312.5	4,687.5	156
Standard 6	1,500	1,250	18,750	625
Standard 7	6,000	5,000	75,000	2,500

Standard	IL-12p70, IL-1β, IL-2, IL-5 (pg/mL)	IL-13, IL-21 (pg/mL)	IL-17A (pg/mL)	IL-4 (pg/mL)	IL-23 (pg/mL)
Standard 1	0.49	0.24	0.73	1.83	7.93
Standard 2	1.95	0.98	2.93	7.32	31.7
Standard 3	7.81	3.91	11.7	29.3	127.0
Standard 4	31.3	15.63	46.9	117.2	507.8
Standard 5	125	62.5	187.5	468.8	2,031.3
Standard 6	500	250	750	1,875	8,125
Standard 7	2,000	1,000	3,000	7,500	32,500

Standard	IL-6 (pg/mL)	IL-7 (pg/mL)	IL-8, MIP-1α (pg/mL)	MIP-1β (pg/mL)	TNFα (pg/mL)
Standard 1	0.18	0.37	0.31	0.92	0.43
Standard 2	0.73	1.46	1.22	3.66	1.71
Standard 3	2.93	5.86	4.88	14.7	6.84
Standard 4	11.7	23.4	19.5	58.6	27.3
Standard 5	46.9	93.8	78.1	234.4	109.4
Standard 6	187.5	375	312.5	937.5	437.5
Standard 7	750	1,500	1,250	3,750	1,750

IMMUNOASSAY PROCEDURE

- Prior to beginning this assay, it is imperative to read this protocol completely and to thoroughly understand the Technical Guidelines.
- Allow all reagents to warm to room temperature (20-25°C) before use in the assay.
- Diagram the placement of Standards [0 (Background), standards 1 through 7], Controls 1 and 2, and Samples on Well Map Worksheet in a vertical configuration. (Note: Most instruments will only read the 96-well plate vertically by default.) It is recommended to run the assay in duplicate.
- If using a filter plate, set the filter plate on a plate holder at all times during reagent dispensing and incubation steps so that the bottom of the plate does not touch any surface.

1. Add 200 µL of Wash Buffer into each well of the plate. Seal and mix on a plate shaker for 10 minutes at room temperature (20-25°C).
2. Decant Wash Buffer and remove the residual amount from all wells by inverting the plate and tapping it smartly onto absorbent towels several times.
3. Add 50 µL of each **diluted** Standard or Quality Control into the appropriate wells (**NOT from Stock Vials**). The **Serum Matrix** should be used for 0 pg/mL standard (background). When assaying tissue culture or other supernatant, use appropriate control culture medium as the background.
4. Add 25 µL of Assay Buffer to the sample wells.
5. Add 25 µL of sample into the sample wells.
6. Vortex Mixing Bottle and add 25 µL of the Mixed or Premixed Beads to each well. (Note: During addition of Beads, shake bead bottle intermittently to avoid settling.)
7. Seal the plate with a plate sealer. Wrap the plate with foil and incubate with agitation on a plate shaker overnight (16-18 hrs) at 4°C

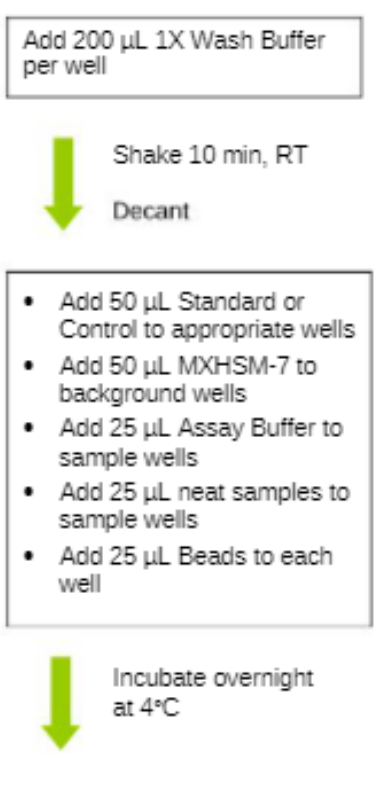

8. Gently remove well contents and wash plate 3 times following instructions listed in the **PLATE WASHING** section.

9. Add 50 µL of Detection Antibodies into each well. (Note: Allow the Detection Antibodies to warm to room temperature prior to addition.)

10. Seal, cover with foil and incubate with agitation on a plate shaker for 1 hour at room temperature (20-25°C). **DO NOT ASPIRATE AFTER INCUBATION.**

11. Add 50 µL Streptavidin-Phycoerythrin to each well containing the 50 µL of Detection Antibodies.

12. Seal, cover with foil and incubate with agitation on a plate shaker for 30 minutes at room temperature (20-25°C).

13. Gently remove well contents and wash plate 3 times following instructions listed in the **PLATE WASHING** section.

14. Add 150 µL of Sheath Fluid (or Drive Fluid if using MAGPIX®) to all wells. Resuspend the beads on a plate shaker for 5 minutes.

15. Run plate on Luminex® 200™, HTS, FLEXMAP 3D® or MAGPIX® with xPONENT® software.

16. Save and analyze the Median Fluorescent Intensity (MFI) data using a 5-parameter logistic or spline curve-fitting method for calculating analyte concentrations in samples and Controls. **(Note: Because of the built-in two-fold sample dilution, for all neat samples, multiply the calculated concentrations by two. For two-fold diluted samples, multiply the calculated concentrations by four. Calculated Quality Control concentrations do not require multiplication by a dilution factor.)**

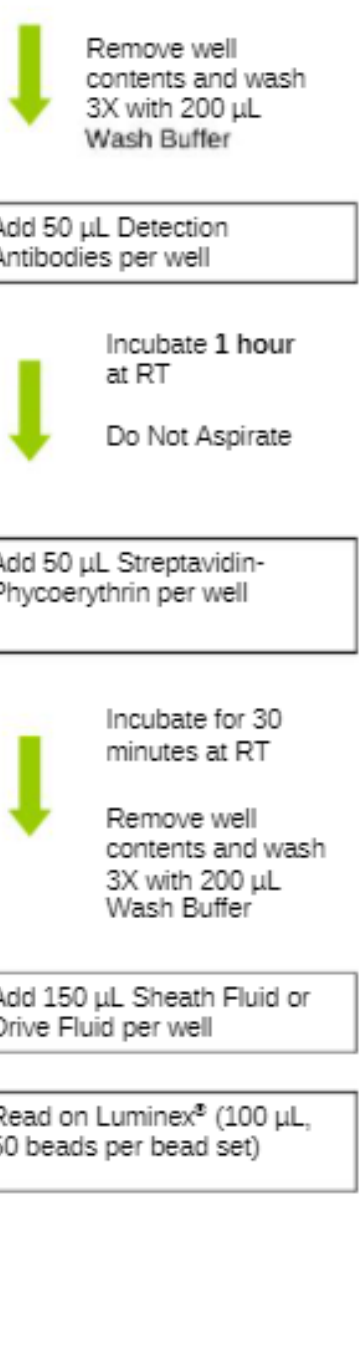

PLATE WASHING

1.) Solid Plate

If using a solid plate, use either a handheld magnet or magnetic plate washer.

A.) Handheld magnet (EMD Millipore Catalog # 40-285) - Rest plate on magnet for 60 seconds to allow complete settling of magnetic beads. Remove well contents by gently decanting the plate in an appropriate waste receptacle and gently tapping on absorbent pads to remove residual liquid. Wash plate with 200 µL of Wash Buffer by removing plate from magnet, adding Wash Buffer, shaking for 30 seconds, reattaching to magnet, letting beads settle for 60 seconds and removing well contents as previously described after each wash. Repeat wash steps as recommended in Assay Procedure.

B.) Magnetic plate washer (EMD Millipore Catalog # 40-094, # 40-095, # 40-096 and # 40-097) - Please refer to specific automatic plate washer manual for appropriate equipment settings. Please note that after the final aspiration, there will be approximately 25 µL of residual wash buffer in each well. This is expected when using the BioTek plate washer and this volume does not need to be aspirated from the plate.

If using an automatic plate washer other than BioTek® 405 LS or 405 TS, please refer to the manufacturer's recommendations for programming instructions.

2.) Filter Plate (EMD Millipore Catalog # MX-PLATE)

If using a filter plate, use a vacuum filtration manifold to remove well contents. Wash plate with 200 µL/well of Wash Buffer, removing Wash Buffer by vacuum filtration after each wash. Repeat wash steps as recommended in the Assay Procedure.

EQUIPMENT SETTINGS

Luminex® 200™, HTS, FLEXMAP 3D®, and MAGPIX® with xPONENT® software:

These specifications are for the Luminex® 200™, Luminex® HTS, Luminex® FLEXMAP 3D®, and Luminex® MAGPIX® with xPONENT® software. Luminex® instruments with other software (e.g. MasterPlex®, StarStation, LiquiChip, Bio-Plex Manager™, LABScan™100) would need to follow instrument instructions for gate settings and additional specifications from the vendors for reading Luminex® magnetic beads.

For magnetic bead assays, the Luminex® 200™ and HTS instruments must be calibrated with the xPONENT® 3.1 compatible Calibration Kit (EMD Millipore Catalog # 40-275) and performance verified with the Performance Verification Kit (EMD Millipore Catalog # 40-276). The Luminex® FLEXMAP 3D® instrument must be calibrated with the FLEXMAP 3D® Calibrator Kit (EMD Millipore Catalog # 40-028) and performance verified with the FLEXMAP 3D® Performance Verification Kit (EMD Millipore Catalog # 40-029). The Luminex® MAGPIX® instrument must be calibrated with the MAGPIX® Calibration Kit (EMD Millipore Catalog # 40-049) and performance verified with the MAGPIX® Performance Verification Kit (EMD Millipore Catalog # 40-050).

NOTE: When setting up a Protocol using the xPONENT® software, you must select MagPlex as the Bead Type in the Acquisition settings.

NOTE: These assays cannot be run on any instruments using Luminex® IS 2.3 or Luminex® 1.7 software.

ANNEX TABLE 4A. Correlations of comorbidities with ultrasound parameters

	Hyperlipidemia	Hypertension	Diabetes Mellitus	COPD	Hearing Loss	Visual Loss	Previous stroke/TIA	Congestive heart failure	Heart disease	Myocardial infarction	Renal disease	Osteoarthritis	Anxiety/ depression	Fracture s/ Osteoporosis	Hepatopathy	Dementia	Connective tissue disease	Previous malignancy	Peripheral vascular disease	Peptic ulcer	Smoking	Alcohol abuse	Feline	Obesity
SFT RF	-.002	-.054	-.024	-.238**	.049	.004	.018	.009	-.053	-.158*	-.049	.090	.238**	.302**	.024	.043	-.082	-.099	-.167*	.062	-.079	-.232**	.139	.306**
MT RF	-.279**	-.303**	-.190**	-.098	-.045	-.281**	-.167*	-.023	-.113	-.093	-.028	-.216**	-.122	-.159*	-.086	-.056	-.202**	-.148*	-.025	-.092	.113	.008	.148*	.004
EI Tr RF	.154*	.087	-.070	.006	.033	.152*	.024	.124	.064	-.065	-.035	.279**	.080	.271**	-.101	.152*	.032	.051	-.083	.054	.021	.005	.133	.213**
EI LRF	.088	.059	-.056	.008	.052	.151*	-.024	.143*	.113	-.072	-.002	.268**	.037	.209**	-.130	.153*	-.001	.067	-.100	.067	-.002	-.032	.122	.202**
PA RF	-.106	-.197**	-.128	-.207**	-.200**	-.177*	-.222**	.024	-.114	-.073	-.052	-.133	-.086	-.033	.011	-.119	-.206**	-.065	-.073	-.049	.122	.012	-.139	-.044
PAC RF	-.012	-.242**	-.222**	-.100	-.178*	-.218**	-.124	-.041	-.135	-.082	-.143	-.159*	-.044	-.055	-.026	-.095	-.016	-.067	.027	-.105	.148	.039	.173*	-.132
MT VI	-.126	-.164*	-.147*	.005	-.007	-.179*	-.191**	.057	-.115	-.060	.007	-.107	-.075	-.091	-.095	-.081	-.026	-.131	-.013	-.126	.094	.147*	-.083	.165*
EI Tr VI	-.041	-.112	-.169*	-.080	-.024	-.074	-.041	.077	-.003	-.157*	.004	.091	-.005	.174*	-.083	.021	-.133	-.138	-.062	.047	.098	-.082	.107	.207**
EI LVI	.051	.101	-.106	-.080	.018	-.046	-.001	.088	.038	-.119	.059	.113	.010	.157*	-.023	.032	-.081	-.080	-.002	.067	-.103	-.106	.144*	.238**
PA VI	-.153	-.148	-.123	-.052	-.023	-.021	-.030	.043	-.033	-.080	.000	-.173*	-.034	-.010	-.034	.002	-.032	-.074	-.031	-.156*	.046	-.135	-.099	-.040
PAC VI	-.205*	-.308**	-.177*	-.127	-.205*	-.257**	-.115	-.114	-.095	-.015	-.082	-.277**	-.131	-.065	-.132	-.047	-.033	-.139	-.001	-.207*	.074	-.022	-.273**	-.143
$FT VM	-.021	-.100	-.100	-.235**	.025	-.041	-.001	-.033	-.074	-.181*	-.074	.095	.172*	.311**	.008	.042	-.079	-.090	-.091	.107	-.121	-.211**	.151*	.302**
MT VM	-.191**	-.198**	-.228**	.067	-.039	-.276**	-.093	-.081	-.051	.003	-.098	.175*	-.209**	-.230**	.003	-.076	-.091	-.170*	-.118	.004	-.001	.041	-.158*	-.011
EI Tr VM	.021	-.049	-.105	-.089	-.069	-.037	-.071	-.117	-.055	-.085	.003	.072	-.033	.118	-.025	-.009	-.024	-.067	.044	.047	.054	-.038	.109	.046
EI L VM	.014	-.010	-.111	-.054	.003	.074	.024	.048	.000	-.026	-.069	.226**	.052	.189**	.010	.103	.004	-.005	-.082	-.026	.042	-.067	.098	.152*
PA VM	-.004	-.060	-.033	-.035	-.016	-.068	-.071	.018	-.061	.009	-.074	-.138	.094	-.146*	-.010	.049	.093	-.018	.006	-.062	-.027	.041	-.069	.046
PAC VM	-.043	-.095	-.095	.024	-.122	-.112	-.022	.089	-.025	.075	.002	-.200**	-.037	-.162*	.077	.030	.129	-.068	-.003	.003	.052	.086	-.159*	.064
$FT VL	-.081	-.103	-.098	-.192**	.055	-.029	-.059	-.039	-.048	-.190**	-.078	.074	.173*	.262**	-.097	-.003	-.125	-.146*	-.158*	-.048	-.084	-.221**	.123	.230**
MT VL	-.113	-.197**	-.126	-.120	-.183*	-.247**	-.026	-.141	-.045	-.005	-.101	-.101	-.096	-.176*	-.048	-.126	.038	-.071	.009	-.121	.028	-.017	-.150*	.081
EI Tr VL	.108	.075	-.103	.027	.094	.127	.003	.187*	.004	-.026	.044	.243**	.095	.255**	-.039	.169*	-.035	.018	-.152*	.046	.012	-.078	.150*	.231**
EI L VL	.115	.124	-.028	.054	.070	.138	.039	.230**	.100	.070	.072	.224**	.051	.224**	-.011	.173*	.017	.078	-.104	.016	.088	.010	.121	.204**
PA VL	-.193**	-.329**	-.122	-.217**	-.191**	-.207**	-.026	-.124	-.053	.006	-.024	-.268**	-.062	-.126	.127	-.131	-.109	-.154*	.014	.060	.054	.065	-.104	.018
PAC VL	-.114	-.202**	-.204**	-.127	-.028	-.210**	-.018	.179*	-.005	-.003	-.103	.149*	-.064	-.094	.054	-.141	-.118	-.144*	.002	.021	.048	.127	-.069	-.028
AREA RF	-.318**	-.340**	-.228**	-.081	-.067	-.295**	-.144*	-.085	-.217**	-.100	-.124	-.241**	.179*	-.213**	-.045	-.228**	-.117	-.197**	-.105	-.034	.109	-.015	-.206**	-.050

**The correlation is significant at the 0.01 level (bilateral).

*The correlation is significant at the 0.05 level (bilateral).

Abbreviations: SFT - superficial fat thickness, MT - muscle thickness, EI - echointensity, PA - pennate angle, PAC pennate angle in contraction, RF - rectus femoris, VI - vastus intermedius, VM - vastus medialis, VL - vastus lateralis, COPD - chronic obstructive pulmonary disease, TIA - transitory ischemic attack

Kendall's τ used for statistical analysis

Annex table 4A Correlation of comorbidities with ultrasound parameters

Annex table 4B Correlation of ultrasound and biochemical parameters

ANNEX TABLE 4B. Correlations of ultrasound and biochemical parameters (N= 61)																									
	SFT RF	MT RF	EI Tr RF	EI LRF	PA RF	PAC RF	MT VI	EI Tr VI	EI LVI	PA VI	PAC VI	SFT VM	MT VM	EI Tr VM	EI L VM	PA VM	PAC VM	SFT VL	MT VL	EI Tr VL	EI L VL	PA VL	PAC VL	AREA RF	Frailty phenotype
Leucocytes	0.125	0.006	0.109	0.061	0.054	0.034	.265*	0.025	0.000	-0.015	0.020	0.052	0.041	-0.159	-0.012	0.000	0.002	0.056	-0.189	0.145	0.054	-0.010	0.185	-0.018	0.176
Neutrophils	0.164	-0.038	0.145	0.117	-0.072	-0.017	.285*	0.019	-0.010	-0.008	0.054	0.114	0.073	-0.209	0.045	-0.129	-0.057	0.043	-0.055	0.156	0.036	-0.053	0.093	-0.065	0.204
Lymphocytes	0.064	0.070	0.025	-0.024	0.225	0.005	0.058	0.079	0.098	0.059	0.027	-0.018	-0.081	0.092	-0.021	0.226	0.216	0.107	-0.154	0.087	0.100	0.116	.253*	0.190	-0.161
RBC	-.267*	0.188	-.324*	-.349**	-0.143	-0.135	0.153	-0.148	-0.120	-0.015	0.062	-.267*	.361**	-0.070	-.285*	.292*	-0.009	-.327**	0.179	-.262*	-.283*	0.172	.253*	.346**	-.328**
HGB	-.359**	0.017	-0.242	-.318*	-0.208	-.303*	-0.050	-0.125	-0.095	-0.151	-0.133	-.367**	.289*	-0.080	-0.203	0.191	-0.031	-.467**	0.003	-0.190	-0.235	-0.086	0.141	0.101	-0.186
HCT	-.289*	0.025	-0.222	-.294*	-0.209	-0.237	-0.008	-0.089	-0.064	-0.124	-0.144	-.262*	.318*	-0.057	-0.165	0.170	-0.038	-.414**	0.035	-0.176	-0.247	-0.029	0.125	0.123	-0.183
MCV	-0.140	-.310*	0.213	0.141	-0.163	-0.103	-0.134	-0.011	-0.029	-0.112	-0.238	-0.094	-0.182	-0.128	0.107	-0.184	-0.026	-0.159	-.346**	0.159	0.103	-.318*	-0.157	-.450**	,428**
MCH	-.392**	-.276*	0.102	0.020	-0.176	-0.244	-0.212	-0.120	-0.117	-0.115	-0.236	-.368**	-0.159	-0.153	0.011	-0.142	0.050	-.360**	-.320*	0.072	0.065	-.354**	-0.132	-.402**	,308*
MCHC	-.425**	0.038	-0.154	-0.216	-0.041	-.298*	-0.211	-0.165	-0.154	-0.005	-0.015	-.441**	-0.001	-0.056	-0.128	-0.011	0.067	-.292*	-0.109	-0.075	-0.039	-0.162	0.082	0.002	-0.185
Platelets	.320*	0.200	0.214	0.153	.316*	0.201	-0.014	.313*	.256*	0.073	0.265	.343**	0.032	0.107	0.168	-0.053	0.035	.388**	-0.094	0.189	0.100	0.080	0.185	0.172	-0.234
Proteins	0.116	0.218	-0.203	-.255*	0.144	0.153	0.170	0.063	0.016	0.064	.309*	0.120	0.223	0.042	-0.182	0.187	-0.121	0.104	0.128	-0.224	-.297*	0.144	.390**	.296*	-,319*
Glucose	0.168	-.307*	0.141	0.159	-0.121	-0.055	0.037	-0.082	-0.112	-0.106	-0.002	0.142	-0.133	0.017	-0.023	-0.002	-0.150	0.122	-0.032	0.132	0.139	-.297*	-0.171	-.323*	,564**
Urea	-0.144	-0.040	0.002	0.063	0.024	-0.171	-0.048	-0.030	-0.021	-0.251	-0.232	-0.096	0.113	-0.014	0.113	-0.146	-.334**	-0.240	0.058	-0.152	-0.075	-0.248	-0.231	-0.129	0.044
Creatinine	-.319*	0.187	-0.209	-0.220	-0.158	-.282*	0.220	-0.161	-0.147	0.150	0.076	-.271*	.439**	-0.232	-0.150	0.049	0.150	-.443**	0.186	-0.237	-0.207	-0.084	0.050	0.130	-0.055
Glomerular filtration rate	-0.007	0.158	-0.197	-0.170	0.190	.348*	0.023	0.131	0.114	0.039	0.176	0.011	-0.010	0.099	-0.132	0.103	0.062	0.082	0.026	-0.118	-0.107	.396**	.256*	0.208	-.330**
Calcium	-0.003	0.156	-0.124	-0.210	0.040	0.064	0.011	0.000	-0.031	0.024	0.215	0.032	0.141	-0.007	-0.222	.277*	0.048	0.027	0.086	-0.085	-0.105	0.103	0.151	0.184	-209
Phosphorus	0.076	0.069	0.125	0.099	0.078	0.025	-0.032	0.230	0.229	0.045	-0.077	0.064	-0.182	0.174	0.151	0.109	0.172	0.206	0.060	0.028	-0.022	0.143	-0.061	0.061	-0.037
ALT	-0.048	0.182	-0.144	-0.174	0.061	-0.100	.327**	-0.029	0.004	0.008	0.125	0.004	.293*	0.070	-.268*	.422**	0.206	-0.007	-0.041	-0.051	-0.052	0.137	0.245	0.114	-0.068
ALP	.271*	-0.022	0.248	0.186	-0.067	-0.044	0.141	0.216	0.147	-0.120	-0.144	.367**	-0.094	0.219	0.194	-0.013	-0.170	0.197	-0.010	.268*	0.164	-0.057	-0.075	-0.051	0.162
Chlorine	-0.036	-0.197	.370**	.319*	-0.050	-0.159	-0.114	0.126	0.096	-0.028	-0.216	-0.052	-.297*	0.140	0.122	-0.198	0.061	-0.008	-.286*	.348**	.293*	-0.164	-0.184	-0.149	0.159
Potassium	-0.115	-0.199	0.099	0.016	-0.058	-0.036	-0.105	-0.035	-0.091	-0.095	-0.127	-0.096	-0.075	0.093	0.108	0.021	-0.063	-0.176	-.277*	0.031	-0.044	-.335**	-0.194	-0.218	0.107
Sodium	0.040	-0.225	.303*	0.201	-0.165	-0.199	-0.218	0.126	0.061	-.278*	-.316*	0.040	-0.152	0.102	0.114	-0.095	0.099	-0.077	-.301*	.270*	.251*	-0.186	-0.102	-0.219	,271*
Total cholesterol	0.196	0.078	.276*	0.226	0.197	0.142	0.054	.251*	0.237	0.079	0.067	0.196	-0.051	.283*	0.246	.336**	0.242	0.118	-0.071	.336**	.410**	0.032	-0.038	0.038	-0.048
Triglycerides	-0.005	-0.044	-0.005	0.041	-0.231	-0.185	.271*	-0.130	-0.067	0.013	-0.039	0.064	0.106	-0.033	-0.111	.295*	0.254	-0.097	-0.006	0.110	0.116	0.020	0.073	-0.044	,276*
HDL cholesterol	0.089	0.104	0.165	0.016	0.211	0.148	-0.195	.275*	0.171	0.061	0.002	0.070	-0.110	0.153	0.180	-0.109	-0.075	0.235	-0.191	0.157	0.097	-0.036	-0.045	0.087	-0.139
LDL cholesterol	0.219	0.004	.309*	.310*	0.239	0.163	0.013	.253*	.257*	0.020	0.086	0.189	-0.126	.290*	.298*	.320*	0.132	0.100	0.012	.316*	.416**	-0.020	-0.110	-0.032	-0.063
CPK	-0.131	0.099	-.295*	-.309*	-0.062	-0.152	-0.172	-0.028	0.044	-0.027	0.030	-0.150	0.060	-0.128	-0.181	0.109	.335**	-0.112	0.041	-0.243	-0.213	0.087	0.083	0.190	-,289*
Total cholesterol/HDL	0.049	-0.063	0.010	0.144	-0.080	0.001	.272*	-0.128	-0.021	-0.002	0.101	0.064	0.049	0.045	-0.036	.385**	0.207	-0.146	0.158	0.070	0.198	0.066	0.016	-0.035	0.133
Homocysteine	-0.091	-0.192	0.094	0.150	-0.213	-0.265	-0.006	-0.163	-0.146	-0.132	-0.278	-0.116	0.086	-0.154	-0.038	-0.218	-0.128	-0.177	-0.153	0.041	0.056	-0.235	-0.125	-0.121	,303*
Ferritin	-.361**	0.047	-0.031	-0.091	-0.123	-0.159	0.176	-0.062	-0.019	-0.025	-0.023	-0.232	0.217	0.003	-0.034	.263*	-0.078	-.468**	0.015	-0.066	-0.047	-0.116	0.044	-0.027	-0.047
Iron	-0.149	-0.146	-0.159	-.261*	-0.184	-.335*	-0.146	-0.232	-0.144	-0.136	-0.027	-0.157	0.090	-0.226	-0.147	0.142	0.041	-0.204	0.030	-0.159	-0.175	0.013	0.243	-0.125	-0.086
TS	-0.221	-0.158	-0.155	-0.250	-.258*	-.423**	-0.104	-.303*	-0.203	-0.128	-0.160	-0.192	0.125	-.274*	-0.143	0.044	-0.019	-.305*	0.063	-0.118	-0.179	-0.009	0.201	-0.147	-0.036
CRP	.331**	0.041	0.176	0.201	0.073	0.123	0.223	-0.015	-0.058	0.177	0.065	.366**	0.036	-0.038	0.083	0.094	0.000	0.224	-0.105	0.244	0.246	-0.047	0.079	-0.035	0.225
Albumin	-0.152	0.101	-0.215	-.282*	-0.017	0.067	0.030	-0.179	-0.189	0.096	0.173	-0.089	0.159	-0.156	-0.203	0.111	0.027	-0.103	-0.041	-0.211	-.292*	0.157	.311*	0.209	-0.112
Vitamin D	-0.109	-0.017	-0.132	-0.147	0.031	0.031	-0.115	-0.047	-0.075	0.032	-0.062	-0.086	-0.019	-0.046	0.034	-0.236	-.257*	0.005	0.086	-0.149	-0.157	-0.158	0.024	-0.007	-0.170

**The correlation is significant at the 0.01 level (bilateral).

*The correlation is significant at the 0.05 level (bilateral).

Abbreviations: MT - muscle thickness, EI - echointensity, PA - pennate angle, PAC pennate angle in contraction, RF - rectus femoris, VI - vastus intermedius, VM - vastus medialis, VL - vastus lateralis, RBC - red blood cells, HGB - hemoglobin, HCT - hematocrit, MCV - mean corpuscular volume, MCH - mean corpuscular hemoglobin, MCHC - mean corpuscular hemoglobin concentration, ALT - alanine aminotransferase, ALP - alkaline phosphatase, HDL - high-density lipoprotein, LDL - low-density lipoprotein, CPK - creatine phosphokinase, TS - transferrin saturation, CRP- C-reactive protein

Rho of Spearman used for statistical analysis

ANNEX TABLE 4C. Correlations of ultrasound parameters and hormones (N = 61)

	$FT RF	MT RF	EI Tr RF	EI LRF	PA RF	PAC RF	MT VI	EI Tr VI	EI LVI	PA VI	PAC VI	$FT VM	MT VM	EI Tr VM	EI L VM	PA VM	PAC VM	$FT VL	MT VL	EI Tr VL	EI L VL	PA VL	PAC VL	AREA RF
Cortisol	0.119	0.161	0.077	0.124	0.119	0.021	0.207	0.017	0.027	0.147	0.022	0.034	0.101	-0.152	-0.118	0.118	0.152	0.164	-0.034	0.113	0.192	.257*	0.043	0.049
Insulin	0.147	-0.039	0.045	0.038	-0.049	0.007	0.125	-0.099	-0.090	0.107	-0.004	0.192	0.022	0.076	0.002	.285*	0.170	0.057	-0.067	0.128	0.158	-0.020	0.073	-0.012
PTH	-0.010	-0.155	0.234	0.252	-0.019	-0.140	-0.179	0.095	0.067	-0.009	-0.085	0.017	-0.175	0.101	0.130	-0.003	0.048	-0.034	-0.112	0.063	0.141	.302*	-0.249	-0.192
IGF 1	0.000	.374**	-.378**	-.299*	0.185	0.257	0.044	0.077	0.040	0.142	.352*	0.024	.358**	0.014	-0.085	-0.144	0.175	-0.006	0.244	-0.169	-0.185	.268*	0.162	.510**
TSH	0.019	0.008	0.181	0.154	-0.003	-0.053	0.129	0.128	0.189	0.059	-0.159	0.022	0.023	0.147	0.199	0.102	0.046	0.049	-0.092	0.098	0.102	0.129	-0.081	0.023

**The correlation is significant at the 0.01 level (bilateral).

*The correlation is significant at the 0.05 level (bilateral).

Abbreviations: MT - muscle thickness, EI - echointensity, PA - pennate angle, PAC pennate angle in contraction, RF - rectus femoris, VI - vastus intermedius, VM - vastus medialis, VL - vastus lateralis, PTH - parathormone, TSH - thyroid stimulating hormone, IGF 1 - Insulin-like growth factor 1

Rho of Spearman used for statistical analysis

ANNEX TABLE 4D. Correlations of ultrasound parameters and cytokines and oxidative stress parameters (N = 61)

	$FT RF	MT RF	EI Tr RF	EI LRF	PA RF	PAC RF	MT VI	EI Tr VI	EI LVI	PA VI	PAC VI	$FT VM	MT VM	EI Tr VM	EI L VM	PA VM	PAC VM	$FT VL	MT VL	EI Tr VL	EI L VL	PA VL	PAC VL	AREA RF
ITAC	0.036	-0.153	0.240	0.210	0.025	-0.050	-0.016	0.153	0.098	0.079	0.067	-0.023	-0.034	0.230	0.113	0.056	-0.046	-0.030	-0.152	0.114	0.109	-0.052	-0.063	-0.198
Fractalkine	0.220	.269*	-0.085	-0.066	0.243	0.183	.369**	0.181	0.114	.302*	.290*	.261*	0.242	0.211	0.030	0.218	0.077	0.152	.260*	0.083	0.077	.424**	.285*	-0.012
IFNγ	0.074	.318*	-0.099	-0.112	0.147	0.114	.397**	0.089	0.023	.312*	.401**	0.062	.271*	0.105	-0.117	0.106	-0.039	0.107	.294*	-0.018	-0.034	.358**	.370**	0.242
IL10	0.231	0.186	0.105	0.134	0.005	0.054	.386**	0.144	0.133	.276*	0.148	0.186	0.061	0.069	-0.022	0.232	0.123	0.184	0.235	0.204	0.166	0.249	.282*	0.056
MIP3a	-0.068	0.167	-0.122	-0.118	-0.035	-0.052	.426**	-0.038	-0.076	.390**	.399**	-0.058	.278*	0.011	-0.171	0.241	0.054	-0.088	.256*	-0.043	-0.074	.262*	.399**	.272*
IL12p70	0.122	0.249	-0.082	-0.096	0.011	-0.105	.269*	0.167	0.091	0.199	0.261	0.126	0.232	0.110	-0.070	0.149	0.052	0.160	.306*	0.076	-0.071	.330*	.327*	0.162
IL13	.340**	0.156	0.025	-0.019	.284*	0.120	0.138	0.136	0.131	0.160	0.246	0.247	0.093	0.183	0.036	0.127	-0.047	.312*	.296*	0.110	0.067	.269*	.255*	0.043
IL17a	0.084	0.225	-0.058	-0.084	0.139	0.101	.369**	0.065	0.031	.299*	.434**	0.062	0.240	0.128	-0.090	0.100	-0.008	0.086	.263*	0.036	0.001	.353**	.418**	0.216
IL1b	0.037	.408**	-0.196	-0.247	0.086	0.138	.293*	0.105	0.017	0.219	0.184	0.061	0.230	-0.055	-0.176	0.066	0.053	0.077	0.215	-0.014	-0.118	.377**	.331**	.296*
IL2	-0.005	.352**	-0.181	-0.217	0.099	0.007	.428**	0.003	-0.077	0.247	0.234	-0.018	.338**	-0.004	-0.181	0.090	0.055	0.058	0.212	0.025	-0.063	.302*	.345**	0.245
IL4	0.183	.288*	-0.063	-0.124	0.196	0.201	.313*	0.070	0.008	0.176	0.259	0.141	0.241	-0.071	-0.085	-0.060	-0.086	0.205	0.071	0.189	0.061	.292*	.328*	0.173
IL23	.308*	0.237	-0.078	-0.136	0.140	-0.044	0.169	0.009	-0.065	0.260	0.091	.307*	0.203	0.014	0.032	0.120	0.046	0.239	0.195	0.077	-0.044	0.215	.272*	-0.025
IL6	0.172	0.119	0.125	0.130	-0.061	-0.140	.340**	0.204	0.150	0.184	0.169	0.130	0.176	0.132	-0.064	0.181	0.125	0.120	.267*	.297*	0.209	0.244	0.168	0.167
IL7	0.170	.296*	0.226	0.123	.339**	0.149	.315*	.338**	.275*	.306*	.294*	0.242	0.184	.360**	.282*	0.157	-0.036	0.124	0.247	.258*	0.225	.337**	0.229	0.023
IL8	-0.236	-.279*	0.205	0.161	-0.232	-.281*	-.297*	-0.048	-0.039	-.470**	-.425**	-0.243	-0.233	-0.037	0.040	-0.069	-0.062	-0.177	-.297*	0.099	0.125	-.316*	-.353**	-0.159
TNFα	-0.176	-0.035	0.004	-0.030	-0.029	-0.129	0.078	-0.035	-0.116	0.011	0.093	-0.189	0.117	-0.013	-0.089	0.141	0.077	-.293*	0.101	-0.025	0.057	-0.148	0.033	-0.098
MDA	-0.178	0.030	-0.171	-0.184	-0.023	0.003	-0.088	-0.010	-0.015	-0.062	-0.049	-0.139	.268*	-0.013	-0.068	0.190	0.158	-.315*	0.119	-0.114	-0.008	0.046	0.070	0.108
Protox	0.246	-0.020	-0.049	-0.091	.268*	0.158	-0.194	-0.070	-0.126	0.102	-0.052	0.246	-0.148	-0.062	0.101	-.330*	-.277*	.294*	-0.049	-0.004	-0.167	0.079	0.097	-0.096

**The correlation is significant at the 0.01 level (bilateral).

*The correlation is significant at the 0.05 level (bilateral).

Abbreviations: MT - muscle thickness, EI - echointensity, PA - pennate angle, PAC pennate angle in contraction, RF - rectus femoris, VI - vastus intermedius, VM - vastus medialis, VL - vastus lateralis, ITAC - interferon-inducible T-cell alpha chemoattractant, IFNγ - interferon gamma, IL - interleukin, MIP - Macrophage Inflammatory Protein, TNFα - Tumour Necrosis Factor Alpha, MDA - malondialdehyde, Protox - oxidized proteins

Rho of Spearman used for statistical analysis

ANNEX TABLE 4E Logistic regression analysis model HIGH AUC						
	Ultrasound parameters			Adjustment with physical characteristics		
	Wald	p	OR	Wald	p	OR
Frailty phenotype (constant)	.157	.692	0.925			
AREA RF	6.645	.010	.660	3.380	.066	.691
MT RF	.277	.599	0.561	0.251	.616	0.527
PAC VI	.080	.777	0.978	.006	.939	.993
MT VM	2.745	.098	.412	1.995	.158	.387
PA VL	2.326	.127	.867	0.731	.392	.908
BMI				6.775	.101	1.125
Sex				2.690	.009	0.076
Muscle strength				7.584	.006	.857
Gait speed				3.024	.082	2.056
Block χ^2 (df)				24,824 (4), p<0.001		
Model χ^2 (df)	48,402 (5), p<0.001			73,226 (9), p<0.001		
Nagelkerke R^2	.504			.683		
Correct prediction	76.5			86.3		

Sample size=128; Abreviations: RF - rectus femoris, VL - vastus lateralis, VM - vastus medialis, VI - vastus intermedius, MT - muscle thickness, PA - pennate angle, PAC - pennate angle in contraction, BMI - body mass index.

Annex table 4E Logistic regression analysis model HIGH AUC

ANNEX TABLE 4F Logistic regression analysis model MT/AREA						
	Ultrasound parameters			Adjustment with physical characteristics		
	Wald	p	OR	Wald	p	OR
Frailty phenotype (constant)	1.326	.250	1.228			
MT RF	1.421	.233	.326	.788	.375	.357
MT VM	2.504	.114	.462	.615	.433	.621
MT VL	3.491	.062	.231	3.322	.068	.162
MT VI	.584	.445	1.724	.051	.821	.793
AREA RF	12.872	.000	.607	6.933	.008	.630
BMI				4.415	.036	1.173
Sex				9.705	.002	.048
Muscle strength				12.021	.001	.826
Gait speed				3.429	.064	1.957
Block χ^2 (df)				35,076 (4), p<0.001		
Model χ^2 (df)	62,979 (5), p<0.001			98,055 (9), p<0.001		
Nagelkerke R^2	.523			.720		
Correct prediction	80.3			89.0		

Sample size=128; Abreviations: RF - rectus femoris, VL - vastus lateralis, VM - vastus medialis, VI - vastus intermedius, MT - muscle thickness, BMI - body mass index.

Annex table 4F Logistic regression analysis model MT/AREA

ANNEX TABLE 4G Logistic regression analysis model RF						
	Ultrasound parameters			Adjustment with physical characteristics		
	Wald	p	OR	Wald	p	OR
Frailty phenotype (constant)	0.035	0.851	1.036			
AREA RF	12.426	.000	.602	7.099	.008	.625
MT RF	1.020	.312	0.382	2.690	.101	.304
SFT RF	0.020	.888	.941	1.531	.216	.222
EI RF	0.301	.583	1.008	0.061	.805	.995
PA RF	0.970	.325	1.120	0.224	.636	1.080
PAC RF	2.941	.086	.844	0.013	.909	.985
BMI				3.905	.048	1.180
Sex				4.617	.032	.112
Muscle strength				11.896	.001	.811
Gait speed				3.141	.076	2.048
Block χ^2 (df)				31,507 (4) p<0,001		
Model χ^2 (df)	51,158 (6) p<0,001			82,665 (10) p<0,001		
Nagelkerke R^2	.482			.688		
Correct prediction	82.5			86.0		

Sample size=128; Abreviations: RF - rectus femoris, MT - muscle thickness, SFT - superficial fat thickness, EI - echointensity, PA - pennate angle, PAC - pennate angle in contraction, BMI - body mass index.

Annex table 4G Logistic regression analysis model RF

ANNEX TABLE 4H Logistic regression analysis model BIO 4									
	Ultrasound parameters			Adjustment with biochemical parameters			Adjustment with physical characteristics		
	Wald	p	OR	Wald	p	OR	Wald	p	OR
Frailty phenotype (constant)	1.599	.206	1.385						
MT RF	15.584	.000	.011	12.559	.000	.008	3.900	.048	.000
MCV				0.830	.362	1.078	1.683	.195	1.237
PROTEINS				4.392	.036	.143	4.409	.036	.001
BMI							3.147	.076	1.409
Sex							4.126	.042	0.001
Muscle strength							4.320	.038	.479
Block χ^2 (df)				8,379 (2) p=0,015			26,552 (3) p<0,001		
Model χ^2 (df)	26,633 (1) p<0,001			35,012 (3) p<0,001			61,565 (6) p<0,001		
Nagelkerke R^2	.470			.580			.847		
Correct prediction	75.8			82.3			91.9		

Sample size=61; Abreviations: MT RF - muscle thicknes of rectus femoris, MCV - mean corpuscular volume, BMI - body mass index.

Annex table 4H Logistic regression analysis model BIO 4

ANNEX TABLE 4I Logistic regression analysis model BIO 5									
	Ultrasound parameters			Adjustment with biochemical parameters			Adjustment with physical characteristics		
	Wald	p	OR	Wald	p	OR	Wald	p	OR
Frailty phenotype (constant)	1.318	.251	1.346						
AREA RF	14.613	.000	.508	12.399	.000	.475	7.216	.007	.438
IL 12				3.228	.072	.572	5.676	.017	.266
IL 17				1.005	.316	.959	.025	.874	1,010
Gait speed							1.882	.170	2.932
Muscle strength							5.377	.020	.841
Block χ^2 (df)				15.714 (2) p<0.001			15.362 (2) p=0.001		
Model χ^2 (df)	25.976 (1) p<0.001			41.691 (3) p<0.001			57.053 (5) p<0.001		
Nagelkerke R^2	.466			.665			.816		
Correct prediction	80.3			83.6			91.8		

Sample size=61; Abreviations: RF - rectus femoris, IL - interleukin.

Annex table 4I Logistic regression model analysis BIO 5

ANNEX TABLE 4.7A Reference values for IGF-1		
Age (y)	Female (ng/ml)	Male (ng/ml)
0-5	33.0-172.0	27.4-113.5
5-8	80.0-244.0	54.9-206.4
8-11	87.0-399.0	85.2-248.8
11-15	188.0-510.0	115.4-498.2
15-20	267.0-471.0	247.3-481.7
20-24	149.1-332.3	187.9-400.0
24-39	107.8-246.7	96.4-227.8
39-54	92.7-244.6	88.3-209.9
>54	45.0-204.4	54.6-185.7

Abbreviations: IGF-1 - Insulin-like growth factor 1

Annex table 4.7A Reference values for IGF-1